# Bulletin
# of
# The Geological Society of America

VOLUME 69 June 1958 NUMBER 6

## CONTENTS


| | Pages |
|---|---|
| Malaspina Glacier, Alaska. By Robert P. Sharp | 617–646 |
| Lower and Middle Cambrian stratigraphy in northern Utah and southeastern Idaho. By George B. Maxey | 647–688 |
| Stratigraphy of Upper Pennsylvanian and Lower Permian rocks in the Sand Canyon area, Otero County, New Mexico. By George O. Bachman and Philip T. Hayes | 689–700 |
| Urano-organic ore at Temple Mountain, Utah. By Dana R. Kelley and Paul F. Kerr | 701–756 |
| Precambrian classification and correlation in the Canadian Shield. By M. E. Wilson | 757–774 |
| Geochemistry of the Sterling Hill zinc deposit, Sussex County, New Jersey. By R. W. Metsger, C. B. Tennant, and J. L. Rodda | 775–788 |
| Short Notes | |
| Formation of badland topography. By Max F. Carman, Jr. | 789–790 |
| Cross-bedding in Pennsylvanian sandstones of central Pennsylvania: A preliminary study. By Richard P. Nickelsen | 791–796 |
| Index (January–June) | 797–802 |


**Subscription $15.00 per year.**

**Printing Office: Mt. Royal & Guilford Aves., Baltimore 2, Md.**

**Communications for publications should be addressed to The Geological Society of America, Dr. H. R. Aldrich, Secretary, 419 West 117 Street, New York, N. Y.**

**Please give notice of change of address 4 weeks in advance. Claims for nonreceipt of the Bulletin of a given month must be sent to the Secretary of the Society before the end of the second succeeding month.**

Entered as second-class matter at the Post Office at Baltimore, Md.
under the Act of Congress of July 16, 1894.
Accepted for mailing at special rate of postage provided for in Section 1103
Act of October 3, 1917, authorized on July 8, 1918.

## PAPERS IN PRESS FOR FORTHCOMING ISSUES

Paleoecology of the Lower Carboniferous Reef Complex and Shelf Limestones, Northwest Derbyshire, England. By G. B. Wolfenden

Sedimentary Breccias in the Southeast Missouri Lead District. By F. G. Snyder and J. W. Odell

Metamorphosed Middle Paleozoic Fossils from Central Massachusetts, Eastern Vermont, and Western New Hampshire. By Arthur J. Boucot, Gordon J. F. MacDonald, Charles Milton, and James B. Thompson, Jr.

Mechanisms of Pegmatite Emplacement. By Robert A. Chadwick

Lower Ordovician Section near Chambersburg, Pennsylvania. By William J. Sando

Stratigraphy of Ocoee Series, Great Smoky Mountains, Tennessee and North Carolina. By Philip B. King, Jarvis B. Hadley, Robert B. Neuman, and Warren Hamilton

BULLETIN OF THE GEOLOGICAL SOCIETY OF AMERICA
VOL. 69, PP. 617-646, 16 FIGS., 4 PLS. JUNE 1958

# MALASPINA GLACIER, ALASKA

BY ROBERT P. SHARP

## ABSTRACT

Malaspina Glacier is a piedmont ice sheet covering approximately 850 square miles on the flat coastal foreland of southern Alaska. The Seward-Malaspina glacier system has experienced marked deficits in 6 out of 9 budget years between 1945 and 1954. In 1 of the remaining 3 years it had a good surplus, and in the other 2 years the economy was about balanced. Variation in precipitation has exerted a major influence on regimen.

Seismic explorations show that the ice, 2000 feet thick, lies in a basin at least 825 and possibly 1000 feet below sea level. Data support speculation that the closure of this basin is due about one-third to glacial erosion and two-thirds to peripheral glacial deposition.

Geometrically and structurally, Malaspina Glacier is simple in broad aspects but complex in detail. An extensive system of radial crevasses, a prevailing foliation, and two sets of tight joints are consistent with the broad lobate form of the sheet and with the stresses causing it to spread out on the coastal foreland. Near the center of the glacier the foliation dips too steeply (75°–85°) to be related to near-surface shearing, so it is attributed to plastic deformation at some depth. An extensive and complex system of folds, spectacularly displayed on the glacier's surface, deforms ice streams and debris bands about near-vertical axes. These structures were formed within the Malaspina and are not inherited from higher in the system. They are attributed to slip folding, or to flowage with minor modification by slippage, and developed in response to the strong shove of ice pouring out of the mountains. The Malaspina Glacier spreads out and at the same time maintains sufficient thickness and surface slope to flow uphill across the coastal foreland by folding up accordian fashion.

Deformation of an aluminum pipe in a 1000-foot borehole near the center of this glacier provides information on internal flow. Differential movement in 1 year between top and bottom of the hole was 5.75 feet, with the top moving the most. Deformation recorded in the uppermost 300 feet over a 3-year period extends to within less than 50 feet of the surface, amounts to 1.5 feet, and follows a similar curve. Malaspina borehole observations do not support the concept of extrusion flow. Plots of these data suggest that the strain rate is not an exponential function of depth, but rather that the stress-strain-rate relationship can be described by the commonly used function $\dot{\gamma} = k\tau^n$, with a value of about 3 for $n$. Yielding appears to have occurred at a shear stress as small as 0.01 bar.

Movement of the Malaspina Glacier seemingly involves basal slip or boundary-layer flow as well as internal flowage. Movement of the ice is controlled primarily by surface slope, and steeper parts of the ice surface overlie ascending as well as descending reaches on the subglacial floor. Simple calculations based upon ablation, surface slope, and horizontal velocity show that surfaceward movement of ice is required near the glacier's margin to maintain elevation and profile. Nye's compressive flow seems the most likely mechanism for producing such surfaceward movement.

## CONTENTS

### TEXT

| | Page |
|---|---|
| Introduction | 618 |
| Acknowledgments | 620 |
| Location and physical setting | 620 |
| Ablation and regimen | 621 |
| General statement | 621 |
| Meteorological conditions | 621 |
| Ablation of firn and ice | 621 |
| Comparison of firn ablation on Malaspina and upper Seward glaciers | 622 |
| Summary of ablation relationships on Malaspina Glacier | 622 |
| Regimen of the Malaspina-Seward glacier system | 622 |
| Nature and origin of the Malaspina Glacier | |

| | Page |
|---|---|
| basin | 624 |
| Introductory statement | 624 |
| Geological relationships | 624 |
| Yakutat Foreland and Yakutat Bay | 625 |
| Offshore relationships | 626 |
| Origin of Malaspina Glacier basin | 627 |
| Structural features in Malaspina Glacier | 628 |
| Introductory statement | 628 |
| Crevasses and joints | 628 |
| Foliation | 630 |
| Crystal size | 630 |
| Crystal fabrics | 631 |
| Folded structures within Malaspina Glacier | 631 |
| Introduction | 631 |
| Constitution of lower Seward Glacier | 631 |
| Debris bands on Malaspina Glacier | 632 |
| Description of folds | 633 |
| Origin of the folded structures | 635 |
| Resurgent activity within Malaspina Glacier | 636 |
| Relationship of velocity to depth | 638 |
| Introduction | 638 |
| Setting | 638 |
| Procedure and equipment | 638 |
| Surveys of pipe | 639 |
| Introduction | 639 |
| Surveys of 1951 | 639 |
| Survey of 1952 | 640 |
| Attempted survey of 1953 | 641 |
| Survey of 1954 | 641 |
| Conclusions drawn from borehole data | 641 |
| Mode of flow in Malaspina Glacier | 642 |
| References cited | 645 |


ILLUSTRATIONS


| Figure | Page |
|---|---|
| 1. Map of Malaspina Glacier and environs | 619 |
| 2. Map of ablation stakes near central camp | 621 |
| 3. Cross section of Malaspina Glacier along geophysical profile | 624 |
| 4. Map of Yakutat Bay hydrographic relationships | 626 |
| 5. Diagrammatic cross section of Malaspina basin | 627 |
| 6. Crevasse, foliation, and joint relationships along geophysical profile | 629 |
| 7. Constitution of lower Seward Glacier | 632 |
| 8. Component parts of Malaspina Glacier | 633 |
| 9. Diagram of Malaspina folds | 634 |
| 10. Structural map of a Malaspina fold | 635 |
| 11. Evolution of Malaspina folds | 637 |
| 12. Design of hotpoint | 639 |
| 13. Plots of borehole deformation | 640 |
| 14. Plot of depth-strain rate relationships | 642 |
| 15. Plot of shear stress-strain rate relationships | 643 |
| 16. Relationship of surface slope to configuration of subglacial floor | 644 |

| Plate | Following page |
|---|---|
| 1. Marginal zones of Malaspina Glacier<br>2. Deformed moraines and ice streams in Malaspina Glacier<br>3. Structures in central Malaspina Glacier<br>4. Malaspina ice crystals and photo mosaic | 630 |


TABLE


| Table | Page |
|---|---|
| 1. Items of Malaspina-Seward regimen and budget-year precipitation at Yakutat | 623 |


## Introduction

The Malaspina is the type specimen of a piedmont glacier (Russell, 1891, p. 57, 122; 1901, p. 2, 109). Located alongside much-traveled southern Alaska sea and air routes, it has been observed and studied by explorers and geologists for over 65 years (Russell, 1891, p. 70–74; 1892; Tarr, 1907; Tarr and Butler, 1909, p. 24–25; Tarr and Martin, 1914, p. 41–58; Washburn, 1935). Nonetheless, it has never been thoroughly investigated, owing to large size, unfavorable weather, and difficulties of access.

Facilities and support provided by "Project Snow Cornice," an endeavor of the Arctic Institute of North America directed by W. A. Wood, afforded exceptional opportunity for the following glaciological work upon the Malaspina during the summer of 1951: (1) determination by geophysical means of ice thickness along a radial profile line through the center of the glacier (Allen and Smith, 1953); (2) recording of the vertical velocity profile by deformation of a pipe installed in a deep borehole (Sharp, 1953); (3) study of crystal fabrics in ice (to be reported by G. P. Rigsby); (4) investigation of megascopic structures including crevasses, foliation, and folds; (5) observations pertinent to glacier regimen, especially measurements of ablation; and (6) mapping of features and deposits in the peripheral zone outside the present ice edge (Hartshorn, 1952).

Earlier observations on the Malaspina by Snow Cornice personnel were made in 1948 by F. B. Leighton, Rigsby, and Sharp, and in 1949 by Henri Bader (1950; 1951), A. B. Robertson, L. F. Nobles, and Sharp. In 1951 a beach camp (Fig. 1) was established and supplied by small aircraft operating out of Yakutat. A central camp on the glacier (Fig. 1) was set up and maintained by a helicopter based at the beach camp. The central glacier camp was occupied for approximately two months by C. R. Allen, D. R. Baker, G. I. Smith, Rigsby, and Sharp. Subsequent trips to this site were made on foot in 1952 by Nobles and Sharp, in 1953 by Allen and Sharp, and in 1954 by J. E. Conel and Sharp.

Project Snow Cornice suffered a severe

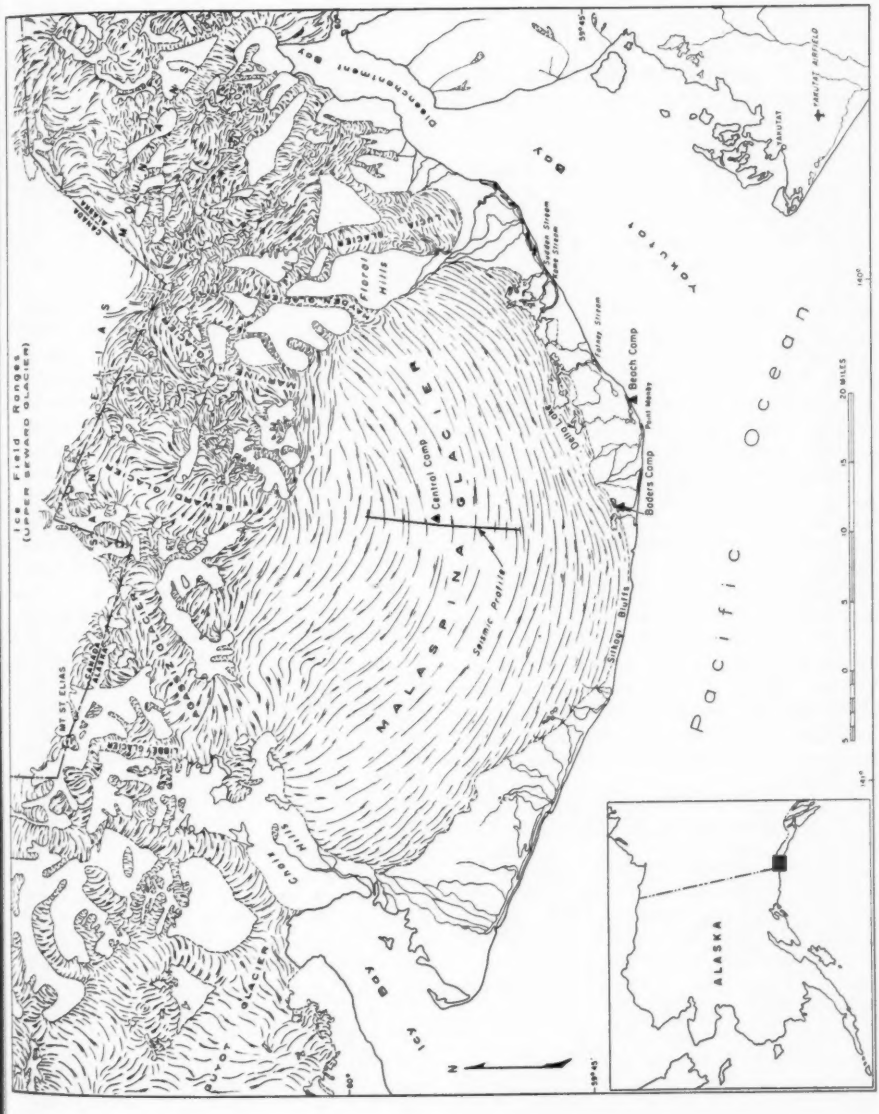
MALASPINA GLACIER
Pacific Ocean
Icy Bay
Disenchantment Bay
Yakutat Bay
Yakutat
Yakutat Airfield
Central Camp
Beach Camp
Boders Camp
Point Manby
Seismic Profile
Sitkagi Bluffs
Fiord Hills
Chaix Hills
Mt. St. Elias
Mt. Cook
Mt. Vancouver
Mt. Augusta
Mt. Logan
Mt. Lucania
Mt. Newton
Mt. Steele
Mt. Wood
Mt. Kennedy
Mt. Hubbard
Mt. Alverstone
Mt. Fairweather
Mt. Crillon
Mt. Quincy Adams
Mt. Root
Mt. Bertha
Mt. Cook

setback on 27 July 1951 with the disappearance of its Norseman aircraft flown by veteran Alaskan bush pilot Maurice King with passengers Foresta and Valerie Wood. This article is dedicated to these people.

## Acknowledgments

This work could not have been accomplished without the generous logistical aid and support of W. A. Wood and Project Snow Cornice. Financial support for the glaciological research was provided by the Office of Naval Research through contract *N6onr-24416* with the California Institute of Technology. Appreciation is expressed for the assistance of all persons named above. A. B. Robertson and G. Hattersley-Smith collected valuable data on the upper Seward Glacier in 1951. A. H. Luke and R. F. Luman respectively piloted and serviced the helicopter used in 1951. Personnel of the Civil Aeronautics Authority, the U. S. Weather Bureau, and the Bellingham Canning Company at Yakutat went out of their way to help. Valuable aid and many courtesies were received from Mr. and Mrs. R. D. Jackson, R. A. Welch, E. R. Pierce, G. S. Clark, and G. H. Luetkehans at Yakutat. Officers and men of the Seventeenth Coast Guard District and of the U. S. Air Force Tenth Air Rescue Squadron provided logistical assistance. An inclinometer and accessories for surveying of the deep borehole were kindly loaned in 1951, 1952, 1953, and 1954 by the Parsons Survey Company of South Gate, California. The manuscript has been improved by critical comments and constructive suggestions from C. R. Allen, M. F. Meier, and R. E. Deane.

## Location and Physical Setting

Malaspina Glacier occupies part of the southern Alaska coastal foreland along the north shore of the Gulf of Alaska (59°52′ N., 140°30′ W.). The nearest settlement is Yakutat, a village and airfield, across Yakutat Bay to the east (Fig. 1). This ice sheet extends from the open sea at Sitkagi Bluffs, where it is almost tidal, 28 miles north to the base of the St. Elias Mountains and 40 miles west from Yakutat Bay to Icy Bay. Planimetric measurements on new maps (Yakutat, Icy Bay, Mount St. Elias, and Bering Glacier, Alaska, 1:250,000) indicate that the Malaspina covers approximately 850 square miles, ignoring the 25 square miles of the now detached Lucia-Atrevida lobe (Plafker and Miller, 1957b, p. 1). The 1500 square miles earlier cited by Russell (1893, p. 224) probably resulted from poor maps and inclusion of the Icy Bay lobe as part of the Malaspina. It cannot be used to determine the shrinkage of this sheet of ice since 1890. The Seward Glacier, which drains a large intermontane basin in the heart of the St. Elias Mountains (Fig. 1), supplies 69 per cent by area of the ice. The remaining 31 per cent is supplied by smaller glaciers flowing from the south face of these mountains, principally the Hayden, Marvine, Seward, Agassiz, and Libbey glaciers. This report deals with that part of the Malaspina supplied by the Seward Glacier.

Altitudes on the ice surface range from about 75 feet at the outer margin to roughly 2500 feet at the debouchment of Seward Glacier. The central camp is at approximately 1370 feet. The glacier surface has a number of broad swells and swales and a few sharp risers. In the marginal zone, the residual debris of medial moraines caps ice ridges up to 300 feet high; closer to the outer edge is a rough chaotic debris-mantled topography characterizing stagnant ice (Pl. 1, fig. 2). In an outermost marginal zone, which averages 1 mile wide, vegetation (Pl. 1, fig. 1) has taken root in thicker, more stable superglacial debris, and a spruce forest with trees up to 100 years old grows on the glacier. This superglacial vegetation and the remnants of interglacial forests in two small areas of deglaciation date the last major advance of Malaspina Glacier at 200 ± 50 years ago (Sharp, 1958). Except for small local areas along the southeastern edge of the glacier, the ice has not receded from the terminal position attained in this last advance (Plafker and Miller, 1957b, p. 11).

On an average, in recent years the firn limit on the Malaspina-Seward system lies at about 2750 feet, a short distance up the lower Seward Glacier. Even under such conditions isolated snow patches may remain upon the Malaspina, and some crevasses contain wedges of snow. In warm dry years, such as 1950–1951, the firn limit recedes far up the lower Seward Glacier to 3500–4000 feet elevation, but in cool wet years, such as 1948–1949, the Malaspina may be nearly half-covered by snow at the end of the ablation season, with a firn limit in the neighborhood of 1000–1200 feet elevation.

## Ablation and Regimen

### *General Statement*

Glacier regimen was not of major concern during this work, but measurements of ablation near the center of the Malaspina furnish a comparison of ablation rates on firn and ice and demonstrate marked differences between ablation on the upper Seward and Malaspina glaciers. The data also permit generalizations concerning the regimen of the Seward-Malaspina system.

### *Meteorological Conditions*

Malaspina weather is that of the maritime south coastal Alaskan environment as recorded by the U. S. Weather Bureau station at Yakutat, on ice-free ground at 28 feet elevation. Yakutat has a mean annual precipitation of 134 inches with extremes of 174 and 86 inches. Mean relative humidity ranges between 79 and 90. Mean annual temperature is 39°F., with recorded extremes of 79°F. and −22°F. Mean hourly wind speed is 8.5, and the prevailing direction is east. Mean sky cover from sunrise to sunset is 8.3. Precipitation of 0.01 inch or greater is recorded on 223 days in an average year, on about 46 of which some snow, hail or sleet occurs. Solid precipitation has been recorded in all months except June, July, and August. Heavy fog occurs on an average of 32 days per year.

The only meteorological element measured at the central Malaspina camp was temperature; wind and cloud cover were estimated. Two aspects of the central-camp meteorological environment merit comment. A cold gravity wind blows 60–70 per cent of the time from the north-northwest with an estimated velocity of 10–15 miles per hour. It is strongest on clear days, slackens at night, and is disrupted by stormy weather. The other aspect is the small diurnal variation in temperature recorded from 4 July to 27 August, 1951, in a ventilated shelter about 4 feet above the ice surface. On 7 out of 55 days, the diurnal range was only 6°F., and on 9 it was 7°F. The median diurnal fluctuation was 8°, and the maximum was 17°. Minimum temperatures of 32°–34°F. were usual, and the daily maxima were for the most part between 40° and 45°F. The maximum of 51° was recorded twice, and the minimum, 32°F., occurred on 15 out of 55 days.

### *Ablation of Firn and Ice*

Measurements were made against dowels set in the firn at the central camp and along the seismic profile to the north. This procedure

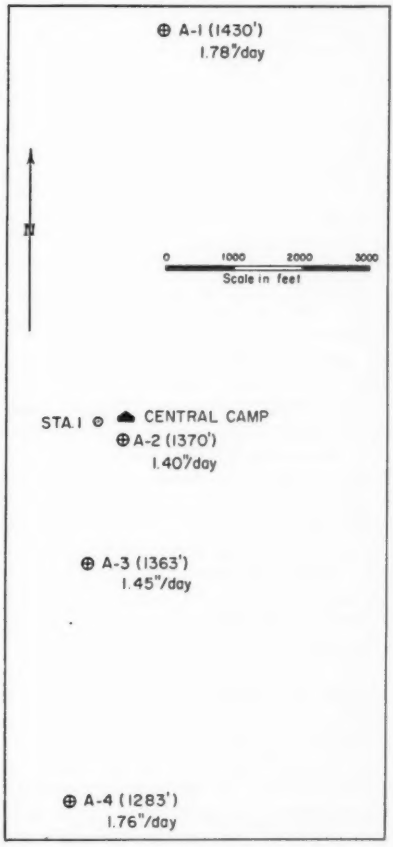


FIGURE 2.—MAP OF ABLATION STAKES NEAR CENTRAL CAMP

Figures in parentheses indicate elevation; figures below are average ablation of ice in inches per day.

yields inaccurate results for short periods, but for longer intervals the errors are not great, as indicated by a mean daily firn ablation of 2.6, 2.5, and 2.7 inches over an 18-day period at three stations along the seismic profile north of the central camp. Firn density was estimated at 0.5–0.55. Daily ablation at the central camp from 3–25 July, 1951, ranged from 1.5 to 3.5 inches of firn. The firn cover

became too thin and patchy for measurements after 25 July.

Ablation of ice was determined at four stations near the central camp (Fig. 2). Measurements were made against 1-inch wooden dowels set 8–9 feet into the ice in snug drill holes. The average daily melt ranged from 1.4 to 1.8 inches of ice (density about 0.89) from 18 July to 27 August, 1951. Daily measurements on pole A-2 at the central camp ranged from 0.5 to 2 inches of ice. The data on Figure 2 suggest a small decrease in ablation northward along the southern half of the line, but pole A-1 at the north end has the highest rather than the lowest rate. In 1949 ablation of ice at a point about 10 miles south of the central camp measured 2.6 inches per day for the corresponding part of the ablation season. This indicates a southward increase in ablation of roughly 0.12 inches of ice per mile per day, which agrees well with the gradient of 0.13 inches per mile between poles A-2 and A-3 but is only one-third that between poles A-2 and A-4. The weak ablation gradient on the Malaspina can be outweighed by local conditions such as direction of exposure, air and water drainage, and nature of the ice. The total ice melt for the ablation season of 1951 at the central camp was 85 inches.

The impression that ice wastes more rapidly than firn on Malaspina Glacier is confirmed by direct measurements at two locations near the central camp, only 365 feet apart, for the same time interval. From 18–25 July, ice melted 1.3 times more rapidly than firn, compared on a water-equivalent basis. A comparison of records from station 1 and pole A-1, 1.1 miles to the north (Fig. 2), shows that ice at A-1 melted 1.8 times more rapidly than firn at station 1. The lower wastage rate on firn is probably due for the most part to its greater albedo.

### *Comparison of Firn Ablation on Malaspina and Upper Seward Glaciers*

Data obtained on upper Seward Glacier by G. Hattersley-Smith, indicate that the ablation of firn on Malaspina Glacier at 1370 feet was 2.5 times greater than on upper Seward Glacier at 5875 feet for the period 6–14 July, 1951. This difference is surprisingly large in view of the intense direct radiation and warmer daytime temperatures of the upper Seward environment. The mean maximum and minimum temperatures for the period were 28°F. and 53°F. on the upper Seward and 33°F. and 47°F. on the Malaspina. Subfreezing temperatures were attained every night during the observation period on the upper Seward but only once on the Malaspina. Each night the upper Seward firn developed a frozen crust which retarded ablation the next morning. Furthermore, since freezing did not usually occur at night on the Malaspina, some melting continued through the night, giving a longer diurnal ablation period. As much as 1 inch of night-time firn ablation was measured at the central camp between 8 p.m. and 8 a.m. Probably the most important factor producing greater ablation on the Malaspina is the prevailing gravity wind which promotes melting by conduction and condensation. The upper Seward by contrast is nearly windless except in times of storm.

### *Summary of Ablation Relationships on Malaspina Glacier*

The greatest ablation on central Malaspina Glacier occurred on warm clear days with a steady gravity wind and on days of heavy rain, possibly because of condensation at the ice-air interface. Clear weather and wind seem more important than high air temperature. Ablation decreased with cloudiness and fog, but these were also times of reduced wind. Ablation continued at a reduced rate during the night if air temperature did not fall to freezing; usually some wind continued into the night. Ice melted about 1.5 times more rapidly than firn on the Malaspina, and firn on the Malaspina melted about 2.5 times more rapidly than firn on the upper Seward Glacier.

### *Regimen of the Malaspina-Seward Glacier System*

Estimates of the regimen of the Malaspina-Seward system were previously made for budget years 1947/48 and 1948/49 (Sharp, 1951, p. 742). An extension of these estimates for the interval from 1945 to 1954 is attempted on the basis of additional information (Table 1).

The estimates (Table 1) suggest that this glacier system experienced marked deficits in 6 out of 9 budget years prior to 1954/55. In 1948/49 it had a surplus, in 1951/52 an approximate balance, and in 1952/53 perhaps a slightly negative regimen. Data are limited,

and the estimates are approximations indicative only of general trends.

Accumulation measurements on upper Seward Glacier (Sharp, 1951, p. 742) suggest that 1945/46 was a modestly unfavorable year and 1946/47 distinctly unfavorable.

When the central Malaspina camp site was revisited in middle August, 1952, 43 inches of snow covered the ice. Since this snow mantle probably survived the ablation season, no melting of ice occurred in 1952 at this location, and wastage on the Malaspina

TABLE 1.—ITEMS OF MALASPINA-SEWARD REGIMEN AND BUDGET-YEAR PRECIPITATION AT YAKUTAT

| Budget year | Accumulation surplus in cubic inches of water* | Wastage in cubic inches of water | Estimated budget balance in cubic inches of water | Precipitation at Yakutat in inches (October to September) | Departure from mean precipitation |
|---|---|---|---|---|---|
| 1945/46 | $8.7 \times 10^{13}$ | ? | Modestly negative | 112.30 | −21.85 |
| 1946/47 | $4.9 \times 10^{13}$ | ? | Strongly negative | 139.68 | +5.53 |
| 1947/48 | $7.5 \times 10^{13}$ | $28.9 \times 10^{13}$ | $-21.4 \times 10^{13}$ | 137.72 | +3.57 |
| 1948/49 | $19.0 \times 10^{13}$ | $10.0 \times 10^{13}$ | $+9.0 \times 10^{13}$ | 162.19 | +28.04 |
| 1949/50 | 3.2 to $4.4 \times 10^{13}$ | High | $-25$ to $-30 \times 10^{13}$ | 106.61 | −27.54 |
| 1950/51 | $2.0 \times 10^{13}$ | $32.0 \times 10^{13}$ | $-30 \times 10^{13}$ | 83.39 | −50.76 |
| 1951/52 | Slightly below normal? | Considerably below normal? | About balanced | 100.88 | −33.27 |
| 1952/53 | Near normal? | Above normal? | Slightly negative? | 123.02 | −11.13 |
| 1953/54 | Below normal? | Above normal? | Strongly negative? | 89.60 | −44.55 |

*1 cubic inch is the equivalent of $0.395 \times 10^{-14}$ cubic miles or $4.33 \times 10^{-3}$ gallons.

Details concerning 1947/48 and 1948/49 have already been presented (Sharp, 1951). In 1949/50 accumulation surplus in the nourishment area was one-third to one-half the average, and the lack of older firn beneath the snow at the Malaspina central camp in 1951 means that wastage for the 1950 ablation season must have been normal or above. Yakutat weather records show 28 inches below average precipitation for 1949/50.

The year 1950/51 was even more unfavorable. Accumulation surplus on the upper Seward Glacier was less than one-third the average of recent years, and wastage on the Malaspina was far above normal. Firn limit near the end of the ablation season was far up the Seward Glacier at an elevation near 4000 feet. Records of ablation on upper Seward Glacier during the summer of 1951 do not suggest excessively rapid ablation, and the excessive wastage on Malaspina Glacier resulted more from early disappearance of an exceptionally thin snow cover than from high rates of melting. The impression that the unfavorable budgetary balance of 1950/51 was due mostly to reduced precipitation is confirmed by Yakutat weather records, which show a deficiency of 51 inches for 1950/51.

was below normal. Nothing is known about accumulation on upper Seward Glacier for 1951/52, but Yakutat weather records show a precipitation about 33 inches below normal. However, budget year 1951/52 may have been about balanced, primarily because of reduced wastage.

In mid-August of both 1953 and 1954 the central Malaspina camp site was bare of snow, and observations from the air showed the firn limit to be far back on the Malaspina in both years. Wastage for these years was normal or above, and Yakutat weather records show a deficiency from average precipitation of 11 inches for 1952/53 and 45 inches for 1953/54. Consequently, 1952/53 probably yielded a small deficit, and 1953/54 a larger one, primarily because of insufficient precipitation.

The magnitude of fluctuation in supply and wastage from year to year in the Seward-Malaspina system is large. Within the period 1947/48 to 1950/51 a sixfold variation of surplus occurred in the accumulation area, and a threefold variation of deficit occurred in the wastage area. It is clear (Table 1) that precipitation has a strong influence on budgetary relationships, for years of marked deficit had exceptionally low precipitation, and the

only year with a demonstrated surplus (1948/49) had abnormally high precipitation. The snow-rain ratio is also significant, not only with respect to nourishment in the accumulation area, but because snow forms a protective blanket which reduces ablation of ice in the wastage area. Unfortunately, the snow-rain ratio for Yakutat, elevation 28 feet, cannot be satisfactorily extrapolated to Malaspina Glacier, elevation 75–2500 feet, or to its accumulation area, elevation 2500–19,850 feet. Variations in this ratio may account for the fact that years such as 1946/47 and 1947/48 with favorable precipitation totals showed marked budgetary deficits, and that year 1951/52 was about balanced although deficient in precipitation.

## Nature and Origin of the Malaspina Glacier Basin

### *Introductory Statement*

The margin of Malaspina Glacier is everywhere a little above sea level, but seismic reflections show that its bottom near the center is at least 825 feet[1] below the sea (Fig. 3). The ice lies in a closed basin that may have been created by erosion, by deposition, or by both, with possibly a slight contribution from isostatic depression. The speculative conclusion is reached that this basin has been created about two-thirds by peripheral deposition and about one-third by erosion. This conclusion bears on the nature and origin of the southern Alaska coastal foreland and the genesis of other depressions and indentations within it.

### *Geological Relationships*

Exposures of bedrock are not known anywhere around the outer margin of Malaspina Glacier between Chaix Hills (Fig. 1) on the northwest and Floral Hills on the northeast (Plafker and Miller, 1957a). Bedrock exposures are also lacking within the Yakutat foreland east of Yakutat Bay except in close proximity to the mountains (Tarr and Butler, 1909, Pl. 37). In so far as can be judged from surface exposures, the rim of the Malaspina basin from Chaix to Floral hills consists of unconsolidated debris.

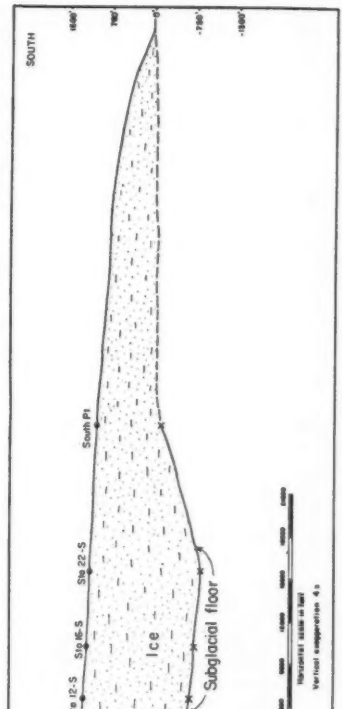


FIGURE 3.—Cross Section of Malaspina Glacier Along Geophysical Profile
Nature of material between base of ice and rock is not known, but it may be till or other similar unconsolidated debris.

[1] The figure of more than 700 feet earlier cited by Allen and Smith (1953, p. 757) referred only to the central part of the seismic profile.

Seismic explorations (Allen and Smith, 1953, p. 755, 758) suggest that consolidated sedimentary rocks, probably of the Yakataga Formation or the Yakutat Group (D. J. Miller, 1957; Plafker and Miller, 1957a), underlie the central part of Malaspina Glacier. The seismic records, however, do not indicate whether the material immediately under the ice is bedrock or unconsolidated debris. For this reason the amount of bedrock closure, if any, remains undetermined. Much of the closure is probably within unconsolidated deposits, because seismic refraction work just outside the southeastern margin of the glacier in the vicinity of Fotney Stream (Fig. 1) shows unconsolidated debris in excess of 500 feet thick (Allen and Smith, 1953, p. 759–760).

This does not necessarily mean that the basin has been created principally by deposition. The Malaspina Glacier might have gouged out a depression within unconsolidated deposits composing a flat foreland like that east of Yakutat Bay (Blackwelder, 1909, p. 461). During its latest major advance, 200 ± 50 years ago, the ice overrode hillocks of till 100–200 feet above sea level in its southeasternmost part (Sharp, 1958). This suggests basin erosion, but it is not a strong point, owing to the peripheral position of the hillocks.

### *Yakutat Foreland and Yakutat Bay*

East of Yakutat Bay is a low featureless coastal plain, the Yakutat foreland, extending in its widest part from the abrupt linear base of the mountains to the ocean 17 miles to the south. The corresponding area west of Yakutat Bay is occupied by Malaspina Glacier, and the shore lines of these two foreland segments form a straight-line continuation except for Yakutat Bay.

Judging from shallow exposures the Yakutat foreland is composed of unconsolidated Quaternary materials including till, outwash, fluvial, eolian, lagoonal, and shore-line accumulations (Blackwelder, 1909; Tarr and Butler, 1909, p. 97–99; Gilbert, 1910, p. 46; Tarr and Martin, 1914, p. 25–26). Much of this material has been supplied by glaciers from the mountains to the north, and the foreland was probably constructed at times when these glaciers were active and occupied advanced positions (Tarr and Butler, 1909, p. 29, 98–99; Tarr and Martin, 1914, p. 25; Plafker and Miller, 1957b, p. 7). Two of the largest of these ice bodies were the Malaspina and the glacier in Yakutat Bay. Yakutat Bay is both a planimetric embayment of the foreland and a basin within it (Fig. 4). It was probably formed in much the same manner as the basin under Malaspina Glacier, so a study of its characteristics should be helpful.

A crescent-shaped boulder-strewn rocky submarine ridge only 38–96 feet beneath the water surface at the mouth of Yakutat Bay has been interpreted as an end moraine (Tarr and Butler, 1909, p. 107; Tarr and Martin, 1914, p. 223). The east limb of this moraine extends northward along the east side of Yakutat Bay from Ocean Cape past Yakutat village. The corresponding west limb is shown passing under the Malaspina Glacier (Plafker and Miller, 1957b, map), and the hillocks of till now exposed by local deglaciation in the southeasternmost part of Malaspina Glacier (Sharp, 1958) are probably part of this morainal ridge. Inside the end moraine, the water of Yakutat Bay attains a maximum depth of more than 1000 feet near Point Latouche (Fig. 4), and topographic closure on the bay floor is 900 feet. The basin beneath Malaspina Glacier is probably at least as deep, for the seismic explorations most likely did not probe the lowest point. The impression that Yakutat Bay was created by the building up of the Yakutat foreland while the bay site was occupied by ice (Tarr and Martin, 1914, p. 26) arises partly from the extensive outwash plain east of the moraine along the east side of the bay. Similar relationships, but with the depression now occupied by a lake, have been described from glaciated parts of central United States (Leverett, 1929, p. 27; 1932, p. 73).

Before accepting the basin occupied by Yakutat Bay as solely the product of deposition, the possibility of glacial erosion should be considered. Yakutat Bay passes northward into Disenchantment Bay, a narrow bedrock fiord penetrating the mountains. The floor of this fiord, well within the mountains, is 700–900 feet below sea level. Either it has been deeply excavated, or considerable recent submergence has occurred. Lack of independent evidence for submergence of this magnitude favors glacial excavation. The possibility that Yakutat Bay, too, may have been subjected to erosion is supported by the 1000-foot depth a scant 3 miles beyond the mountain front.

The relationships in Yakutat Bay suggest

Nature of material between base of ice and rock is not known, but it may be till or other similar unconsolidated debris.

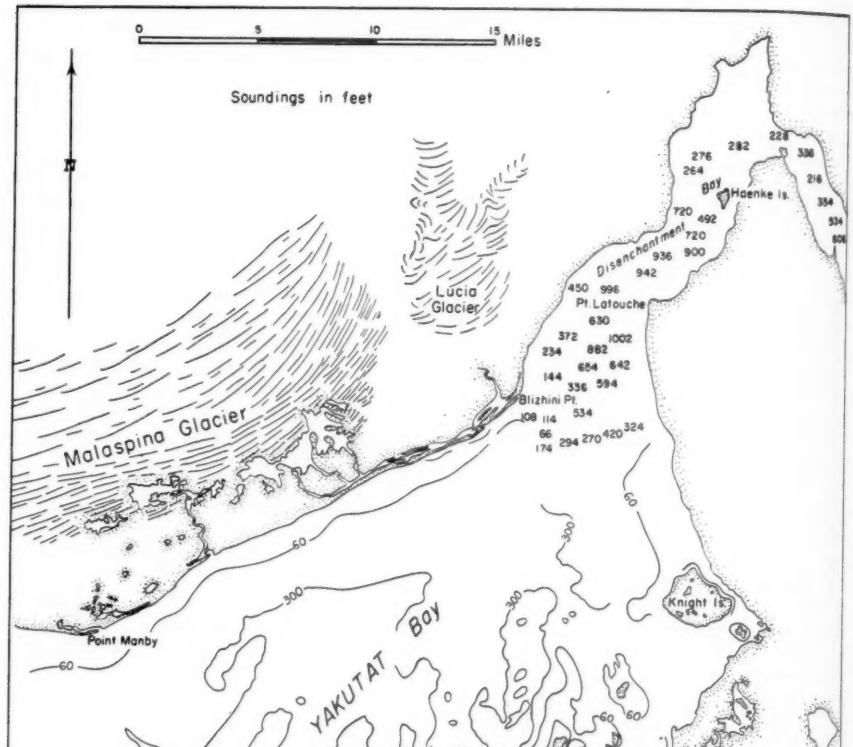


FIGURE 4.—MAP OF YAKUTAT BAY HYDROGRAPHIC RELATIONSHIPS

Water depth in feet, adapted from U. S. Hydrographic Office Chart and U. S. Geological Survey Yakutat, Alaska map (1:250,000).

that the Malaspina basin may be as much as 1000 feet deep and that much of the closure can be due to deposition, although some contribution from erosion is possible or even likely.

### *Offshore Relationships*

The continental shelf extends at least 50 miles beyond the present shore line in the vicinity of Malaspina Glacier. The depth of water over this shelf is about 600 feet (Fig. 5) except for a shallow valley extending eastward to a point off the mouth of Yakutat Bay. A wholly depositional origin for the Yakutat Bay and Malaspina basins, with depths of 900–1000 feet, would mean that the sea floor was originally at least this deep and that a layer of material 300–400 feet thick was spread across the 50-mile width of the present conti-

nental shelf. This seems unlikely and is one of the stronger arguments for some erosion in these basins.

*Origin of Malaspina Glacier Basin*

It is suggested that the basin beneath Malaspina Glacier, with a closure of 825–1000 feet below sea level, has been created about two-thirds by peripheral deposition and about one-third by erosion. In support of this, the following points are listed:

(1) The south face of the St. Elias Mountains is probably a fault scarp, and the initial depth of water offshore could have been sufficient for the basin to have been created for the most part by deposition.

(2) The Yakutat foreland has been built up at least in part of debris derived from glaciers at a time when they lay in advanced positions. Since areas occupied by glacier ice were the sites of relatively little deposition, they were left as depressions within the foreland when the ice receded.

(3) Surficially, the entire outer rim of the Malaspina basin consists of unconsolidated material, and seismic refractions indicate a thickness of unconsolidated debris in excess of 500 feet at the southeastern edge of the ice.

(4) No part of the Malaspina-basin closure is known to be in bedrock.

(5) The bedrock under the Malaspina Glacier is sedimentary, probably of the Yakataga and Kulthieth formations and the Yakutat Group (Plafker and Miller, 1957a). If the basin were wholly an erosional feature in these formations, considerable rock debris from them would be expected in the peripheral deposits. The debris on, in, and at the margin of the present Malaspina Glacier consists almost wholly of crystalline metamorphic and igneous rocks from the higher parts of the St. Elias Mountains. Therefore extensive erosion of the sedimentary formations named seems unlikely. This argument has less weight if the basin has been eroded out of foreland sediments, or if it has been created by erosion at an earlier stage of glaciation.

(6) The gradient on the sea floor in the first 10 miles off the Malaspina Glacier is 60 feet per mile. The remaining 40 miles of the continental shelf are relatively flat. If sea level were lowered 600 feet, and the Malaspina Glacier removed, one would see around the outer margin of its basin a broad embankment

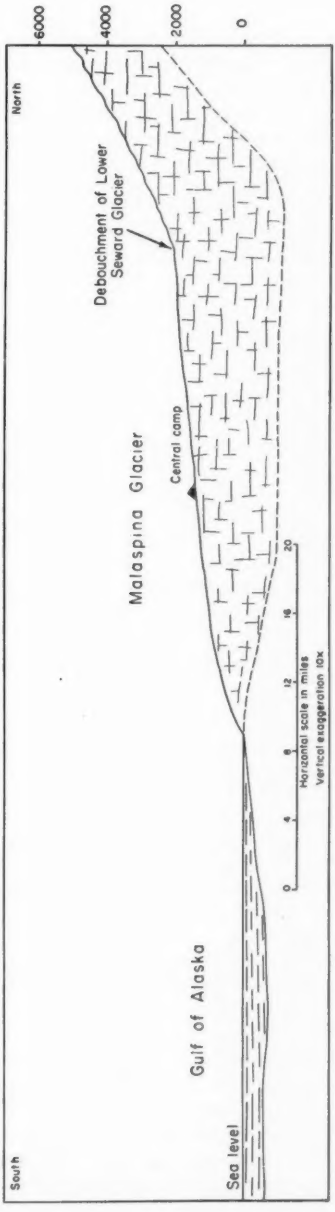


FIGURE 5.—DIAGRAMMATIC CROSS SECTION OF MALASPINA BASIN

rising 600–700 feet above the continental shelf (Fig. 5). The basin has at least 100 and possibly 400 feet additional closure. Unless the mantle of deposits laid down on the flat part of the continental shelf farther offshore is of similar thickness, which seems unlikely, 100–400 feet has been glacially excavated.

Neither the Malaspina basin nor Yakutat Bay need have been created solely by a single glacial advance. No evidence has been found, however, for an expansion of the Malaspina to a position much beyond the maximum of its last advance, 200 years ago. Patches of till a mile or so beyond the southeastern and southwestern margins of the glacier may have been laid down by glaciers occupying Yakutat and Icy bays (Plafker and Miller, 1957b, map). Glacial-marine deposits in the Gulf of Alaska are attributed to debris dropped from floating ice and do not require a great expansion of land-borne ice (Menard, 1953, p. 1282). Capps (1931, p. 4) is inclined to think that the glaciers along the south coast of Alaska pushed far out to sea, but the evidence is not strong, and Flint (1947, p. 223) gives reasons for doubt. In the Malaspina area there is no good firsthand evidence indicating that any of the glaciers pushed very far beyond the present shore line (Plafker and Miller, 1957b).

## Structural Features in Malaspina Glacier

### *Introductory Statement*

The larger geometric relationships and some of the major structures of the Malaspina are simple. Much of the ice, however, has traveled 50–60 miles along an irregular and in part narrowly confined course before spreading into an unconfined piedmont sheet, so it is not suprising that the structural details are complex. Structural observations were made principally along the geophysical profile through the central camp and along the route between central camp and Delta Lake. Supplementary information was obtained from numerous air flights over the glacier and from vertical air photographs. Much of the information available from air photos is presented on the recent map of Plafker and Miller (1957b). Attention is given to crevasses and associated joints, foliation, crystal orientation, and complexly folded ice streams and morainal septa. Radial crevasses, joints, foliation, and folds are probably related products of a single stress system.

### *Crevasses and Joints*

The crevasses of Malaspina Glacier are principally of two sets, radial and transverse, with respect to the inferred direction of flow. All are essentially vertical, none is especially deep (60–70 feet), overly wide (1–10 feet), nor particularly long (most are a few hundred yards).

Radial crevasses are widely distributed and generally consistent in trend, size, and arrangement. They are more numerous and wider over swells and steep reaches. They trend approximately normal to the lobate border of the ice sheet and converge toward the mouth of Seward Glacier. They strike essentially perpendicular to the trace of the axial planes of folds (Pl. 2, fig. 2) and to the foliation (Fig. 6). Radial crevasses have a strong échelon habit, and the narrowing of one crevasse is usually accompanied by the widening of one or more of its neighbors. The orientation and arrangement of radial crevasses suggest that they are related to the spreading out of the ice onto the coastal foreland.

Transverse crevasses are localized to swells and steep reaches of the ice surface which presumably reflect irregularities in the subglacial floor. They usually intersect the radial set at a high angle. An impulse of renewed activity, first observed in the summer of 1954, created many new, sharp-edged, smooth-walled transverse crevasses, especially over swells on the ice surface.

At many localities two sets of tight joints were observed. They strike at about 90° to each other, with vertical to steep northward dip. In places, the radial crevasses bisect the angle between the joint sets, but elsewhere the bisectrix is rotated as much as 40° clockwise from the radial crevasses. The geometric relationships of joints, radial crevasses, and foliation at a number of localities are shown in Figure 6. These joints look like shear planes, and small lateral offsets have been observed along some. They are not always equally developed, and in places only one set was observed. If the radial crevasses are the product of transverse spreading, and the strike of the foliation is at right angles to a compression, then it follows that the joints are probably shear planes related to a near-surface stress pattern in which the intermediate stress axis is perpendicular to the glacier surface. Clockwise rotation of

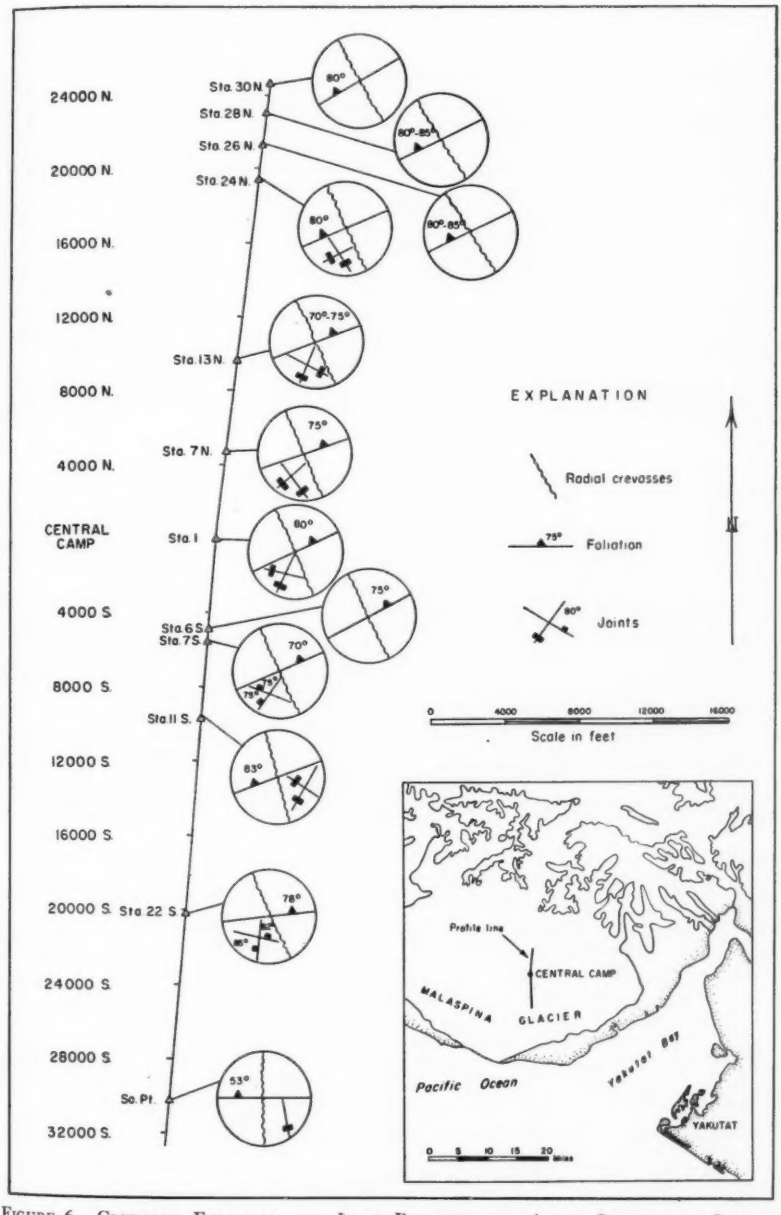


FIGURE 6.—CREVASSE, FOLIATION, AND JOINT RELATIONSHIPS ALONG GEOPHYSICAL PROFILE

the joints with respect to the radial crevasses is puzzling. Possibly one of these structures formed earlier than the other, and the apparent rotation is due to a local change of stress orientation as the ice moved forward.

### *Foliation*

In spite of considerable study during the past century, the origin of foliation in glacier ice is not yet well understood. The mechanism by which alternate layers of whitish and bluish ice are formed, the place and depth at which this structure originates, its relationship to the stress system, and its significance with respect to mode and mechanism of glacier flow remain unsettled. Data on foliation obtained from the Malaspina may contribute to an eventual solution of these problems. Glacier foliation is generally regarded as the product of shearing along discrete planes, accompanied by or followed by recrystallization (Perutz and Seligman, 1939, p. 355–357; Drygalski and Machatschek, 1942, p. 123–129).

The trace of foliation planes on the surface of Malaspina Glacier is conformable with the bulbous outline of the lobe. In the central camp area, for at least 5 miles to the north, and for a mile or two to the south, the dip is 75°–85° north. Along a line from the central camp to Delta Lake it decreases gradually to about 45° near the edge. The lower dip in the marginal zone is consistent with observations of foliation in other glaciers and with inferences concerning its general attitude, but the steep dips of 75°–85° near and northward from the central camp are puzzling.

Foliation with steep dips in some cirque and valley glaciers is attributed to rotation (Lewis, 1956, p. 696) or remains unexplained (Untersteiner, 1954, p. 234–235). Sufficient rotation in the right direction to give steep dips seems out of the question for the Malaspina Glacier. The maintenance of surface profile and elevation in the ablation area requires surfaceward movement of ice. Some investigators think foliation is due to shearing related to such surfaceward movement. If foliation is produced by shearing, it should be expected to have a classical relationship to the axes of principal stress. The foliation plane should strike parallel to the intermediate stress, and make an angle of roughly 45° with the greatest compressive stress. The attitude of foliation planes near the center of Malaspina Glacier requires that the greatest compressive stress be directed toward the surface at an angle of 30°–40°. Since the principal stresses cannot have this orientation at the surface, the foliation would have to form at depth within the glacier. This is possible, but the steep inclination required for the greatest compressive stress makes one look for other relationships or explanations.

The radial crevasses indicate extension in the surface ice in a direction parallel to the strike of the foliation. A similar extension must occur at depth in the glacier, but it is produced by some other mechanism, for the crevasses are scarcely 100 feet deep. Extension at depth may occur by a sort of plastic yielding or flow involving slippage along a series of closely spaced parallel planes which now appear on the surface as foliation. Their strike would be essentially at right angles to the direction of maximum compression, and the original nearly vertical, dip could have been reduced to 75°–85° by rotation during flow as would be expected from the known vertical velocity distribution (Fig. 13). The gentler dips near the glacier's margin may indicate still more rotation and the increasing influence of drag on the subglacial floor.

### *Crystal Size*

The size of crystals in stagnant ice near the edge of Malaspina Glacier has been investigated in considerable detail by Bader (1951, p. 523–526), who demonstrated that the inter-

PLATE 1.—MARGINAL ZONES OF MALASPINA GLACIER

FIGURE 1.—Stagnant ice near Malaspina margin. Ablation debris on surface supports dense growth of alders, 1949.

FIGURE 2.—Coarse ablation debris on stagnant marginal ice of Malaspina Glacier, 1948.

FIGURE 3.—Slip displacement of moraines at fold apexes, east edge of Seward Glacier lobe of the Malaspina, 1951, air photo.

PLATE 2.—DEFORMED MORAINES AND ICE STREAMS IN MALASPINA GLACIER

FIGURE 1.—Structures in west part of Malaspina lobe supplied by Seward Glacier. Agassiz Glacier and Mount St. Elias in background. Air photo by U. S. Coast Guard, 1953.

FIGURE 2.—Structures near east margin of lobe of Malaspina Glacier fed by Seward Glacier, which debouches from upper left. Radial crevasses about perpendicular to traces of axial planes of folds. Air photo by U. S. Coast Guard, 1953.

FIGURE 1

FIGURE 2

FIGURE 3

MARGINAL ZONES OF MALASPINA GLACIER

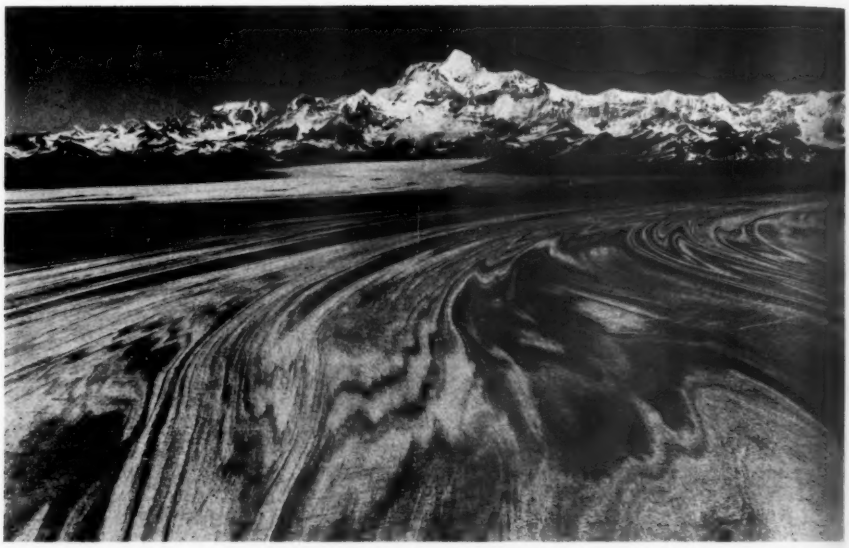

FIGURE 1

FIGURE 2
DEFORMED MORAINES AND ICE STREAMS IN MALASPINA GLACIER

FIGURE 1

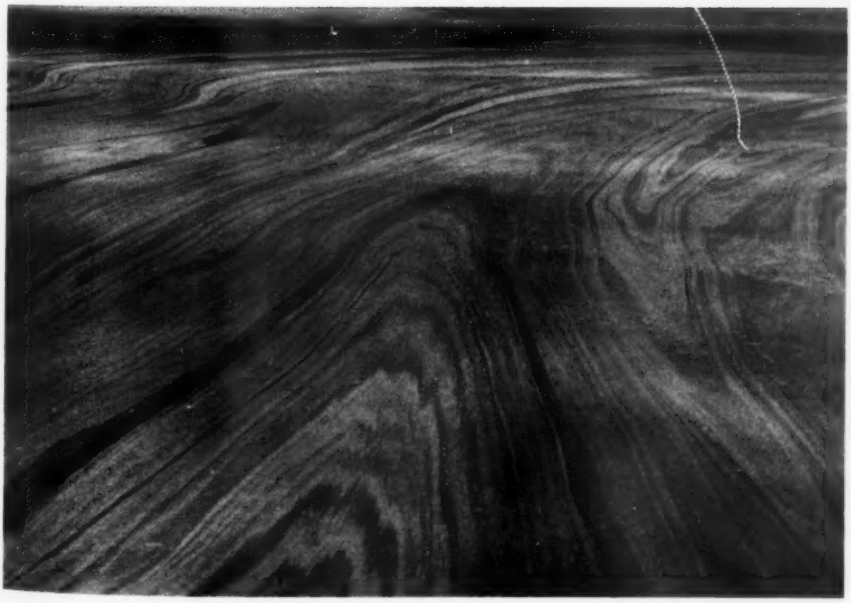

FIGURE 2

STRUCTURES IN CENTRAL MALASPINA GLACIER

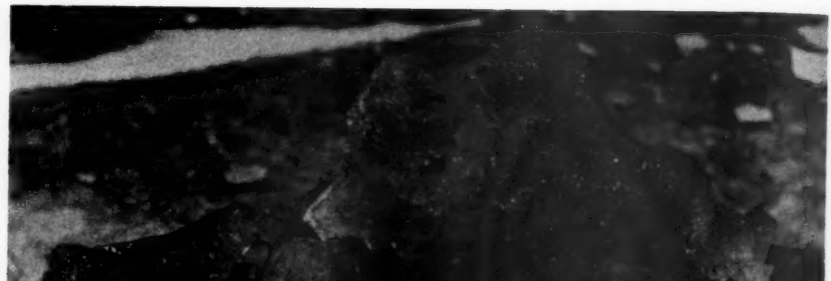

FIGURE 1

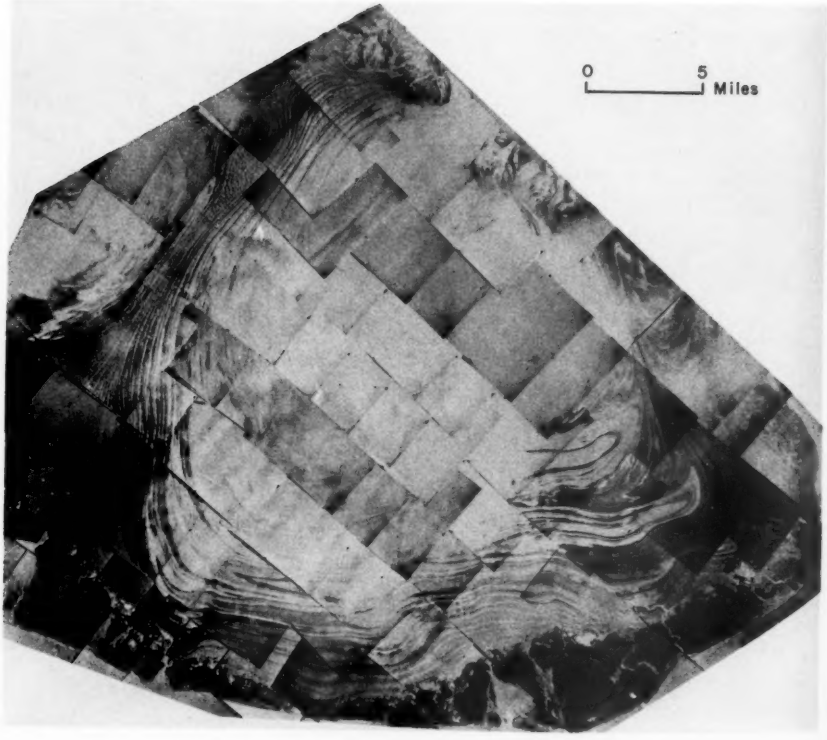


FIGURE 2

MALASPINA ICE CRYSTALS AND PHOTO MOSAIC

crystalline relationships are complex and that individual crystals may attain a length of several feet. Crystal size increases gradually from an estimated mean of about 2½ inches at the central camp to about 6 inches at the glacier's margin (Pl. 4, fig. 1). The increase is not regular, and marked variations were noted between individual streams. For example, about 4 miles from the southeast margin is a band of clean ice composed almost entirely of crystals 6–9 inches in diameter. Something in the constitution or past history of this particular ice endowed it with an ability to develop uniformly large crystals. Since the crystals are larger than in the neighboring ice streams, the difference must be related to some aspect of the environment back in the mountains, although the large crystals probably developed after the ice became part of the Malaspina. This stream cannot be traced to its source, so the conditions favoring development of large crystals remain undetermined.

### *Crystal Fabrics*

Orientation of crystals has been investigated near the margin of Malaspina Glacier (Bader, 1951, p. 526–535) and more extensively near the central camp by Rigsby, who will make an independent report. Malaspina ice shows relatively strong fabric patterns (Fig. 10) similar to, but not as strong as, those previously recorded from the Emmons Glacier (Rigsby, 1951, p. 594–597). They are stronger than the patterns of the upper Saskatchewan Glacier and about comparable to the best in the lower part of the Saskatchewan (Meier, Rigsby, and Sharp, 1954, p. 21–24). On the Malaspina the pole to the foliation plane lies off the center of the pattern defined by the maxima. The patterns show no consistent relationship to any megascopic structure in the ice, so that they may be the product of near-surface recrystallization and, therefore, need bear only a second-order relationship to flow deeper within the glacier.

### *Folded Structures Within Malaspina Glacier*

*Introduction.*—In a dry year, when the snow cover on Malaspina Glacier has been removed by ablation, an extensive system of complex folds is visible (Pls. 1–4). Although these structures look like plunging anticlines and synclines truncated by erosion, they are not properly described as such, because they involve individual ice streams and intervening morainal septa lying side by side. The contact surfaces between ice streams and moraines were steeply inclined before deformation, and there is no systematic age relationship among them as in a sequence of sedimentary layers.

Early explorers observed the Malaspina folds from high points in the mountains to the north, and Tarr and Martin (1914, p. 204) noted that "a determining of their nature would be a matter of great interest." Washburn (1935, p. 1881–1882) photographed the folds from the air and attributed them to spasmodic variations in volume of the many tributary ice streams in the Seward-Malaspina system. The interpretation arrived at herein is that they are not inherited from higher in the system but developed within the Malaspina as it spread out on the flat coastal foreland. Attention is confined to that part of the Malaspina fed by Seward Glacier.

*Constitution of lower Seward Glacier.*—Before dealing with the Malaspina folds, it is necessary to consider the constitution of lower Seward Glacier at the point of debouchment. Upper Seward Glacier gathers most of its substance in a large intermontane basin in the heart of the St. Elias Range. The slopes and canyons surrounding this basin and discharging into it provide a basal layer (Fig. 7, *A*) upon which the snow layers that accumulate in the basin are laid (Fig. 7, *B*).

PLATE 3.—STRUCTURES IN CENTRAL MALASPINA GLACIER

FIGURE 1.—Folds in southeast central part of Malaspina Glacier viewed west-southwest. Dark bands are medial moraines, 1951, air photo.

FIGURE 2.—Folds a little south of central part of Malaspina Glacier, viewed westward. Darker bands are, for the most part, fine surface silt of Part *B* (Fig. 8), 1951, air photo.

PLATE 4.—MALASPINA ICE CRYSTALS AND PHOTO MOSAIC

FIGURE 1.—Ice crystals separated by melting near outer edge of Malaspina Glacier.

FIGURE 2.—Composite air-photo mosaic of Malaspina Glacier, 1948. Considerable snow on glacier. U. S. Navy photos.

The basal layer consists of many individual ice streams separated by medial moraines, and, judging from the area of accumulation, it composes about one-third by volume of the upper Seward Glacier. The sedimentary accumulation of the basin is faintly stratified and includes some thin septa of dirty ice containing debris derived from the flanks of nunataks. At the outlet of upper Seward Glacier total ice thickness is estimated at 3000–4000 feet, from seismic and gravity data farther back in the basin. Although the flow is funneled into a channel 3.5–4 miles wide at this point, the thickness probably does not increase much, since the discharge is accommodated by increased velocity generated by a marked steepening of gradient.

As the ice descends through lower Seward Glacier it undergoes much flow metamorphism, the ice streams of part *A* are probably greatly compressed, and the medial moraines between them become nearly vertical. The sedimentary layering of part *B* is masked and perhaps destroyed by recrystallization and by the formation of secondary foliation. During this descent the ice is still above the firn limit, and it receives an additional coating of sedimentary snow and firn (Fig. 7, *C*). In addition, ice streams from canyons tributary to lower Seward Glacier make up a fourth part of the the Seward Glacier (Fig. 7, *D*). The medial moraines associated with these ice streams are the first to be uncovered by ablation and are the only ones visible on lower Seward Glacier. The four units, *A*-*D* (Fig. 7), compose distinct parts of the Malaspina in about the relationships sketched in Figure 8.

The medial moraines of *A* and *D* constitute the prominent debris bands in the peripheral zone of the Malaspina (Pl. 3, fig. 1). Some of these morainal septa may exist in an inset position (Sharp, 1948) rather than extending to the base of the glacier, but any such relationship is obscured by the complexity of deformation. Most glaciers consist primarily of *A*, *C*, and *D* in the above scheme. The Malaspina is unusual in the large size of *B*, which originates in the huge intermontane basin of upper Seward Glacier.

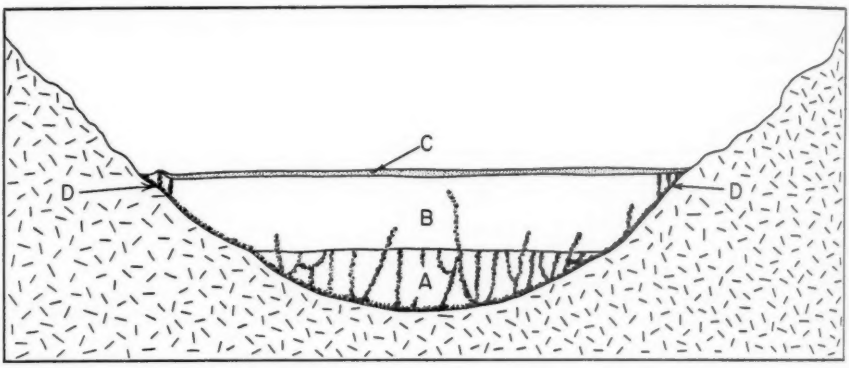


FIGURE 7.—CONSTITUTION OF LOWER SEWARD GLACIER

*A*—Ice streams and moraines tributary to upper Seward basin; *B*—ice formed by direct accumulation in upper Seward basin; *C*—sedimentary ice and firn accumulated directly upon lower Seward Glacier; *D*—ice streams and moraines tributary to lower Seward Glacier.

*Debris bands on Malaspina Glacier.*—The Malaspina folds are most clearly outlined by two types of debris bands. The more prominent bands are medial moraines that consist of surficial accumulations of coarse angular rock debris marking the debris-rich ice septa between individual ice streams. The lithologic constitution of most moraines is distinctive, so they can be followed through the folds by an observer on foot; some are so distinctive that they can be traced even on air photographs.

Moraines in the southern peripheral zone of the Malaspina are composed of crystalline rocks derived from far back in the St. Elias Mountains. Some consist largely of quartz diorite, and others are composed predominantly of one or more metamorphic rocks, some so distinctive that they can be used to identify individual moraines. Although lithologic mixtures are found, these debris bands are too

distinctively individual to represent debris sheared into the ice from a heterogeneous layer of ground moraine; they are truly medial moraines. Some of the outermost moraines on the northeast and northwest flanks should be composed of material derived from the Yakataga Formation and the Yakutat Group which are exposed in the foothills to the north. This has been confirmed by firsthand observation only at the northwest corner of the glacier (C. R. Allen, Personal communication.)

Because of burial by layer *B* (Figs. 7 and 8), the medial moraines have been exposed by ablation only in a peripheral zone of the ice sheet 5–6 miles wide. In time, owing to insulation by debris, ice ridges up to 300 feet high develop along the traces of these outermost moraines. With continued ablation the amount of rock material on the surface increases and spreads laterally, giving a debris band far wider than the underlying debris-rich ice septa. Eventually, adjacent morainal debris bands merge, obscuring the ice stream between them. This occurs within the outermost 3 or 4 miles of the glacier (Pl. 1, fig. 2), and here the folded structures are not so easily discerned.

A second type of dirty band outlining folds is less prominent and wholly surficial. It is best seen in the central part of the glacier (Fig. 8, *B*), where coarse debris is lacking. This type of band consists of accumulations of dark silt in little holes and depressions on the surface of the ice. The silt is mostly fine debris incorporated in snow of the accumulation area and released by subsequent melting of the ice, but it may include some material blown onto the surface of Malaspina Glacier from surrounding soil and rock areas. The ice under silt-covered areas contains no more of this debris than ice under clean areas. Since most of the silt-bearing depressions are breached air bubbles, bands of bubble-rich ice are discolored by silt washed off the smooth surface of bubble-free ice and trapped on the rough surface of bubble-rich ice. This type of debris band is not readily recognized unless previously identified from the air (Pl. 3, fig. 2). The considerable width of these bands precludes the possibility that they represent the traces of original dirty strata inherited from the layers of the accumulation area.

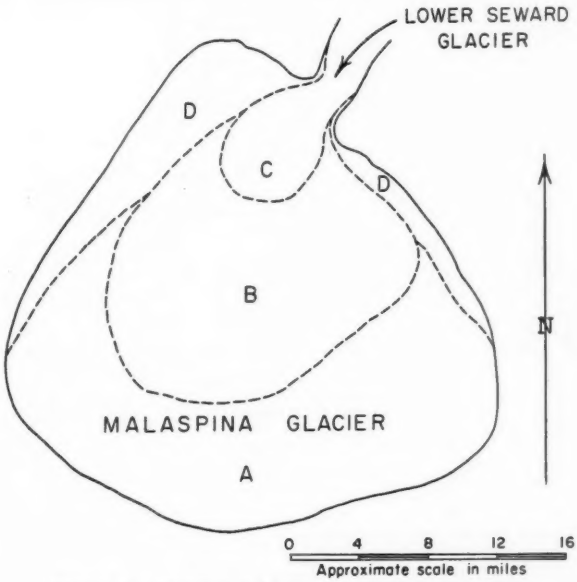


FIGURE 8.—COMPONENT PARTS OF MALASPINA GLACIER

*A*, *B*, *C*, and *D* represent units which correspond to those of lower Seward Glacier (shown in Figure 7).

*Description of folds.*—The terminology of wave forms is more suitable for describing these Malaspina structures than the termin-

ology ordinarily used for geological folds. The wave length of the structures ranges up to 3 miles, and the double amplitude attains a maximum of 20 miles. The peaks of the waves range from rounded to sharp, and many are rendered jagged by superimposed small waves and offsets by shearing (Pl. 1, fig. 3). The structures as exposed on the surface appear to be predominantly tight, isoclinal, and symmetrical (Fig. 9). Traces of the axial planes are bowed or bent into conformity with the bulbous outline of the ice lobe, and they are conformable with the foliation in strike (Fig. 10). Large neighboring folds are essentially harmonious, although minor plications within them are not (Fig. 9).

Individual morainal bands can be traced through the folded structures as they appear on air photos only to a limited degree, owing to structural complexity, lack of strong distinguishing characteristics of the moraines, and an obscuring snow cover. Some moraines have been traced through as many as 15 separate waves, and one moraine would have a length of 115 miles if unfolded. The moraines do not join across the central part of the glacier, those on the east side being different from those on the west. This is consistent with the deduced constitution of the Malaspina Glacier.

In tightly folded sections, the individual ice streams appear to be greatly thinned. In part, this is a mistaken impression created by lateral spreading of debris from medial moraines. However, some bands of ice now only one or two hundred feet across must represent valley glaciers originally many

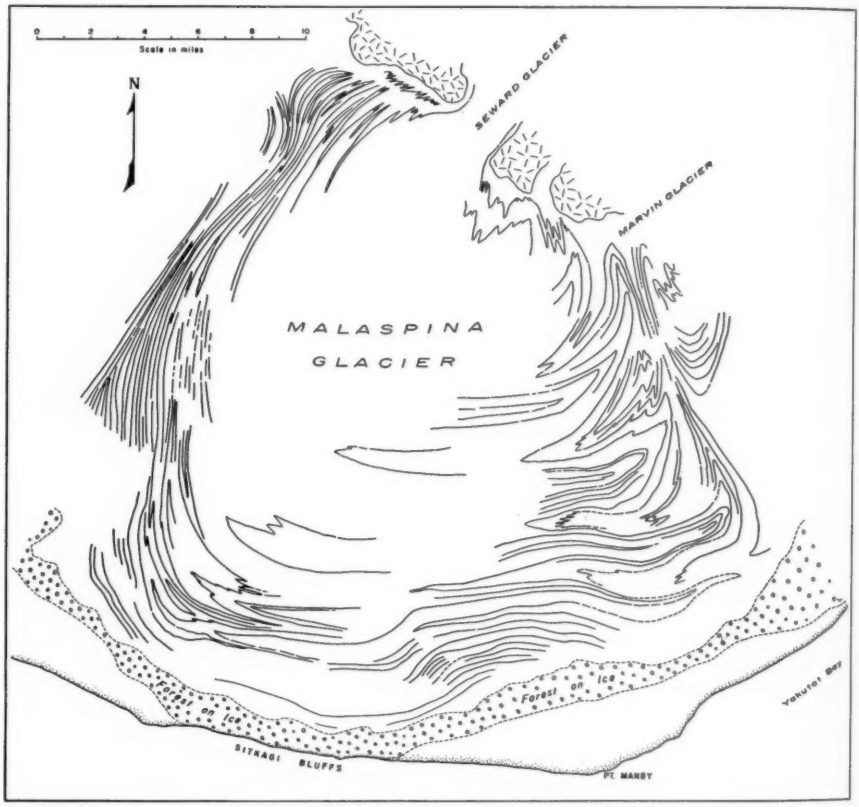


FIGURE 9.—DIAGRAM OF MALASPINA FOLDS
As worked out from composite air-photo mosaic (Pl. 4, fig. 2).

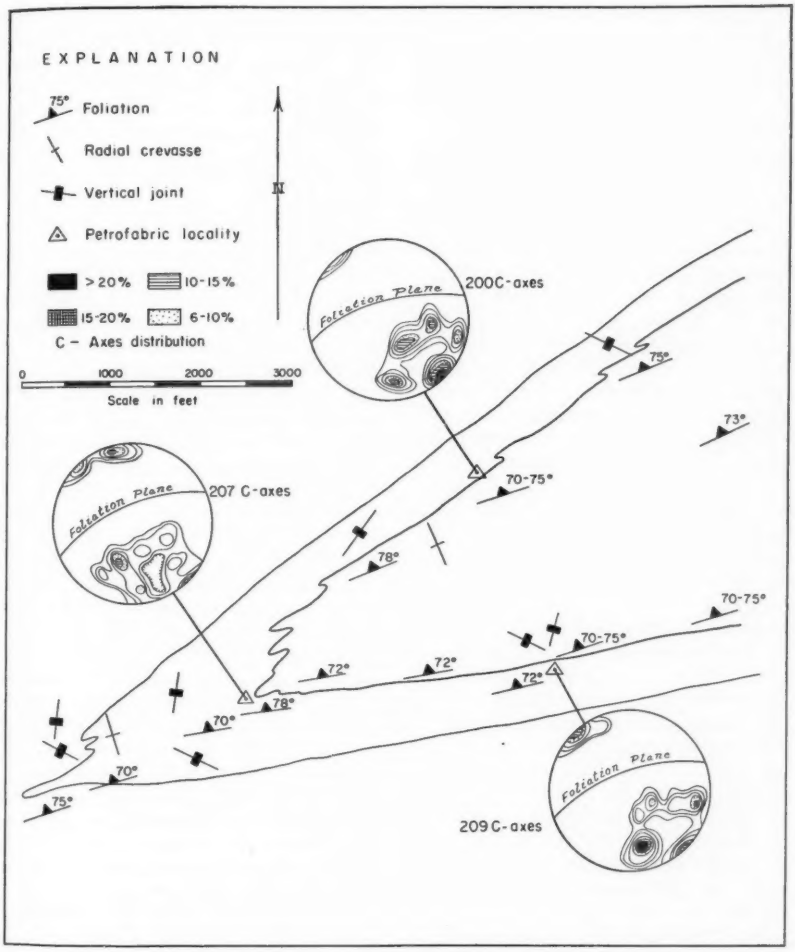


FIGURE 10.—STRUCTURAL MAP OF A MALASPINA FOLD

Location is just northwest of the central camp. Fabric diagrams by G. P. Rigsby, structural mapping by D. R. Baker.

times wider. Some thinning probably resulted from squeezing within the lower Seward Glacier, but much of it occurs within the Malaspina.

*Origin of the folded structures.*—Evidence suggests that the Malaspina folds are the product of deformation within this ice sheet as it spreads out on the coastal foreland and are not inherited from higher in the system. This interpretation is best supported by the behavior of medial moraines visible on the surface on both sides of lower Seward Glacier just above the point of debouchment into the Malaspina. These moraines are undeformed in the Seward Glacier and extend a mile or two into the Malaspina before becoming involved in the typical fold patterns. They lie in that part of the Malaspina supplied by tributaries of lower Seward Glacier (Fig. 7, *D*), but their folds conform with structures in ice supplied by other components of the Seward system. Although some of the moraines within *A* (Fig. 8) of the Malaspina may have been somewhat deformed before reaching

that glacier, the general conformity of structures involving these moraines with the structures in *B* and *D* (Fig. 8) and with the general outlines of the ice lobe indicates that most of the deformation occurred within the Malaspina.

Malaspina Glacier lies in a broad basin extending to at least 825 feet below sea level; judging from the depth of water in the Disenchantment Bay fiord, the floor of Malaspina basin may be well below sea level at the point of debouchment of lower Seward Glacier. This means that the ice not only spreads out radially but also moves uphill for much, if not all, of the 28 miles from the point of debouchment to the outer margin. The ability of a glacier to flow over a flat surface or up an opposing slope is dependent primarily upon the slope of the ice surface (Nye, 1952b, p. 91–92). To flow across such a terrain a glacier must not only possess a sufficient surface slope, but it must also maintain a thickness great enough to handle the discharge. Malaspina Glacier is faced with the conflicting tasks of spreading out, which tends to produce thinness, and of developing or maintaining sufficient surface slope and thickness to flow uphill. Two mechanisms could fulfill this dual task. The first involves surfaceward movement of ice along numerous slip surfaces, and the second involves folding of the ice streams in accordion fashion about steeply inclined axes.

As the ice spread out into a lobe on the coastal foreland it could have maintained or even increased its surface slope and thickness by surfaceward displacement along concentrically arranged inward-dipping slip planes, and the foliation now visible in the ice might be regarded as the product of such displacements. However, dip-slip displacements on such planes would produce little offset of the steep contacts between ice streams and morainal septa. Oblique- or strike-slip displacements would be more effective and more consistent with the lateral spreading of the ice. Some folds require at least 6 miles total offset of contacts by slippage distributed over a width of about a quarter of a mile. The spacing of foliation planes in the ice is irregular, but about 1 per inch is a generous estimate. A strike-slip displacement of 2 inches on each foliation plane would be required to produce a 6-mile offset; this seems reasonable. Field observations and photographs (Pl. 1, fig. 3) indicate some displacement of debris bands by distributed slippage along planes conformable in strike at least with the foliation. Although the Malaspina folds may have been produced entirely by this mechanism, it is just as likely that they were formed mostly by flowage with only minor modification through slippage. Evidence is not sufficient to permit a choice between these alternatives. The more puzzling problem is the cause for and the stresses related to the genesis of the individual folds, whether formed by flowage or slippage.

The ice folded up in accordion fashion as it moved across the foreland. This was probably due to a combination of resistance to outward flow offered by the uphill slope of the glacier floor and by the push from behind provided by the outpouring of ice from lower Seward Glacier. Individual folds formed in zones where the yielding to one side from a radial flow line was especially easy or was favored by some earlier minor flexing. This lateral yielding was part of the process of spreading out into a sheet. The folds became larger, more complex, and tighter as the process continued (Fig. 11). The trace of the axial planes came to lie normal to the direction of flow and conformably with the outlines of the ice lobe. The increased tightness of folding and the elongation parallel to axial planes caused thinning of the individual ice streams. No single morainal septa should extend around the entire periphery of the present ice lobe, and indeed the moraines on opposite sides of the lobe cannot be traced continuously from one side to the other.

All of the above may be correct, but they do not account for the formation of the individual folds. The evidence is good that they were formed within the Malaspina, and although they may be related to variations of or irregularities in the movement of that body, it is not clear just what these were.

## Resurgent Activity Within Malaspina Glacier

The broad marginal zone of stagnant ice in the Malaspina Glacier indicates waning activity, which is consistent with the known negative regimen. Therefore, the unmistakable signs of renewed activity extending well out toward the borders of this glacier, as first observed in the summer of 1954, came as a considerable surprise. The resurgence may have been underway prior to 1954 in parts of the glacier closer to the mountains, and it was continuing in 1955 (C. R. Allen, Per-

sonal communication). J. H. Hartshorn (Personal communication) observed renewed activity in formerly stagnant ice close to the south edge of the Malaspina in the summer of 1956.

The following evidence of resurgent activity was noted in 1954:

(1) A marked increase in the number and the size of crevasses between August 1953 and August 1954 made areas of ice between Delta Lake and central camp, which had been traversed easily on foot, impassable. Old crevasses were much larger than at any time since 1948. New transverse crevasses with smooth vertical walls and sharp unmelted edges formed. Changes in crevasses occurred in many places over the glacier's surface, but they were particularly marked on the crests of swells.

(2) The topographic relief on the glacier's surface as expressed by swales and swells seemed greater in 1954 than in 1953. This is a subjective impression unconfirmed by actual measurements.

(3) Noises from the cracking of ice and the falling of blocks in crevasses were common in the summer of 1954, whereas in earlier years most of the noises from the glacier were made by water pouring into moulins or crevasses.

(4) Breaking of the pipe at a depth of 300 feet in the borehole at the central camp between the summers of 1953 and 1954 was probably caused by this renewed activity.

Since these surface manifestations of the resurgence developed at many widely separated places on the glacier in the relatively short time of 12 months, a surge must have been moving rapidly through this glacier. Surges observed in valley glaciers (Finsterwalder, 1937, p. 99; Perutz, 1947, p. 49; Klebelsberg, 1948, p. 87–88; Deeley and Parr, 1914, p. 165–166; Hess, 1933, p. 94–95; Harrison, 1951, p. 10–11; 1956, p. 675–676) travel with speeds of 700–10,000 feet per year. They can be caused by a sudden increase in accumulation arising from favorable meteorological conditions or from abnormal events, such as earthquakes, which shake snow off of surrounding slopes (Tarr, 1907, p. 282; Tarr and Martin, 1914, p. 168–172, 185). Budget year 1948/49 is known to have been exceptionally favorable for the Seward-Malaspina system. However, the average velocity of surges arising from the 1899 Yakutat Bay earthquake in valley glaciers of this area was about 1.75 miles per year (Tarr and Martin, 1914, p. 172). At this velocity a minimum of 10–20 years would be required to transmit an impulse from the upper Seward basin to Malaspina Glacier. Thus, the resurgence in 1954 probably had its origin some time prior to 1948/49, perhaps during a more extended period of heavy accumulation related to abnormally high precipitation suggested by Yakutat records for the interval from 1937 to 1943.

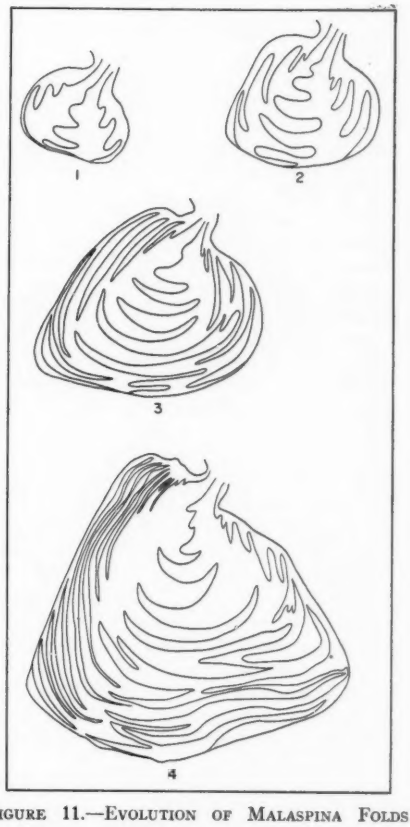


FIGURE 11.—EVOLUTION OF MALASPINA FOLDS

Wholly diagrammatic and shown with only three medial moraines for simplicity's sake.

That part of the Malaspina fed by Marvine Glacier was reactivated in 1906 by a surge attributed to the Yakutat Bay earthquake of 1899 (Tarr and Butler, 1909, p. 83–88; Tarr and Martin, 1914, p. 54–56). Consideration was given to the possibility that the 1954 reactivation in the Seward-fed part of the Malaspina was of the same origin. However, the velocity of transmission of the 1954 surge through the Malaspina, although not accurately known, was probably in excess of 5

miles per year, which is much too high for it to have started in the upper reaches of the Seward-Glacier as far back as 1899.

## Relationship of Velocity to Depth

### *Introduction*

Magnitude and variations of surface velocities on glaciers have been measured in many places, but data on velocity distribution in depth are sparse. The concept of extrusion flow (Streiff-Becker, 1938, p. 10–11; Demorest, 1942, p. 31–38; 1943, p. 365–373) stimulated interest in subsurface velocities, for they are pertinent to an evaluation of this concept. In response to this need, Perutz (1949) and his associates bored a vertical hole through the Jungfraufirn in the Swiss Alps and measured the year-to-year deformation of a steel pipe therein. This well-conceived and successfully executed experiment yielded a vertical velocity profile with a decreasing velocity in depth which is not consistent with extrusion flow (Gerrard, Perutz, and Roch, 1952, p. 552). Since it is not clear that the geometrical relationships of the Jungfraufirn require extrusion flow, similar experiments in different settings are desirable. Several have been initiated; those in North America are on the Juneau Ice Field (M. M. Miller, 1953, p. 50) and the Malaspina Glacier in Alaska, on the Saskatchewan (Meier, Rigsby, and Sharp, 1954, p. 12–13) and Salmon glaciers in Canada (Mathews, 1957) and on the Blue Glacier in Washington. The Juneau Ice Field and the Saskatchewan Glacier holes are shallow and will yield information only on near-surface flow.

Malaspina Glacier affords a nearly ideal subject for a field test of the extrusion-flow hypothesis. It is a sheet of ice with gentle surface slope which lies in a basin. Over most and possibly all of the distance outward from the mountains it moves uphill over its subglacial floor.

### *Setting*

The site selected for a borehole was on clean ice at the central camp (Fig. 1), where the surface is without marked topographic configuration and is relatively free of crevasses. A 10-mile transit-stadia profile on a north-south line through the site shows a surface slope of 34.8 feet per mile in the immediate vicinity of the hole and a southward slope for the entire 10 miles of 60.5 feet per mile.

Seismic reflections (Allen and Smith, 1953, p. 755–758) indicate an ice thickness of 1995 feet at the borehole site. The altitude here is approximately 1370 feet, so the floor of the glacier is 625 feet below sea level. Geophysical data show that the glacier floor slopes northward 380 feet per mile just south of the borehole and an average of 70 feet per mile northward over the 10.5 miles between the south margin of the glacier and the borehole. Direction of flow at the site as judged from foliation and radial crevasses is about S.25° E., but the location is too far from any fixed points to permit measurement of magnitude or direction of surface movement over a time interval of only a few years. Consequently, the data reported here pertain to a floating system.

### *Procedure and Equipment*

Earlier experience on upper Seward Glacier and the success of similar efforts in other areas (Nizery, 1951; M. M. Miller, 1952) suggested that the best hope for making a deep hole in the Malaspina with a minimum of expense and equipment was by means of an electrical hotpoint. The task was simplified by the temperate condition of the ice (Ahlmann, 1948, p. 66), which eliminated the problem of drill-stem freezing during the operation.

Hotpoints of the design and specification shown in Figure 12 were made in the Electrical and Mechanical Shop of the California Institute of Technology. They have an outer diameter of 1.75 inches and produce approximately a 2-inch hole. The drill stem was aluminum pipe of 1.38 inches inner diameter and 1.65 inches outer diameter in 10-foot sections joined by aluminum couplings. A well-insulated heavy (number 8) copper cable was strung through the pipe, and the pipe itself was used to complete the circuit. Energy was supplied by a small gas-engine generator producing 220 volts at 2500 watts. This system was operated at about 7 amperes, controlled by a variable resistance.

Boring rates ranged from 19.3 feet to 6.4 feet per hour, with an average of 11.3 feet per hour, omitting occasions when no penetration was obtained. This happened several times, even though all the equipment seemed to be working satisfactorily. On such occasions the operation was shut down for 12–24 hours, following which further penetration was obtained. Boring was carried on at intervals over a 9-day period to a depth slightly greater than 1000 feet. Here penetration suddenly ceased with a

sharp drop in amperage attributed to a short circuit caused by water leaking into the hotpoint.

Aluminum pipe was used for the drill stem because the magnetic needle in the inclinometer used to survey the hole would not function properly in a steel pipe. Owing to shortages caused by the Korean conflict, only 1000 feet of aluminum pipe could be obtained, and all of it had been put into the hole when the hotpoint failed. Although an additional 500 feet of steel pipe was on hand, it was decided not to risk losing the hole by pulling the pipe in order to install a new hotpoint.

The electrical cable had to be withdrawn from inside the pipe to allow passage of the inclinometer. Provision for this had been made by attaching the cable to the hotpoint with a push-pull plug. The strenuous efforts of four men pulling on the cable failed to free it; an improvised winch finally separated a splice in the cable at a depth of 500 feet. Thus, the pipe had to be removed from the borehole to clear the remaining cable. This was easily done, as the aluminum pipe was almost afloat. In the process, it was discovered that joints in the pipe at depths in excess of 300 feet were not waterproof under the pressure of water in the hole outside the pipe. Consequently, water leaking into the pipe had frozen under the lower (1 atmosphere) inside pressure. At depths of 650–700 feet, ice filled the pipe, firmly binding the cable. After removing this ice, the pipe was reinserted in the hole and filled with saline water to prevent further inside freezing which would have blocked passage of the inclinometer. After the inclinometer surveys were completed, the top 60 feet were filled with antifreeze to guard against freezing during winter. Initially, some fear had been felt that the pipe might be seized by flowage or by slippage along a shear plane before boring was completed. This did not occur, and the pipe was still free in the hole 13 days after the boring was started.

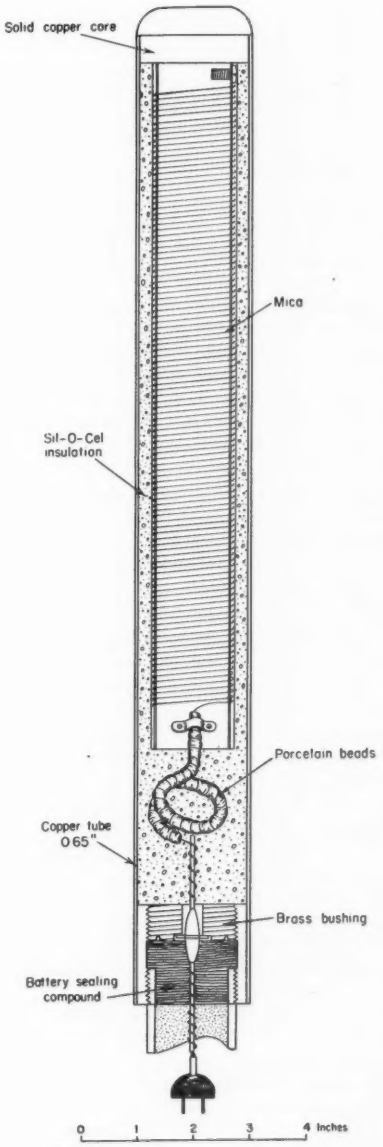


FIGURE 12.—DESIGN OF HOTPOINT

### *Surveys of Pipe*

*Introduction.*—A small-diameter single-shot inclinometer, generously loaned by the Parsons Survey Company of South Gate, California, was used to determine the inclination and orientation of the pipe. This instrument measures inclination accurately to 5 minutes and direction accurately to 3°. Since the pipe was full of water, the inclinometer had to be enclosed in a waterproof casing, the outer diameter of which was about 1.25 inches. Records were made at 50-foot intervals. Repetition of observations demonstrated a reproducibility within the limits noted above.

*Surveys of 1951.*—The pipe was first surveyed in late July 1951, 10 days after boring was completed. Deviations from the vertical

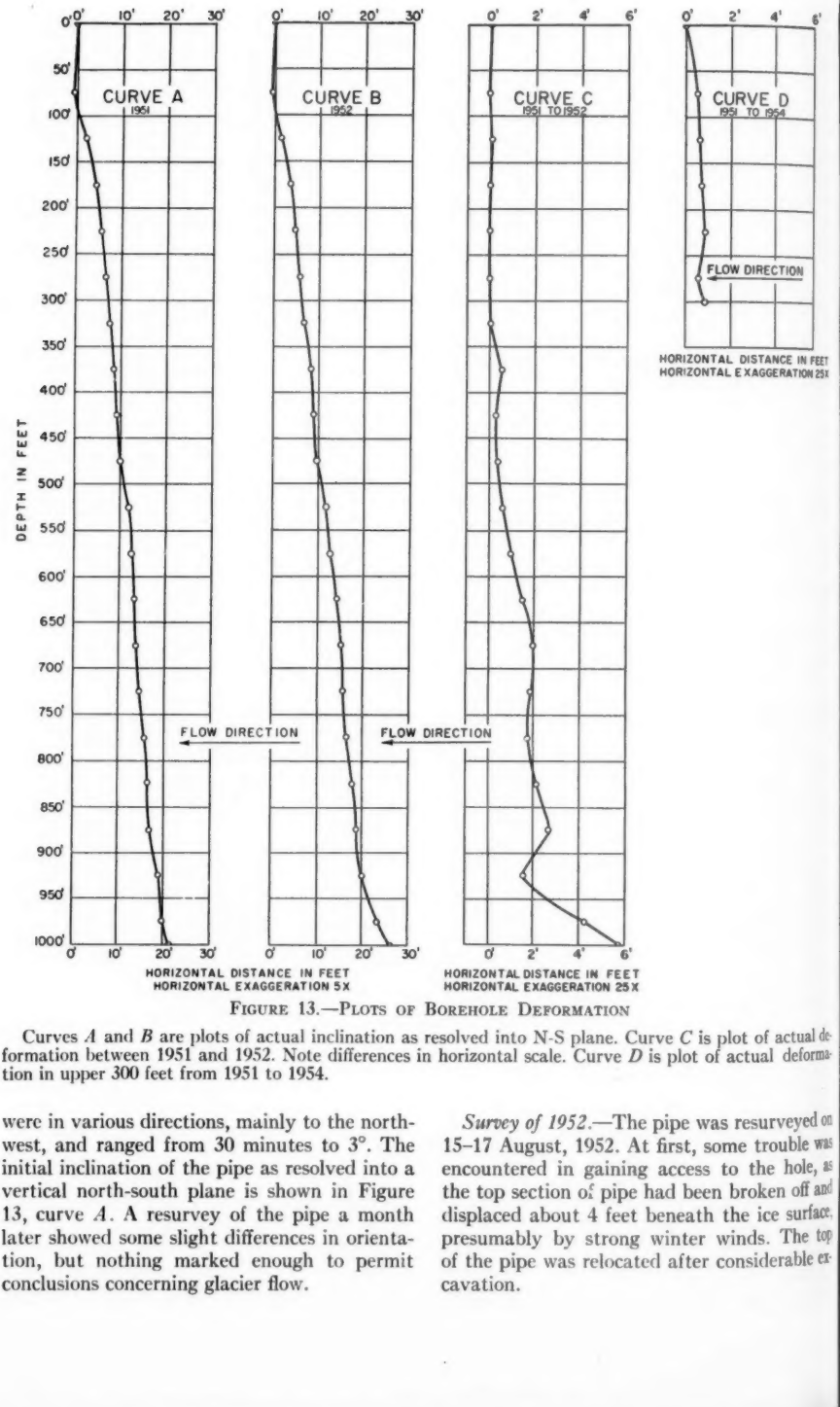


FIGURE 13.—PLOTS OF BOREHOLE DEFORMATION

Curves *A* and *B* are plots of actual inclination as resolved into N-S plane. Curve *C* is plot of actual deformation between 1951 and 1952. Note differences in horizontal scale. Curve *D* is plot of actual deformation in upper 300 feet from 1951 to 1954.

were in various directions, mainly to the northwest, and ranged from 30 minutes to 3°. The initial inclination of the pipe as resolved into a vertical north-south plane is shown in Figure 13, curve *A*. A resurvey of the pipe a month later showed some slight differences in orientation, but nothing marked enough to permit conclusions concerning glacier flow.

*Survey of 1952.*—The pipe was resurveyed on 15–17 August, 1952. At first, some trouble was encountered in gaining access to the hole, as the top section of pipe had been broken off and displaced about 4 feet beneath the ice surface, presumably by strong winter winds. The top of the pipe was relocated after considerable excavation.

The survey of 1952 showed no measurable deformation in the upper 300 feet during the first year. Below 300 feet the deformation was at a relatively uniform rate with only minor variation to a depth of about 925 feet, where it showed a marked increase (Fig. 13, curve *B*). The greatest angular deviation from vertical was at the bottom, but even here it was less than 4°. Differential movement between the top and bottom of the 1000-foot pipe was 5.75 feet. Since this is a floating system without a tie to any fixed point, nothing is known about the total movement of the pipe and the glacier at this site. The effects of deformation during the first year are best shown when plotted as deviations from a vertical line as in Figure 13, curve *C*.

*Attempted survey of 1953.*—Much of the antifreeze in the upper part of the pipe was flushed out during the survey of 1952. This loss had not been anticipated, and it was not possible to obtain a new supply. Therefore, in 1953 some ice was expected in the upper part of the pipe, and drilling equipment was provided for its removal. The site was reached on 15 August, and the pipe was found to contain a solid core of ice. Fifty-three feet of drill rod had been provided, but this was not sufficient to penetrate the total thickness of ice in the pipe. Since the winter chill on Malaspina Glacier probably penetrates no more than 30–40 feet into the ice, this abnormal depth of freezing must have been due to conduction along the pipe. Other attempts at removing the ice from the pipe failed, and no survey was possible in 1953. The upper 53 feet of the pipe which had been cleaned out by drilling was filled with antifreeze.

*Survey of 1954.*—The borehole site was reached on 9 August, 1954; the pipe was free of ice and without liquid to a depth of 125 feet. An inclinometer survey was initiated and extended to a depth of 300 feet, beyond which passage was blocked. The pipe was either obstructed, crushed, or broken at this depth. Since about 125 feet of liquid had escaped from the pipe a break must have occurred. This was probably caused by deformation related to the surge that started moving through this part of the Malaspina Glacier between the summers of 1953 and 1954.

Measurements obtained in the upper 300 feet in 1954 are significant. No deformation was recorded in the upper 300 feet during 1951–1952, but over the 3-year period from 1951 to 1954, the differential movement between top and bottom of the 300-foot section amounted to 1.5 feet, and some of this occurred within the uppermost 50 feet. These data give a flow curve (Fig. 13, curve *D*) for the upper 300 feet, which is of the same type obtained in 1952 for the entire hole.

### *Conclusions Drawn from Borehole Data*

(1) Extrusion flow does not occur in the uppermost 1000 feet of this ice sheet, although the geometrical relationships are almost ideal for it.

(2) Whatever the mode of movement, it produced a flow curve in which the top moved the greater distance. Deformation of the pipe may not give a true measure of total differential displacement because of ice flowage past the pipe. Even though this may be true, the displacement of the pipe must be in the proper direction and therefore truly indicative of the mode of flow. The curve of 1954 for the upper 300 feet of the Malaspina hole shows a similar velocity distribution with some deformation within 50 feet of the surface (Fig. 13).

(3) Data from the Malaspina borehole surveys have been plotted in several different ways, but the scatter of points is such that curves cannot be drawn with much confidence. On a semilogarithmic plot of shear-strain rate against depth (Fig. 14), the points at and below a depth of 700 feet fit nicely on a curved line, suggesting that the relationship of shear-strain rate to depth is not exponential. The points on a log-log plot of shear-strain rate against shear stress (Fig. 15) are more suggestive of a straight-line relationship, possibly of the type $\dot{\gamma} = k\tau^n$ [2] proposed by Perutz (1950, p. 65) and applied to the creep of metals. This is seemingly confirmed by laboratory experiments (Glen, 1952, p. 113; 1955, p. 528; Steinemann, 1954, p. 408), observations in a borehole (Gerrard, Perutz, and Roch, 1952, p. 554), and in tunnels (Nye, 1953, p. 484–485). The Malaspina curve yields an approximate value for $n$ of 3, which fits well with the data from other sources (Gerrard, Perutz, and Roch, 1952, p. 554: Glen, 1952, 1953, 1955: Nye, 1953: Steinemann, 1954). The Malaspina observations also suggest a yield stress for ice as low as 0.01 bar, supporting Steinemann's (1954, p. 410) conclusion that the yield stress for ice must be less than 0.2 bar.

---

[2] $\dot{\gamma}$ = mean strain rate, $\tau$ = shear stress, $k$ and $n$ are constants. $\dot{\gamma}$ is simply the measure of deformation of the pipe and $\tau$ is calculated from the formula $\tau = \rho g h \sin \alpha$; $h$ = depth beneath the surface and $\alpha$ is angle of surface slope.

## Mode of Flow in Malaspina Glacier

A prime question is how a sheet of ice like Malaspina Glacier can move 28 miles across the coastal foreland over a subglacial floor sloping back toward the mountains. The ratio of horizontal extent to average thickness of this body is somewhat greater than 100 to 1. Sufficient stress to cause flow at the outer margin could not possibly be transmitted through a sheet of ice of these dimensions. Rather the slope of the ice surface and its thickness combine to produce a shear stress sufficient to produce flow. The thrust from debouching valley glaciers causes the glacier to thicken until it has developed a sufficient surface slope and depth to flow across whatever type of floor lies before it. This is the basic assumption underlying most treatments of ice flow across flat or back-sloping floors (Demorest, 1943, p. 366; Nye, 1952a, p. 529; 1952b, p. 85-86; 1952c, p. 104; Bodvarsson, 1955, p. 5).

A demonstration of the relationship between surface slope and flow is afforded by surface features and subsurface data in the vicinity of the central camp on Malaspina Glacier. Just south of the camp is a ridge or knob on the subglacial floor about 300 feet high. This feature restricts the cross section of flow, so that discharge must be maintained either by a velocity increase or by a lateral divergence. If the adjustment is made by velocity increase, the surface slope on the glacier should steepen over the top of the knob and for some distance upstream therefrom, not just over the downstream side. Data from seismic explorations

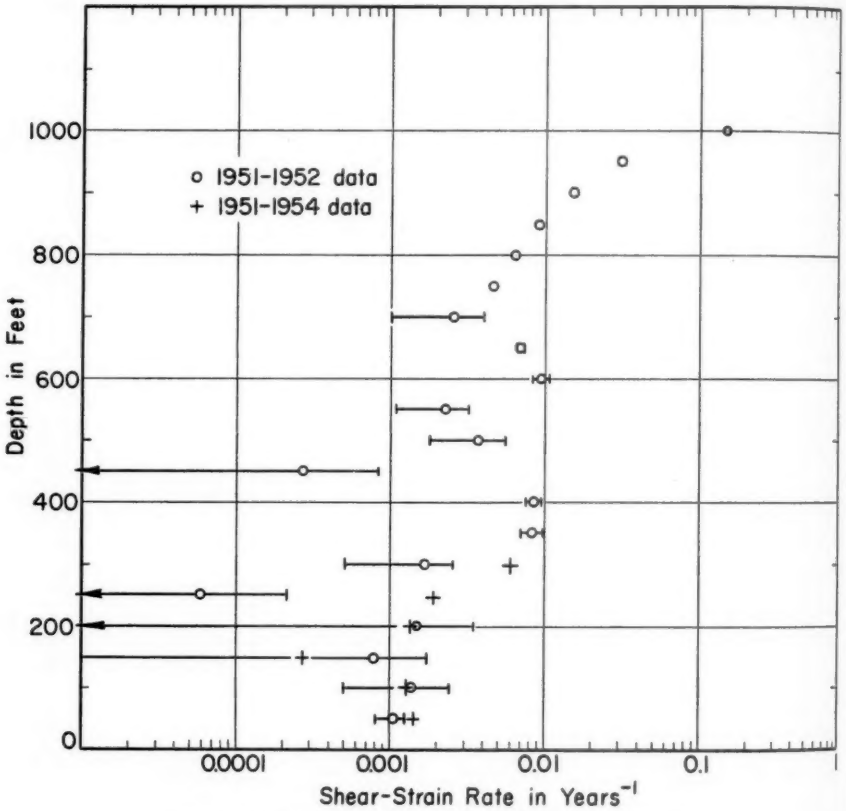


Figure 14.—Plot of Depth-Strain Rate Relationships

Lines indicate limits of error. Upper points suggest curve rather than straight-line relationships.

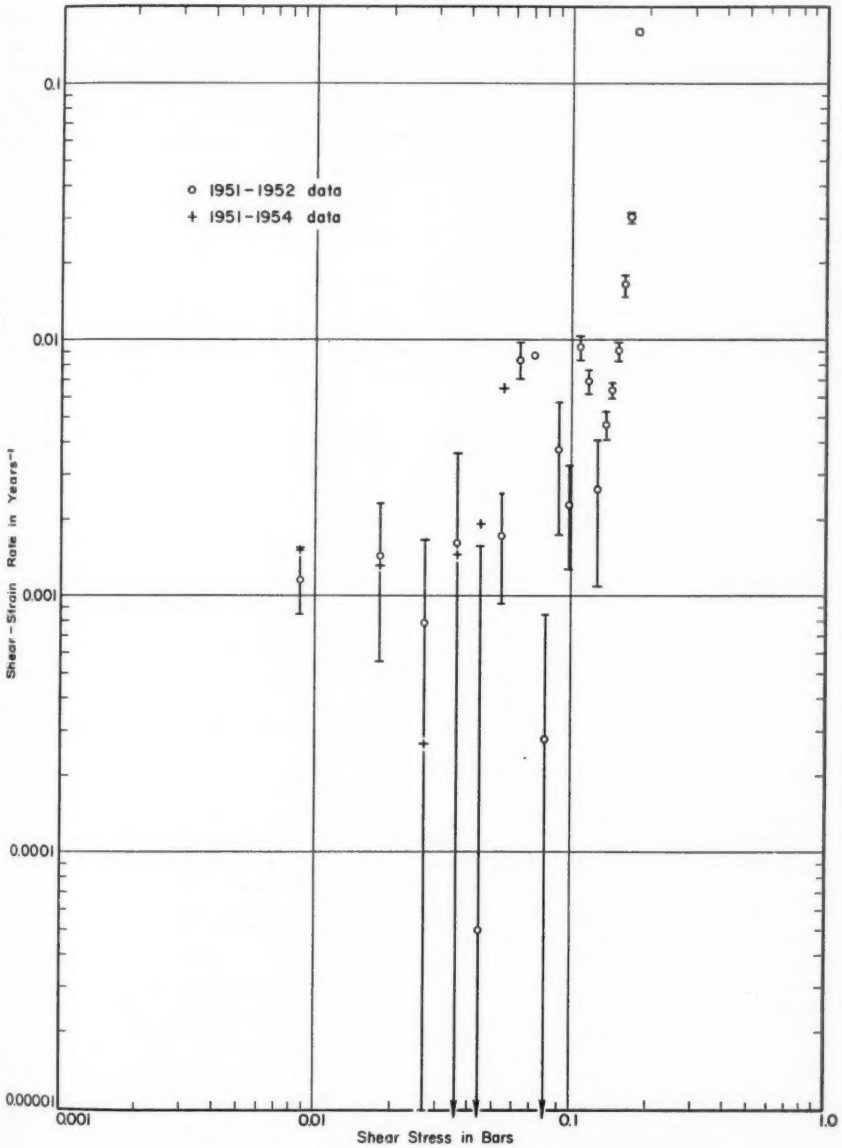


FIGURE 15.—PLOT OF SHEAR STRESS-STRAIN RATE RELATIONSHIPS
Lines represent limits of error.

and a transit-stadia survey show that this is the relationship (Fig. 16). In general, one is inclined to regard steeper reaches on the surface of an otherwise gently sloping glacier as underlain by steeper slopes on the subglacial floor. On the Malaspina they may be underlain by an ascending as well as a descending floor.

The movement of any glacier can be comprised of two principal elements: slippage over the bed and internal deformation. Their relative

roles have been reported to range from major (as much as 90 per cent) basal slippage in thin masses of cold ice on steep slopes (McCall, 1952, p. 126; Ward, 1955, p. 597), to possibly as little as 10–20 per cent in thicker masses of temperate ice on gentle slopes (Deeley and Parr, 1913, p. 99–100; Hess, 1933, p. 42; Haefeli, 1951, p. 496). In most instances, it is not possible to distinguish between basal slip and an abnormally high rate of flow in a basal layer (Bodvarsson, 1955, p. 4), which can be called boundary flow.

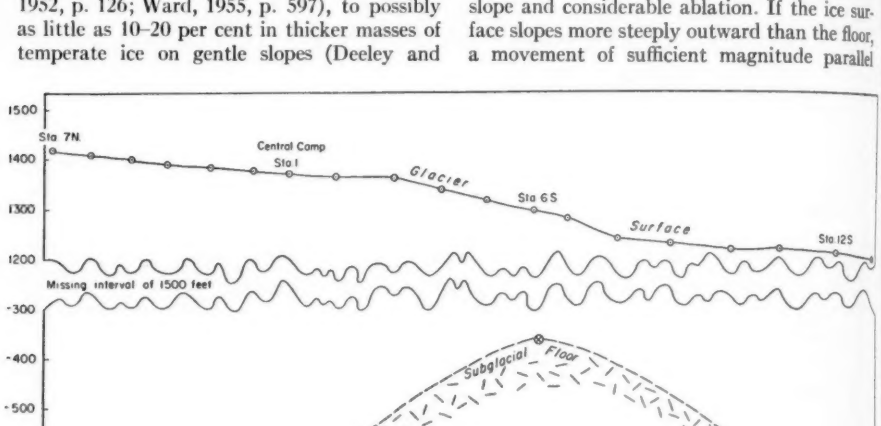


FIGURE 16.—RELATIONSHIP OF SURFACE SLOPE TO CONFIGURATION OF SUBGLACIAL FLOOR
Data on subglacial floor obtained by seismic reflections.

Data are not adequate for a quantitative evaluation of the role of basal slip or boundary flow in the movement of Malaspina Glacier, but the indications are that either one or the other occurs. The Malaspina borehole at the central camp extends about halfway through the glacier. Extrapolation of the curve obtained from this hole suggests that internal flow is probably not less than 25 and possibly as great as 75 feet per year. No allowance is made for flow of ice past the pipe, so the above figures are possibly low. An approximate mean movement of 200–300 feet per year can be calculated for the central camp site from data on discharge derived from earlier studies of accumulation and ablation on the Seward-Malaspina system. From these figures it appears that much of the movement at this site must be due to a relatively high rate of boundary flow or to basal slip, or possibly both.

The absolute direction of flow within the Malaspina sheet is important with respect to the maintenance of surface elevation and profile, especially on this glacier with its gentle slope and considerable ablation. If the ice surface slopes more steeply outward than the floor, a movement of sufficient magnitude parallel to the floor could maintain the surface in spite of ablation. Calculation of the required velocity is most easily made for the central camp, where surface slope is 35 feet per mile to the south, the floor slopes 255 feet per mile to the north, and the total ablation of ice in 1951 was 7 feet. The velocity parallel to the floor required to maintain the profile is about 145 feet per year under these conditions. The mean velocity of 200–300 feet per year calculated from discharge suggests that no independent surfaceward movement within the ice is required to maintain the surface profile at this location. The subglacial floor slopes north at an exceptionally high angle here, so that the conditions are not representative.

Similar calculations for sites closer to the glacier's margin with 15–20 feet of ice ablation per year, show that the movement parallel to the floor required to maintain the elevation and profile of the ice surface is 700–1000 feet per year. Even though the glacier is probably not in equilibrium, this seems much too high, and an upward movement of ice independent of that related to the rise upon the subglacial floor must occur near the margin.

The hypotheses of obstructed extrusion flow

(Demorest, 1943, p. 367–369) and of compressive flow (Nye, 1952b, p. 86–89) can both produce a surfaceward component of movement. Cogent objections have been advanced against any type of extrusion flow, and its occurrence here is considered unlikely. The rising floor of the Malaspina and the signs of decreasing velocity outward toward the margin are favorable to compressive flow. This is considered the most likely explanation yet advanced for surfaceward flow of ice in Malaspina Glacier.

In summation, the motion of Malaspina Glacier is thought to occur partly by basal slippage or boundary-layer flow and partly by internal flowage. The surface velocity parallel to the floor at the central camp probably does not exceed 200–300 feet per year. Close to the glacier's margin it is considerably less, decreasing to zero in the stagnant marginal zone. Some surfaceward movement of ice results from motion over the rising subglacial floor, but this rise is not sufficient to maintain the elevation and profile of the ice surface against lowering by ablation near the outer edge of the glacier. An independent surfaceward movement of ice is required, and it is postulated that this occurs because of compressive flow. Although Nye's (1951, p. 565–568; 1952b, p. 88) analysis shows that in compressive flow, the trajectories of maximum shear-strain rate rise out of the surface at a 45-degree angle, the velocity vector makes a much lower angle with the surface.

## References Cited


Ahlmann, H. W., 1948, Glaciological research on the North Atlantic coasts: Royal Geog. Soc., Research ser. no. 1, 83 p.

Allen, C. R., and Smith, G. I., 1953, Seismic and gravity investigations on the Malaspina Glacier, Alaska: Am. Geophys. Union Trans., v. 34, p. 755–760

Bader, Henri, 1950, The significance of air bubbles in glacier ice: Jour. Glaciology, v. 1, p. 443–451

—— 1951, Introduction to ice petrofabrics: Jour. Geology, v. 59, p. 519–536

Blackwelder, Eliot, 1909, The Yakutat coastal plain of Alaska; A combined terrestrial and marine formation: Am. Jour. Sci., v. 27, 4th ser., p. 459–466

Bodvarsson, Gunnar, 1955, On the flow of ice-sheets and glaciers: Jökull, Ar. 5, p. 1–8

Capps, S. R., 1931, Glaciation in Alaska: U. S. Geol. Survey Prof. Paper 170-A, 8 p.

Deeley, R. M., and Parr, P. H., 1913, The viscosity of glacier ice: Philos. Mag. and Jour. Sci., v. 26, p. 85–111

—— 1914, The Hintereis Glacier: Philos. Mag. and Jour. Sci., v. 27, p. 153–176

Demorest, Max, 1942, Glacier regimens and ice movement within glaciers: Am. Jour. Sci., v. 240, p. 31–66

—— 1943, Ice sheets: Geol. Soc. America Bull., v. 54, p. 363–400

Drygalski, E. v., and Machatschek, Fritz, 1942, Gletscherkunde: Enzyklopadie der Erdkunde, Franz Deuticke, Vienna, 261 p.

Finsterwalder, Richard, 1937, Die Gletscher des Nanga Parbat: Zeit. f. Gletscherk., v. 25, p. 57–108

Flint, R. F., 1947, Glacial geology and the Pleistocene Epoch: New York, John Wiley and Sons, 589 p.

Gerrard, J. A. F., Perutz, M. F., and Roch, André, 1952, Measurement of the velocity distribution along a vertical line through a glacier: Royal Soc. London, Proc. A., v. 213, p. 546–558

Gilbert, G. K., 1910, Glaciers and glaciation: Harriman Alaska Ser., Smithsonian Inst., v. 3, 231 p.

Glen, J. W., 1952, Experiments on the deformation of ice: Jour. Glaciology, v. 2, p. 111–114

Glen, J. W., 1953, Rate of flow of polycrystalline ice: Nature, v. 172, p. 721

—— 1955, The creep of polycrystalline ice: Royal Soc. London, Proc. A, v. 228, p. 519–538

Haefeli, R., 1951, Some observations on glacier flow: Jour. Glaciology, v. 1, p. 496–498

Harrison, A. E., 1951, Ice advances during the recession of Nisqually Glacier: The Mountaineer, v. 43, p. 7–12

—— 1956, Fluctuations of the Nisqually Glacier, Mt. Ranier, Washington, since 1750: Jour. Glaciology, v. 2, p. 675–683

Hartshorn, J. H., 1952, Superglacial and proglacial geology of the Malaspina Glacier, Alaska, and its bearing on glacial features of New England (Abstract): Geol. Soc. America Bull., v. 63, p. 1259–1260

Hess, Hans, 1933, Das Eis der Erde: Handbuch der Geophysic, v. 7, sec. 1, p. 1–121

Klebelsberg, R. v., 1948, Handbuch der Gletscherkunde und Glazialgeologie: v. 1, Springer, Vienna, 403 p.

Lewis, W. V., 1956, Future lines of progress in glaciology: Jour. Glaciology, v. 2, p. 695–697

Leverett, Frank, 1929, Moraines and shorelines of the Lake Superior region: U. S. Geol. Survey Prof. Paper 154, 72 p.

—— 1932, Quaternary geology of Minnesota and parts of adjacent States: U. S. Geol. Survey Prof. Paper 161, 149 p.

Mathews, W. H., 1957, Vertical distribution of velocity in Salmon Glacier, British Columbia (abstract): Geol. Soc. America Bull., v. 68, p. 1835

McCall, J. G., 1952, The internal structure of a cirque glacier: Jour. Glaciology, v. 2, p. 122–130

Meier, M. F., Rigsby, G. P., and Sharp, R. P., 1954, Preliminary data from Saskatchewan Glacier, Alberta, Canada: Arctic, v. 7, p. 3–26

Menard, H. W., 1953, Pleistocene and Recent sediment from the floor of the northeastern Pacific Ocean: Geol. Soc. America Bull., v. 64, p. 1279–1294

Miller, D. J., 1957, Geology of the southeastern part of the Robinson Mountains, Yakataga District, Alaska: U.S.G.S. Oil and Gas Investigation Map OM 187

Miller, M. M., 1952, The application of electrothermic boring methods to englacial research: Arctic Inst. North America, Internal Memo. 6 (mimeo.), 35 p.

Miller, M. M., 1953, Juneau Ice Field research project, 1951 winter season: Am. Geog. Soc., Rept. 8 (mimeo.), 51 p.
Nizery, A., 1951, Electrothermic rig for the boring of glaciers: Am. Geophys. Union Trans., v. 32, p. 66–72
Nye, J. F., 1951, The flow of glaciers and ice-sheets as a problem in plasticity: Royal Soc. London, Proc. A., v. 207, p. 554–572
Nye, J. F., 1952a, A method of calculating the thickness of the ice-sheets: Nature, v. 169, p. 529–530
—— 1952b, The mechanics of glacier flow: Jour. Glaciology, v. 2, p. 82–93
—— 1952c, A comparison between the theoretical and the measured long profile of the Unteraar Glacier: Jour. Glaciology, v. 2, p. 103–107
—— 1953, The flow law of ice from measurements in glacier tunnels, laboratory experiments and the Jungfraufirn borehole experiment: Royal Soc. London, Proc. A, v. 219, p. 477–489
Perutz, M. F., 1947, Report on problems relating to the flow of glaciers: Jour. Glaciology, v. 1, p. 47–51
—— 1949, Direct measurement of the velocity distribution in a vertical profile through a glacier: Jour. Glaciology, v. 1, p. 249
—— 1950, Glaciology—the flow of glaciers: The Observatory, v. 70, p. 64–65
Perutz, M. F., and Seligman, Gerald, 1939, A crystallographic investigation of glacier structure and the mechanism of glacier flow: Royal Soc. London, Proc. A., v. 172, p. 335–360
Plafker, George, and Miller, D. J., 1957a, Reconnaissance geology of the Malaspina District, Alaska: U. S. Geol. Survey Oil and Gas Investigation Map OM 189
—— 1957b, Glacial features and surficial deposits of the Malaspina district, Alaska: U.S.G.S. Prelim. Rept., 13 p.
Rigsby, G. P., 1951, Crystal fabric studies on Emmons Glacier, Mount Rainier, Washington: Jour. Geology, v. 59, p. 590–598
Russell, I. C., 1891, An expedition to Mount St. Elias, Alaska: Nat. Geog. Mag., v. 3, p. 53–204
—— 1892, Mt. St. Elias and its glaciers: Am. Jour. Sci., v. 43 (3rd ser.), p. 169–182
—— 1893, Malaspina Glacier: Jour. Geology, v. 1, p. 219–245
—— 1901, Glaciers of North America: Boston, Mass., Ginn and Company, 210 p.
Sharp, R. P., 1948, Constitution of valley glaciers: Jour. Glaciology, v. 1, p. 182–189
—— 1951, Accumulation and ablation on the Seward-Malaspina Glacier system, Canada-Alaska: Geol. Soc. America Bull., v. 62, p. 725–744
—— 1953, Deformation of bore hole in Malaspina Glacier, Alaska: Geol. Soc. America Bull., v. 64, p. 97–100
—— 1958, The latest major advance of Malaspina Glacier, Alaska: Geographical Review, v. 48, p. 16–26
Steinemann, Samuel, 1954, Results of preliminary experiments on the plasticity of ice crystals: Jour. Glaciology, v. 2, p. 404–412
Streiff-Becker, R., 1938, Zur Dynamik des Firneises: Zeit. f. Gletscherk., v. 26, p. 1–21
Tarr, R. S., 1907, The Malaspina Glacier: Am. Geog. Soc. Bull., v. 39, pl 273–285
Tarr, R. S., and Butler, B. S., 1909, The Yakutat Bay region: U. S. Geol. Survey Prof. Paper 64, 183 p.
Tarr, R. S., and Martin, Lawrence, 1914, Alaskan glacier studies: Nat. Geog. Soc., 498 p.
Untersteiner, N., 1954, Über die Feinbänderung und Bewegung des Gletschereises: Arch. f. Met., Geophys. und Biokl., Ser. A, Bd. 7, p. 231–242
Ward, W. H., 1955, The flow of Highway Glacier: Jour. Glaciology, v. 2, p. 592–598
Washburn, H. B., 1935, Morainic banding of Malaspina and other Alaskan glaciers: Geol. Soc. America Bull., v. 46, p. 1879–1890

Division of Geological Sciences, California Institute of Technology, Pasadena, California

Manuscript Received by the Secretary of the Society, August 1, 1957

BULLETIN OF THE GEOLOGICAL SOCIETY OF AMERICA
VOL. 69, PP. 647-688, 3 FIGS. JUNE 1958

# LOWER AND MIDDLE CAMBRIAN STRATIGRAPHY IN NORTHERN UTAH AND SOUTHEASTERN IDAHO

BY GEORGE B. MAXEY

## ABSTRACT

The stratigraphic succession of Lower and Middle Cambrian sediments in northern Utah and southeastern Idaho as determined from 13 measured sections includes the basal medium- to coarse-grained Prospect Mountain Quartzite overlain by interbedded fine- and coarse-grained clastic rocks (Pioche Formation) that in turn are overlain by several hundred to a few thousand feet of carbonate rocks with a few thinly interbedded layers of fine clastics. The carbonate sequence includes the Langston Formation, Ute Limestone, Blacksmith Dolomite, and Bloomington Formation.

Known occurrences of fossils are listed for the formations. Seventeen faunal groups are identified, and a sequence of faunizones is proposed.

Cambrian deposits may be separated into (1) orthoquartzite; (2) greenish-brown, micaceous and arenaceous shale; (3) brown-weathering, calcareous sandstone; (4) rusty-brown-weathering dolomite; (5) green and buff fissile shale; (6) calcareous black shale; (7) mottled, silty, aphanitic, thinly bedded limestone; (8) *Girvanella* limestone; (9) intraformational conglomerate; (10) oölitic limestone; (11) "undifferentiated limestone"; and (12) "undifferentiated dolomite" facies.

All these sediments probably were deposited in a shallow, chiefly transgressive, though oscillating, sea. This sea transgressed a low-lying but mature topography eastward to western Utah by earliest Cambrian (pre-Olenellus?) time and to eastern Utah by the end of Early Cambrian time. The area remained submerged during Medial Cambrian and much of Late Cambrian time.

## CONTENTS

### TEXT

| | Page |
|---|---|
| Introduction | 648 |
| Location and general description of sections studied | 649 |
| General statement | 649 |
| Portneuf and Bannock ranges, Idaho | 649 |
| Malad Range, Idaho | 649 |
| Bear River Range, Utah and Idaho | 650 |
| General description | 650 |
| High Creek section | 651 |
| Section on the North Fork of Mill Creek and Spence Gulch section | 655 |
| Section in the Left Fork of Blacksmith Fork Canyon | 656 |
| South Cottonwood Canyon section, Blacksmith Fork | 658 |
| Blacksmith Fork section | 658 |
| North part of the Wasatch Range, Utah | 659 |
| General statement | 659 |
| Calls Fort section | 659 |
| Willard Peak section | 662 |
| Ogden Canyon section | 664 |
| Big Cottonwood Creek and Neffs Canyon sections | 664 |
| Summary | 666 |
| Promontory Range, Utah | 666 |
| Lower and Middle Cambrian formations in northeastern Utah and southeastern Idaho and their regional relationships | 667 |
| Prospect Mountain Quartzite (Lower Cambrian) | 667 |
| Pioche Formation | 668 |
| Langston Formation (Lower and Middle Cambrian) | 669 |
| Ute Formation | 671 |
| Blacksmith Dolomite | 672 |
| Bloomington Formation | 672 |
| Early and Medial Cambrian faunules in Utah and southeastern Idaho | 673 |
| Zonation of the faunules | 676 |
| General statement | 676 |
| *Olenellus* zone | 676 |
| *Glossopleura-Zacanthoides* zone | 677 |
| *Bathyuriscus-Elrathina* zone | 678 |
| *Thompsonaspis* zone | 678 |
| *Asaphiscus-Bolaspidella* zone | 678 |
| Discussion | 678 |
| Early and Medial Cambrian sedimentation and paleogeography | 679 |
| Description of the lithofacies | 679 |
| Interpretation and paleogeography | 685 |
| Selected references | 686 |

### ILLUSTRATIONS

| Figure | | Page |
|---|---|---|
| 1. | Location of the stratigraphic sections studied and outcrops of Cambrian rocks in the region | 648 |
| 2. | Lithologic variations within some Lower and Middle Cambrian formations in northern Utah and southeastern Idaho | 670 |
| 3. | Regional correlation and Early and Medial Cambrian faunules and faunizones | 673 |

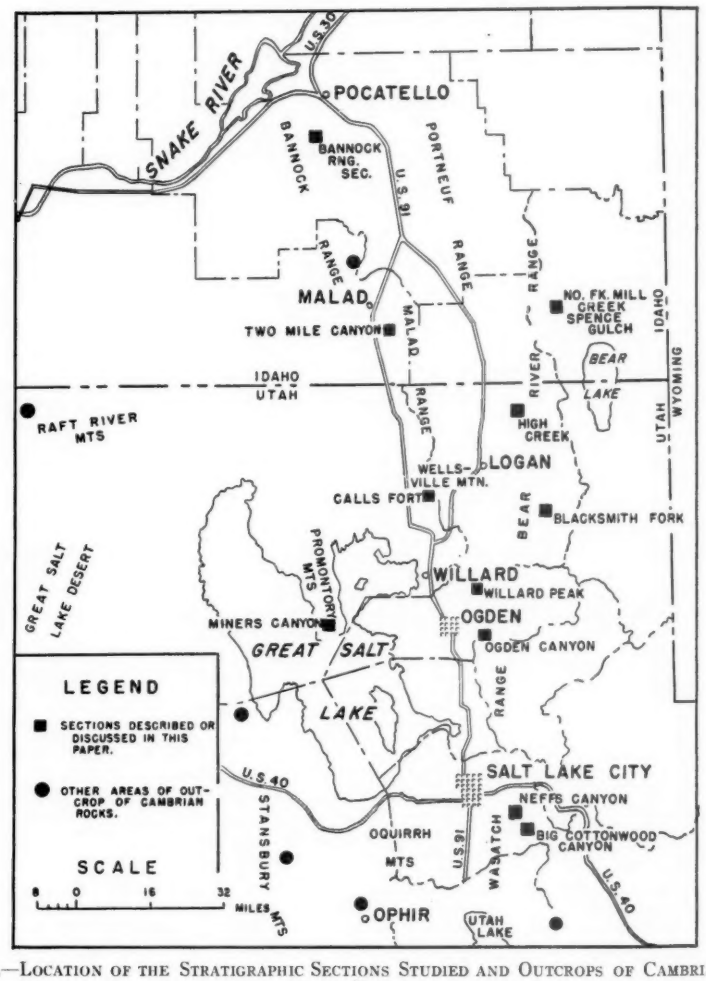


FIGURE 1.—LOCATION OF THE STRATIGRAPHIC SECTIONS STUDIED AND OUTCROPS OF CAMBRIAN ROCKS IN THE REGION

## INTRODUCTION

As part of a regional investigation of the Cambrian rocks of the Great Basin which has been conducted sporadically since 1939, the writer studied several sections of Lower and Middle Cambrian rocks in northeastern Utah and southeastern Idaho (Fig. 1). New information resulting from this study constitutes the main body of this paper. Suggestions are also included for simplifying and correcting Cambrian formational and biostratigraphic nomenclature which seems to be unnecessarily complex and partly in error on the basis of modern principles and concepts of regional stratigraphy. Many of the conclusions here presented are tentative because the field and laboratory study is still in progress. Additional information and more dependable conclusions will be made available as the study progresses.

The writer gratefully acknowledges the advice and assistance of Dr. Charles Deiss and Dr. J. Stewart Williams, both of whom encouraged him to begin and continue these studies. Dr. B. F. Howell consistently and patiently advised the writer throughout the

study; assisted him with many problems, chief among these the identification of most of the fossils; and finally read the manuscript. Without this advice and assistance the study would probably have never been completed, and for this the writer is sincerely grateful. Dr. Erling Dorf and Dr. Franklin Van Houten also read the manuscript and offered helpful suggestions. Thanks are extended to Dr. Norman Denson, Mr. Donald Duncan, Dr. Franco Rasetti, the late Dr. Charles E. Resser, Dr. John F. Mason, and the late Mr. Frank Beckwith, all of whom contributed much time and many ideas.

Funds to finance the field and laboratory work were furnished in part by the Departments of Geology of Princeton University and Utah State Agricultural College. The University of Connecticut also contributed funds for laboratory equipment and freed the writer from excessive academic tasks during 1949 and 1950. Field assistants included John W. Wetzler (Summer, 1939), Kent O. Bushnell, and Arthur Reimer (Summer, 1950). To these organizations and individuals the writer is indebted and extends his warmest thanks.

All sections described for the first time by the writer were measured with a Brunton compass and steel tape; adjustments were made to obtain the correct thicknesses of stratigraphic units where necessary. These adjustments were usually made by reference to Mertie's chart (1922, Pl. VI). Rock colors were determined in the field by use of a standard rock color chart (Goldman and Merwin, 1928). The color names corresponding to the color chips on the chart are from Ridgway (1912, p. 1–53).

## Location and General Description of Sections Studied

### *General Statement*

Most of the outcrop areas (Fig. 1) in northeastern Utah and southern Idaho were visited by the writer during the period 1940–1951 when he measured one or more detailed sections of rocks of Early and Medial Cambrian age in several of the areas. When detailed sections, described by other geologists were available, they were carefully studied in the field. Collections made from these sections were accurately located within the sections. Significant lithologic variations were likewise noted and carefully checked in the field. Detailed descriptions are given here for only those sections which have not been published.

### *Portneuf and Bannock Ranges, Idaho*

Detailed descriptions of sections of Cambrian rocks in the north part of the Bannock Range have been published by Ludlum (1943, p. 973–986). In the vicinity of Pocatello and Inkom, Idaho, he found that 3200 feet of Prospect Mountain ("Brigham") Quartzite unconformably overlies the Precambrian Blackrock Limestone. This is one of the few localities in Idaho and northern Utah, outside the Wasatch Range, where the base of the Prospect Mountain Formation is exposed. The formation is pink to red, thick-bedded, vitreous, medium-grained quartzose sandstone interbedded with beds of coarse sandstone and pebble conglomerate. The upper 600 feet of the formation as described by Ludlum is thin-bedded and contains much green or buff siltstone and shale. The lower part of this shaly and silty sequence may be the lithogenetic equivalent of the Pioche Shale, and the upper part the equivalent of the Spence Shale Member of the Langston Formation. The quartzite is conformably overlain by 4250 feet of sparsely fossiliferous limestones interbedded with a little shale and sandstone.

In the vicinity of Scout Mountain about 10 miles south of Pocatello, Idaho, the writer identified lithologic equivalents of the Langston, Ute, and Bloomington Formations which also crop out in adjacent areas of Idaho and northern Utah. Time did not allow detailed measurement of this section, but several lithologic units and formations were recognized, including the Spence Shale Member of the Langston Formation and the Hodges and Calls Fort Shale Members of the Bloomington Formation. An equivalent of the Blacksmith Dolomite probably is absent in this locality.

A section in the south part of the Bannock Range, about 3 miles north of Malad City, Idaho, was also examined. Lithologic equivalents of the above-mentioned formations, except the Blacksmith Dolomite, were also recognized in this area.

### *Malad Range, Idaho*

The Two Mile Canyon section is exposed approximately 2 miles southeast of Malad City, Idaho (Fig. 1), in a small canyon in the Malad Range, a northward extension of the Wasatch Range of Utah. The Cambrian rocks that crop out in the vicinity of Two Mile Canyon were first studied in detail by Walcott in 1898 and 1906 (Resser, 1939b, p. 4, 9–11). Meek had earlier made collections and notes. Walcott

measured and described in detail a partial section of the Prospect Mountain ("Brigham") Quartzite and a complete section of the formations of Medial Cambrian age. The description of this section was not published until 1939 when Resser (1939b, p. 10–11) included it in his discussion of the "*Ptarmigania* strata" (Naomi Peak Limestome Member of the Langston Formation).

The writer visited the Two Mile Canyon section several times between May 1939 (accompanied by Deiss) and June 1941. The rocks are complexly faulted in Two Mile Canyon, and a careful search for a place to measure an undisturbed sequence of rocks of Medial Cambrian age was unsuccessful. However, an undisturbed but incomplete section from well down in the Prospect Mountain Quartzite ("Brigham") to high in the Spence Shale Member of the Langston Formation was carefully measured and described, and fossils were collected from several horizons. The lower part of Walcott's section described by Resser (1939b, p. 10–11), including the Prospect Mountain ("Brigham") Quartzite, Walcott's "Langston" limestone, and the Spence Shale, corresponds very closely in lithologic detail to the section measured by the writer. Therefore the section is not described here.

Walcott's description of the Two Mile Canyon section may be correct as far as sequence of lithologic types is concerned, but his assignment of those types to the Middle Cambrian formations which occur in adjacent areas does not appear to be accurate. The Spence Shale and some overlying units are now known to occur low in the Langston Formation rather than at the base of the Ute Formation (Williams and Maxey, 1941, p. 276–285). Probably the Spence Shale and the three overlying units in Walcott's description of the Ute Formation (Resser, 1939b, p. 10) should be referred to the Langston Formation. Moreover, the basal beds of the Nounan Formation contain fossils of Late Cambrian age. Accurate measurement of the thickness of the various lithologic units may not be possible in an unmapped area of such complex structure. For example, the apparent thinness of the Bloomington Formation and the apparent thickness of the Blacksmith Dolomite in Walcott's Two Mile Canyon section may be the result of cutting out and duplication of beds by faulting. However, the section in Two Mile Canyon contains the lithogenetic equivalents of the section in adjacent areas in northern Utah and southern Idaho. The faunas contained in the Langston Formation at two Mile Canyon are identical with those in the same formation in closely adjacent areas.

### *Bear River Range, Utah and Idaho*

*General description.*—The Bear River Range is an eastward prong of the Wasatch Range and extends northward nearly 95 miles from Sharp's Mountain, east of Brigham City, Utah, to Soda Point, 45 miles north of the Utah-Idaho boundary. The southern part of the range in Logan quadrangle, Utah, is underlain by a broad syncline, broken on the west along the range front and near the center of the range by normal faults of considerable throw. Rocks of Cambrian age crop out along the west front of the range nearly as far south as Logan, Utah, and, in the center and east parts of the Range, to its southern extremity. The northern part of the range in Idaho has not been completely mapped, and the boundaries of the outcrops of Cambrian rocks are not accurately known. However, much of the northern part of the range is underlain by rocks of this age.

The Cambrian rocks in the Bear River Range were probably first studied by Hague and Emmons (1877, p. 340–417) during the Fortieth Parallel Survey (1867–1877). Peale (1879, p. 598–600), with the Green River Division of the Hayden Survey, also worked in the range in 1877. Many of the data collected by these field parties were later studied and described by Walcott, who first visited the area in 1898. He followed this work with extended studies of the Blacksmith Fork and Mill Creek areas in 1906 and published the original Blacksmith Fork Cambrian section in 1908 (Walcott, 1908a, p. 5–9; 1908b, p. 191–200). Walcott was assisted by Burling and others in the later study. Further results of these studies were published in 1912 (Walcott, 1912, p. 148–153).

Richardson described the Cambrian rocks in the eastern part of the range in the Randolph quadrangle in 1913 (p. 406–409) and in 1941 (p. 7–14). He noted that the section is similar to the Blacksmith Fork section and described and named the Hodges Shale Member at the base of the Bloomington Formation and the Worm Creek Quartzite Member at the base of the St. Charles Formation (Upper Cambrian). Mansfield (1927, p. 52–56), on the basis of work of geologists of the United States Geological Survey between 1909 and 1916, gave detailed descriptions of sections of the Cambrian rocks in southeastern Idaho, chiefly east of the Bear River Range. He adopted the formational names of Walcott's Blacksmith Fork section

and recognized the Hodges Shale and Worm Creek Quartzite of Richardson.

Deiss (1938) remeasured and emended the Blacksmith Fork section and designated type localities for the formations of Medial Cambrian age. He also described the *Glossopleura* horizon at the base of the Ute Formation and correctly stated that "the shale at the base of the Ute Formation cannot be correlated with the Spence shale of Idaho" (1938, p. 116).

Resser (1939a; 1939b) described the faunas of the lower part of the Langston Formation. He recognized the Spence Shale Member but incorrectly assigned it to the base of the Ute Formation, and he described in the detail the "*Ptarmigania* fauna" at the base of the Langston. These descriptions were based chiefly on unpublished field notes and undescribed material collected by the Walcott expeditions of 1898 and 1906.

Williams and Maxey (1941, p. 276–285) showed that the Spence Shale Member occurs near the base of the Langston Formation and is not a member of the Ute Limestone. Most of the detailed field date collected during those field seasons is incorporated in the present report. On the basis of these data and later study, Williams (1948, p. 1131–1135) briefly described the Cambrian formations of the Logan quadrangle and discussed lithologic and faunal variations within that area.

Denson (1942) described and named the Calls Fort Shale Member of the Bloomington Formation and, on the basis of fossils, showed that the top of the Bloomington Formation was deposited in latest Medial Cambrian time. He described three new and important faunules in the Bloomington Formation and showed that these faunules were present in uppermost Middle Cambrian rocks in Wyoming, Montana, British Columbia, and Alberta.

The sections given below were measured by the writer during the field seasons of 1939 and 1940 and were checked and emended by him in the summer of 1950.

*High Creek section.*—Rocks of Early and Medial Cambrian age are well exposed from far down in the Prospect Mountain Formation to the contact of the Bloomington and Nounan (Upper Cambrian) Formations. Exposures of the Spence Shale Member and the Prospect Mountain, Ute, Blacksmith, and Bloomington Formations are as good as any in northern Utah and southern Idaho. More fossil zones were found in this section than in any other measured or observed section in the Bear River and Wasatch ranges. Outcrops are numerous, especially along the high ridges between the larger streams. The base of the measured section is at the contact of the Pioche (?) shale and the Langston Formation on the main ridge between the North and South forks of High Creek in section 11, T. 14 N., R. 2 E., approximately 7 miles northeast of Richmond, Utah (Fig. 1). The line of the section follows northeasterly up the ridge, on the South Fork side of the ridge.

*High Creek Section, Bear River Range*

UPPER CAMBRIAN

Nounan Formation

| | Feet |
|---|---|
| 45. Dolomite and limestone: neutral-gray, thin-bedded medium-crystalline dolomite interbedded with dark-gray thin-bedded, finely crystalline limestone in first 20 feet of unit overlain by neutral-gray, thin- to medium-bedded (1 inch to 6 inches), finely crystalline dolomite; weathers to speckled white and gray surfaces; poorly exposed outcrops | 60 |
| Total thickness of Nounan Formation | 1125 |

MIDDLE CAMBRIAN

Bloomington Formation

*Calls Fort Shale Member*

| | |
|---|---|
| 44. Limestone: dark blackish gray, thin-bedded, finely crystalline, platy; weathers to blue-gray and colonial-buff-stained plates; some arenaceous, shaly, dolomitized layers in top | 60 |
| 43. Limestone: dark gray, thin-bedded, conglomeratic with very small, well-rounded, limestone pebbles and much limonite; weathers to lighter-gray and limonite-stained rough-surfaced plates 1–2 feet square. Fossil locality 101 s24 at base (of this unit) | 30 |

Fossils:

*Homagnostus* cf. *pisiformis pater* (Holm and Westergard)
*Elrathia dubia* Denson
Unidentified and undescribed trilobite genera
*Hyolithes*
*Stenotheca*

42. Limestone and shale: neutral-gray, thin-bedded, finely crystalline

| | Feet |
|---|---|
| shaly limestone interbedded with thin beds of dark-gray limestone; near deep-olive, thin-bedded, finely chunky to fissile shale. Limestones weather to light bluish-gray, colonial-buff-stained ½- to 1-foot quadrangular plates; shales weather to tea-green chunks and very thin small plates. Poorly exposed outcrops | 90 |
| Total thickness of Calls Fort Shale | 180 |
| 41. Limestone: dark blue gray, medium crystalline, oölitic; has very few dark-gray bands and spots; weathers to lighter bluish-gray chunks | 40 |
| 40. Limestone: neutral gray, irregularly and thinly bedded, finely crystalline; contains many buff clay partings; slightly nodular, some beds more nodular and darker gray than others especially toward top; weathers to very light-bluish-gray chunks; at base is very thin-bedded and weathers to colonial-buff plates; few beds of more finely crystalline, thicker-bedded, slightly darker limestone toward center of unit which form good 4- to 5-foot outcrops | 155 |
| 39. Limestone: dark neutral gray, thick-bedded, finely crystalline oölitic | 50 |
| 38. Limestone: dark neutral gray with tannish tinge, thick-bedded finely crystalline, oölitic; smaller oölites and lighter color than above | 70 |
| 37. Limestone: dark neutral gray, thick-bedded, finely crystalline, oölitic | 165 |
| 36. Limestone: dark bluish gray, thick-bedded, finely crystalline, oölitic; contains few small limestone pebbles ¼–1 inch in diameter; weathers to lighter-bluish-gray, limonite-stained low outcrops; interbedded with very dark-bluish-gray, very compact limestone which contains few small crystals of calcite and few small splotches of tan limonite, and which weathers to limonite-stained, lighter-blue-gray, low outcrops | 100 |
| 35. Limestone: dark bluish gray, thin- to thick-bedded (beds 2 inches to 2 feet thick), compact, brittle, nodular; contains some buff to tan limonitic blobs on weathered surfaces; weathers to lighter-bluish-gray rough chunks and plates. Nonfossiliferous | 15 |
| 34. Covered interval: float indicates beds similar to unit 35 | 70 |
| 33. Limestone: similar to unit 34 except fossiliferous at the base. Fossil locality 101 a10 | 55 |
| Fossils: | |
| *Olenoides*, sp. | |
| Undescribed and unidentified trilobite genera | |
| *Hodges Shale Member* | |
| 32. Limestone and shale: dark-bluish-gray, thick-bedded finely crystalline, oölitic limestone interbedded with three 4- to 6-foot phases of andora-green, very thin-bedded (beds 1/16–¼ inch thick), calcareous shale that weathers to small tea-green chips. Fossil locality 101 s7 in basal oölite layers of this unit | 40 |
| Fossils: | |
| *Olenoides*, sp. | |
| Undescribed and unidentified trilobite genera | |
| 31. Limestone, shale, and sandstone: 2 feet of vinaceous-pink, very thin and unevenly bedded, micaceous, calcareous, shaly, very finely- to medium-grained sandstone at base; this sandstone overlain by dark-neutral-gray, thin-bedded, compact nodular, arenaceous, unevenly bedded limestone with many shale partings, overlain by andora-green, very thin-bedded calcareous shale that weathers to small tea-green chips; shale and limestone thinly interbedded on top part. Much of the unit poorly exposed | 100 |
| 30. Limestone and shale: mouse-gray, thin-bedded, finely crystalline limestone with some clay partings; some shale as described in unit 31 interbedded; 2 feet of graphalium-green, thin-bedded, very pure, compact limestone in center of unit; all outcrops poorly exposed | 55 |
| 29. Covered interval: probably interbedded shale and limestone is indicated by float, animal burrows, and few very poor outcrops | 70 |
| 28. Limestone and shale: dark-grayish-olive, thin-bedded, micaceous, cal- | |

| | Feet |
|---|---|
| careous shale which forms low, even light-buff slopes; interbedded with thin beds of dark-gray, thin-bedded, finely crystalline, arenaceous, shaly limestone that weathers to light bluish gray in thin, platy, low outcrop; bedding planes uneven; poorly exposed outcrops | 130 |
| 27. Limestone: dark neutral gray, thin-bedded, finely crystalline, at bottom of unit bedding is in thin laminations (3/16–1 inch thick); bedding becomes thicker and there are chert layers 1 inch thick toward the middle of the unit; one 4-foot bed of oölitic, finely crystalline, thin-bedded limestone near middle of unit; limestone tends to become nodular with uneven bedding planes toward top. Fossiliferous at top. Fossil locality 101 s | 200 |
| Fossils: | |
| *Olenoides*, sp. | |
| cf. *Clyphaspidella* | |
| *Blainia gregaria* Walcott | |
| *Helcionella*, sp. | |
| Undescribed and unidentified trilobite genera | |
| Total thickness of Hodges Shale Member | 540 |
| Total thickness of Bloomington Formation | 1495 |
| Blacksmith Formation | |
| 26. Dolomite: light gray unevenly banded with neutral gray, thick-bedded, medium-crystalline; weathers to low sloping outcrops with rough sugary surfaces | 80 |
| 25. Limestone: dark bluish gray, thin- to medium-bedded with uneven bedding planes; weathers to dark-bluish-gray rough surfaces | 60 |
| 24. Dolomite: very light gray, thick-bedded, medium-crystalline, and interbedded with thicker, more numerous beds of a blotchy mottled thick-bedded dolomite of same colors | 145 |
| 23. Dolomite: very light gray, thick-bedded, medium-crystalline; some limonite stains in the weathered pieces; weathers to very light-buff sugary surface | 50 |
| 22. Dolomite: dark medium gray, thick-bedded, medium-crystalline; arenaceous | 55 |
| 21. Dolomite: very light gray, thick-bedded; contains many small calcite crystals and some limonite flakes and pseudomorphs after pyrite; weathers to drab, very light-buff sugary surface; some beds with dark-gray streaks and mottles in them | 95 |
| Total thickness of Blacksmith Formation | 485 |
| Ute Formation | |
| 20. Limestone: light-neutral-gray, thick-bedded, finely crystalline, slightly arenaceous limestone containing many small crystals of calcite; weathers to high light-neutral-gray ledges with rough sugary surfaces at base of unit; middle part of unit weathers to light lavender-tinged gray surface; upper part is darker gray and weathers to dark-gray ledges | 225 |
| 19. Limestone and sandstone: dark-blue-gray, thin-bedded, finely crystalline limestone interbedded with light-blue-gray, thin-bedded, fine-grained calcareous sandstone. *"Girvanella,"* ½–1½ inches in diameter, very common | 125 |
| 18. Limestone: dark blue gray, medium-bedded, finely crystalline, arenaceous; some beds more sandy than others; interbedded with thinner beds of very dark-blue-gray, very thin-bedded, medium-grained, oölitic, fossiliferous limestone. Fossil locality 101 ml | 110 |
| Fossils: (101 ml) | |
| *Olenoides*, sp. | |
| *Alokistocare*, sp. | |
| 17. Shale: tea-green, thin-bedded shale which weathers on outcrops to mahogany-red platy pieces | 30 |
| 16. Limestone: dark-blue-gray, thin-bedded, finely crystalline limestone; some beds arenaceous; some dark-gray, rather nodular, fossiliferous limestone thinly interbedded at top of unit. *"Girvanella"* common and smaller than in unit 19 | 75 |
| 15. Shale: tea-green, thin-bedded shale which weathers to mahogany-red platy pieces | 35 |
| 14. Limestone: dark blue gray, finely crystalline, brittle; has ¼–½-inch thick arenaceous layers every ½–1 | |

| | Feet |
|---|---|
| inch which weather to light tan yellow; limestone weathers to light blue gray. In upper part of unit a very few *"Girvanella"* appear | 85 |
| 13. Shale: dull-greenish-citrine, thin-bedded, micaceous, arenaceous shale which weathers to a duller, drabber color | 15 |
| 12. Limestone and shale: citrine-yellow, thin-bedded micaceous, arenaceous shale interbedded with amber-brown to light-gray thin-bedded arenaceous finely crystalline limestone containing much limonite | 20 |
| 11. Limestone and shale: dull-citrine to citrine-yellow, thin-bedded, fine-grained, arenaceous, micaceous shale intercalated with thin layers of dark-bluish-gray thicker-bedded, finely crystalline, oölitic limestone, both of which are interbedded with 1–2-foot layers of dark-livid-brown to warm-blackish-brown, thick-bedded, finely crystalline, oölitic limestone | 10 |
| 10. Sandstone and limestone: citrine-yellow, thin-bedded, fine-grained, calcareous, shaly, micaceous sandstone interbedded with mottled neutral-gray and deep-livid-brown, thin-bedded, finely crystalline, silty limestone which weathers to dull mahogany red and which is overlain by a bed of purer dark-green-blue-gray finely crystalline, slightly arenaceous limestone which shows shadows of oölitic structure | 15 |
| Total thickness of the Ute Formation | 745 |
| Langston Formation | |
| 9. Limestone: medium bluish gray, thick-bedded, finely crystalline; weathers to very light bluish gray, lined with very light-gray streaks parallel to bedding | 35 |
| 8. Dolomite: mottled, neutral gray to dark neutral gray, thick-bedded, finely crystalline; becomes less mottled, lighter in color, and arenaceous toward top of unit; weathers to reddish-buff, sugary-surfaced chunks | 35 |
| 7. Limestone: dark neutral gray to bluish gray, thick-bedded, finely crystalline; some small veins light tan to buff on weathered surfaces; some beds slightly nodular; *"Girvanella"* in upper part of unit but not numerous | 155 |
| 6. Covered interval: much limestone float; bank in lower part as well as scarcity of limestone float indicate contact of shale (described below) and limestone in lower part of interval | 35 |
| *Spence Shale Member* | |
| 5. Shale: dark grayish olive to olivaceous black, calcareous; weathers to small deep-olive-buff to olive-buff chips, fossiliferous; forms smooth low slopes | 185 |
| 4. Limestone and shale: vinaceous-fawn-colored, thin-bedded, calcareous, fossiliferous shale containing lenses of finely crystalline, dark-gray limestone. Fossil localities 101 a2d and 101 a2c at top of this unit | 7 |
| Fossils: (101 a2d and 101 a2c) | |
| *"Agnostus"* | |
| *Alokistocare*, sp. | |
| *Bathyuriscus* | |
| *Chancia* | |
| *Clappaspis* | |
| *Clavaspidella* | |
| *Elrathia* | |
| *Kochina* | |
| *Olenoides* | |
| *Oryctocephalus* | |
| *Pachyaspis* | |
| *Pagetia* | |
| *Spencia* | |
| *Taxioura* (*Ogygopsis*) | |
| Total thickness of Spence Shale Member | 192 |
| *Naomi Peak Limestone Member* | |
| 3. Limestone, shale, and calcareous sandstone: dark-bluish-gray, thick- to thin-bedded, finely crystalline to medium-crystalline, fossiliferous, slightly arenaceous limestone interbedded and intercalated with vinaceous-fawn-colored, calcareous, fossiliferous shale. Few feet of dark-neutral-gray, medium-bedded, medium-grained, very calcareous sandstone at base: sandstone weathers to between deep olive buff and olive buff low outcrops; calcareous cement leaches out easily on weathered surfaces and is not present ½–1 inch from outside | |

| | Feet |
|---|---|
| surface. Fossil localities 101 a2, 101, a2a, 101 a2b. | |
| Fossils: ("*Ptarmigania*" strata) | |
| *Albertella* | |
| *Clavaspidella* | |
| *Dolichometopsis* | |
| *Kochaspis* | |
| *Kochiella* | |
| *Kochina* | |
| *Oryctocephalus* | |
| *Poulsenia* | |
| *Prozacanthoides* | |
| *Ptarmigania* | |
| Thickness of Naomi Peak Member..... | 32 |
| Total thickness of Langston Formation.. | 484 |

LOWER CAMBRIAN AND PRECAMBRIAN (?)

Pioche (?) Shale

2. Shale and quartzite: greenish-buff, micaceous, fucoidal, sandy, and silty shale in beds 2–4 feet thick interbedded with thin- to medium-bedded, fine- to medium-grained, dark-reddish-brown, purple, green, and pink sandstone and quartzite in beds 10–20 feet thick. Weathers darker brown than underlying quartzite and contains much more shale. Thickness of formation not measured but estimated to be about 150 feet on south side of High Creek Canyon at forks.

Prospect Mountain Quartzite

1. Quartzite: pink to red, medium-grained, cross-bedded thick-bedded units interbedded with few purple and green units. Not measured, but estimated to exceed 3000 feet. (Thickness in south part of Preston quadrangle, about 10 miles north of High Creek, given by Williams (1948, p. 1132) as 4800 feet with base not exposed).

*Section on the North Fork of Mill Creek and Spence Gulch section.*—Spence Gulch, the type locality of the Spence Shale Member of the Langston Formation, is a tributary of the Left Fork of Mill Creek. It joins this fork in sec. 12, T. 13 S., R. 42 E. (Boise Base and Merid ian), and extends about 1 mile southeastward from the junction before it opens into a rather wide basin. Only parts of the Prospect Mountain Quartzite and Spence Shale are well exposed, and other formations are covered with soil. The Spence Shale, however, can be traced northward along the strike to excellently exposed outcrops of the lower Middle Cambrian formations in sec. 2, T. 13 S., R. 42 E., on the divide between Mill Creek and the North Fork of Mill Creek. Here, a partial section, including the lower part of the Ute Formation, the Langston Formation, and the upper part of the Prospect Mountain Quartzite, was measured and described by the writer in 1940. This locality is probably the same as, or very close to, the locality where Walcott described the Middle Cambrian formations on "Mill Creek, west of Liberty" (Resser, 1939b, p. 13–14) in 1906. Walcott's descriptions, especially of the Langston Formation, do not agree with the observations of the writer, whose Mill Creek section is given here.

*North Fork of Mill Creek Section, Bear River Range*

MIDDLE CAMBRIAN

| | Feet |
|---|---|
| Ute Formation | |
| 7. Limestone and shale: poorly exposed outcrops of light-green to greenish-tan fissile shale interbedded with dark-gray, compact, thin- to medium-bedded argillaceous limestone..... | not measured |
| Langston Formation | |
| 6. Dolomite: light gray to dark gray, finely to coarsely crystalline, compact to porous with much limonite along joint cracks and bedding planes, medium-bedded to massive; weathers to bright orange-tan slopes and to dull, dark-tan, blocky, sugary-surfaced outcrops..... | 155 |
| 5. Limestone: dark neutral gray, finely crystalline, thin- to medium-bedded; some beds contain silty partings and mottles..... | 170 |
| 4. Limestone and shale: very poorly exposed outcrops of unit 5 shale in lowe ¾ of unit..... | 80 |
| *Spence Shale Member* | |
| 3. Shale: fuscous black and light tea green poorly exposed, argillaceous, fossiliferous..... | 65 |
| 2. Covered interval: contact of the shale with "*Ptarmigania* strata", and contact of Naomi Peak member with Prospect Mountain quartzite (?) probably concealed by soil in this interval..... | 20 |

| | Feet |
|---|---|
| Total thickness of Spence Shale and Naomi Peak Member | 85 |
| Total thickness of Langston Formation | 490 |

LOWER CAMBRIAN AND PRECAMBRIAN (?)

Prospect Mountain Quartzite (?)

1. Sandstone: army brown, medium-grained, slightly calcareous, micaceous, medium-bedded....not measured

The writer also measured, described, and collected from the Spence Shale at the type locality. R. A. Spence, son of the discoverer of the Spence Shale at Spence Gulch, showed the writer the exact place in Spence Gulch where he recalled that Walcott measured and collected from the Spence Shale Member. Spence Gulch is a strike valley cut in the Spence Shale; the east side of the valley is a dip slope of the more resistant Prospect Mountain quartzite, and the west side is formed of the limestone and dolomite overlying the Spence shale. Most of the shale member is covered, but, midway between the head and mouth, the stream has undercut the west side of the gulch and removed the soil, thus exposing a steep outcrop which Walcott designated the type locality of the Spence shale. The writer re-measured and collected from the Spence at this locality (Fig. 1).

MIDDLE CAMBRIAN

Feet

Langston Formation

5. Dolomite: very light to dark gray, finely to coarsely crystalline, compact to porous with much limonite along joint cracks and bedding planes, medium-bedded to massive; weathers to bright orange-tan slopes....not measured
4. Limestone: dark neutral gray, compact, thin- to medium-bedded not measured

*Spence Shale Member*

3. Covered interval....not measured
2. Shale; fuscous black and light tea green; argillaceous, fossiliferous.... 50

Fossil locality 111a

Fossils: (111a)

| | |
|---|---|
| *"Agnostus"* | *Elrathia* |
| *Alokistocare* | *Zacanthoides* |
| *Bythicheilus* | *Acrotreta* |
| *Bathyuriscus* | *Acrothele* |
| *Chancia* | *Iphidella* |
| *Clappaspis* | *Hyolithes* |

| | Feet |
|---|---|
| Covered interval | 20 |
| Total thickness of Spence Shale | 70 |

LOWER CAMBRIAN AND PRECAMBRIAN (?)

Prospect Mountain Quartzite (?)

1. Sandstone and quartzite: poorly exposed outcrop of white, medium-grained, medium-bedded sandstone with flecks of limonite which overlies purplish to maroon, medium-grained, medium-bedded quartzite not measured

*Section in the Left Fork of Blacksmith Fork Canyon.*—This section is on the north side of the canyon (Fig. 1); the base of the measured section is in the NW ¼ sec. 23, T. 11 N., R. 3 E., on the prominent spur about a quarter of a mile east of the Lucky Star mine. The line of the section runs northerly up the spur.

Outcrops of lower Middle Cambrian formations are well exposed from the Prospect Mountain-Langston contact upward to the Blacksmith-Bloomington contact. The Spence Shale Member is absent at this locality as at Blacksmith Fork and at Temple Ridge, and the lower dolomite of the Langston is thicker and conformable with the Prospect Mountain Quartzite.

MIDDLE CAMBRIAN

Feet

Bloomington Formation....not measured

Blacksmith Formation

23. Dolomite: between medium and dark neutral gray, finely crystalline, thin- to medium-bedded; many beds are oölitic; one bed near the top of the unit is light mouse gray, compact, saccharoidal.... 85
22. Dolomite: banded neutral gray and dark gray, darker bands approximately 6 feet thick, light bands approximately 20 feet thick; light band composed of very compact, very dolomitic limestone and dolomite which is laminated and weathers to smoke-gray surfaces; contains splotches of limonitic, silty material; dark-gray bands are composed of coarsely crystalline, medium-bedded dolomite. Mud cracks observed in the basal light band.... 45

| | Feet |
|---|---|
| 21. Dolomitic limestone: neutral gray, laminated, very compact; laminae show very plainly on smoke-gray weathered surfaces; laminae slightly silty at base of unit, siltier and sandy up section | 45 |
| 20. Dolomite: light neutral gray, finely crystalline, thick-bedded; saccharoidal | 25 |
| 19. Dolomite: blackish gray, very finely crystalline, compact, thin- to medium-bedded; very uneven bedding planes; contains veinlets of calcite and limonite; slightly fetid; weathers to low outcrops slightly darker | 15 |
| 18. Dolomite: light neutral grav, finely crystalline, thick-bedded; sugary-textured | 80 |
| 17. Dolomite: dark neutral gray, very finely crystalline, medium-bedded; weathers to sugary-surfaced, slightly lighter-gray, prominent outcrops; banding due to slightly different grain size of lighter and darker shades of gray at the base | 30 |
| Total thickness of the Blacksmith Formation | 325 |
| *Ute Formation* | |
| 16. Limestone: dark gray, finely crystalline, compact, brittle, thin- to medium-bedded; weathers to tan-surfaced, blocky ledges; silty partings or relatively even bedding planes; some bedding planes very uneven; fossiliferous in middle part of unit | 85 |
| 15. Oölitic limestone: light-gray matrix with dark-gray oölites approximately 1 mm. in diameter; thick to thin-bedded | 70 |
| 14. Limestone: dark gray, very finely crystalline, compact, thin- to medium-bedded, very pure; fossiliferous at base of unit; some algal and intraformational conglomerate beds; some beds sandy | 235 |
| Fossil locality 105 k | |
| Fossils: (105 k) | |
| *Olenoides* | |
| *Alokistocare* | |
| *Acrotreta* | |
| 13. Covered interval: float indicates that unit is similar to unit 14 | 50 |
| 12. Silty limestone and shale: very light-bluish-gray, laminated, silty limestone interbedded with dark-olive shale; few interbedded layers of dark-gray, very finely crystalline, thin- to medium-bedded, pure limestone. Outcrops poorly exposed | 15 |
| 11. Limestone: light gray, finely crystalline, thin-bedded, silty; interbedded with dark-gray, very finely crystalline, compact, thin- to thick-bedded limestone with many silty-concentrated layers and areas which stand in relief on weathered surfaces and which weather light tan | 85 |
| 10. Siltstone and shale: very light-bluish-gray, laminated, calcareous siltstone which grades into, and is interbedded with, very pure, dark-olive to citrine-drab shale | 15 |
| 9. Limestone: dark gray, finely crystalline, thin- to medium-bedded; silty; contains siltier mottles and streaks which weather to dull light tan and stand in relief on weathered surfaces; outcrops poorly exposed; some limestone very pure | 80 |
| 8. Covered interval: talus-covered slope; talus resembles unit 9 | 30 |
| 7. Shale: citrine drab, laminated; weathers to argus-brown; fissile; outcrops on well-exposed slopes | 10 |
| Fossils: (105 F) | |
| *Elrathina?* | |
| Total thickness of Ute Formation | 675 |
| Langston Formation | |
| 6. Dolomite: dark gray, finely crystalline, medium-bedded to massive, weathers to dark-tan, sugary-surfaced, high ledges | 65 |
| 5. Limestone: dark gray, finely crystalline, thick-bedded, many flecks of limonite disseminated throughout rocks; few beds of intraformational conglomerate and algal limestone; fossiliferous. Fossil locality 105 D 20 feet from base of unit | 40 |
| Fossils: (105 D) | |
| *Glossopleura* | |
| *Glyphaspis?* | |
| 4. Limestone: light neutral gray, very finely crystalline, compact, laminated, saccharoidal; weathers to smooth light-tan surfaces | 8 |
| 3. Dolomite: light neutral gray, medium crystalline, massive; weathers to tan, sugary-surfaced, high ledges | 125 |
| 2. Dolomite: medium gray, finely crystal- | |

| | Feet |
|---|---|
| line, compact, medium-bedded to massive; very sandy at base, less sandy upward in section; weathers to dark-tan, sugary-surfaced outcrops | 100 |
| Total thickness of Langston Formation | 338 |

LOWER CAMBRIAN AND PRECAMBRIAN (?)

Prospect Mountain Quartzite (?)

1. Sandstone and shale: brownish-white, medium-bedded to massive, medium- to fine-grained sandstone of speckled appearance due to fine limonite grains disseminated throughout; thin layers of interbedded, tawny-olive, micaceous, limonitic shale ..... not measured

*South Cottonwood Canyon section, Blacksmith Fork.*—South Cottonwood Canyon is approximately 11 miles east of Hyrum, Utah, and is a tributary to Blacksmith Fork. The following section was measured on the west side of the canyon in SE ¼ sec. 18, T. 10 N., R. 3 E. The base of the section is approximately 1 mile south of the base of the section Deiss measured in 1937.

In this section, as in the sections in Blacksmith Fork, in the Left Fork of Blacksmith, and on Temple Ridge, the Spence Shale Member is not present, and the lower dolomites of the Langston Formation are thicker and conformable with the Prospect Mountain Quartzite (?).

MIDDLE CAMBRIAN

Langston Formation

| | Feet |
|---|---|
| 4. Dolomite: light to dark gray, finely to coarsely crystalline, compact to porous with much limonite along joint cracks and bedding planes, medium-bedded; weathers to bright orange-tan slopes and to dull tan, blocky, sugary-surfaced outcrops; nonfossiliferous | 285 |
| 3. Limestone: dark neutral gray, compact, thin- to medium-bedded, nodular; contains many buff to tawny-olive limonitic partings; several beds of intraformational conglomerate; few algal and oölitic beds; fossiliferous at center of unit. Fossil locality 97 b 25 feet from base of unit | 50 |
| Fossils: (97 b) *Glossopleura* *Clavaspidella?* | |
| 2. Dolomite: dark-gray, finely crystalline, pact, limonitic dolomite, unfossiliferous | 55 |
| Total thickness of Langston Formation | 390 |

LOWER CAMBRIAN AND PRECAMBRIAN (?)

Prospect Mountain Quartzite (?)

1. Sandstone: brownish white, medium-bedded to massive, medium- to fine-grained; characteristic speckled appearance due to fine grains of limonite shot through the sandstone; weathers to dark reddish-tan, poorly exposed outcrops ..... not measured

*Blacksmith Fork section.*—This section was measured by Walcott (1908a, p. 5–9) and was established by him as one of the most important Cambrian sections in the Western Cordillera. All the formations named by him have been recognized throughout northeastern Utah and southeastern Idaho. Adoption and use of the formational names by geologists of the U. S. Geological Survey (Mansfield, 1927; Blackwelder, 1909; Richardson, 1913; 1941) and Deiss' (1938, p. 1105–1124) excellent redefinition of them bolstered their validity and greatly extended the area in which they were used. Resser's (1939b, p. 6–7) discussion of the Cambrian section in the area further influenced geologists to accept the Blacksmith Fork section as the standard for northern Utah and southern Idaho.

The observations of the writer coincide with Deiss' (1938, p. 1105–1124) descriptions. Therefore, the section is not redescribed in this report. The Blacksmith Fork section (Fig. 1) is not the most representative or "typical" of Cambrian stratigraphy in the Bear River Range. Two near-by sections, the High Creek and Calls Fort sections, are better exposed and more easily accessible, and contain more typical formations and more faunal horizons. The prominent lithofacies change in the Langston Formation where the Spence Shale and Naomi Peak Limestone Members pinch out to the southeast begins only a few miles north and west of Blacksmith Fork, and these two members are missing in the Blacksmith Fork section. They are important markers throughout the rest of the area from the Logan River to the

Bannock Range and from the east side of the Bear River Range to west of the Wasatch Range and Wellsville Mountain. Thus the High Creek section, which is thicker and more centrally located within the area of outcrop of the formations, contains formations with more typical facies and more numerous faunal horizons. For these reasons, the High Creek section is considered the "standard" for northeastern Utah and southeastern Idaho in this paper.

### *North Part of the Wasatch Range, Utah*

*General statement.*—The Wasatch Range extends from Mt. Nebo, just northeast of Nephi, Utah, northward approximately 140 miles to the north end of Wellsville Mountain, about 20 miles north of Brigham City, Utah. Northward from Wellsville Mountain is a broad low gap through which Bear River has cut a deep canyon. This gap is bounded on the north by the south end of the Malad Range. The Bear River Range is an east prong of the Wasatch Range which branches eastward from the main range in the latitude of Brigham City and then parallels it on the opoosite side of Cache Valley for early 30 miles. The Wasatch Range is complexly folded and faulted, and outcrops of rocks of Cambrian age are common especially along the west front. Well-known exposures occur on Wellsville Mountain, especially east of the Calls Fort monument, about 7 miles north of Brigham City, Utah; in the vicinity of Ogden Canyon east of Ogden, Utah; and in Big Cottonwood Canyon, east of Salt Lake City, Utah (Fig. 1). The formations in Wellsville Mountain are all lithogenetic equivalents of the formations in the Bear River Range, and the Cambrian section near Calls Fort is probably as nearly complete as any section in northern Utah. South of Brigham City, Utah, the Cambrian section is incomplete, and evidence presented in the following paragraphs suggests that most of Medial Cambrian and all of Late Cambrian time is unrepresented by rocks in most of the Wasatch Range. Cambrian sediments similar to those in the Bear River Range were probably deposited but were removed by erosion before Late Devonian time, although the Medial Cambrian-Devonian hiatus in the Wasatch Range may, in part, also represent a period of nondeposition.

*Calls Fort section.*—Cambrian rocks are well exposed in the Calls Fort area on the west side of Wellsville Mountain from far down in the Prospect Mountain Formation to the contact of the St. Charles Formation (Upper Cambrian) with the Garden City Limestone (Ordovician). The west side of the mountain is steep, and the rock outcrops occur chiefly as cliffs and high ledges. These excellently exposed outcrops extend from the latitude of Brigham City to a few miles north of the Calls Fort monument, a distance of more than 8 miles.

Field parties of the 40th Parallel Survey (1867–1877) were probably the first geologists to examine and collect fossils from the Cambrian rocks in this area. During this period, Meek collected fossils from the formations between the Prospect Mountain ("Brigham") Quartzite and the Blacksmith Formation (Resser, 1939b, p. 8, 12), and Resser and others collected from a near-by locality in 1926 (Resser, 1939b, p. 8, 12). Although this section is one of the most extensive, best exposed, and most readily accessible of the Cordilleran Cambrian sections, none of these workers measured and described it in detail. Walcott (1908a, p. 8–9) named it the type locality for the Brigham quartzite and published an estimated thickness of 2000 feet for it. Resser (1939b, p. 12) described former work in the vicinity of Brigham City, published an incomplete description of part of the Ute Formation, and listed fossils which are from mixed collections but presumably came from the Naomi Peak Limestone Member (his "*Ptarmigania* strata"). He had previously (1939a, p. 2–3) listed the same fossil localities for collections of specimens which he said were presumably from the Spence Shale Member.

Williams and Maxey (1941, p. 276–285) briefly mentioned the significance of the sequence of Cambrian formations in the Calls Fort section. Denson (1942, p. 23–27) measured the upper part of the Middle Cambrian section in 1941 and collected from three important fossil zones. He also described the Calls Fort Shale Member of the Bloomington Formation and designated the west side of Wellsville Mountain, near the Calls Fort monument, as its type locality. Williams (1948, p. 1131–1135) mentioned the Cambrian rocks in Wellsville Mountain and briefly described the relationships between the formations there and in the Logan quadrangle.

The following section was measured and described by the writer in 1940. The lower part was further examined and remeasured in 1950. The base of the section is on the ridge between the second and third canyons south of a point due east of the Calls Fort monument (Fig. 1) and is in the SE ¼ of sec. 14, T. 10 N., R. 2 W.

The line of the section follows the ridge upward and northeastward. The upper part of the section (from the top of the middle member of the Bloomington Formation to the top of the Bloomington Formation) was measured on the second spur to the north, on the north side of Precipice Canyon.

The best and most readily accessible exposures of the Spence Shale Member and the Bloomington Formation in northern Utah and southeastern Idaho occur on Wellsville Mountain. Walcott's type locality of the Brigham quartzite is approximately 5 miles south on the first prominent spur of the Mountain, north of Brigham City.

*Calls Fort Section, Wasatch Range*

UPPER CAMBRIAN

Nounan Formation

| | Feet |
|---|---|
| 31. Dolomite: neutral gray, finely crystalline, thin-bedded to laminated; weathers to lighter-gray sugary-outcrops | 85 |

MIDDLE CAMBRIAN

Bloomington Formation

| | |
|---|---|
| 30. Limestone: dark neutral gray, finely crystalline, medium- to thick-bedded; fossiliferous; contains two oölitic beds near top of unit | 35 |
| *Calls Fort Shale Member* | |
| 29. Shale and limestone: neutral-gray, slightly calcareous shale; contains nodules of slightly lighter-gray limestone which tend to weather out, leaving holes on the faces of well-exposed outcrops; shale weathers to dark-olive-buff, blocky outcrops. Few interbedded thin layers of oölitic dark-gray limestone and dark-neutral-gray, finely crystalline thin-bedded limestone throughout | 200 |
| Total thickness of Calls Fort Shale Member | 200 |
| 28. Limestone: dark neutral gray, finely crystalline, thin-bedded; irregularly interbedded and intermingled with thin beds and irregular masses of fawn-colored siltstone and shale which stand in relief on weathered surfaces at base of unit; this is overlain by dark-neutral-gray to neutral-gray, thin-bedded, finely crystalline limestone shot through with very thin shaly partings and specks and veinlets of calcite. Top of unit contains a few oölitic beds which have sandy and silty partings which weather in relief to very light buff | 515 |
| *Hodges Shale Member* | |
| 27. Shale and silty limestone: dark-mouse-gray, micaceous shale which weathers to drab (when well exposed weathers to between army brown and natal brown); limestone is dark neutral gray, finely crystalline, thin-bedded; irregularly interbedded and intermingled with thin beds and irregular masses of fawn-colored siltstone and shale which stand in relief on weathered surfaces. In weathered outcrops units is tawny olive. Fossiliferous, brachiopods throughout upper part of unit. Fossil locality 103 cc at top of unit | 335 |
| Fossils: (103 cc)<br>*Olenoides*<br>*Hyolithes*<br>*Westonia*<br>*Lingulella*<br>*Obolus* | |
| Fossils locality 103 ccl is 125 feet from top of unit. | |
| Fossils: (103 ccl)<br>*Olenoides*<br>Undescribed genera | |
| Fossil localities 103 cc2 and 103 cc3 are 175 feet from top of unit. | |
| Fossils: (103 cc2) (103 cc3)<br>*Olenoides*<br>Undescribed genera | |
| Total thickness of Hodges Shale Member | 335 |
| Total thickness of Bloomington Formation | 1085 |

Blacksmith Formation

| | |
|---|---|
| 26. Dolomite and dolomitic limestone: mostly light neutral gray with few beds of dark neutral gray, compact to medium crystalline; not remarkably banded in contrast to unit 25; some laminated beds; weathers to pale smoke gray. Dolomitic limestone chiefly in upper fourth of unit | 395 |
| 25. Dolomite: neutral gray and dark neutral gray, fine to medium crystal- | |

| | Feet |
|---|---|
| line, massive; cliffs banded by alternating lighter and darker shades; cross-bedding common; some oölitic beds | 410 |
| Total thickness of the Blacksmith Formation | 805 |
| Ute Formation | |
| 24. Limestone: dark neutral gray, finely crystalline, thin-bedded, sandy; silty and sandy partings present but not conspicuous; upper third of unit notable for irregular streaking of dark neutral and light neutral gray; grades into dolomite | 90 |
| 23. Sandstone: dark neutral gray, fine-grained, thin-bedded, calcareous, micaceous; silty and sandy partings and sandier beds weather to tawny-olive surfaces; some cross-bedding | 113 |
| 22. Shale: citrine drab, laminated, micaceous, weathers to argus brown on well-exposed surfaces | 5 |
| 21. Limestone: dark neutral gray, finely crystalline, thin-bedded, sandy; bedding marked by very conspicuous laminae of fine sand and silt that weather into relief to between natal and bone brown; gray layers weather to much lighter gray | 30 |
| 20. Shale: citrine crab, laminated; weathers to argus brown on well-exposed surfaces; fossiliferous. Fossil locality 103 t at base of this unit | 40 |
| Fossils: (103 t) | |
| *Olenoides* | |
| *Ehmaniella* (?) | |
| *Obolus* | |
| 19. Limestone: neutral gray to dark neutral gray, oölitic and finely crystalline; lower compact phase thin-bedded; upper oölitic phase medium-bedded to massive; conspicuous beds of edgewise-conglomerate at base of unit; conglomerate contains pebbles 1–1½ inches long. Oölitic bed 50 feet from top of unit is fossiliferous. Fossil locality 103 s | 80 |
| Fossils: (103 2) | |
| *Olenoides* | |
| *Alokistocare* | |
| 18. Shale: citrine drab, laminated; weathers to argus brown on well-exposed surfaces | 6 |
| 17. Limestone; dark neutral gray, finely crystalline, thin-bedded, sandy; bedding marked by very conspicuous laminae of fine sand and silt, between natal and bone brown that weather into relief; gray layers weather to much lighter gray | 30 |
| 16. Shale; citrine drab, laminated, weathers to argus brown on well-exposed surfaces | 3 |
| 15. Limestone: dark neutral gray, finely crystalline, thin-bedded, sandy; bedding marked by very conspicuous laminae of fine sand and silt, natal and bone brown that weather into relief; gray layers weather to much lighter gray | 26 |
| 14. Shale: citrine drab, laminated; weathers to argus brown on well-exposed surfaces | 3 |
| 13. Limestone: dark neutral gray, algal (*Girvanella?*), oölitic, finely crystalline; thin- to medium-bedded, sandy; characterized by silt and clay partings which weather to tawny olive and stand in relief on weathered surfaces; upper part of unit is thin-bedded | 80 |
| 12. Shale; citrine drab, laminated, weathers to argus brown on well-exposed surfaces | 7 |
| 11. Limestone: dark neutral gray, oölitic, thin-bedded, some cross-bedded; lower and upper quarters of unit characterized by conspicuous silty partings which weather to tawny olive and stand in relief. *Girvanella?* conspicuous in upper part | 40 |
| 10. Shale: citrine drab, laminated; weathers to argus brown on well-exposed surfaces | 3 |
| 9. Limestone: dark neutral gray, massive, oölitic; upper third of unit lighter color and thinner-bedded with conspicuous silt partings | 35 |
| 8. Shale: citrine drab, laminated; weathers to argus brown on well-exposed surfaces; fossiliferous. Fossil locality 103 F | 4 |
| Fossils: (103 F) | |
| *Glossopleura*, sp. | |
| *Kootenia* | |
| *Zacanthoides* | |
| *Acrotreta* | |
| *Acrothele* | |
| *Iphidella* | |

| | Feet |
|---|---|
| *Hyolithes* | |
| Total thickness of Ute Formation | 621 |
| Langston Formation | |
| 7. Dolomite: light gray, fine to medium crystalline, massive; weathers to buff-brown, sugary surfaces; middle portion characterized by irregular banding due to slightly different crystal size expressed in color on weathered surfaces, the finely crystalline parts appearing slightly darker | 90 |
| 6. Limestone and siltstone: dark-neutral-gray, finely crystalline, nodularly bedded limestone with irregular partings of silty limestone which stand in relief on weathered surfaces and weather to between natal and bone brown. Siltstone is smoke gray, calcareous, laminated; forms upper three quarters of unit | 20 |
| *Spence Shale Member* | |
| 5. Shale: neutral gray, laminated, calcareous; weathers to citrine olive and, on well-exposed outcrop surfaces and edges; to mahogany red; unit remarkably uniform; fossiliferous; lower 15 feet fuscous-black, laminated shale which weathers to light-drab surfaces. Fossil locality 103 c | 125 |
| Fossils: (103 c) | |
| *Bathyuriscus* | *Spencia* |
| *Alokistocare* | *Clavaspidella* |
| *"Agnostus"* | *Acrothele* |
| *Elrathia* | *Iphidella* |
| *Chancia* | *Wimanella* |
| *Glossopleura* | *Hyolithes* |
| *Taxioura-Ogygopsis* | |
| 4. Silty limestone and shale: thin-bedded to laminated silty limestone; laminations marked by clay-rich laminae, between natal and bone brown that stand in relief on weathered surfaces; lower half of unit with 2 layers of fuscous-black, laminated, calcareous, fossiliferous shale | 50 |
| Total thickness of Spence Shale Member | 175 |
| *Naomi Peak Limestone Member* | |
| 3. Limestone: saccharoidal, light neutral gray, finely to medium crystalline, porous, some oölites; massive, sandy throughout, some sand concentrated in wavy, discontinuous partings that stand in relief on weathered surfaces. These are Resser's *"Ptarmigania* strata". Fossil locality 103 A | 25 |
| Fossils: (103 A) | |
| *Ptarmigania* | |
| *Albertella* | |
| *Taxioura (Ogygopsis)* | |
| *Clavaspidella* | |
| *Kochaspis* | |
| *Prozacanthoides* | |
| *Oryctocephalus* | |
| Total thickness of Langston Formation | 310 |

LOWER CAMBRIAN

Pioche (?) formation

2. Quartzite and shale: reddish-brown, medium-grained and purple quartzite interbedded with a few dark-green, medium-grained quartzite layers; all quartzite thin- to medium-bedded and interbedded with numerous thin (2 inches to 4 feet thick) beds of green and tan, micaceous, fucoidal shale ..... 125

LOWER CAMBRIAN AND PRECAMBRIAN (?)

Prospect Mountain Quartzite

1. Quartzite: red and pink, generally medium-bedded to massive medium-grained quartzite flecked with limonite pseudomorphs and some beds containing a few pebbles interbedded with a few thin beds of dark-green, medium-bedded, medium-grained quartzite; weathers to brownish-red and pink slopes, much lighter in hue than overlying Pioche (?) formation. Not measured, but estimated by Walcott to be 2000+ feet thick. Base not exposed.

*Willard Peak section.*—Willard Peak is about 10 miles south of Box Elder Canyon and 4 miles southeast of the town of Willard, Utah (Fig. 1). It is the nearest point south of Wellsville Mountain at which a sequence of Cambrian quartzite, shale, and limestone is exposed, because between Brigham City and Willard the range is complexly faulted, and exposures consist chiefly of poorly exposed, brecciated quartzite. No-

where on the long north-south ridge of which Willard Peak is the highest point is there a complete section of Lower and Middle Cambrian formations. However, a considerable thickness of sediments, including the Prospect Mountain Quartzite, Pioche (?) shale, and part of the Langston Formation, are exposed as part of a thrust sheet near the top of the mountain. The upper part of the Langston Formation is cut off by a thrust fault, and along the trace of this fault Prospect Mountain Quartzite overlies the limestone. This incomplete section is of considerable significance in the Cambrian stratigraphy of the Wasatch Range because the complete section of the Prospect Mountain Quartzite is exposed, lying unconformably on Precambrian gneiss and schist. The section has been briefly mentioned by Blackwelder (1909, p. 519–526) and by Eardley and Hatch (1940, p. 835–837).

The base of the section is about 2000 feet down from the crest of the ridge near the head of Willard Canyon and at the contact of the Precambrian gneiss and the Prospect Mountain Quartzite. The line of the section runs eastward and up the cliffs to within about 300 feet of the crest of the ridge, where the trace of an overthrust mass of Prospect Mountain Quartzite cuts off the upper part of the Langston Formation.

*Willard Peak Section, Wasatch Range*

LOWER CAMBRIAN AND PRECAMBRIAN (?)

Prospect Mountain Quartzite

| | Feet |
|---|---|
| 10. Quartzite: red, yellow, and white, medium-grained, medium-bedded to massive, much shattered and deformed. Thickness not measured. | |
| Trace of thrust fault | |
| 9. Poorly exposed interval covered with small shattered fragments of quartzite and mylonitic material. | |

MIDDLE CAMBRIAN

Langston Formation

| | |
|---|---|
| 8. Limestone and dolomite: dark-gray, finely crystalline thin- to medium-bedded limestone with silty and shaley partings; weathers to light-gray ledges and cliffs; interbedded with several 4- to 10-foot thick green, phyllitic or slaty shale units with few beds of green micaceous fine- to medium-grained sandstone. | 100 |
| 7. Limestone: similar to limestone unit 8 but with no phyllitic shale | 75 |
| 6. Shale: green, phyllitic or slaty, arenaceous with many micaceous layers | 58 |
| 5. Limestone and dolomite: dark-gray, finely crystalline thin- to medium-bedded argillaceous limestone with many silty partings; weathers to light-grey ledges and is interbedded with a few 1- to 4-foot thick units of steel-gray, finely crystalline, medium-bedded dolomite which weathers to tan and dark-brown blocky ledges | 95 |
| 4. Shale: greenish brown, phyllitic or slaty; weathers to light-gray-green ledges | 62 |
| 3. Limestone and dolomite: similar to limestone and dolomite of unit 5 but with considerably more dolomite and a few sandy limestone beds near base of unit | 18 |
| Total thickness of Langston Formation measured | 408 |

LOWER CAMBRIAN

Pioche Shale

| | |
|---|---|
| 2. Shale, sandstone, and quartzite: greenish-brown phyllitic and slaty shale units ranging from a few inches to 30 feet thick interbedded with brown and red, fine- to medium-grained, medium-bedded sandstone and quartzite in units 1–3 feet thick; forms slope at base of limestone cliffs and top of quartzite cliffs (see below) | 140 |
| Total thickness of Pioche Shale | 140 |

LOWER CAMBRIAN AND PRECAMBRIAN (?)

Prospect Mountain Quartzite

| | |
|---|---|
| 1. Quartzite: pink and light reddish tan, medium- to coarse-grained, thin-bedded to massive, with little interbedded shale. Estimated thickness 1200 feet, but thickness estimated to range from 700 to 1500 feet along strike within a mile north and south of line of section. Unconformably overlies Precambrian gneisses and schists. Estimated thickness | 1200 |
| Total thickness of Cambrian strata measured and estimated | 1750 |

*Ogden Canyon section.*—Ogden Canyon runs eastward from Ogden and is about 10 miles south of the Willard Peak area (Fig. 1). The same Cambrian formations are exposed in the Ogden Canyon area and between Willard and Ogden Canyon as are exposed in Willard Peak. These formations are parts of thrust sheets and in most places are only incompletely exposed and somewhat metamorphosed. The rocks of Cambrian age exposed in this area have been briefly discussed by Blackwelder (1909) and Eardley and Hatch (1940).

The Prospect Mountain Quartzite ranges from 1000 to 1500 feet in thickness. It unconformably overlies a thick series of gneisses, schists, quartzites, and argillites that have been referred to the Proterozoic and "Archean" by Blackwelder (1909, p. 520–526) and Eardley and Hatch (1940, p. 834–840). It is conformably overlain by a thin (125- to 175-foot thick) shale and quartzite unit, the Pioche Formation, which, in turn, is overlain by the limestone and shale beds of the Langston Formation. Probably nowhere in this part of the Wasatch Range is more than 500 or 600 feet of shale or limestone of Cambrian age exposed above the Prospect Mountain Quartzite. The writer has found unidentifiable fossil fragments only in these shales and limestones. Both Blackwelder (1909, p. 523) and Eardley and Hatch (1940, p. 835–837) reported that the limestone was fossiliferous, but published no fossil lists.

*Big Cottonwood Creek and Neffs Canyon sections.*—Cambrian rocks are poorly exposed in the Wasatch Range from just south of Ogden Canyon to Neffs Canyon, about 6 miles southeast of Salt Lake City, Utah, but in this canyon and in Big Cottonwood Creek Canyon, approximately 5 miles southeast, Cambrian formations are exposed as a part of a large fold which also contains older and younger rocks. As in Ogden Canyon and at Willard Peak, the rocks have been considerably folded and faulted and are somewhat metamorphosed.

Descriptions of the Cambrian formations in Big Cottonwood Canyon were published in the reports of the Fortieth Parallel Survey (Hague and Emmons, 1877, p. 366–378). The Cambrian rocks were divided into (1) Cambrian quartzites and slates, (2) primordial slates, and (3) "Ute" limestone. Fossils and lithologic samples collected by members of the surveys were further described by Walcott (1886, p. 38–39; 1890, p. 549–550; 1891, p. 156–160; 1908a, p. 12). Walcott (1908, p. 12) recognized that the "Primordial slates" were the equivalent of the Pioche Formation, but he did not describe the overlying limestone or the underlying quartzite. He considered the basal Cambrian quartzite conformable with the great thickness of quartzites and slates underlying it, which he called Algonkian (1890, p. 549–550). Only the Pioche Shale, which contains *Olenellus gilberti*, did he consider Cambrian. Blackwelder (1909, p. 520–523) discovered the angular unconformity between the quartzite of Cambrian age and the Algonkain (?) quartzite and slate, and pointed out that the Cambrian quartzite ranges from 1000 to 1500 feet in thickness and is conformable with the overlying Pioche Shale. Hintze (1913, p. 103–105) discussed the Big Cottonwood Canyon section and the unconformity at the base of the quartzite and suggested the name "Alta shale" for the shale between the basal quartzite and the limestone of Medial Cambrian age. He postulated an unconformity at the top of the shale, suggested that the limestone be called the Maxfield limestone, and recognized, as had Walcott and others, the unconformity between the top of the limestone and beds of Mississippian age. Burling (1914, p. 111–112) pointed out that the term "Alta shale" was not necessary and that there was probably no hiatus between the Pioche Shale and the "Maxfield limestone" because both contained faunas of early Medial Cambrian age. Since 1913, the U. S. Geological Survey (Calkins and Butler, 1943, p. 9–18) has applied the term "Ophir formation" to the shale and has accepted Hintze's "Maxfield limestone". Most workers have referred the quartzite at the base of the section to the "Tintic quartzite".

The writer measured the Cambrian shale and part of the limestone in Big Cottonwood Canyon (Fig. 1) in 1950 when he collected fossils from about the middle part of the limestone. The base of the measured section is at the top of the Prospect Mountain Quartzite in sec. 13, T. 2 S., R. 2 E. (Salt Lake Base and Meridian) and about 800 feet west of the Maxfield Mine. The line of the section is northeasterly up the slope. The formations are poorly exposed in this area, and many of the thicknesses are only estimates. However, the sequence of units is correct.

*Section in Big Cottonwood Creek Canyon, Wasatch Range*

MIDDLE CAMBRIAN

Langston Formation

6. Covered interval: drift suggests bedrock is limestone as in unit 5. Not measured.

Feet

5. Limestone: black gray to steel gray, finely crystalline thin-bedded, fossiliferous; with shaly and silty partings. Fossil locality CC1–50, about 20 feet above base ..... 50
Fossils:
*Glossopleura* cf. *producta* (Hall and Whitfield) *Spencia*, sp.
4. Quartzite: brownish tan, very fine-grained, laminated, somewhat calcareous; interbedded with a few beds of siltstone; weathers to blocky, dark-brown ledges ..... 20
3. Limestone: light gray, finely crystalline to porcellaneous-textured, contains some silty and shaly flecks and partings ..... 35
Total thickness of Langston Formation measured ..... 105

LOWER AND MIDDLE CAMBRIAN

Pioche Shale

2. Shale: greenish black, phyllitic shale and slate with many fucoidal markings on bedding planes ..... 175

LOWER CAMBRIAN AND PRECAMBRIAN (?)

Prospect Mountain Quartzite

1. Quartzite: brown, pink, and red, medium- to coarse-grained, thin-bedded to massive quartzite interbedded with a few thin (1–2 feet) layers of dark-green and brown phyllitic shale with many fucoidal markings. Not measured, but approximately 1000 feet thick. Unconformable with underlying Precambrian slate and quartzite.

In Neffs Canyon the Cambrian rocks are better exposed than in Big Cottonwood Canyon, and a stratigraphic section from the unconformity at the base of the Prospect Mountain Quartzite to the unconformity at the base of the Mississippian rocks was observed and measured in part. The base of the measured section is at the contact of the Pioche Shale and Prospect Mountain Quartzite on the first small south tributary of Neffs Canyon (Fig. 1) in sec. 6, T. 2 S., R. 2 E. (Salt Lake Base and Meridian). The line of the section is northwesterly up the slope to the top of the ridge, where the Mississippian limestones crop out as prominent ledges and cliffs.

*Neffs Canyon Section. Wasatch Range*

MISSISSIPPIAN

Feet

7. Limestone: massive, gray to dark gray finely to coarsely crystalline. Forms prominent ledges and cliffs. Not measured.

*Unconformity*

MIDDLE CAMBRIAN

Langston Formation

6. Dolomite: steel gray, finely crystalline, thin and irregularly bedded; weathers to light-gray ledges and forms top of cliffs above shale slopes; contains many shaly and silty partings ..... 62
5. Quartzite and sandstone: pinkish-white, fine- to coarse-grained, thin- to medium-bedded quartzite interbedded with tan fine-grained, calcareous sandstone and quartzite which weathers into thin brown plates; top of unit is pinkish-white pebble conglomerate about 4 feet thick ..... 14
4. Limestone: light gray, very finely crystalline (some beds porcellaneous-textured), thin-bedded to laminated with many shaly and silty partings; weathers to light-gray and tan ledges at base of cliffs above shale slopes. Limestone becomes arenaceous and irregularly bedded toward top of unit ..... 66
Total thickness of Langston Formation ..... 142

LOWER AND MIDDLE CAMBRIAN

Pioche Formation

3. Shale and quartzite: greenish-brown and olive-green, laminated, sandy, micaceous fucoidal shale interbedded with a few thin (1–4 inches) layers of thin-bedded, fine- to medium-grained, brown micaceous quartzites 98
2. Shale, quartzite, and sandstone: greenish-brown and olive-green, laminated, arenaceous, micaceous, fucoidal shale interbedded with brown and greenish-brown, fine- to medium-grained, thin- to thick-bedded micaceous sandstone and quartzite. Much shale and little

| | Feet |
|---|---|
| coarser material at top of unit; considerably more coarsely clastic toward base of unit | 100 |
| Total thickness of Pioche Formation | 198 |

LOWER CAMBRIAN AND PRECAMBRIAN (?)

Prospect Mountain Quartzite

1. Quartzite: white and pinkish white, medium- to coarse-grained (some beds of small pebble conglomerate), medium-bedded with some cross-bedding; interbedded with a few thin (1–2 feet) layers of greenish-brown shale in upper 100 feet of formation. Not measured, but estimated to be 1000 feet thick.

| | |
|---|---|
| Total thickness of Prospect Mountain Quartzite | 1000 |
| Total measured and estimated thickness of rocks of Cambrian age | 1340 |

The units in these sections compare closely with those described by Hintze (1913, p. 103–105), and the general sequence is the same as other published descriptions (Walcott, 1890, p. 549–550; Blackwelder, 1909, p. 520–527; Calkins and Butler, 1943, p. 9–18). Also the formations are lithologically similar to those recognized by the writer in the Ogden Canyon and Willard Peak areas except that the unconformity at the top is not recognized in those areas.

*Summary.*—The data presented indicate that the Cambrian sequence in the north part of the Wasatch Range, north of Boxelder Canyon (Wellsville Mountain), is essentially the same as the sequence in the Bear River Range in Utah and in southeastern Idaho. South of Boxelder Canyon, only the lower part of the sequence is known, and the upper part was either never deposited or was removed by erosion. Thus, the "standard" Cambrian sequence in this part of the Wasatch Range consists of:

(1) a basal quartzite unit of variable thickness, here referred to the Prospect Mountain Quartzite, unconformably overlying the Precambrian gneiss, schist, slate, and quartzite and conformably overlain by

(2) a thinner sequence of predominantly shaly beds with considerable intercalated and interbedded coarser clastics, here referred to the Pioche Shale, ranging from about 150 to 200 feet in thickness, and conformably overlain by

(3) a thin limestone and/or dolomite unit with some intercalated and interbedded shale and sandstone, the Langston Formation, which is truncated by an erosional unconformity or by a thrust fault. This unit is overlain unconformably either by older beds in faulted contact or by dolomite and limestone of Devonian (Calkins and Butler, 1943, p. 18; Baker, 1947, chart) age or limestone of Mississippian age (Williams, 1943, p. 599–600).

From these characteristics, the Big Cottonwood Creek section is considered the "standard" section for most of the Wasatch Range.

### *Promontory Range, Utah*

Early and Middle Cambrian rocks in the Promontory Range have been mentioned briefly by Butler and Heikes (Butler *et al.*, 1920, p. 499–501), Resser (1939b, p. 6), and Eardley and Hatch (1940, p. 801–802), all of whom recognized that the sequence on Promontory Point at the south end of the range was similar to that in the Bear River Range. Resser (1939b, p. 6) reported Early Cambrian fossils from these rocks but did not give the species or locate the zones. In 1950 the writer examined the section in Miner's Canyon, about 3 miles northwest of the Crystal Lake Salt Company buildings at the southwest end of Promontory Point.

The strata in Miner's Canyon are much disturbed by thrusts and small normal faults and by folds. It was possible, however, to recognize the entire sequence of the Bear River Range. Because of complex faulting, and because only a few fossil-bearing zones were found, no detailed study was made. Estimates of thickness indicate that the Langston Formation and the Blacksmith Dolomite may be thinner here than at Calls Fort or in Blacksmith Fork Canyon; the Ute Formation may be considerably thicker, and the Bloomington Formation is less shaly but is about the same thickness. As at Calls Fort and High Creek, the shale and quartzite beds between the Prospect Mountain Quartzite and the Langston Formation are doubtfully referred to the Pioche Formation. The Prospect Mountain Quartzite is approximately 1000 feet thick and unconformably overlies Precambrian strata. The Pioche (?) formation, the Spence Shale Member of the Langston, and the shale at the base of the Ute Formation contain fragments of fossils. Forms characteristic of the Spence Shale fauna elsewhere in Utah and

southeastern Idaho were recognized in the Spence Shale Member at Miner's Canyon.

## Lower and Middle Cambrian Formations in Northeastern Utah and Southeastern Idaho and Their Regional Relationships

### *Prospect Mountain Quartzite (Lower Cambrian)*

DEFINITION AND DISTRIBUTION: The Prospect Mountain Quartzite was first defined by Hague (1883, p. 27; 1883, p. 254), who designated the west side of Prospect Peak near Eureka, Nevada, as the type locality. In the type area, the formation consists chiefly of reddish-brown to pink, medium-grained, thick- to thin-bedded quartzite interbedded and intercalated with a few thin layers and lenses of micaceous arenaceous shale and, near the base of the exposed section, with quartzitic conglomerate. Hague gives the thickness as 1500 feet at the type locality, where the base is not exposed and the quartzite is conformably overlain by the Pioche Formation. Detailed descriptions of the formation are given in another part of this paper.

The formation has been recognized in sections throughout Nevada, Utah, eastern California, northern Arizona, and southeastern Idaho in an area roughly the same as the Great Basin province, but which extends northward and southward beyond its boundaries. The Prospect Mountain Quartzite is unusually uniform and in nearly all areas is conformably overlain by shales containing late Early Cambrian or early Medial Cambrian fossils. The base of the formation has been positively recognized in only a few localities in Utah and southeastern Idaho. It unconformably overlies Precambrian formations in the Bannock Range (Ludlum, 1943, p. 973), in the central southern parts of the Wasatch Range, and on Promontory Point. In the Sheeprock Mountains, Utah, the quartzite is questionably unconformable upon Precambrian rocks. Elsewhere in Utah and Idaho the base of the Prospect Mountain quartzite is covered or has not been recognized. The quartzite is 3200 feet thick in the Bannock Range, approximately 1000 feet thick on Promontory Point, and ranges from approximately 700 feet to 1200 feet in the Wasatch. Eardley and Hatch (1940, p. 825–826) report 3500 feet of quartzite above a questionable unconformity in the Sheeprock Range. Known thicknesses of the quartzite in the other areas of outcrop in Utah and Idaho range from 300 feet near Ophir, Utah, to more than 6000 feet in the Tintic district, Utah. However, the thickness in the Tintic district may be the result of duplication by folding and faulting, or an unconformity may be present within the quartzite. The largest well-exposed and unquestioned thickness in the area under discussion is in the Bear River Range near the Utah-Idaho boundary, where Williams (1948, p. 1132) and Church measured 4800 feet of quartzite beds (probably includes approximately 150 feet of the Pioche (?) formation), and the base of the formation is not exposed. The maximum known thickness of the formation is more than 7855 feet (Humphrey, 1945, p. 25–26) in the Groom district, Nevada. Wheeler (1948, p. 20) reported thicknesses of 4750 feet in the Deep Creek Range, Utah, and 4128 feet in the Nopah Range, California. Nolan (1929, p. 463) reported a thickness of 3700 feet of Prospect Mountain Quartzite (Stirling quartzite) in the Spring Mountains, Nevada, and the writer has observed approximately 4000 feet in the Desert Range, 20 miles northeast of the Spring Mountains.

Within the area of this study the rocks previously assigned to the "Tintic quartzite" belong in the Prospect Mountain Formation, as do rocks assigned to all but the uppermost shaly units of the so-called "Brigham quartzite". The uppermost shaly units are here doubtfully referred to the Pioche Formation.

AGE: As far as the writer knows, diagnostic fossils have not been found in the Prospect Mountain Quartzite. The only fossils found in the formation are numerous worm borings, fucoids (?), annelid and trilobite trails, and one common phoronid (?) boring (*Skolithos*), none of which indicates the age of the formation. Fossils from the overlying Pioche Shale show that that formation is partly within the *Olenellus* zone in western Utah and in the central and southern Wasatch Range, and here the Prospect Mountain Quartzite certainly is Early Cambrian or older. In the northern Wasatch, in the Bear River Range, and in southeastern Idaho the oldest known diagnostic fossils occur in the Langston Formation and belong within the earliest Middle Cambrian zone (*Albertella-Kochaspis* subzone). Thus here also the quartzite is probably Early Cambrian or older.

Wheeler (1947, p. 157–159) proposed that the base of the *Olenellus* zone be recognized as the base of the Cambrian system in western North America. This suggestion may be highly satisfactory for the Cambrian of the Cordillera for the reasons that Wheeler has so ably pre-

sented. However, two important difficulties arise: (1) although the top of the *Olenellus* zone is well defined and easily recognized in many areas, its base is not accurately defined and apparently has not been recognized in western North America; (2) in eastern North America and northwestern Europe well-defined and easily recognized faunal zones older than the *Olenellus* zone have been found. In those regions the base of the Cambrian system has been defined so as to coincide with the base of the lowermost (*Obolella*) zone (Howell *et al.*, 1944, chart).

On the basis of physical characteristics, including lithologic features, conformity with the overlying Pioche Shale, etc., Wheeler (1948, p. 20, Fig. 5) doubtfully included the upper part of the quartzites in the Lower Cambrian series in three western Utah sections, even though diagnostic fossils of the *Olenellus* zone do not occur in the quartzite. Probably in Utah and Idaho, where the quartzites nearly everywhere conformably underlie the Pioche Shale and where *Olenellus* occurs in that formation, the Prospect Mountain Quartzite is of Early Cambrian age. The formation was apparently deposited during part, or all, of the time when faunas that antedate the *Olenellus* fauna were thriving in other regions. Further study of the quartzite and other Lower Cambrian formations in the Great Basin may yield evidence allowing a more precise definition of Lower Cambrian faunal zones and thus permit a more accurate age assignment of the formation.

### *Pioche Formation*

DEFINITION AND DISTRIBUTION: The Pioche Shale was first described at the type locality near Pioche, Nevada, by Walcott (1908a, p. 11–12) as 210 feet of "arenaceous and argillaceous shaly layers with some thin layers and bands of limestone more or less irregularly interbedded and limited in horizontal distribution". He correctly pointed out that the formation crops out in the House and Wasatch ranges, in Utah, where it also lies conformably between the Prospect Mountain Quartzite and the overlying Cambrian limestones. Westgate and Knopf (1927, p. 8–10) redescribed the formation, emended the original definition, and pointed out that the true thickness of the formation is approximately 1120 feet at the type locality. Deiss (1938, p. 1152–1160), on paleontological evidence, incorrectly divided this lithogenetic and mappable unit into two formations, "the Pioche shale (restricted)" and the "Comet shale". Wheeler and Lemmon (1939, p. 34–35) restored the formation to its proper status. Wheeler (1943, p. 1781–1982) indicated the wide geographic occurrence of the Pioche Formation in Utah, Nevada, and Arizona and in 1948 (p. 25) stated that, among other terms, the "Ophir" and "Cabin" shales were synonyms of Pioche.

Data presented here prove the presence of the Pioche Formation throughout most of west-central and northern Utah and suggest its presence in the northern Wasatch, in part of the Bear River Range, and in southeastern Idaho. In the two last-named areas, the beds lithogenetically equivalent to the Pioche Formation seem to pinch out to the east and were not observed at Spence Gulch or in the Blacksmith Fork drainage area (Figs. 2, 3). Elsewhere in the Wasatch and southeastern Idaho these beds have heretofore been included in the "Brigham formation". In the central Wasatch Mountains the basal shales of the "Ophir formation" constitute the Pioche Formation. In Utah and southeastern Idaho it is composed of arenaceous and argillaceous shales, generally interbedded and intercalated with quartzite and sandstone layers and lenses. The quartzite and sandstone beds are lithologically similar to those of the underlying Prospect Mountain Formation. Only a few carbonate layers or lenses are interbedded with the shales. Sparseness or lack of carbonate beds is the chief criterion used in many places to distinguish the Pioche Formation and the conformably overlying carbonate beds of the Langston Formation. Further, the Pioche shales are predominantly argillaceous and micaceous, whereas the overlying shales are mostly calcareous. The formation thins eastward and northward from the type locality (Wheeler, 1943, Pl. 1; 1948, Fig. 5), and in at least one section in northeastern Utah (Blacksmith Fork) it is not present. In northeastern Utah and southeastern Idaho the arenaceous beds constitute so much of the formation at the expense of the argillaceous shale that it is only arbitrarily distinguishable from the underlying Prospect Mountain Quartzite. The Pioche ranges in thickness from 265 feet in the House Range to approximately 100 feet in the Ophir Canyon section.

AGE: Fossils of Early Cambrian age belonging to the *Olenellus* zone have been found in the Pioche Formation in Utah. Fossil localities include the House Range, Ophir Canyon, and Big Cottonwood Creek Canyon. *Olenellus* has been

reported from the Pioche Shale of the Wasatch Mountains east of Provo (P. E. Dennis, personal communication) and in rocks now assigned to the Pioche Shale of the Promontory Range (Resser, 1939b, p. 6). The Langston Formation conformably overlies the Pioche Shale and contains fossils belonging to the *Albertella-Kochaspis* subzone, which contains the earliest Medial Cambrian fossils in the Great Basin. Thus, the fossils indicate that the Pioche Formation is of late Early Cambrian and early Medial Cambrian age throughout northern Utah and southern Idaho. Like the overlying Langston Formation, it transgresses the Early-Medial Cambrian boundary.

### *Langston Formation (Lower and Middle Cambrian)*

DEFINITION AND DISTRIBUTION: The Langston formation was named by Walcott (1908a, p. 8; 1908b, p. 198–199) who described it as "massive-bedded, bluish-gray limestone with many round concretions" and gave its thickness as 107 feet in Blacksmith Fork Canyon, Utah, its probable type locality (1908a, p. 8). Later, he (Walcott, 1908b, p. 188–199) redescribed it and included 390 feet of "massive-bedded, dark arenaceous limestone, passing at about 150 feet down into a calcareous sandstone, and then a gray sandstone". In the later description he listed fossils and made Blacksmith Fork Canyon the type locality, although Langston Creek (where the formation is also exposed) is some distance from Blacksmith Fork. In both papers he states that the Langston Limestone conformably overlies the Prospect Mountain Quartzite ("Brigham") and comfortably underlies the Spence Shale, which he considered the basal member of the Ute Formation. Walcott's definition was generally accepted, and Deiss (1938, p. 1112–1119) remeasured and redescribed the formation and designated a new "type" locality in Blacksmith Fork Canyon. In 1941, Williams and Maxey (1941, p. 279) stated that the Langston Formation is

> "a sequence of shales, limestone, and dolomites that, though changing laterally to some extent, constitutes a satisfactory mappable (lithologic) unit. The Spence shale is a member of the Langston formation separated in normal sequence from the Brigham quartzite by only a few feet of crystalline limestone."

They pointed out that the Langston Formation at the "type" localities in Blacksmith Fork consists of an abnormal development of the dolomite members at the expense of the shale and limestone members. The sections upon which Williams and Maxey's (1941) paper was based are detailed in the present paper.

The writer has recognized the Langston Formation in all areas described in this paper and suggests that the north side of the High Creek Canyon is the best and most nearly typical exposure of the Langston Formation. The formation is characteristically developed with all members present, whereas to the southeast (toward Blacksmith Fork) the Spence Shale and Naomi Peak Members pinch out into the thick basal dolomite (Fig. 2), and to the south and west they finger into a maze of thinly interbedded and intercalated shale and limestone beds.

In the Wasatch Range, from Willard Peak south and west to beyond the central Wasatch, the formation consists of these interbedded limestones and shales and a few sandy beds. Throughout most of Utah and southern Idaho the Langston Formation marks the beginning of the long period of deposition of predominantly carbonate rocks which characterize the Middle and Upper Cambrian Series, whereas the underlying formations are predominantly detrital and arenaceous. Thus the base of the formation is usually drawn at the first distinctive limestone bed above the Prospect Mountain Quartzite.

Beds formerly assigned to the upper part of the "Ophir formation" and to the "Maxfield" formation are here assigned to the Langston Formation.

Two units within the Langston Limestone are locally distinct lithologic markers. Resser (1939b) described a fauna from the basal limestone beds of the Langston Formation superjacent to the shaly quartzite beds of the Pioche (?) Formation (Brigham) and subjacent to the Spence Shale Member. He called this the *Ptarmigania* fauna, and the limestone in which it occurs he referred to as the "*Ptarmigania* strata". He neither adequately defined the member nor designated a type locality, probably because he was not aware of its exact stratigraphic position. Further, the term "*Ptarmigania* strata" is likely to become confused with the term Ptarmigan Formation, an already accepted name for a Middle Cambrian formation in Canada. The detailed descriptions of sections in the northern Wasatch Mountains, in the Bear River Range, and in southeastern Idaho indicate that these limestones are a distinctive rock unit. In the field this unit is an excellent stratigraphic marker or "key bed", because (1) it is the first limestone in the sec-

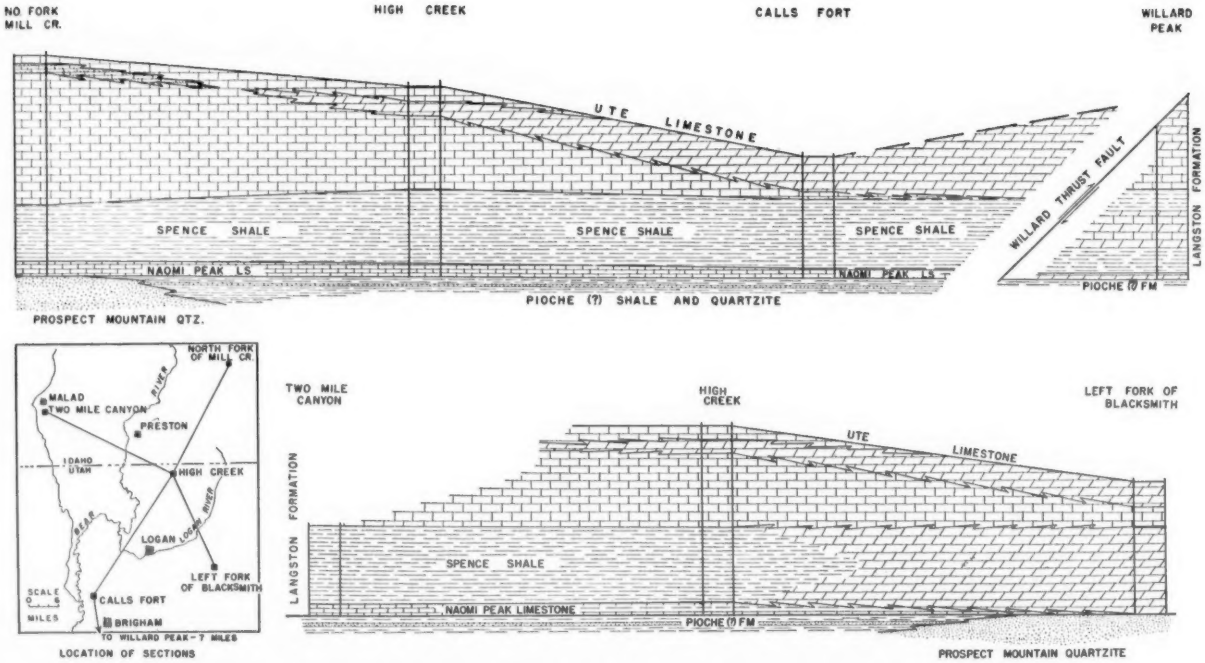


FIGURE 2.—LITHOLOGIC VARIATIONS WITHIN SOME LOWER AND MIDDLE CAMBRIAN FORMATIONS IN NORTHERN UTAH AND SOUTHEASTERN IDAHO

tion above the arenaceous sediments of the Pioche (?) and Prospect Mountain formations, (2) it contains in all known outcrops the distinctive, easily recognized fossils of the *Ptarmigania* fauna, and (3) it is nearly always excellently exposed because it forms the first ledges under the slopes formed on the Spence Shale and caps the prominent cliffs and ledges of the underlying resistant arenaceous sediments. This unit is here designated the Naomi Peak Limestone Member of the Langston Formation.

ORIGINAL DESCRIPTION: The Naomi Peak Member is composed of light- to medium-neutral-gray, finely crystalline, arenaceous limestone with numerous lenses of coarsely crystalline, very fossiliferous, pure limestone. In many places few thin beds of gray, medium-grained, brown-weathering, calcareous or dolomitic sandstone occur near the base of the member. It conformably overlies the Pioche (?) Shale and underlies the Spence Shale Member of the Langston Formation. It constitutes the basal 32 feet of the Langston in the excellent section on the north side of the North Fork of High Creek, approximately 6½ miles northeast of Richmond, Utah. The known outcrop area of the Naomi Peak Limestone Member extends from the Left Fork of Blacksmith Fork River northward beyond Spence Gulch and Malad, Idaho, and from the east side of the Bear River Range to Wellsville Mountain. The member is 40 feet thick at the North Fork of Mill Creek, 2½ miles north of Spence Gulch, Idaho; 32 feet thick at Two Mile Canyon, Idaho; 32 feet thick at High Creek, Utah; 25 feet thick at Wellsville Mountain; and 40 feet thick at Temple Ridge, in the central part of the Bear River Range. It is not recognized in the Left Fork of Blacksmith Fork, in Blacksmith Fork, in the Promontory Range, or in central or western Utah.

The Spence Shale was designated by Walcott (1908a, p. 8) as the basal member of the Ute Formation. He described it as 30 feet of argillaceous shales in the type locality at Spence Gulch, Idaho. Williams and Maxey (1941, p. 276–285) redescribed the member as part of the Langston Formation immediately superjacent to the Naomi Peak Limestone. As Williams and Maxey (1941, p. 280) state, the formation is not wholly exposed at Walcott's type locality, but approximately 1 mile north-northwest along the strike, on the west side of the Left Fork of Mill Creek, it is well exposed and is 125 feet thick. Here, as at the type locality, it consists of black and olive-green, fissile, somewhat calcareous shale with numerous fossils in the lower beds and with some interbedded thin layers of tan siltstone and silty shale in the upper part. The area of outcrop of the Spence Shale is somewhat larger than that of the Naomi Peak Member because it crops out in the Promontory and Bannock ranges and may extend northward beyond the Snake River in Idaho. However, it was not recognized in Utah south of the latitude of Brigham City or west of Promontory Point (Fig. 2).

AGE: The faunas of the Naomi Peak Limestone and Spence Shale Members are assigned to the *Albertella-Kochaspis* subzone and unquestionably show that the basal Langston was deposited in earliest Medial Cambrian time. The "*Ptarmigania* fauna" contains several forms that have Early Cambrian affinities. The Langston Formation in the House Range contains only these early forms or their ancestors and, in so far as known, no typically Medial Cambrian types. This fauna in the House Range is tentatively placed in the *Antagmus-Onchocephalus* zone of late Early Cambrian age. This suggests that the sedimentary environment of the Langston transgressed slowly eastward and that the Langston Formation may transgress the Early-Medial Cambrian boundary in the western Great Basin. The upper beds of the Langston are everywhere clearly Medial Cambrian, for they contain fossils belonging to the *Glossopleura-Zacanthoides* zone or they are conformably overlain by beds assigned to that zone.

### *Ute Formation*

DEFINITION AND DISTRIBUTION: The name Ute Limestone was applied by King (1878, p. 232–233) to the 2000 feet of limestones overlying the Cambrian quartzites. Walcott (1908a, p. 7) redescribed the lower 759 feet in Blacksmith Fork and restricted the name to these lower beds. This restricted usage has been followed, and Deiss (1938, p. 1120–1121) remeasured the thickness and emended the description of the beds in the Blacksmith Fork section. Deiss retained Blacksmith Fork Canyon as the type locality of the emended Ute Limestone. Williams and Maxey (1941, p. 281) defined the Ute Formation as the "thin-bedded, silty limestone and green shales" conformably overlying the Langston Formation and underlying the Blacksmith Dolomite, both persistent

and readily recognized. This definition and Deiss' description are here recognized as essentially correct. Outside the Bear River Range the Ute Formation has been readily recognized throughout northern Utah and southern Idaho. According to Deiss (1938, p. 1113–1114) the Ute Formation is 685 feet thick in Blacksmith Fork. Its maximum measured thickness (745 feet) in northern Utah and southeastern Idaho is at High Creek, Utah. An estimate of its thickness at Promontory Point, Utah, is 790 feet.

AGE: The basal shales of the Ute Formation in southeastern Idaho and northern Utah contain fossils assigned to the *Glossopleura-Zacanthoides* zone. In central Utah the basal beds conformably overlie rocks containing similar fossils. *Olenoides*, *Ehmaniella* (?), *Alokistocare*, and *Obolus*, all typical Medial Cambrian forms characteristic of the *Bathyuriscus-Elrathina* zone, occur approximately 400 feet above the base of the formation in northern Utah. Further, elements of the *Bathyuriscus-Elrathina* zone are reported from near the base of the conformably overlying Blacksmith Dolomite. Thus, the Ute Formation is Medial Cambrian.

### *Blacksmith Dolomite*

Walcott (1908a, p. 7) designated "Blacksmith Fork Canyon, about 8 miles above its mouth and 15 miles east of Hyrum, Cache County, Utah," as the type locality of the Blacksmith Dolomite. He incorrectly described the formation as 570 feet of "gray arenaceous limestone in massive layers." Deiss (1938, p. 1112–1113, 1121) emended this definition and correctly stated that the formation was essentially all thick-bedded gray dolomite and interbedded magnesian limestones. These beds are approximately 450 feet thick at the type locality in Blacksmith Fork and about 485 feet thick at High Creek. The formation thins northward and is not recognized in the northern extremity of the Bear River Range near Lava Hot Springs. Walcott (1908a, p. 8) reports that it is only 23 feet thick in the section west of Liberty, Idaho. It apparently thickens westward and southward because it is more than 500 feet thick on Promontory Point and is thicker at Calls Fort than at High Creek.

The only fossils reported from the Blacksmith Dolomite are forms belonging to the "*Thompsonaspis* faunule" of Denson (1942, p. 26) and to the *Bathyuriscus-Elrathina* zone. Denson's *Thompsonaspis* faunule is probably the same as the *Palella-Thompsonaspis* zone of authors (Howell *et al.*, 1944, Chart).

### *Bloomington Formation*

DEFINITION AND DISTRIBUTION: The Bloomington Formation conformably overlies the Blacksmith Dolomite throughout northern and northeastern Utah and in most of southern Idaho. It was named by Walcott (1908a, p. 7), who designated the type locality as "Bear River Range, about 6 miles west of the town of Bloomington, Bear Lake County, Idaho. A second easily accessible locality is in Blacksmith Fork Canyon, east of Hyrum, Cache County, Utah."

He described the formation as "bluish gray, more or less thin-bedded limestones and argillaceous shales. Small rounded nodules of calcite occur scattered regularly through many of the layers of limestone." Richardson (1913, p. 406) described the basal shale beds of the Bloomington Formation as the Hodges Shale Member in the Randolph quadrangle, Utah. Mansfield (1927, p. 55) redescribed the formation in southeastern Idaho, recognized the Hodges Shale Member at the base, and changed the type locality to Mill Creek, near Liberty, Idaho. Deiss (1938, p. 1121–1132) redescribed the Bloomington in the Blacksmith Fork area and pointed out that the Hodges Shale Member was thinner there. Williams and Maxey (1941, p. 381) described the formation in the Logan quadrangle and vicinity as 1200 feet of thin-bedded limestone and shale with the Hodges Shale Member at the base and a thick shale member at the top. This upper thick shale member was designated by Denson (1942, p. 24) as the Calls Fort Shale. Thus, the Bloomington Formation consists of (1) a basal tawny-olive shale and interbedded thin layers of light- to dark-gray limestone (the Hodges Shale Member), overlain by (2) a middle unit of thinly to thickly bedded, light- to dark-gray limestone which weathers to slopes strewn with thin plates of limestone, overlain by (3) an upper tawny-olive shale unit with some interbedded platy limestone, the Call's Fort Member.

The Bloomington Formation crops out throughout southeastern Idaho and northeastern Utah as far south as the northern margin of Great Salt Lake and Brigham City. It has been recognized in the Lakeside Range, on the west margin of Great Salt Lake. In the Wasatch Range it was probably removed by late or post-Cambrian erosion, or it may never have been deposited.

AGE: Denson (1942 p. 24) places the Bloomington Formation in the latest Medial Cambrian zones on the basis of faunules, as yet not published, which occur in the Calls Fort and Hodges Shale Members. The writer tentatively

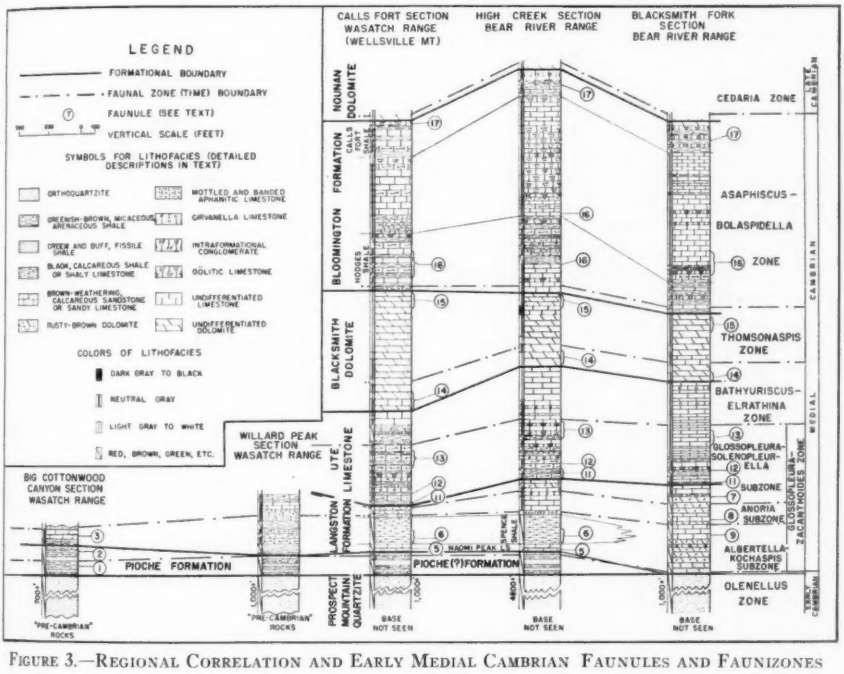


FIGURE 3.—REGIONAL CORRELATION AND EARLY MEDIAL CAMBRIAN FAUNULES AND FAUNIZONES

places these members in the *Asaphiscus-Bolaspidella* zone. The top of the *Thompsonaspis* zone occurs just below the base of the formation, in the top of the Blacksmith Dolomite, at High Creek, Utah. The base of the Lower *Cedaria* zone (Upper Cambrian) is drawn near the base of the Nounan Formation, which lies conformably on the Calls Fort Member of the Bloomington Formation.

## EARLY AND MEDIAL CAMBRIAN FAUNULES IN UTAH AND SOUTHEASTERN IDAHO

The writer here lists all reported occurrences of diagnostic Lower and Middle Cambrian fossils in the region. The zones in which these faunules occur are designated on Figure 3 by the numbers heading each list. Zonation of the faunules is discussed. Since no diagnostic fossils are known from the Prospect Mountain quartzite, this formation is not included.

### PIOCHE SHALE

Wasatch Range, Big Cottonwood Canyon; base of the formation (Walcott, 1891, p. 319; Hintze, 1913, p. 104–105; Burling, 1914, p. 8)

1. *Olenellus gilberti* (Meek)
   *Cruziana*, sp.

Same: 100 feet above base of formation (Walcott, 1890, p. 319; Hintze, 1913, p. 104–105; Burling, 1914, p. 3)

2. *Obolus* (Westonia) *ella* (Hall and Whitfield)
   *Micromitra* (*Iphidella*) *pannula* (White)
   *Hyolithes billingsi* (Walcott)
   *Tuzoia argenta* (Walcott)
   *Ehmaniella* (?) *quadrans* (Hall and Whitfield)
   *Glossopleura producta* (Hall and Whitfield)

### LANGSTON FORMATION

Wasatch Range, Big Cottonwood Canyon; 70 feet above base of formation

3. *Spencia*, sp. undet.
   *Glossopleura utahensis* (Resser)
   *Anoria utahensis* (Resser)

Promontory Range; 15 to 100 feet above base of formation

4. Many species from the Spence Shale, including *Taxioura*, sp. undet. *Hyolithes*, sp.; and *Elrathia*, sp. undet.

Bear River and Malad ranges and Wellsville Mountain; basal 32 to 40 feet of formation (Naomi Peak Limestone Member) (Resser, 1939b, p. 20–72)

5. Brachiopoda
   - *Acrothele artemis* Walcott
   - *A. parilis* Resser
   - *Acrothyra minor* Walcott
   - *Acrotreta eucharis* Resser
   - *A. sulcata* Walcott
   - *Iphidella maladensis* Walcott
   - *Lingulella eucharis* Resser
   - *Micromitra haydeni* Walcott
   - *Paterina hirta* Resser
   - *Wimanella maladensis* Resser

   Gastropoda
   - *Helcionella aequa* Resser
   - *H. arguta* Resser
   - *H. burlingi* Resser
   - *Hyolithes prolixus* Resser

   Agnostia
   - *Agnostus lautus* Resser

   Trilobita
   - *Albertella*, sp. undet.
   - *Alokistocare brighamensis* Resser
   - *A. euchare* Resser
   - *Alokistocare euzona* Resser
   - *Alokistocarella occidens* Resser
   - *Bathyuriscus politus* Resser
   - *Clavaspidella excavata* Resser
   - *C. wasatchensis* Resser
   - *Dolichometopsis alia* Resser
   - *D. comis* Resser
   - *D. communis* Resser
   - *D. gravis* Resser
   - *D. gregalis* Resser
   - *D. lepida* Resser
   - *D. mansfieldi* Resser
   - *D. media* Resser
   - *D. potena* Resser
   - *D. poulseni* Resser
   - *D. propinqua* Resser
   - *D. stella* Resser
   - *Ehmaniella maladensis* Resser
   - *Inglefieldia idahoensis* Resser
   - *Kochaspis dispar* Resser
   - *K. maladensis* Resser
   - *Kochiella arenosa* Resser
   - *K. mansfieldi* Resser
   - *Kochina* (?) *elongata* Resser
   - *K.* (?) *libertyensis* Resser
   - *K. venusta* Resser
   - *K. vestita* Resser
   - *K. wasatchensis* Resser
   - *Kootenia acicularis* Resser
   - *K. bearensis* Resser
   - *K. brevispina* Resser
   - *K. convoluta* Resser
   - *K. germana* Resser
   - *K. granulosa* Resser
   - *K. libertyensis* Resser
   - *K. maladensis* Resser
   - *K. mendosa* Resser
   - *K. venusta* Resser
   - *Olenoides maladensis* Resser
   - *Oryctocephalites typicalis* Resser
   - *Oryctocephalus maladensis* Resser
   - *Pachyaspis typicalis* Resser
   - *Pagetia clytia* Walcott
   - *P. maladensis* Resser
   - *Poliella dignata* Resser
   - *P. germana* Resser
   - *P. sobrina* Resser
   - *P. wasatchensis* Resser
   - *P.*, sp. undet.
   - *Poulsenia bearensis* Resser
   - *P. granosa* Resser
   - *P. occidens* Resser
   - *Prozacanthoides aequus* Resser
   - *P. alatus* Resser
   - *P. decorosus* Resser
   - *P. exilis* Resser
   - *P. libertyensis* Resser
   - *P. optatus* Resser
   - *Ptarmigania agrestis* Resser
   - *P. altilus* Resser
   - *P. aurita* Resser
   - *P. exigua* Resser
   - *P. natalis* Resser
   - *P. ornata* Resser
   - *Taxioura magna* Resser (*Ogygopsis*)
   - *T. typicalis* Resser (*Ogygopsis*)
   - *Tonkinella idahoensis* Resser

   Unidentified species and genera of trilobites and brachiopods

Same: beds between approximately 40 feet and 230 feet above base of formation (Spence Shale Member). The fossils occur chiefly in the basal 60 feet of the member (Resser, 1939a, p. 3–24).

6. Algae
   - *Morania*, sp. undet.

   Echinoderma
   - *Eocrinus longidactylus* (Walcott)

   Worms
   - *Selkerkia spencei* Resser

   Brachiopoda
   - *Acrothele affinis* Resser

*Acrotreta definita* Walcott
*A. levata* Resser
*Iphidella grata* Resser
*Lingulella eucharis* Resser
*Micromitra lepida* Resser
*Wimanella nantes* (Walcott)
*W. rara* (Walcott)
*W. spencei* (Walcott)
Gastropoda
*Hyolithes cecrops* Walcott
*H. ornatellus* Resser
*"Orthotheca" sola* Resser
Agnostia
*Agnostus bonnerensis* Resser
*A. brighamensis* Resser
Trilobita
*Albertella*, sp. undet.
*Alokistocare brighamense* Resser
*A. idahoense* Resser
*A. laticaudum* Resser
*A. punctatum* Resser
*A. septum* Resser
*A. spencense* Resser
*Alokistocarella spencei* Resser
*Bathyuriscus atossa* Walcott
*B. brighamensis* Resser
*Bythicheilus alveatum* Resser
*B. typicum* Resser
*Chancia augusta* Resser
*C. ebdome* Resser
*C. evax* Resser
*Clappaspis coriacea* Resser
*C. dotis* Resser
*C. idahoensis* Resser
*C. lanata* Resser
*C. spencei* Resser
*Clavaspidella anax* (Walcott)
*C. bithus* (Walcott)
*Elrathia spencei* Resser
*Ehmaniella quadrans* (Hall and Whitfield)
*Glossopleura bion* (Walcott)
*G. gigantea* Resser
*G. similaris* Resser
*G. utahensis* Resser
*Kootenia idahoensis* Resser
*K. mathewsi* Resser
*K. spencei* Resser
*Olenoides brighamensis* Resser
*O. evansi* Resser
*O. wasatchensis* (Hall and Whitfield)
*Oryctocare geikei* Walcott
*Oryctocephalus walcotti* Resser
*Pagetia clytia* Walcott
*Poliella anteros* (Walcott)
*P. ceranus* (Walcott)
*Stauroholcus typicalis* Resser
*Spencia plena* Resser
*S. typicalis* Resser
*Taxioura*, sp. undet. (*Ogygopsis*)
*Utia curio* Walcott
*Vistoia* (?) *minuta* Resser
*Zacanthoides abbreviatus* Resser
*Zacanthoides adjunctis* Resser
*Z. gradatus* Resser
*Z. holopygus* Resser
*Z. idahoensis* Walcott
*Z. serratus* Resser

Several unidentified species and genera of trilobites; many embryonic forms

Bear River Range and Wellsville Mountain; 85 feet below top of formation in the Left Fork of Blacksmith Fork Canyon
7. *Glossopleura*, sp. undet.
*Glyphaspis* (?), sp. undet.

Same: approximately 220 feet below top of formation in Blacksmith Fork Canyon
8. *Glyphaspis* (?), sp. undet. (Deiss, 1938, p. 1115)

Same: approximately 310 feet below top of formation in Blacksmith Fork Canyon
9. *Glossopleura*, sp. undet.
*Clavaspidella* (?), sp. undet.

UTE FORMATION

Promontory Range; at base of the formation
10. *Glossopleura* cf. *producta* (Hall and Whitfield)
*Elrathina* (?), sp.

Bear River Range and Wellsville Mountain; basal 4 to 15 feet of the formation (Deiss, 1938, p. 1114)
11. *Alokistocare*, sp.
*Elrathina* (?), sp.
*Glossopleura producta* (Hall and Whitfield)
*Glossopleura*, n. sp.
*Kochina*, n. sp.
*Kootenia*, sp.
*Zacanthoides*, sp.
*Micromitra*, sp.
*Acrotreta*, sp.
*Acrothele*, sp.
*Iphidella*, sp.
*Hyolithes*, sp.

Same: 105 to 109 feet above the base of the formation
12. *Anomalocephalus*, n. sp.
*Ehmaniella*, n. sp.

Same: 275 to 375 feet above the base of the formation
13. *Olenoides*, sp.
*Ehmaniella* (?), sp.

*Alokistocare subcoronatum* (Hall and Whitfield)
*Kootenia quadriceps* (Hall and Whitfield)

BLACKSMITH DOLOMITE

Bear River Range and Wellsville Mountain; near the base of the formation
14. See Howell et al. (1944, Chart)
Same: near top of formation (Denson, 1942)
15. *Anomocare*
*Palella*

BLOOMINGTON FORMATION

Bear River Range and Wellsville Mountain; 160 to 335 feet above the base of the formation (Hodges Shale Member)
16. *Bolaspidella*
*Blainia* cf. *gregaria* Walcott
*Blainia gregaria* Walcott
*Olenoides*
*Solenopleura*
*Helcionella*, sp.
Undescribed genera of trilobites and brachiopods
Same: 10 feet above top of Hodges Shale Member
16a. *Olenoides*, sp.
Undescribed genera of brachiopods and trilobites
Same: 90 to 110 feet below the top of the formation near top of Calls Fort Member
17. *Asaphiscus*
*Pachyrhachis oweni* Walcott
*Parehmania*
*Bolaspis* (?)
*Howellaspis* (?)
*Acrocephalops* (?) cf. *A. gracilis* Resser
*Elrathia*
*Homagnostus* cf. *pisiformis pater* (Holm and Westergaard)
Undescribed genera of trilobites and brachiopods

## ZONATION OF THE FAUNULES

### *General Statement*

Five faunal zones are recognized in the Lower and Middle Cambrian strata of Utah and southeastern Idaho, of which one, the *Olenellus*, is of Early Cambrian age. The zones are discussed in detail and compared with zones of comparable age recognized in other areas.

### Olenellus *Zone*

The oldest diagnostic fossils recognized in Utah and southern Idaho are members of the trilobite genus, *Olenellus*, chiefly *Olenellus gilberti* (Meek), and the brachiopod species *Obolus* (*Westonia*) *ella* (Hall and Whitfield). These forms are sparse in the Pioche Shale of the Wasatch Range. *Olenellus* fossils are unknown in any other sections in the area and in most areas are confined to the lower beds of the Pioche, but *Obolus* occurs higher in the section in most parts of the area.

Genera of the Olenellidae occur in many Lower Cambrian rocks in North America and northwest Europe. Howell *et al.* (1944, chart) indicate that the *Olenellus* zone is underlain by three zones in Europe and northeastern North America and by two zones in the Appalachian region of the United States. Further, a section of Lower Cambrian rocks in the Inyo Range of California and Nevada, not shown on the chart, contains fossils of Early Cambrian age which probably antedate the forms in the Pioche Shale. The *Olenellus* zone in western Utah (House Range) is immediately subjacent to and conformable with strata containing elements of the *Antagmus-Onchocephalus* zone (*Syspacephalus* zone of Howell's chart) which has not been recognized in northeastern Utah and Idaho and is of latest Early Cambrian age.

Lochman (1953, p. 487–488) states that on the basis of present knowledge " . . . the entire Lower Cambrian should be correctly labeled the *Olenellus* zone . . . " She also describes two subdivisions of the zone: (1) a lower subzone characterized not only by Olenellidae but by primitive nontrilobitic forms including the brachiopod, *Obolella*, and (2) an upper subzone characterized by Olenellidae associated with Eodiscidae, general of the Corynexochidae, and primitive opisthoparian genera. Presumably this upper subzone would correspond with the *Syspacephalus* zone of Howell *et al.* (1944, chart) and with the *Antagmus-Onchocephalus* zone. The *Bonnia-Olenellus* zone of Rasetti (1951, p. 81–83, 109) apparently is essentially synonymous with the *Olenellus* zone of Lochman.

In northern Utah and southeastern Idaho the *Olenellus* zone as defined above is recognizable and of stratigraphic value, although it appears that we are dealing with fossils that appear in the upper part of the zone in other areas.

### Glossopleura-Zacanthoides *Zone*

Faunas in those beds of the Langston and Pioche Formations which directly overlie the beds containing Early Cambrian fossils characteristically contain the trilobite genera *Glossopleura* and *Zacanthoides*. One, and usually both, genera occur commonly in the strata of the Langston and basal Ute Formations of central and northern Utah and southeastern Idaho. Numerous distinctive forms belonging to both trilobite and inarticulate brachiopod genera occur with them in some areas (see fauna numbers in the preceding section and in Figure 3). Neither form has been observed in strata overlying the topmost rocks of the Ute Formation. On the basis of the distinctly limited range of these two genera, it is here proposed that the beds in which they occur be designated the *Glossopleura-Zacanthoides* zone.

Trilobite genera most common near the base of this zone include *Dolichometopsis*, *Ptarmigania*, *Chancia*, *Clavaspidella*, *Oryctocephalus*, *Kootenia*, *Kochina*, *Kochaspis*, *Taxioura*, *Oryctocare*, *Alokistocare*, *Ehmaniella*, *Clappaspis*, and *Albertella*. Of these, *Albertella* is one of the more uncommon trilobite genera. Only a few specimens of this genus are known from Utah and Idaho. However, *Albertella* occurs at or near the base of the Middle Cambrian in many localities in the Western Cordillera. Because of this widespread occurrence, members of the genus are Middle Cambrian guide fossils. Similarly, some species of *Kochaspis* are guide fossils in the lowest Middle Cambrian beds in Utah, Nevada, Idaho, and Canada. In Utah and Idaho, species of *Kochaspis* occur in the same basal Middle Cambrian beds with *Albertella* (the Naomi Peak and Spence shale members). It is here proposed that the basal beds of the *Glossopleura-Zacanthoides* zone be placed in the *Albertella-Kochaspis* subzone.

The beds between the *Albertella-Kochaspis* subzone and the uppermost Langston strata in northern Utah and southern Idaho are only sparsely fossiliferous. Members of the trilobite genera *Glossopleura*, *Zacanthoides*, *Kootenia*, *Kochina*, and *Glyphaspis* have been observed occasionally. These forms are common in beds in a similar stratigraphic position in other areas, where they are usually referred to as the "*Zacanthoides-Anoria* zone" (Howell *et al.*, 1944, Chart). *Zacanthoides* occurs in Utah throughout a considerably thicker interval and may be most practicably utilized as a guide fossil for that interval. Further, *Anoria* has been reported from only the interval in question. Therefore, it is suggested that this sequence of beds be tentatively referred to as the *Anoria* subzone of the *Glossopleura-Zacanthoides* zone in Utah and Idaho.

The beds in the upper part of the *Glossopleura-Zacanthoides* zone, between the uppermost Langston or basal Ute Formations and the base of the Blacksmith Dolomite, commonly contain the trilobite genera *Glossopleura*, *Zacanthoides*, *Solenopleura*, *Kootenia*, *Kochina*, *Elrathina*, *Ehmaniella*, *Dolichometopsis*, *Clappaspis*, *Anomalocephalus*, and *Alokistocare*. Howell *et al.* (1944, p. 995) listed the trilobite genus *Solenopleurella* as a fossil common to the "*Glossopleura-Kootenia* zone." Since this is the only form that does not commonly occur elsewhere in the *Glossopleura-Zacanthoides* zone in Utah and Idaho it may be tentatively referred to as the *Glossopleura-Solenopleurella* subzone.

This zonation agrees with the zones proposed by other authors. Lochman (1952, p. 79–81) has recognized two zones, the *Albertella* and the *Glossopleura-Kootenia* which closely compare in range, faunule succession, and faunal content to the interval here proposed as the *Glossopleura-Zacanthoides* zone. Presumably an interval containing elements of the *Anoria* subzone is not present in Sonora, or these elements are blended with one or the other or both of Lochman's zones and are not recognizable there, perhaps as a result of facies differences in the corresponding parts of the stratigraphic section.

Rasetti (1951, p. 93–99, 109) also recognizes two zones, the *Albertella* and the *Glossopleura* which again closely correspond with the *Glossopleura-Zacanthoides* zone, and differ in perhaps the same manner and for the same reasons given above. Rasetti, however, recognizes two zones beneath his *Albertella* zone and above the *Olenellus* zone (his *Bonnia-Olenellus* zone), the *Wenkchemnia-Stephenaspis* zone and the *Plaguira-Kochaspis* zone. Lochman (1953, p. 486–487), who did not recognize these zones in Sonora (Lochman, 1952, p. 80), suggests that they may merge in other areas. Rasetti (1951, p. 80) also suggests this possibility. Lochman further states that faunas which should be assigned to a merged zone may have been collected several places in the western United States and Sonora but that adequate evidence is not yet available to assign them to this zone. Many forms found in the Naomi Peak Limestone associated with *Kochaspis* and

*Albertella* are similar to those listed by Rasetti from his zones. Thus, more extensive collection and study of the fossils may result in recognition of these zones or of a merging of the two zones in Utah and Idaho.

### Bathyuriscus-Elrathina *Zone*

Trilobite genera related to *Ehmania* and *Ehmaniella* have been reported by Howell *et al.* (1944 chart) from the base of the Blacksmith formation in northern Utah. They are included in the *Bolaspis-Glyphaspis* zone of Howell. A fauna consisting of genera of "*Agnostus*", *Elrathia*, and *Bolaspidella* was found by Denson in the lower part of the upper beds of the Blacksmith Dolomite and was assigned by Howell to the *Elrathiella-Triplagnostus-Clappaspis* zone (Howell *et al.*, 1944, chart). The writer found only fragmental fossils not subject to accurate identification in the upper beds of the Ute Limestone and in all but the uppermost interval of the Blacksmith Dolomite.

Although Deiss (1938, p. 1105–1124, 1161–1163) did not find fossils in this interval of the Blacksmith Fork section he found faunules comparable to those mentioned above in Montana and in the House Range and later (1939, p. 1016–1022; 1940, p. 731–794) in the Canadian Rockies. He included these forms in his *Ehmania*, "*Agnostus*"-*Bathyuriscus*, *Bathyuriscus-Elrathia*, and *Bathyuriscus-Elrathina* faunas. These faunas succeeded his *Glossopleura* fauna and preceded his *Thompsonaspis* or *Olenoides* (*Neolenus*) fauna. The interval in which he found these fossils corresponds stratigraphically and in sequence of faunules to the interval between the *Glossopleura-Zacanthoides* zone and the *Thompsonaspis* zone of this paper.

Rasetti (1951, p. 99–109) has studied this stratigraphic interval in the Canadian Rockies and has proposed that it be called the *Bathyuriscus-Elrathina* zone.

On the basis of present knowledge it appears proper to apply Rasetti's zone name in northeastern Utah for the interval between the *Glossopleura-Zacanthoides* and *Thompsonaspis* zones even though Rasetti does not find *Ehmania* or *Bolaspis-Glyphaspis* zone forms in the Canadian Rocky sections. Thus, the *Bathyuriscus-Elrathina* zone as used in this paper includes the *Bolaspis-Glyphaspis* zone of Howell *et al.* and of Lochman; the *Elrathiella-Triplagnostus-Clappaspis* zone of Howell *et al.*, the *Elrathiella-Clappaspis* zone of Lochman; it is essentially equivalent to the *Bathyuriscus-Elrathina* zone of Rasetti.

### Thompsonaspis *Zone*

In the Bear River Range Denson (1942, p. 26) and the writer collected trilobites from the uppermost beds of the Blacksmith Dolomite which are the same forms as those Denson refers to a *Thompsonaspis* faunule that occurs in Wyoming. Deiss (1938, p. 1018–1019) recognizes in sections in the Cordilleran and Canadian Rocky regions a faunule composed of essentially the same forms which he calls the *Olenoides-Thompsonaspis* fauna. In all these areas this faunule is found in rocks which overlie strata of the *Bathyuriscus-Elrathina* zone and underlie rocks containing elements of the distinctive *Asaphiscus-Bolaspidella* zone. This interval containing *Thompsonaspis* and associated forms is here referred to as the *Thompsonaspis* zone.

### Asaphiscus-Bolaspidella *Zone*

The beds constituting the Bloomington Formation in northern Utah and southern Idaho contain genera of trilobites including *Asaphiscus*, *Bolaspidella* (*Deissella* of some authors), *Blainia*, *Olenoides*, *Solenopleura*, *Parehmania*, *Bolaspis* (?), *Acrocephalops*, *Elrathia*, *Homagnostus*, and several undescribed genera (see fauna numbers 16, 16a, and 17 in the preceding section). Similar faunas occur in the lower and middle parts of the Marjum Formation in the House Range of Utah and in upper Middle Cambrian formations in Montana. *Asaphiscus* and closely allied forms and *Bolaspidella* (*Deissella* of Denson and others) are common elements in all these faunas and seem to be restricted to this interval of the Cambrian system. Therefore it is proposed that these beds be designated the *Asaphiscus-Bolaspidella* zone.

Denson (1942, p. 26) divided this zone into two "faunules," basing his evidence for this subdivision on genera for which descriptions have not yet been published. Preliminary work in this and other areas indicate that such a division will probably prove satisfactory.

The *Asaphiscus-Bolaspidella* zone is the uppermost zone of the Middle Cambrian and is conformably overlain by beds (Nounan Formation) containing the Lower *Cedaria* zone of Late Cambrian age.

#### *Discussion*

The names of some of the faunal zones described here do not conform with those sug-

gested by the Cambrian subcommittee (Howell *et al.*, 1944, chart) nor with those described by Lochman (1952, p. 73–78) for northwestern Sonora in Mexico. The writer firmly believes that, wherever possible, a faunal zone should be named for a diagnostic fossil or assemblage of fossils and, further, that, where practicable, it should include all beds in which that diagnostic fossil or fossil assemblage occurs. Such a procedure will undoubtedly render faunal zones far more usable. For example, the Cambrian subcommittee lists four faunal zones (the *Kochaspis liliana*, *Albertella*, *Zacanthoides-Anoria*, and *Glossopleura-Kootenia* zones), and Lochman lists two (the *Albertella* and *Glossopleura-Kootenia* zones) in which the two trilobite genera *Glossopleura* and *Zacanthoides* commonly occur. To the writer's knowledge the two genera do not occur in any other zones in Utah and southern Idaho. Two of the zones of the subcommittee, the *Kochaspis liliana* zone and the *Albertella* zone, appear to be a single unit, as was suggested by Williams and Maxey (1941, p. 284) and as was later recognized by Lochman (Wheeler, 1948, p. 46). One other zone, the *Glossopleura-Kootenia* zone, is named for one genus that commonly occurs well below the designated lower boundary of the zone and for another genus that occurs both above and below the designated boundaries of the zone. The writer, therefore, has described and proposed the *Glossopleura-Zacanthoides* zone, which includes all the beds in which the two genera for which it is named are known to occur. Further, he has suggested subdivisions of the zone, or subzones, named after guide fossils within the zone.

Fossil evidence does not indicate the same sequence of forms for Utah that is suggested by the zones proposed by the Cambrian subcommittee (Howell *et al.*, 1944, chart), especially the zones of late Medial Cambrian age. The available published material indicates that *Thompsonaspsis* and associated forms occur before *Marjumia* and with forms closely related to early-appearing members of the writer's *Asaphiscus-Bolaspidella* zone. For example, Howell's chart (1944) shows *Marjumia* appearing before *Thompsonaspsis*. Actually *Marjumia* has been found only in the top of the *Asaphiscus-Bolaspidella* zone and in overlying Upper Cambrian strata. Also *Bolaspidella* (*Deissella*) appears in the lower part of the *Asaphiscus-Bolaspidella* zone and has not been found with *Marjumia* and related elements. Although *Olenoides* occurs throughout the Middle Cambrian section, members of the genus are most common and varied in the upper part of the *Asaphiscus-Bolaspidella* zone, especially in the Marjum Formation of the House Range and in the Bloomington Formation of northern Utah and southern Idaho rather than before *Thompsonaspis*. In Utah and Idaho, beds containing *Thompsonaspis* underlie beds containing the late Medial Cambrian forms of *Olenoides*, *Orria*, and *Bolaspidella*, and *Bolaspidella* occurs throughout the interval in which *Orria*, *Asaphiscus* and allied forms, and *Olenoides* are found.

The sequence of zones for the Lower and Middle Cambrian given by the Cambrian subcommittee (Howell *et al.*, 1944), Lochman (1952, p. 80; 1953, p. 486–488), Rasetti (1951, p. 109), and the sequence proposed in this paper for Utah and Idaho are as shown on p. 680.

## Early and Medial Cambrian Sedimentation and Paleogeography

### *Description of the Lithofacies*

Several lithofacies of Early and Medial Cambrian age are common throughout Utah and southeastern Idaho. Many of these lithofacies are distinctive and are easily identified by common macroscopic methods. The distinguishing characteristics are valuable clues to their origin. The facies include: (1) the orthoquartzite facies, composed chiefly of medium to coarse quartz particles with some interbedded lenses of quartz pebbles; (2) greenish-brown, micaceous, and finely arenaceous shale, normally interbedded with layers of the orthoquartzite; (3) brown-weathering calcareous sandstone; (4) rusty-brown-weathering dolomite; (5) green and buff fissile shale; (6) highly calcareous, dark-gray to black shale and dark-gray, shaly, platy, aphanitic limestone; (7) mottled, silty, aphanitic and thin-bedded limestone; (8) the *Girvanella* limestone; (9) intraformational conglomerate; and (10) oölitic limestone. Certain other lithofacies are composed of nondescript types, all carbonate, which are here placed in one of two groups—the "undifferentiated limestones" and "undifferentiated dolomites."

Recognition of the lithofacies is based chiefly upon their macroscopic features. Undoubtedly sedimentological or statistical studies would reveal evidence which might provide a basis for revision in both the recognition and the interpretation of the lithofacies; however, the writer believes that the presently recognized

| Cambrian Correlation Chart (Howell et al., 1944) | Lochman (1952; 1953) | Rasetti (1951) | This paper |
|---|---|---|---|
| | | Late Cambrian | Lower Cedaria zone |
| | | Medial Cambrian | |
| *Deisella-Centropleura vermontensis* zone<br>*Palella-Thompsonaspis* zone<br>*Olenoides-Orria-Marjumia* | | | *Asaphiscus-Bolaspidella* zone |
| | | | *Thompsonaspis* zone |
| *Elrathiella-Triplagnostus Clappaspis* zone<br>*Bolaspis-Glyphaspis* zone | *Elrathiella Clappaspis* zone<br>*Bolaspis-Glyphaspis* zone | *Bathyuriscus Elrathina* zone | *Bathyuriscus-Elrathina* zone |
| *Glossopleura-Kootenia* zone | | | |
| | *Glossopleura Kootenia* zone | *Glossopleura* zone | *Glossopleura-Zacanthoides* zone |
| *Zacanthoides-Anoria* zone | | | |
| *Albertella* zone<br>*Kochaspis liliana* | *Albertella* zone | *Albertella* zone<br>*Plagiura-Kochaspis* zone<br>*Wenkchemnia-Stephenaspis* zone | |
| | | Medial Cambrian | |
| | | Early Cambrian | |
| *Syspacephalus* zone<br>*Olenellus* zone<br>*Bonnia* zone<br>*Obelella* zone | *Olenellus* zone | *Bonnia-Olenellus* zone | *Olenellus* zone |

facies and the interpretations based upon them add considerably to the understanding of Early and Medial Cambrian sedimentation and paleogeography. In many instances the facies correspond closely to those recognized by McKee (1945, p. 1–168) in the Grand Canyon region where the excellently exposed, continuous outcrops of the Cambrian formations allow opportunity for far more detailed study than do the widely separated outcrops in the Great Basin region. Much of McKee's evidence and interpretation is here recognized as the best available explanation for many lithologic and stratigraphic phenomena observed during the present study.

ORTHOQUARTZITE: The dominant facies of the Lower Cambrian strata in the area is medium- to coarse-grained "clean" orthoquartzite (rarely containing lenses of quartz conglomerate) which constitutes the principal part of the Prospect Mountain Quartzite and a considerable part of the Pioche Formation. It consists of quartz particles most of which are subangular and firmly cemented with silica or, only occasionally, with iron oxide. When iron-oxide cement predominates the rock is somewhat friable. Labile mineral particles, mostly feldspar, occur locally. The pink, red, purple, and green of the various strata are probably due to dissemination of iron oxide. Most of the strata are medium- to thick-bedded (4–12 inches thick), but many are massive (more than 12 inches thick). Some syngenetic structures, such as common and characteristic cross-lamination and current ripple marks, are of inorganic origin. Probable organic structures which commonly occur, especially as casts on bedding planes, are burrows, tracks, and trails which may indicate the passage of trilobites, phoronids, and worms. Most of these markings have

been described under the generic terms of *Cruziana* (trail-like markings) and *Skolithos* (worm or phoronid burrows) and are the only fossils reported from this facies.

The conglomeratic phases of the facies appear ordinarily at the base of the Porspect Mountain Formation. Lenses of the conglomerate at this horizon in the few outcrops where the formational base is exposed are commonly composed of unusually coarse, in places very angular particles as large as boulders. The writer has noted such outcrops in the central part of the Wasatch Range, and Eardley (1933, p. 315–316) has reported them in the southern part of the Wasatch. Conglomeratic lenses are not confined to the basal part of the formation but also occur occasionally throughout its thickness and in the orthoquartzite facies of the Pioche Formation. Most of the particles in these upper lenses are small, well-rounded quartz pebbles in a medium- to coarse-grained sand matrix.

Inasmuch as the orthoquartzite facies composes most of the Prospect Mountain Quartzite, it is widespread in the Great Basin and locally is several thousand feet thick. In many sections it is interbedded with green, micaceous, and silty shale in the Pioche Formation and in the upper transitional beds of the Prospect Mountain Quartzite. Therefore, the environment which it represents apparently returned for several brief periods after the main deposition of the orthoquartzite. The orthoquartzite was not observed in formations overlying the Pioche Formation.

At the base of the Cambrian section in the Grand Canyon area McKee reports a conglomerate and a coarse sand facies that resemble this orthoquartzite facies. However, the Grand Canyon facies is less quartzitic, occurs in thinner layers, and contains much less silica and much more iron-oxide cement. After a detailed study McKee (1945, p. 38, 47–51) concluded that the Grand Canyon conglomerate facies was deposited in a near-shore marine environment and that the coarse sand facies was probably deposited in waters less than a mile to 15 or 20 miles from shore ranging in depth from 20 to 60 feet. The writer believes these interpretations more or less accurately describe the environment of deposition of the orthoquartzite facies in the Great Basin area.

GREENISH-BROWN, MICACEOUS AND FINELY ARENACEOUS SHALE: Most of the Lower Cambrian strata in Utah and southeastern Idaho except the orthoquartzite facies are normally composed of greenish-brown and gray-green, micaceous, finely arenaceous, hard shale much of which is flaggy but seldom fissile. Some beds contain a little calcareous cement. In many places the bedding planes are covered with worm-burrow castings, trails, and fucoidal structures. In Utah a few inarticulate brachiopod shells and the remains of one poorly preserved trilobite are the only fossils reported. Inorganic syngenetic structures include ripple marks, occasional cross-lamination, and crater-like pits on the bedding planes. In most localities the shale is interbedded with strata of the orthoquartzite facies in the transitional beds near the top of the Prospect Mountain Quartzite and throughout the Pioche Formation. It rarely occurs higher in the section in those areas where it is interbedded with limestones of the Langston, Ute, and Bloomington Formations. It apparently is one of several lithologic types deposited seaward from the orthoquartzite facies and nearer shore than the carbonate facies. It may well have been deposited near shore in place of the orthoquartzite facies when coarse clastic material was lacking.

BROWN-WEATHERING CALCAREOUS SANDSTONE AND SANDY LIMESTONE: This facies is characteristic of the basal part of the Langston Formation in the Wasatch and Bear River ranges. It appears higher in the Langston and Ute Formations where very thin beds and lenses of it are intercalated between relatively great thicknesses of the limestone facies. In most places it is composed of angular and subangular, fine quartz grains embedded in calcareous or dolomitic cement. In some places it is quartzitic and hard but it is usually friable. Calcareous or dolomitic cement is predominant and forms a finely to medium-crystalline, steel-gray to dull neutral-gray matrix which may be flecked with small irregular limonitic stains. The strata of this facies are usually irregularly bedded and channeled; the channels are filled with fragments of trilobite cranidia and pygidia and inarticulate brachiopods. Although it is gray on fresh fracture, it weathers to rusty-brown or orange-brown outcrops and is valuable as a marker. The brown-weathered surfaces result from concentration of silt and iron stain when the calcareous material is leached. In most places the calcareous sandstone and sandy limestone overlies and interfingers with the upper part of the greenish-brown, micaceous shale facies and underlies and interfingers with the lower part of one of the carbonate facies. These relationships suggest that it was probably

deposited seaward from the shale and landward from the carbonates. However, the writer deems interpretations of environment based on existing evidence afforded by the facies rather unsatisfactory. It was probably deposited in an environment similar to that in which the rusty-brown dolomite was formed. In many places this latter facies replaces the calcareous sandstone in the stratigraphic sequence in the south part of the Bear River Mountains in northeastern Utah. The rusty-brown dolomite seems to occur only eastward from the sandstone in this area. McKee (1945, p. 59–62) studied rusty-brown dolomites in the Grand Canyon region and concluded they were the depositional product of a transgressng sea in a specialized environment.

RUSTY-BROWN DOLOMITE: A steel-gray to dull-gray, silty and sandy, finely to coarsely crystalline, medium- to thick-bedded dolomite is common in the Langston Fromation in the northern part of the Wasatch Range and in the Bear River Range. It also occurs sparingly in the Cambrian rocks in other parts of Utah and Idaho. It forms lenses and tongues which interfinger with the brown-weathering calcareous sandstone and sandy limestone. Both facies weather to buff-tan, rusty-brown, or red-brown, limonite-stained, silty surfaces and are commonly indistinguishable in the field unless fresh surfaces are carefully examined and treated with dilute acid. The rusty-brown dolomite of the Langston Formation occurs in thin, irregularly bedded lenses and tongues in the Spence Shale and Naomi Peak Limestone on Wellsville Mountain, Willard Peak, and Promontory Point. Because these intervals thicken eastward the dolomite constitutes most of the lower part of the Langston in Blacksmith Fork where it is thickly interbedded with units of crystalline and algal limestone and other dolomitic facies.

McKee (1945, p. 59–62), who described a similar rock type from the Grand Canyon region, concluded that (p. 60):

> "The distribution of the various tongues of rusty-brown dolomite in the Grand Canyon shows that they are developed, without exception, among the deposits formed at times of a transgressing sea and not among those of regression. Furthermore, they are all located on the eastern margins of limestone facies and between these and areas of clastic sediments. They are associated almost everywhere with iron oxides and in most places with glauconite. Algal or *Girvanella* limestones, wherever present, form a facies between the dolomites and aphanitic, mottled limestones to the west."

and (p. 62):

> "The following events and factors are believed by the writer to have led up to the development of the rusty-brown dolomite facies in the Cambrian deposits of Grand Canyon:
>
> Periodic rapid sinking of the basin caused the sea to advance eastward relatively rapidly, from time to time, for distances of 25 to 100 miles, and as a result of each transgression, the zone of clastic deposition likewise shifted far eastward. Meanwhile, conditions favorable to calcium carbonate accumulation apparently did not move shoreward a corresponding amount, so a specialized facies developed, intermediate in position between the areas of clastic and pure-lime deposition. This facies was controlled by waters of fairly high concentration, as indicated by dolomitic sediments and as suggested by the near-shore position. Furthermore, it was an area of less deposition than to seaward, as is shown both by the abundance of glauconite and by the accumulation of a far smaller amount of nonclastic sediment there than in the corresponding or synchronous limestone facies to the west."

The writer believes this interpretation is probably accurate in regard to the rusty-brown dolomite facies of Utah and that the brown-weathering calcareous sandstone and sandy limestone facies was perhaps deposited seaward from the dolomite in an otherwise similar environment.

GREEN AND BUFF FISSILE SHALE: Green and buff argillaceous and in places micaceous, fissile shale beds ranging from a few inches to several tens of feet thick are commonly interbedded with the various limestone facies of the Ute and Bloomington Formations and with the greenish-brown arenaceous shale facies of the Pioche Shale. Generally, this facies occurs in very thin layers intercalated between relatively thick coarser clastic and limestone beds. The green fissile shale contains calcareous nodules and small (about 1–10 feet long and a few inches thick), thin, crystalline, commonly fossiliferous limestone lenses. Trilobite and inarticulate brachiopod fossils are abundant in the shale beds, and the bedding planes are marked by many fucoidal structures, worm burrows, and trails.

In most instances, these shale beds seem to be regressive clastic tongues deposited as a result of minor oscillations of the sea. In other outcrops they appear to be the product of mud deposition between the coarser clastics which were deposited landward and the carbonate deposition far from shore.

BLACK TO DARK-GRAY, HIGHLY CALCAREOUS SHALE OR SHALY LIMESTONE: This facies makes up much of the Spence Shale Member of the

Langston Formation. It also occurs sparingly as thin intercalations in the Naomi Peak Limestone Member of the Langston Formation. As its name implies, the facies consists chiefly of highly calcareous, thin-bedded to fissile shale or very shaly thin-bedded, aphanitic limestone. It contains many well-preserved trilobite fossils, much pyrite and limonite (usually in pseudomorphs after pyrite), and generally weathers to low, light- to medium-gray ledges and plate-strewn slopes. Commonly the ledges weather to light-brown or tan surfaces. Intervals ranging from a few inches to 100 feet of the calcareous shale are interbedded with intervals of the shaly limestone of approximately the same thickness. Thin intercalations and beds of buff or greenish shales are commonly interbedded with this facies.

These black shales and black shaly limestones do not correspond lithologically with most black shales because they contain relatively large amounts of calcium carbonate, numerous benthonic fossil remains, and are not interbedded or associated with coarser clastics (Twenhofel, 1950, p. 333–337; Pettijohn, 1949, p. 289). It appears that occurrences of this lithologic type are relatively rare. Perhaps the black, calcareous, pyritic shales and limestones of the Upper Cretaceous rocks of the Black Hills region resemble this facies more than other described black shales. Rubey (1930, p. 13) concluded that

> "... the conditions most favorable for the formation and preservation of calcium carbonate, organic material, and pyrite together would be relatively shallow water and a rapid rate of accumulation and burial of organic matter. Under these conditions much organic matter and carbonate would be preserved by burial, and iron sulfide would form abundantly in the putrefying ooze—that is, chiefly below its upper surface."

He cites evidence from the studies of Recent sediments by Murray and Irvine (1891; 1895) that such depositional conditions are common in modern seas. The writer tentatively accepts this interpretation as an explanation of the origin of the Middle Cambrian black, calcareous shale and shaly limestone facies. Further detailed sedimentological and stratigraphic study of the facies is needed.

MOTTLED AND BANDED, APHANITIC, THIN-BEDDED LIMESTONE: Much of the limestone assigned to the Lower and Middle Cambrian formations in Utah and southeastern Idaho consists of dark-gray, silty, aphanitic, thin-bedded limestone and dolomitic limestone which weathers to low, light- to medium-gray ledges with yellow-brown or reddish-brown mottling or irregular, wavy, thin ridges on the weathered surfaces. Thin layers and partings of greenish-gray shale and tan silt are generally intercalated with the thin beds of limestone. Flakes and nodules of the silt and clay are irregularly distributed throughout the limestone matrix and are seldom distinguishable except on weathered surfaces. The mottled thin-bedded limestone facies is commonly interbedded with oölitic limestone and algal beds. The intervals of the mottled facies are normally much thicker than the other facies. Although numerous poorly preserved fossils, especially trilobites, are found on weathered surfaces, well-preserved fossils are rare in the unweathered rock. Better preserved and more easily recoverable fossils are generally found in the thin intercalations and layers of shale between the limestone beds. Structures resembling the casts of worm burrows and trails are common in these beds.

As McKee (1945, p. 71–77) has suggested, these silty limestone beds seem to be indurated calcareous ooze mixed with fine clastic material which was deposited too far from shore to be diluted with large amounts of coarser clastic material. He indicates that the dolomitic mottled rock may have originally been limestone which was replaced by dolomite before and during lithification.

*Girvanella* LIMESTONE: McKee (1945, p. 62–64) described a limestone characterized by spherical and ovoid nodules scattered throughout a finely crystalline matrix. The nodules have concentric structure and are considered algal deposits referable to the form genus, *Girvanella*. Numerous students of the western Cambrian formations have commented upon these algal limestones. They form a rather common facies in the formations of Utah and southeastern Idaho and occur in the section above the coarse clastic facies interbedded with the fissile green shale and with strata of the other limestone facies. Normally the intervals of *Girvanella* limestone are relatively thin, but some of them are more than 100 feet thick. They seem to represent an environment developed somewhat far from shore, one that probably was seaward from that in which the rusty-brown dolomite and brown-weathering calcareous sandstone facies was deposited. The *Girvanella* limestone is especially common in the Langston and Ute Formations, but is scarce in the Blacksmith and Bloomington Formations.

INTRAFORMATIONAL CONGLOMERATE: This facies is composed of thin, flat pebbles oriented in one or more directions, composed of locally derived limestone embedded in a limy matrix. It has been referred to as "edgewise conglomerate" (Nason, 1901, p. 360; Grabau, 1924, p. 785). Units of the conglomerate are relatively thin, and most of them are interbedded with other types of limestone or with dolomite. It occurs chiefly in beds a few inches to a few feet thick in the Langston and Bloomington Formations, but is rare in the other limestone formations.

McKee (1945, p. 65–70) suggests various modes of origin for these conglomerates. He shows that the intraformational conglomerates of different beds in the Grand Canyon area have generally similar features, are commonly found in deposits formed at times of regression, and are located exclusively along shoreward margins of other limestone facies. This means that they were deposited, for the most part, more than 100 miles seaward from the shore line and were probably deposited when the rate of sinking of the depositional basin slowed down so that parts of it were above the profile of equilibrium and caused regression of the sea (McKee, 1945, p. 68–69).

Since all observable data on the origin of the conglomerates in Utah seem to bear out McKee's interpretation, it is tentatively accepted as valid in this area.

OÖLITIC LIMESTONE: Dark-gray to black, fine- to medium-crystalline, medium- to thick-bedded limestone containing oölites ½–1 mm in diameter is commonly interbedded with other limestone facies in the Middle Cambrian formations of Utah. Most of the units of oölitic limestone are thinner than the units of other limestone facies with which they are interbedded. They are commonly interbedded with the *Girvanella* limestone and the intraformational conglomerate, and less generally with the silty, aphanitic limestone.

According to Eardley (1938, p. 1359–1387) who described the formation of oölites in Great Salt Lake, Utah, calcareous oölites normally form as the result of limestone deposition around nuclei in open shallow, strongly agitated waters. Probably the Cambrian oölitic beds were deposited in a somewhat similar environment for they are closely associated with other beds that were also deposited in shallow seas.

UNDIFFERENTIATED CRYSTALLINE LIMESTONES: Considerable thicknesses of finely to coarsely crystalline limestones characterize much of the Middle Cambrian section. Wide variance in color, bedding habit, texture, and weathered surfaces was noted but few distinctive features were observed. However, more detailed investigation might reveal such features. Conditions for deposition of these limestones were probably somewhat similar to those described for some of the other limestone facies except that, in general, these undifferentiated limestones were probably formed in deeper waters and farther from shore than the other facies.

UNDIFFERENTIATED DOLOMITES: As in the case of the undifferentiated limestones mentioned above, considerable thicknesses of dolomites are also present in the Middle Cambrian section. Sufficient time for further study of these dolomites was not available and the problem of the origin of the dolomites is beyond the scope of this paper. Although a detailed study was not made, several kinds of dolomite were observed. Three types are similar to dolomites described by McKee (1945, p. 77–79): (1) a very light-colored (usually white or light-gray), crystalline, thick-bedded dolomite; (2) a light-gray to steel-gray, finely crystalline, laminated dolomite which weathers to cream-colored surfaces; and (3) a medium- to light-gray, usually thinly bedded, platy-weathering dolomite which often forms light- and dark-gray streaked and mottled outcrops.

McKee (1945, p. 77–79) suggested a mode of origin for the "undifferentiated dolomites" in the Grand Canyon region. His conclusions are that the dolomites

> "... were all formed in waters of a regressive sea. The dolomite probably was developed on the sea floor either through direct precipitation or from penecontemporaneous replacement, as is indicated by its uniform distribution over wide areas, and its representation as clastic grains within various beds. Nowhere, so far as is known, does it show evidence of being the result of secondary action. The suggestion is made, therefore, that these deposits are the result of shoaling waters with sea bottom near the base level of deposition, which, as is pointed out by Twenhofel (1939, p. 358), favor higher concentration and dolomite development."

The results of the writer's study concur, in general, with McKee's. Only in a few local instances was evidence observed of secondary dolomitization in the vicinity of faults and other structural features. This dolomitization seems to border fault zones and joints and is similar to that described by Hewett (1931, p. 57–60) in the Goodsprings area, Nevada. A detailed study of the widely distributed and

apparently syngenetic or penecontemporaneous Cambrian dolomites and their relationships with the limestones and other facies might well yield interesting and valuable data concerning the mode of origin of dolomite.

### *Interpretation and Paleogeography*

The evidence presented indicates that the sediments of Early and Medial Cambrian age in Utah and southwestern Idaho were deposited in an oscillating shallow sea which transgressed eastward from beyond the western border of Utah. The surface over which this sea advanced was probably mature with considerable relief because the lowermost Cambrian formation (the Prospect Mountain Quartzite) ranges considerably in thickness and has at its base in some localities a coarse subangular conglomerate. These conditions suggest adjacent highlands. For example, between the northern part (Wellsville Mountain) and the central part of the Wasatch Range the orthoquartzite thins southward from more than 3000 feet to about 900 feet, and near Ogden, Salt Lake City, and Provo, Utah, where the base of the orthoquartzite is exposed, the conglomerates commonly constitute the basal member of the formation. This is the locale of the Precambrian Northern Utah Highland (Eardley, 1939, p. 1277–1310) which probably persisted as a highland during earliest Cambrian time. Very early in Cambrian time, perhaps even in late Precambrian (Wheeler, 1948, p. 19–20, Fig. 5), the eastward-transgressing sea had inundated the lands to the west in Nevada and southern California and was advancing across western Utah. The biostratigraphic relationships of the Lower and Middle Cambrian formations of Utah, Idaho, and Wyoming indicate that the strand line reached the eastern boundary of Utah near the close of the Early Cambrian epoch.

The descriptions of the various facies and faunas indicate that the Early Cambrian was primarily an epoch of clastic deposition through Utah. The source of the clastic sediments has been suggested by Deiss (1941, p. 1090) as ". . . the isolated granitic areas to the east and north." The writer did not observe conclusive evidence that this interpretation is wholly valid. Much of the material must have been derived from the east because the sea was transgressing in that direction and adjacent areas in Nevada were covered by it. On the other hand, the Busby Quartzite of the Deep Creek Range (Nolan, 1935, p. 7–8) seems to interfinger with the Langston Formation in the House Range (Wheeler, 1948, p. 28–29) and in the Sheeprock Range. This suggests that some clastics, at least in late Early Cambrian time, were derived from the west. Detailed studies, similar to those made by McKee (1945, p. 38–51) of the Tapeats Sandstone in the Grand Canyon region, are needed before further conclusions about source areas can be made.

That the strand line of the eastward-transgressing sea constantly oscillated, especially in late Early Cambrian time, is indicated by the interbedded strata of orthoquartzite and arenaceous greenish-brown shale composing the upper transitional beds of the Prospect Mountain and the Pioche Formations. Probably these oscillations resulted from periodic rapid subsidence followed by decreased subsidence or still-stand, when the sea would temporarily regress as the basin was gradually filled to above the profile of equilibrium.

By Medial Cambrian time, Utah and southeastern Idaho were inundated, and the Precambrian highlands were sites of deposition. The strand line was far to the east, and the seas were probably somewhat deeper in most places than they had been in the Early Cambrian. Thus, in Utah this epoch was primarily a period of carbonate and mud deposition in an environment closely approximating the epineritic and shallower parts of the infraneritic zones of modern seas. Oscillations of the strand line continued throughout the epoch and are attested to by the alternate interbedding and interfingering of layers of regressive shallow-water facies such as the green fissile shale, the oölitic limestone, and the intraformational conglomerates with strata of the deeper-water facies. No evidence of unequal subsidence and the resulting formation of separate basins was observed. Highland areas, except far to the east, were probably inundated. The area of the old Northern Utah Highland was re-elevated and deeply eroded in post-Medial Cambrian time, and all of the Upper Cambrian and most of the Middle Cambrian formations are missing. However, the formations that are exposed exhibit no thinning, and some formations thicken from the north across this area. Therefore, the Highland was inundated throughout Medial Cambrian time. No physical evidence of disconformity or biologic evidence of discontinuity was found between the Middle and Upper Cambrian rocks, and it is believed that sedimenta-

tion continued without a break into the Late Cambrian.

## Selected References


Baker, A. A., 1947, Stratigraphy of the Wasatch Mountains in the vicinity of Provo, Utah: U. S. Geol. Survey, Oil and Gas Inv., Prelim. Chart 30

Blackwelder, Eliot, 1909, New light on the geology of the Wasatch Mountains, Utah: Geol. Soc. America Bull., v. 21, p. 517–542

Burling, L. D., 1914, Early Cambrian stratigraphy in the North American Cordillera, with discussion of the *Albertella* and related faunas: Geol. Survey Canada Mus. Bull., no. 2, p. 93–129

Butler, B. S., and others, 1920, The ore deposits of Utah: U. S. Geol Survey Prof. Paper 111 672 p.

Calkins, F. C., and Butler, B. S., 1943, Geology and ore deposits of the Cottonwood: American Fork area, Utah: U. S. Geol. Survey Prof. Paper 201, 152 p.

Deiss, C. F., 1938, Cambrian formations and sections in part of the Cordilleran Trough: Geol. Soc. America Bull., v. 49, p. 1067–1168

—— 1939, Cambrian formations of southwestern Alberta and southeastern British Columbia: Geol. Soc. America Bull., v. 50, p. 951–1026

—— 1941, Cambrian geography and sedimentation in the central Cordilleran region: Geol. Soc. America Bull., v. 52, p. 1085–1116, 10 figs.

Denson, Norman, 1942, Late Middle Cambrian trilobite faunas and stratigraphy of Alberta, Montana, Wyoming, and Utah: unpublished doctoral thesis, 76 p. Princeton University.

Eardley, A. J., 1933, Stratigraphy of the southern Wasatch Mountains, Utah: Mich. Acad. Sci. Papers, v. 18, p. 307–344

—— 1938, Sediments of Great Salt Lake, Utah: Am. Assoc. Petroleum Geologists Bull., v. 22, p. 1359–1387

—— 1939, Structure of the Wasatch-Great Basin region: Geol. Soc. America Bull., v. 50, p. 1277–1310

Eardley, A. J., and Hatch, R. A., 1940, Proterozoic (?) rocks in Utah: Geol. Soc. America Bull., v. 51, p. 795–844

Goldman, M. I., and Merwin, H. E., 1928, Color chart of the Committee on Sedimentation of the National Research Council: Am. Assoc. Petroleum Geologists Bull., v. 9, p. 1018–1019

Grabau, A. W., 1924, Principles of stratigraphy: 2nd ed. New York, A. G. Seiler, p. 785

Hague, Arnold, 1883, Abstract of report on the geology of the Eureka district, Nevada: U. S. Geol. Survey 3rd Ann. Rept., p. 237–290

Hague, Arnold, and Emmons, S. F., 1877, Descriptive geology: U. S. Geol. Explor. 40th Par. (King), v. 2, 890 p.

Hewett, D. F., 1931, Geology and ore deposits of the Goodsprings quadrangle, Nevada: U. S. Geol. Survey Prof. Paper 162, p. 57–60

Hintze, F. F., 1913, A contribution to the geology of the Wasatch Mountains, Utah: New York Acad. Sci. Annals 23, p. 85–149

Howell, B. F., *et al.*, 1944, Correlation of the Cambrian formations of North America: Geol. Soc. America Bull., v. 55, p. 993–1003, chart no. 1.

Howell, E. E., 1875, The geology of portions of Utah, Nevada, Arizona, and New Mexico: Geol. Geog. Explor. Surveys West of the One Hundredth Meridian, v. 3, p. 231–306

Humphrey, F. L., 1945, Geology of the Groom district, Lincoln County, Nevada: Univ. Nev. Bull., v. 39, no. 5, Geol. and Min. Ser., no. 42, 53 p., 17 figs.

King, Clarence, 1878, Systematic geology: U. S. Geol. Explor. 40th Parallel, v. 1, p. 127–227

Lochman, Christina, 1952, *in* Cooper, G. A. *et al.*, Cambrian stratigraphy and paleontology near Caborca, Northwestern Sonora, Mexico: Smithson. Misc. Coll. v. 119, no. 1, 184 p., 13 pls.

—— 1953, Corrections to trilobites in "Cambrian Stratigraphy and Paleontology near Caborca, Northwestern Sonora, Mexico": Jour. Paleontology, v. 27, p. 486–488

Ludlum, John C., 1943, Structure and stratigraphy of part of the Bannock Range, Idaho: Geol. Soc. America Bull., v. 54, p. 973–986

Mansfield, G. R., 1927, Geography, geology and mineral resources of part of southeastern Idaho: U. S. Geol. Survey Prof. Paper 152, p. 48–58

McKee, E. D., 1945, Cambrian history of the Grand Canyon Region, Part I, Stratigraphy and ecology of the Grand Canyon Cambrian: Carnegie Inst. Wash. Publ. 563, 168 p., 12 figs., 15 pls.

Mertie, J. B., 1922, Graphic and mechanical computation of thickness of strata and distance to a stratum: U. S. Geol. Survey Prof. Paper 129, p. 39–52

Murray, John, and Renard, A. F., 1891, Deep-sea deposits: Challenger Rept., p. 229–233

Murray, John, and Irvine, Robert, 1895, On the chemical changes which take place in the composition of the sea-water associated with blue muds on the floor of the ocean: Royal Soc. Edinburgh Trans., v. 37, p. 481–507

Nason, F. L., 1901, The geological relations and the age of the St. Joseph and Potosi limestones of St. Francois County, Missouri: Am. Jour. Sci., ser. 4, v. 12, p. 360

Nolan, T. B. 1929, Notes on the stratigraphy and structure of the northwest portion of Spring Mountain, Nevada: Am. Jour. Sci., 5th Ser., vol. 17, no. 101, p. 461–472, 4 figs.

—— 1935, The Gold Hill mining district, Utah: U. S. Geol. Survey Prof. Paper 177, 172 p.

Peale, A. C., 1879, Report of the geology of the Green River district, Wyo.: U. S. Geol. Geog. Survey Terr. (Hayden), Ann. Rept. 11, 720 p.

Pettijohn, F. J., 1949, Sedimentary rocks: New York, Harper and Bros., 526 p.

Rasetti, Franco, 1951, Middle Cambrian stratigraphy and faunas of the Canadian Rocky Mountains: Smithson. Misc. Coll., v. 116, no. 5, 277 p.

Resser, C. E., 1939a, The Spence shale and its fauna: Smithson. Misc. Coll., v. 97, no. 2, p. 1–29

—— 1939b, The *Ptarmigania* strata of the northern Wasatch Mountains: Smithson. Misc. Coll., v. 98, p. 1–72

Richardson, C. B., 1913, The Paleozoic section in northern Utah: Am. Jour. Sci., 4th ser., v. 36, p. 406–416
—— 1941, Geology and mineral resources of the Randolph quadrangle, Utah-Idaho: U. S. Geol. Survey Bull. 923, 54 p.
Ridgway, R., 1912, Color standards and nomenclature: Baltimore, A. Hoen and Co., 43 p., 53 pls.
Rubey, W. W., 1930, Lithologic studies of fine-grained Upper Cretaceous sedimentary rocks of the Black Hills region: U. S. Geol. Survey Prof. Paper 165-A, p. 1–54
Twenhofel, W. H., 1939, Principles of sedimentation: New York, McGraw-Hill Book Co., Inc., p. 358
—— 1950, Principles of sedimentation: New York, McGraw-Hill Book Co., Inc., 673 p.
Walcott, C. D., 1886, Second contribution to the studies on the Cambrian faunas of North America: U. S. Geol. Survey Bull. 30, 369 p.
—— 1890, The faunas of the Lower Cambrian or *Olenellus* zone: U. S. Geol. Survey 10th Ann. Rept., pt. I, p. 511–568
—— 1891, Cambrian correlation papers: U. S. Geol. Survey Bull. 81, 447 p.
—— 1908a, Nomenclature of some Cambrian Cordilleran formation: Smithson. Misc. Coll., v. 53, no. 1, p. 1–12
—— 1908b, Cambrian sections of the Cordilleran area: Smithson. Misc. Coll., v. 53, no. 5 p. 167–230
—— 1908c, Cambrian trilobites: Smithson. Misc. Coll., v. 53, no. 2, p. 13–52
—— 1912, Cambrian Brachiopoda: U. S. Geol. Survey Mon. 51, pt. 1, 872 p.
—— 1916, Cambrian trilobites: Smithson, Misc. Coll., v. 64, no. 5, 454 p.
Westgate, L. G., and Knopf, Adolf, 1927, Geology and ore deposits of the Pioche district, Nevada, pt. 1, General geology: U. S. Geol. Survey Prof. Paper 171, p. 1–44
Wheeler, H. E., 1943, Lower and Middle Cambrian stratigraphy of the Great Basin area: Geol. Soc. America Bull., v. 54, p. 1781–1982, 2 pls., 5 figs.
—— 1947, Base of the Cambrian System: Jour. Geology, v. 55, p. 153–159, 1 fig.
—— 1948, Late Pre–Cambrian–Cambrian stratigraphic cross-section through southern Nevada: Univ. Nev. Bull., Geol. and Min. Ser., no. 47, 58 p.
Wheeler, H. E., and Lemmon, D. M., 1939, Cambrian formations of the Eureka and Pioche districts, Nevada: Univ. Nev. Bull. 4, v. 33, no. 3, Geol. and Min. Ser., no. 31, 60 p.
Williams, J. Stewart, 1943, Carboniferous formations of the Uinta and northern Wasatch Mountains, Utah: Geol. Soc. America Bull., v. 54, p. 591–624
Williams, J. Stewart, 1948, Geology of the Paleozoic rocks, Logan quadrangle, Utah: Geol. Soc. America Bull., v. 59, p. 1121–1164
Williams, J. Stewart, and Maxey, G. B., 1941, The Cambrian section in the Logan quadrangle, Utah and vicinity: Am. Jour. Sci., vol. 239, p. 276–285

Illinois State Geological Survey, Urbana Ill.

Manuscript Received by the Secretary of the Society, July 3, 1952

BULLETIN OF THE GEOLOGICAL SOCIETY OF AMERICA
VOL. 69, PP. 689-700, 5 FIGS. JUNE 1958

# STRATIGRAPHY OF UPPER PENNSYLVANIAN AND LOWER PERMIAN ROCKS IN THE SAND CANYON AREA, OTERO COUNTY, NEW MEXICO

BY GEORGE O. BACHMAN AND PHILIP T. HAYES

## ABSTRACT

The Magdalena Group of Pennsylvanian age and, in ascending order, the lower tongue of the Abo Sandstone (herein named the Danley Ranch Tongue), the Hueco Limestone, the upper tongue of the Abo Sandstone (herein named the Lee Ranch Tongue), and the Yeso Formation of Permian age are well displayed in the southern part of the Sacramento Mountains. The contact of the Pennsylvanian rocks with the overlying Permian rocks is unconformable throughout the area. Locally the relief before deposition of the Abo was so great that in places the Danley Ranch Tongue of the Abo is absent because of nondeposition. At these places there is prominent angular discordance between the Pennsylvanian and Permian rocks.

The red beds of the Danley Ranch Tongue interfinger with and grade southward into the overlying Hueco Limestone. Red beds of the Lee Ranch Tongue of the Abo Sandstone also grade southward into the Hueco and cannot be traced south of the southern part of the Sacramento Mountains. The Lee Ranch Tongue is believed to be stratigraphically lower than the Deer Mountain Red Shale Member of the type Hueco Limestone. The herein named Otero Mesa Member of the Yeso Formation is believed to occupy an intermediate stratigraphic position between the Lee Ranch Tongue and the Deer Mountain Red Shale.

## CONTENTS

### TEXT

| | Page |
|---|---|
| Introduction and acknowledgments | 689 |
| Stratigraphy | 691 |
| General statement | 691 |
| Pennsylvanian System | 691 |
| Permian System | 692 |
| General statement | 692 |
| Danley Ranch Tongue of the Abo sandstone | 692 |
| Hueco Limestone | 695 |
| Lee Ranch Tongue of the Abo Sandstone | 695 |
| Yeso and San Andres formations | 697 |
| Geologic structure | 699 |
| Depositional history | 699 |
| References cited | 700 |

### ILLUSTRATIONS

| Figure | Page |
|---|---|
| 1. Geologic map of Sand Canyon area | 690 |
| 2. Graphic sections of lower Permian strata, Sand Canyon area | 693 |
| 3. Diagram showing stratigraphic relations of rocks in the Sand Canyon area | 694 |
| 4. Graphic sections of Lee Ranch Tongue and lower part of Yeso Formation, southward from Sand Canyon area | 696 |
| 5. Correlation diagram of lower Permian rocks | 698 |

## INTRODUCTION AND ACKNOWLEDGMENTS

The Sand Canyon area includes about 15 square miles in the southern part of the Sacramento Mountains, Otero County, New Mexico, in parts of Ts. 19 and 20 S., Rs. 11 and 12 E. (Fig. 1). Stratigraphic relationships of upper Pennsylvanian and lower Permian strata are exceptionally well displayed. The Abo Sandstone of early Permian age is divided into a lower and an upper tongue by interfingering with the Hueco Limestone. The lower tongue of the Abo Sandstone is here named the Danley Ranch Tongue, and the upper tongue of the Abo Sandstone is named the Lee Ranch Tongue. Relationships of the Abo Sandstone with the unconformity which underlies the Abo in the Sacramento Moun-

FIGURE 1.—GEOLOGIC MAP OF SAND CANYON AREA

tains also are well displayed in the Sand Canyon area.

Field work was done to clarify relationships of the several stratigraphic units before compilation of this part of the new geologic map of New Mexico. Bachman did reconnaissance mapping and measurement of stratigraphic sections in and adjacent to the area during a 2-week period in the summer of 1955. More detailed mapping was done, and most of the sections were measured by the writers during the first 2 weeks of December 1955. These sections were measured by compass and hand-level methods.

Valuable suggestions were given in the field by C. H. Dane. E. H. Baltz and R. L. Koogle assisted in part of the field work.

## Stratigraphy

### *General Statement*

Sedimentary rocks of all Paleozoic systems crop out in the Sacramento Mountains. A few miles north of the Sand Canyon area rocks of Late Cambrian age crop out and rest on quartzite presumed to be Precambrian. The Upper Cambrian rocks are overlain by a sequence of strata representing the Ordovician, Silurian, Devonian, Mississippian, Pennsylvanian, and Permian systems. The general stratigraphy has been studied by Darton (1928) and Pray (1954). Numerous workers have contributed detailed information on individual formations and systems.

The rocks mapped by the writers in the southern part of the Sacramento Mountains include part of the Magdalena Group of Pennsylvanian and Permian ages, and the Abo, Hueco, and Yeso formations of early Permian age. Relatively small outcrops of the Permian San Andres Formation form the caprock on higher mountain peaks in the eastern part of the map area, but they were not studied.

### *Pennsylvanian System*

The Pennsylvanian System is represented in the southern part of the Sacramento Mountains by the Magdalena Group. The Magdalena Group here consists of clastic and carbonate rocks. In the northern part of the Sacramento Mountains the Magdalena Group includes the Bursum Formation of early Permian age, but this formation was not recognized in the Sand Canyon area. Pray (1954, p. 93) suggested the revision of the nomenclature of the Pennsylvanian rocks in the Sacramento Mountains, but the name Magdalena Group is adequate for the present purpose.

The Magdalena Group in the Sand Canyon area is divisible into two informal units. The lower unit consists of several hundred feet of thin- to thick-bedded marine limestone that is at most places medium gray and weathers to a lighter gray. Dark-gray chert nodules and stringers are common along bedding planes.

The upper unit of the Magdalena Group varies in thickness, but it averages about 1000 feet in the southern part of the Sacramento Mountains. It consists of fine- to coarse-grained clastic rocks with some interbedded limestone. The clastic rocks include gray to tan or brown shale and siltstone, greenish-gray to reddish graywacke, arkose, and conglomerate. The constituents of the coarser clastic rocks are varied and include quartzite, rock fragments, and a variety of heavy minerals. In some places numerous fossil logs are preserved within the clastic sediments. In the S½ sec. 9, T. 20 S., R. 11 E., the upper unit of the Magdalena Group contains several hundred feet of limestone pebble and cobble conglomerate, reddish-brown shale and siltstone, and a thin bed of fusulinid-bearing limestone. These beds are lithologically similar to the Bursum Formation of Permian age in the northern part of the Sacramento Mountains, but no evidence for the Permian age of these red beds in the Magdalena Group at the south end of the mountains has been found. Apparently the red beds in the upper part of the Magdalena at the south end of the mountains were derived from local uplifting that began in late Pennsylvanian. Similar red-bed sequences of late Pennsylvanian age are locally present throughout south-central New Mexico.

The limestone beds in the upper part of the Magdalena Group average 1–3 feet thick. Many of the limestone beds are lenticular but are not comparable texturally to biohermal limestones. Locally, beds have been observed to thicken to 20 or 30 feet within a few hundred yards along their strike. Most limestone beds in the upper unit of the Magdalena Group are noncherty, but locally detrital chert may be associated with the clastic rocks. Stratigraphic sections of the Magdalena Group were not measured.

FIGURE 1.—GEOLOGIC MAP OF SAND CANYON AREA

The contact of the Pennsylvanian sequence with the overlying Permian rocks varies from one of angular unconformity to one of disconformity within relatively short distances. Locally, strata were strongly folded and faulted before deposition of sediments of the Abo. This relationship is similar to the one Pray described (1949, p. 1914) north of the map area.

### *Permian System*

*General statement.*—Permian rocks in the southern part of the Sacramento Mountains are the Abo, Hueco, Yeso, and San Andres formations. The Bursum Formation which lies at the base of the Permian System at the northern end of the Sacramento Mountains has not been recognized in the southern part of the mountains.

Intertonguing reflects the northward lateral gradation of the Hueco Limestone into red beds of the Abo Sandstone. About 15 miles north of the Sand Canyon area, the Hueco Limestone wedges out between the upper and lower parts of the Abo (Pray, 1954, p. 101).

*Danley Ranch Tongue of the Abo Sandstone.*—The lower tongue of the Abo Sandstone, here named the Danley Ranch Tongue, crops out in the Sand Canyon area in a narrow, discontinuous band from the northeast edge of the area to the north fork of Culp Canyon (Fig. 1). Southward from Culp Canyon it is covered by alluvium of Quaternary age except for incomplete exposures southwest of the Sand Canyon area.

The Danley Ranch Tongue of the Abo Sandstone is named for the Danley Ranch on which the unit is well exposed. The type stratigraphic section is exposed in the SW¼ sec. 35, T. 19 S., R. 11 E., about 1 mile east of the Danley Ranch headquarters (Fig. 2*D*).

Soft red shale, reddish-brown cross-laminated shaly siltstone, and very fine-grained sandstone are the predominant rocks of the Danley Ranch Tongue. However, thin ledges of thin-bedded tannish-weathering light-olive-gray limestone, which probably represent minor tongues of the Hueco Limestone, are present in the unit at most places. Beds of conglomerate are present in most localities in the lower part of the tongue.

Four types of conglomerate have been recognized in the Danley Ranch Tongue in the map area. The beds of conglomerate vary in lithology and are believed to have been derived in part from local source areas. The first type of conglomerate is found immediately north of the map area at the base of the Danley Ranch Tongue (Fig. 2*A*). Most of granules and pebbles in this conglomerate are quartzite fragments, but fragments of a distinctive rhyolite porphyry are common. Fragments of rhyolite porphyry have been observed in the Abo Sandstone northward from the Sand Canyon area to at least the latitude of Tularosa, New Mexico, and are believed to have been derived from an area northeast of the present Sacramento Mountains. A second type of conglomerate was observed near the base of the Danley Ranch Tongue in the bottom of a small draw in the SE¼ sec. 3, T. 20 S., R. 11 E. At that locality there is a limestone boulder conglomerate which contains subangular slabs of limestone of Pennsylvanian age ranging from 1 or 2 inches to more than 10 inches in diameter in a matrix of reddish-brown, coarse-grained, angular to subangular, arkosic sandstone. The writers believe that the slabs of limestone in this conglomerate had a local source and were derived from the near-by Pennsylvanian mendip described below. The third type of conglomerate is common in resistant beds from 1 to 5 feet thick in the SE¼ sec. 9, T. 20 S., R. 11 E. Most of this conglomerate consists of subrounded pebbles and cobbles of limestone in a calcareous sandstone matrix. Pebbles of brownish sandstone and angular chert also are present but are not common. This conglomerate probably had a local source, but transportation of the sediments permitted some rounding of the constituents. The fourth type of conglomerate was examined in the NW¼ sec. 11, T. 20 S., R. 11 E., and consists of angular chert fragments ranging up to 10 inches in diameter in a resistant reddish-brown fine-grained matrix which is probably an iron-rich carbonate. This conglomerate probably represents the remnants of a regolith. A soil that contained chert nodules may have been developed at this point, on the lower part of the Magdalena Group, during Permian time. The development of such soil as the result of weathering of calcareous rocks is described by Merrill (1906, p. 216). The finer particles of soil have been removed, and a lag gravel of chert nodules in an iron-rich carbonate matrix is left.

In most of the map area the red beds and conglomerates of the Danley Ranch Tongue

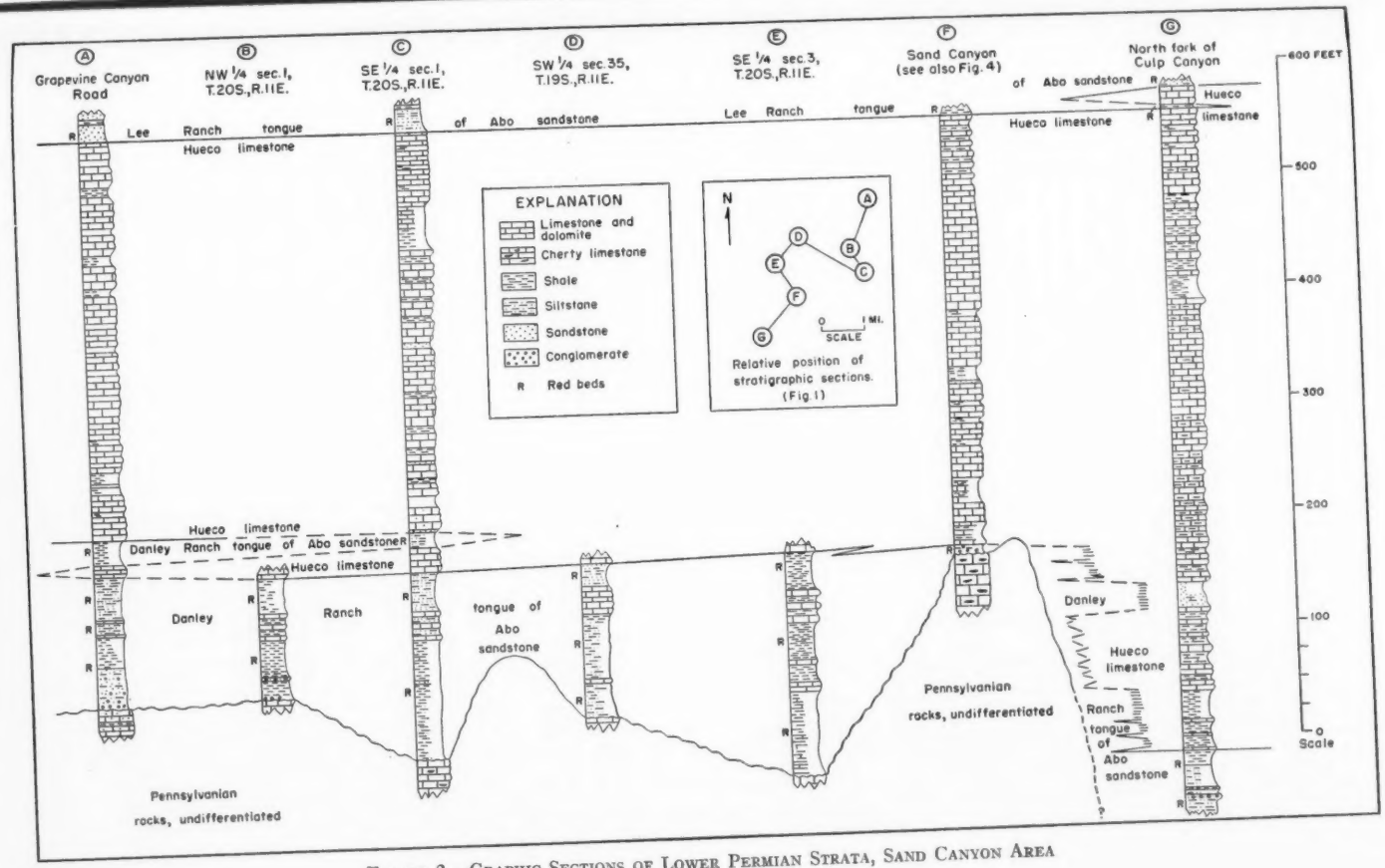


FIGURE 2.—GRAPHIC SECTIONS OF LOWER PERMIAN STRATA, SAND CANYON AREA

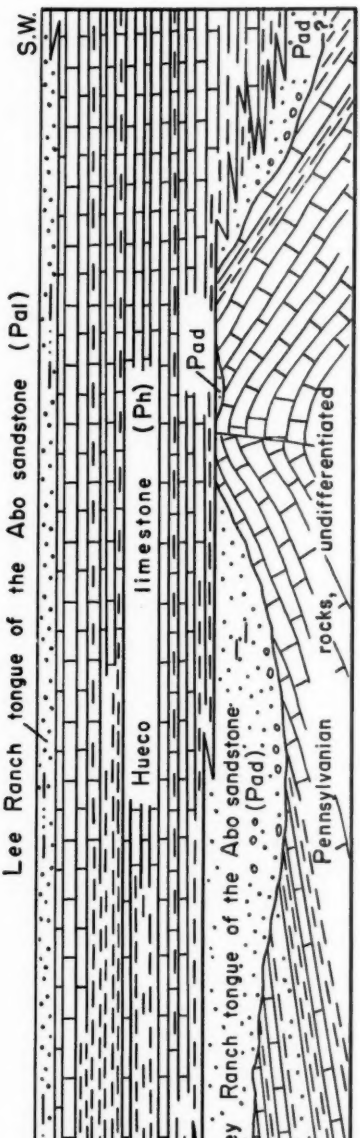


FIGURE 3.—DIAGRAM SHOWING STRATIGRAPHIC RELATIONS OF ROCKS IN THE SAND CANYON AREA

of the Abo Sandstone rest with sharp angular unconformity on grayish limestone and shale beds of the Pennsylvanian sequence. Most commonly the rocks underlying the Danley Ranch Tongue belong to the upper unit of the Magdalena Group. However, in local areas where there was pronounced uplift and erosion before Abo deposition the Danley Ranch Tongue rests directly on the lower limestone unit of the Magdalena. The pre-Abo relief was so great locally in Sand Canyon that the Danley Ranch Tongue is absent altogether owing to nondeposition, and strongly folded beds of the lower unit of the Magdalena Group are overlain by the Hueco Limestone (Fig. 3). These angular relationships do not extend to the southwest corner of the area, however. In the S½ sec. 9, T. 20 S., R. 11 E., the Danley Ranch Tongue overlies the upper part of the Magdalena sequence with a disconformable contact. There at the top of the Magdalena several hundred feet of interbedded red beds and limestone containing *Triticites sp.* are present. These strata do not occur elsewhere in the map area. They are somewhat similar in lithology to the Permian Bursum Formation in the northern part of the Sacramento Mountains but apparently do not contain Permian fusulinids.

The Danley Ranch Tongue has an interfingering relationship with the overlying Hueco Limestone. Some of the interfingering is of sufficient magnitude to be indicated on the geologic map (Fig. 1, SE¼ sec. 3, T. 20 S., R. 11 E.; *see* Figs. 2, and 3), but in most places the contact is transitional and was mapped at the top of the highest red bed. As a result of the transitional nature of the contact, thin limestone tongues of the Hueco are usually present in the upper part of the Danley Ranch Tongue. Red-shale tongues of the Danley Ranch Tongue grade laterally southward into gray shale beds of the Hueco Limestone. Conversely, the limestone tongues of Hueco in the Danley Ranch Tongue either pinch out northward or grade to shaly limestone, thence to limy gray shale, thence to red shale. The southward tonguing and lateral gradation of the Danley Ranch Tongue into the lower part of the Hueco Limestone take place at several localities in the area but are much more common off the flanks of the buried Pennsylvanian mendips.

The thickness of the Danley Ranch Tongue varies widely in the southern part of the Sacramento Mountains as a result of the

intertonguing with the Hueco Limestone and from the marked relief of the erosional surface on which the Abo was deposited. The maximum measured thickness of the Danley Ranch Tongue within the area is nearly 200 feet in the E½ sec. 3, T. 20 S., R. 11 E. Less than 1 mile south of that point the tongue is absent, and the Hueco Limestone lies directly on the lower unit of the Magdalena Group. In the southwestern part of the area an accurate measurement of the Danley Ranch Tongue is not possible owing to the disconformable nature of the contact and to poor exposures. The average thickness of the Danley Ranch Tongue in all the sections measured is about 100 feet.

Fossils were not found in the Danley Ranch Tongue, but because of its intertonguing relationships with the lower part of the Hueco Limestone it is considered to be middle and late Wolfcamp. Within 13 miles south-southwest of this area C. C. Branson collected ammonoids "from about 900 feet above the base of the Hueco" which are considered late Wolfcamp (*in* Miller and Parizek, 1948).

The Danley Ranch Tongue and the Powwow Conglomerate Member of the Hueco (King and Knight, 1945) were probably deposited under similar environmental conditions just before the deposition of the sediments of the Hueco (Fig. 5). Inasmuch as the Powwow Conglomerate is not traceable northward into New Mexico from the type locality, the Danley Ranch Tongue of the Abo Formation is here considered to be a separate unit.

*Hueco Limestone.*—The Hueco Limestone in the Sand Canyon area crops out in relatively steep ledgy slopes in a south-southwestward-trending band which averages about 1 mile in width. Limestone makes up at least half of the Hueco, and shale makes up most of the rest; the percentage of shale increases from south to north. Thin units of sandstone and siltstone are present. Most of the limestone is light olive gray to medium gray, fine-grained, and occurs in beds ranging from 1 inch to 1 foot thick. Many beds contain poorly preserved fossils of several types. Fusulinids were not found within the map area by the writers, but gastropods and ostracods are common. Most of the shale in the Hueco is gray and calcareous. The sandstone and siltstone beds are brownish, thin-bedded, and most of them are cross-laminated and grade northward into thin tongues similar in lithology to the Abo Sandstone.

In most of the mapped area, the Hueco Limestone is conformably underlain by the Danley Ranch Tongue of the Abo Sandstone into which it grades laterally northward. Locally, however, in the vicinity of Sand Canyon, the Hueco rests with angular unconformity on the lower part of the Magdalena Group. The upper part of the Hueco Limestone grades laterally into, and is conformably overlain by, a sequence of red beds which is here referred to as the Lee Ranch Tongue of the Abo Sandstone. The lateral gradation of the Hueco into the Lee Ranch Tongue in a general northward direction is similar in character to the intertonguing of the Hueco and the Danley Ranch Tongue but occurs on a much smaller scale. The only tonguing of the Hueco and the Lee Ranch Tongue observed in the field takes place in the S½ sec. 15, T. 20 S., R. 11 E. (Figs. 1, 2*G*). The Hueco Limestone thickens from about 350 feet 1 mile north of the map area to nearly 600 feet near Culp Canyon, a distance of about 5 miles. Most of this gain in thickness is attributed to intertonguing of the Hueco Limestone with the Abo Sandstone. However, some of the gain may be attributed to the variation in relief of the surface on which the Hueco Limestone was deposited (Fig. 2).

All but the uppermost part of the Hueco is probably Wolfcamp, as in the Hueco Mountains (King and Knight, 1945; Lloyd, 1949; Jones, 1953). The uppermost beds of the Hueco at the south end of the Sand Canyon area, however, are known to be lateral equivalents of part of the Lee Ranch Tongue of the Abo Sandstone which is apparently early Leonard.

*Lee Ranch Tongue of the Abo Sandstone.*—The Lee Ranch Tongue of the Abo Sandstone, here named for exposures in the SE¼ sec. 11, T. 20 S., R. 11 E., about 7 miles southwest of the O. M. Lee Ranch headquarters, is generally rather poorly exposed in a narrow slope-forming outcrop on the backslope of the topographic shelf formed by the Hueco Limestone. At the type locality the Lee Ranch Tongue is 106 feet thick and consists predominantly of salmon-red shale and siltstone, but some thin-bedded fine-grained soft-weathering sandstone beds are present (Fig. 4*F*). In the northern part of the area it consists predominantly of reddish-brown, very thin-bedded, cross-laminated, very fine-grained sandstone and siltstone.

The Lee Ranch Tongue rests conformably

upon the Hueco Limestone and intertongues with it near the south end of the mapped area. Most of the Lee Ranch Tongue grades and sandstone beds and locally by white gypsum of the Yeso Formation. The contact is gradational and therefore arbitrary, but the zone of grada-

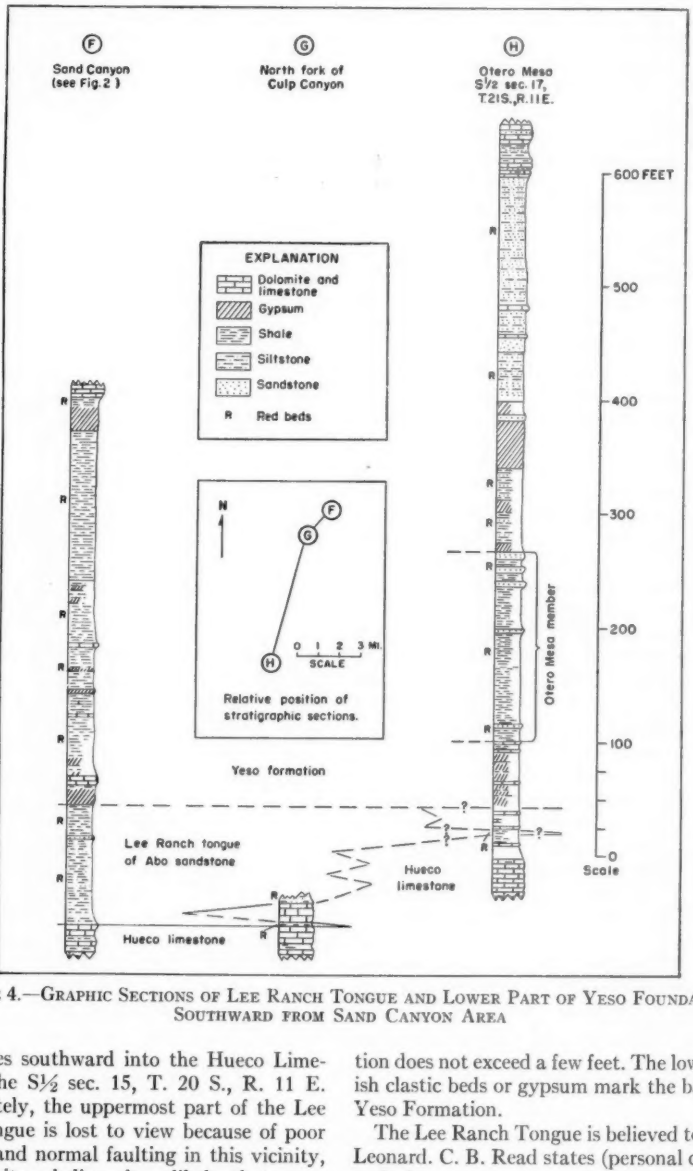


FIGURE 4.—GRAPHIC SECTIONS OF LEE RANCH TONGUE AND LOWER PART OF YESO FOUNDATION, SOUTHWARD FROM SAND CANYON AREA

intertongues southward into the Hueco Limestone in the S½ sec. 15, T. 20 S., R. 11 E. Unfortunately, the uppermost part of the Lee Ranch Tongue is lost to view because of poor exposures and normal faulting in this vicinity, but the writers believe it unlikely that more than about 30 or 40 feet of the unit could extend southward from Culp Canyon.

The red beds of the Lee Ranch Tongue are conformably overlain by pinkish siltstone and tion does not exceed a few feet. The lowest pinkish clastic beds or gypsum mark the base of the Yeso Formation.

The Lee Ranch Tongue is believed to be early Leonard. C. B. Read states (personal communication):

"In Caballero Canyon (above angular unconformity in the uppermost beds of the Abo sandstone) a florule has been collected which contains elements of the *Gigantopteris* flora. Similar floras

have been obtained from the Belle Plains formation of north Texas. Inasmuch as the *Gigantopteris* flora is underlain by the *Callipteris* flora both in New Mexico and in Texas, it is an established fact that the *Gigantopteris* flora can not be older than uppermost Wolfcamp and most paleobotanists regard it as lower Leonard in age. About 11 miles east of Orogrande a collection of fossil plants was obtained from the uppermost beds of the Abo sandstone as mapped by Darton (1928). Included in the collection were numerous specimens of *Supaia sp.* and *Brachyphyllum arizonicum.* This florule is a part of the *Supaia* flora which makes its appearance in the uppermost beds of the Abo sandstone and its equivalents in much of New Mexico and Arizona. The *Supaia* flora and the *Gigantopteris* flora are believed to be lateral or facies equivalents. In consequence, the *Supaia* flora, like the *Gigantopteris* flora, is regarded as Leonard in age. The vertebrate sequence, in a general way, corroborates the floral sequence and the inferences regarding the Leonard age."

Thompson (1954, p. 19) stated that the upper part of the Hueco Limestone in the Hueco Mountains contains an assemblage of fusulinids which is "more similar to subjacent Hueco faunas than to younger Permian faunas." At the type locality of the Wolfcamp Series in the Glass Mountains in western Texas the uppermost strata of the Wolfcamp have been removed by erosion (King, 1930, p. 55; Thompson, 1954, p. 19). Thompson proposed that the Wolfcamp Series be redefined to include the upper part of the Hueco Limestone in the Hueco Mountains. However, in view of the evidence of Leonard age of the upper part of the Abo Sandstone and the lower part of the Yeso Formation, both of which appear to interfinger with the upper part of the Hueco Limestone, the writers prefer to include the upper part of the Hueco Limestone in the Leonard Series.

The writers believe that the uppermost beds of the Abo Sandstone in Caballero Canyon are essentially equivalent to the Lee Ranch Tongue of the Abo Sandstone in the Sand Canyon area—hence the early Leonard age designation of the Lee Ranch Tongue. However, the "uppermost beds of the Abo sandstone" (Read, above quotation) about 11 miles east of Orogrande (approximately 14 miles south of Culp Canyon) do not appear to be lateral equivalents of the Lee Ranch Tongue of the Abo Sandstone. Although Pray (1954) believed that "the upper tongue of the Abo red beds can be traced nearly to the Texas border and forms the Deer Mountain red shale of the Hueco limestone", the writers were unable to trace the Lee Ranch Tongue farther south than Culp Canyon where it goes under an alluvial cover 4 miles wide.

*Yeso and San Andres formations.*—Four miles south of Culp Canyon a red-bed sequence occurs which is somewhat similar lithologically to the upper part of the Abo Sandstone of central New Mexico but unlike the Lee Ranch Tongue of the Sand Canyon area. Miller and Parizek (1948) considered that this red-bed sequence is the Abo Sandstone as used by Darton (1928); Pray (1954) and Thompson (1954, p. 20–21, Fig. 5) also considered it to be a continuation of the upper part of the Abo. However, this sequence is not traceable into nor herein correlated with the thinner Lee Ranch Tongue of the Abo. It is underlain by a gypsum-bearing sequence at a number of localities as observed by the writers and other workers in the area (Darton, 1928; Miller and Parizek, 1948) and is considered to be a part of the Yeso Formation (Figs. 4, 5). It is here named the Otero Mesa Member.

The Otero Mesa Member of the Yeso Formation is named for fairly good exposures at the base of Otero Mesa. The type section is in a westward-facing cuesta in S½ sec. 17, T. 21 S., R. 11 E., about 5 miles south of Culp Canyon where it consists of 168 feet of red to maroon shale and resistant ledges of reddish-brown to tan cross-laminated sandstone (Fig. 4*H*). The Otero Mesa Member lies conformably on a poorly exposed sequence of gypsum, gray shale, and thin-bedded dolomite about 50 feet thick, which is designated as the basal part of the Yeso Formation. It is overlain by a poorly exposed sequence of gypsum, pink shale, and fine-grained sandstone. The Otero Mesa Member here described is continuous with the beds "about 11 miles east of Orogrande" (Read, above quotation).

In summary, rocks that previous workers have identified as the Abo Formation south of Culp Canyon are interpreted as a distinct unit and herein named the Otero Mesa Member of the Yeso Formation for the following reasons:

(1) The Otero Mesa Member is underlain by gypsum, shale, and thin-bedded dolomite which are considered to be more closely related genetically to the Yeso Formation than to the underlying Hueco Limestone.

(2) The Otero Mesa Member includes a larger proportion of sandstone than the southernmost exposures of the upper part of the Abo Sandstone (the Lee Ranch Tongue) near Culp Canyon.

(3) The Lee Ranch Tongue thins greatly southward and is only about 30–40 feet thick at the exposures near Culp Canyon, whereas the

Otero Mesa Member is 168 feet thick at the type locality 5 miles south of Culp Canyon.

Pray (1954, p. 101) stated that "the upper tongue of Abo red beds (the entire Abo of Darton) can be traced nearly to the Texas red beds in the Yeso Formation which overlies the Otero Mesa Member is nearly continuous southward from the apparent wedge edge of the Otero Mesa Member and is well exposed in sec. 13, T. 25 S., R. 10 E.

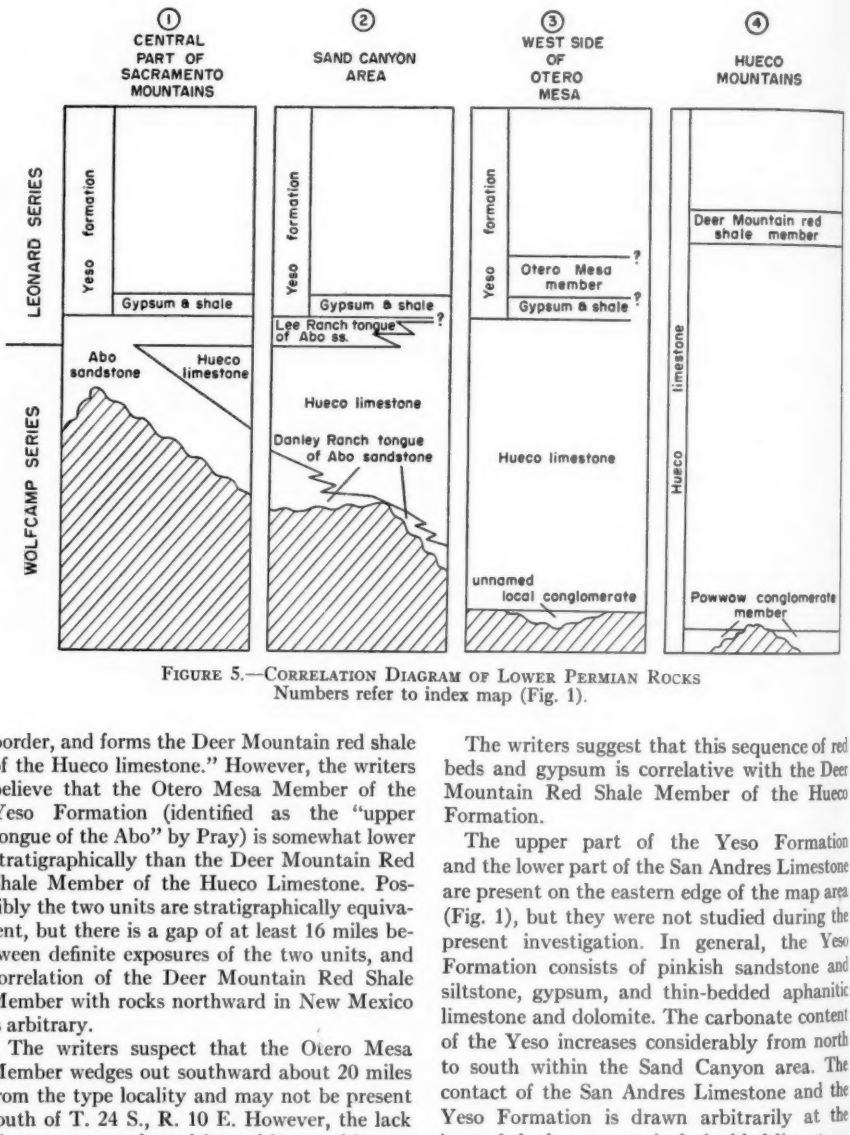


FIGURE 5.—CORRELATION DIAGRAM OF LOWER PERMIAN ROCKS
Numbers refer to index map (Fig. 1).

border, and forms the Deer Mountain red shale of the Hueco limestone." However, the writers believe that the Otero Mesa Member of the Yeso Formation (identified as the "upper tongue of the Abo" by Pray) is somewhat lower stratigraphically than the Deer Mountain Red Shale Member of the Hueco Limestone. Possibly the two units are stratigraphically equivalent, but there is a gap of at least 16 miles between definite exposures of the two units, and correlation of the Deer Mountain Red Shale Member with rocks northward in New Mexico is arbitrary.

The writers suspect that the Otero Mesa Member wedges out southward about 20 miles from the type locality and may not be present south of T. 24 S., R. 10 E. However, the lack of exposures southward from this township prohibits further tracing of the interval occupied by the Otero Mesa Member. The sequence of red beds and gypsum is correlative with the Deer Mountain Red Shale Member of the Hueco Formation.

The writers suggest that this sequence of red beds and gypsum is correlative with the Deer Mountain Red Shale Member of the Hueco Formation.

The upper part of the Yeso Formation and the lower part of the San Andres Limestone are present on the eastern edge of the map area (Fig. 1), but they were not studied during the present investigation. In general, the Yeso Formation consists of pinkish sandstone and siltstone, gypsum, and thin-bedded aphanitic limestone and dolomite. The carbonate content of the Yeso increases considerably from north to south within the Sand Canyon area. The contact of the San Andres Limestone and the Yeso Formation is drawn arbitrarily at the base of the lowest massively bedded limestone. This contact is somewhat lower than that used by Northup and Pray (*in* Lloyd, 1949).

## Geologic Structure

The outcrop pattern of Paleozoic rocks in the Sacramento Mountains trends generally south to southeast. South of Grapevine Canyon, however, the trend changes to southwest. Regionally, sedimentary rocks of the Sacramento Mountains dip toward the east from a west-facing frontal scarp which overlooks the Tularosa Basin. Locally, the direction of dip is variable, and reversal of dip is common along the front of the mountains.

Local folding and faulting are common in the Sand Canyon area, and at some places the rocks are highly distorted. This deformation may be attributed to at least two periods of orogeny. The earliest movement indicated is late Pennsylvanian and early Permian and the second orogenic episode was probably during Tertiary time.

Evidence for the earliest period of folding and faulting in the map area may be observed in the NE¼ sec. 10, T. 20 S., R. 11 E., where Pennsylvanian strata are strongly folded into a northward-trending faulted anticline which is overlain by less disturbed Permian rocks. Dips on the west limb of the fold average about 40°. The eastern limb is less steep, and dips probably do not exceed 30°.

The anticline was partially eroded before deposition of the sediments of the Abo Sandstone and the Hueco Limestone. Along the axis of this anticline cherty limestone beds of the lower unit of the Magdalena Group are exposed and are overlain by strata of the Abo and Hueco sequence of Permian age. The absence of the upper unit of the Magdalena Group at this locality is evidence that erosion stripped away at least 1000 feet of strata before Permian deposition. The axis of this Pennsylvanian fold may be projected southward into the SE¼ sec. 10, T. 20 S., R. 11 E., where a small inlier of the lower unit of the Magdalena is present in the bottom of an unnamed canyon. The axis of this structure may also be projected northward out of the map area into a large faulted anticline north of the Grapevine Canyon road. Evidence is not now available to prove the age of folding of the geologic structure north of the Grapevine Canyon road, but analogy with similar folding that can be dated indicates that much of this folding occurred during late Pennsylvanian.

The coarse clastic material in the upper unit of the Magdalena Group indicates that some uplifting occurred in surrounding areas in late Pennsylvanian time. In the Sand Canyon area local folding and deposition were probably concurrent near the close of Pennsylvanian time, as beds of limestone cobble conglomerate of late Pennsylvanian age lap onto the western side of the above-mentioned Pennsylvanian anticline in the NE¼ sec. 10, T. 20 S., R. 11 E.

Orogeny of probable Tertiary age resulted in regional uplift and local folding and faulting. Permian strata dip generally eastward and reflect this period of uplift. Locally, however, the Hueco Limestone is strongly folded in the SE¼ sec. 10 and the NE¼ sec. 15, T. 20 S., R. 11 E. At some places in this area there is a suggestion of an unconformable relationship within the Hueco, but careful study of individual beds failed to prove this relationslip.

Only four normal faults of probable Tertiary age have been indicated on the geologic map (Fig. 1). Stratigraphic displacement of the faults is variable but probably does not exceed 350 feet on any of these faults. They trend generally north and are parallel to the front of the Sacramento Mountains.

## Depositional History

The Sand Canyon area is significant for the detailed stratigraphic relations of uppermost Pennsylvanian and lower Permian rocks that are observed there. From these details the depositional history may be interpreted in part.

Late in Pennsylvanian time there was strong local folding on the sea bottom within the Sand Canyon area and possibly immediately north, as well as about 20 miles north in the Sacramento Mountains (Pray, 1949). The uplifted areas were eroded and contibuted conglomeratic sediments to the surrounding low areas intermittently from late Pennsylvanian into early Permian. At about the close of Pennsylvanian there was regional uplift, and throughout earliest Wolfcamp, when interbedded limestone and red beds of the Bursum Formation were being deposited farther north, the Sand Canyon area was being subjected to erosion. By middle Wolfcamp the sea began to transgress from the south, and fluviatile deposits of the lower part of the Abo Sandstone were deposited in the Sand Canyon area. Most of these sediments were probably derived from the north and east, but some locally derived conglomeratic sediments also came from the strongly folded Pennsylvanian rocks. Some of these Pennsylvanian rocks remained as mendips of bedrock in the coastal plain and were therefore never covered or only slightly covered by red-bed deposits of the Danley Ranch Tongue.

During most of the time that the red beds of the Danley Ranch Tongue were being deposited north of Sand Canyon the marine limestone and shale of the Hueco Limestone were being deposited at the extreme southern end of the area. The general northward transgression of the sea during Hueco time was intermittently interrupted by minor regressions which are reflected by the many thin beds of the Danley Ranch Tongue that interfinger with the Hueco Limestone. These interfingering relations are particularly common near the areas of marked relief before deposition of the Abo and suggest that very slight movement continued into Hueco time. After the sea covered the highest Pennsylvanian hills near Sand Canyon during Hueco time, it transgressed much more rapidly with only minor periods of retreat, as indicated by the less abrupt interfingering in the northern part of the area. Thus, interfingering of the Danley Ranch Tongue with the lower part of the Hueco Limestone is of two types: (1) local complex interfingering as a result of local supply of sediments of the Abo from mendips which existed well into Hueco time, and (2) regional interfingering of the two formations as a result of the transgressive onlap of the sea during Hueco time. The advance of the sea ended late in Wolfcamp or early in Leonard about 15 miles north of the Sand Canyon area. The sea then retreated quite rapidly but with some fluctuation. Interfingering between the Hueco Limestone and the Lee Ranch Tongue just north of Culp Canyon reflects some of this fluctuation.

The total thickness of marine sediments left by the sea during Hueco time ranges from about 350 feet at the north end of the Sand Canyon area to about 600 feet at the south end. Red-bed sediments of the Lee Ranch Tongue were deposited to a thickness of about 100 feet over the Sand Canyon area while deposition of the Hueco Limestone was continuing to the south. The close of late Abo time was marked by the beginning of evaporite and carbonate deposition alternating with deposition of red beds of the Yeso Formation.

## References Cited


Darton, N. H., 1928, "Red beds" and associated formations in New Mexico: U. S. Geol. Survey Bull. 794, 356 p.

Jones, T. S., 1953, Stratigraphy of the Permian basin of West Texas: West Texas Geol. Soc., 63 p.

King, P 1930, Geology of the Glass Mountains, T... Pt. 1, Descriptive geology: Univ. Texas Bull. 3038, 167 p.

King, P. B., and Knight, J. B., 1945, Geology of Hueco Mountains, El Paso and Hudspeth counties, Texas: U. S. Geol. Survey Prelim. Map 36, Oil and Gas Inves. Ser.

Lloyd, E. R., 1949, Pre-San Andres stratigraphy and oil-producing zones in southeastern New Mexico: N. Mex. Bur. Mines and Min. Res. Bull. 29, 79 p.

Merrill, G. P., 1906, Rocks, rock-weathering and soils: N. Y., Macmillan Co., 400 p.

Miller, A. K., and Parizek, E. J., 1948, A lower Permian ammonoid fauna from New Mexico: Jour. Paleontology, v. 22, p. 350–358

Pray, L. C., 1949, Pre-Abo deformation in the Sacramento Mountains, New Mexico (Abstract): Geol. Soc. America Bull., v. 60, p. 1914-1915

——1954, Outline of the stratigraphy and structure of the Sacramento Mountain escarpment: N. Mex. Geol. Soc. Guidebook 5th Field Conf. p. 92–107

Thompson, M. L., 1954, American Wolfcampian fusulinids: Univ. Kansas Paleont. Contr., Protozoa, Art. 5, 226 p.


U. S. Geological Survey, Box 4083, Station A, Albuquerque, N. Mex.

Manuscript Received by the Secretary of the Society, April 23, 1957

Publication Authorized by the Director U. S. Geological Survey

BULLETIN OF THE GEOLOGICAL SOCIETY OF AMERICA
VOL. 69, PP. 701–756, 21 FIGS, 6 PLS. JUNE 1958

# URANO-ORGANIC ORE AT TEMPLE MOUNTAIN, UTAH

By DANA R. KELLEY AND PAUL F. KERR

## ABSTRACT

Urano-organic substances form essential constituents of the uranium ore at Temple Mountain, Utah. These occur in the vicinity of highly altered collapse structures associated with carbonaceous and petroliferous materials. Chemically, the ore is similar to low-rank coals. Geological conditions, the uranium distribution, texture, physical properties, and microscopic characteristics are indicative of a petroliferous origin. The ore is considered a uranium analogue corresponding to thucolite, the thorium and rare-earth radioactive mineral. The writers believe that induration resulted from polymerization and oxidation-devolatilization of hydrocarbons, caused by the interaction of ore solutions and organic materials at elevated temperatures. The limits of temperature postulated are a minimum of 100° C. and a maximum possibly as high as 350° C.

A characteristic group of metallic elements is present in the ore, as shown by the X-ray spectrograph. A rough zonal relation exists. Arsenic, cobalt, and selenium are concentrated near the collapse, whereas uranium, zinc, and vanadium appear more abundant in the mining area away from the collapse. Small particles of uraninite and sphalerite are disseminated throughout the ore, but the zonal relation is emphasized by the occurrence of native arsenic near the collapse and by the occurrence of montroseite, the primary vanadium oxide, in the mining area. The distribution of supergene oxidation minerals of vanadium and arsenic is further confirmation.

Ore textures suggest the emplacement of uranium-bearing organic material by the flocculation and subsequent accretion of hydrocarbons immiscible in aqueous ore solutions. Replacement of the sediments took place under the corrosive influence of the ore and pre-ore solutions. Contemporaneously, metallic elements were extracted from the solutions by the organic material. During emplacement and induration, dispersed particles of metallic minerals were formed. Banded nodules of the organic material and associated metallic minerals developed as the intensity, composition, and quantity of the solutions varied through time.

A change in the character of the ore solutions is indicated in the vicinity of the collapse by the presence of large replacement masses of dolomite and siderite above the ore horizon, abundant late hydrothermal jarosite in the Chinle, marcasite below the ore horizon, and the replacement of carbonate at depth. Slightly acidic conditions prevailed at depth, and neutral to slightly alkaline conditions prevailed above the ore horizon. Collapse features provided channels for the migration of organic materials and for the penetration of hydrothermal solutions.

The occurrence of native arsenic, $2M_1$ mica clay, and large masses of dolomite, and the character of the urano-organic ore indicate heating in excess of the effects ordinarily attributed to ground water. The distribution and character of the alteration, the ore-mineral suite, and the presence of collapse structures suggest an epithermal hot-spring origin for the uranium mineralization. The features at Temple Mountain are significant in the delineation of centers of uranium mineralization elsewhere on the Colorado Plateau.

## CONTENTS

### TEXT

| | Page |
|---|---|
| Introduction | 702 |
| Acknowledgments | 705 |
| Techniques of investigation | 705 |
| General statement | 705 |
| Microhardness | 705 |
| Differential thermal analysis | 705 |
| X-ray spectrographic analysis | 706 |
| X-ray diffraction | 706 |
| Organic materials | 707 |
| General statement | 707 |
| Relics of vegetation | 707 |
| Range in uranium content | 707 |
| Silicified logs | 708 |
| Coalified wood trash | 708 |
| Organic material of petroliferous origin | 709 |
| Range in uranium content | 709 |
| Fluid and semifluid tar | 709 |

| | Page |
|---|---|
| Dry oil impregnating sandstone | 709 |
| Asphalt | 710 |
| Urano-organic materials | 713 |
| Distribution | 713 |
| Description | 715 |
| Origin of urano-organic constituents | 723 |
| Extraction of uranium from solution | 725 |
| Induration of the organic ore | 726 |
| Metallic element suite | 727 |
| Metallic minerals of the ore | 732 |
| General statement | 732 |
| Arsenic minerals | 733 |
| Iron minerals | 734 |
| Lead minerals | 735 |
| Uranium minerals | 735 |
| Vanadium minerals | 736 |
| Zinc minerals | 736 |
| Distribution of metallic minerals | 737 |
| Ore aggregates | 738 |
| General statement | 738 |
| Included metallic minerals | 742 |
| Other ore textures | 743 |
| Mineral sequence | 744 |
| Alteration associated with mineralization | 744 |
| Hypogene alteration | 744 |
| Supergene alteration | 748 |
| Conclusion | 751 |
| References cited | 753 |


## ILLUSTRATIONS


| Figure | Page |
|---|---|
| 1. Sketch map showing the location of Temple Mountain | 703 |
| 2. Columnar section of formations in the vicinity of Temple Mountain | 704 |
| 3. X-ray spectrograph calibration curve for uranium | 707 |
| 4. Differential thermal analysis of Temple Mountain "asphalt" | 712 |
| 5. Schematic cross-section through Temple Mountain mining district | 713 |
| 6. Distribution of urano-organic ore, Temple Mountain mining district | 714 |
| 7. Hardness of Temple Mountain urano-organic ore | 715 |
| 8. Comparison of hardness and equivalent per cent $U_3O_8$ of urano-organic materials | 716 |
| 9. Differential thermal analysis, indurated hydrocarbons | 717 |
| 10. Differential thermal analysis, low-rank coals and urano-organic ore | 718 |
| 11. Range of reaction maxima of differential thermal analyses of representative organic materials | 719 |
| 12. Urano-organic ore-impregnated log | 719 |
| 13. Loss of weight and hardness upon heating Temple Mountain hydrocarbons | 721 |
| 14. Urano-organic ore along bedding and fracture | 738 |
| 15. Urano-organic ore pod along lithologic contact | 738 |
| 16. Urano-organic ore along fracture | 739 |
| 17. Diagrammatic development of masses of urano-organic material | 740 |
| 18. Some ore-bearing nodules | 741 |
| 19. Composite electron micrographs of urano-organic ore | 742 |
| 20. Paragenesis of alteration and mineralization of the Moss Back Sandstone | 744 |
| 21. Pre-ore alteration in upper and lower strata | 745 |

| Plate | Facing Page |
|---|---|
| 1. Textures observed in hand specimens | 708 |
| 2. Photomicrographs: Some textures in non-uranium-bearing organic materials | 709 |

| | Following page |
|---|---|
| 3. Photomicrographs: Some minerals associated with the organic materials | 742 |
| 4. Electron photomicrographs of urano-organic ore | |
| 5. Photomicrographs: Urano-organic ore | |
| 6. Photomicrographs: Silicification and jarosite | |


## TABLES


| Table | Page |
|---|---|
| 1. Microhardness of some organic materials | 711 |
| 2. Loss of weight on heating of hydrocarbons | 720 |
| 3. Analysis of Temple Mountain asphalt and urano-organic ore | 722 |
| 4. Ash and moisture-free elemental analysis of some organic materials | 723 |
| 5. Comparison of physical properties of some organic materials | 725 |
| 6. Percentage loss of weight in time from heating semifluid tar | 727 |
| 7. Metallic elements in the ash of petroliferous materials | 727 |
| 8. Metallic trace elements | 728 |
| 9. X-ray spectrographic distribution with relation to the collapse area | 729 |
| 10. X-ray diffraction of some organic materials from Temple Mountain | 730 |
| 11. X-ray diffraction of native arsenic | 732 |
| 12. X-ray measurements for heavy-mineral mixture | 733 |
| 13. Partial X-ray-diffraction measurements of iron sulfides | 734 |
| 14. X-ray-diffraction measurements of two varieties of urano-organic materials | 735 |
| 15. X-ray-diffraction measurements of montroseite | 735 |
| 16. X-ray-diffraction measurements of sphalerite | 736 |
| 17. Heavy metallic minerals separated from selected ore zones | 737 |
| 18. Metallic-element distribution in argillic alteration associated with urano-organic materials | 746 |
| 19. Minerals of the Temple Mountain uranium area | 747 |
| 20. X-ray diffraction of jarosite from the Camp Bird mines | 748 |
| 21. X-ray diffraction of jarosite, Temple Mountain | 749 |
| 22. X-ray-diffraction measurements of faintly translucent material associated with organic materials | 750 |


## Introduction

Temple Mountain first became an important mining area during the epoch of radium exploration, about 1920. The search for uranium revived mining operations in recent years. The mining district has lately been one of the major uranium producers on the Colorado Plateau.

The ore is a urano-organic material. Such

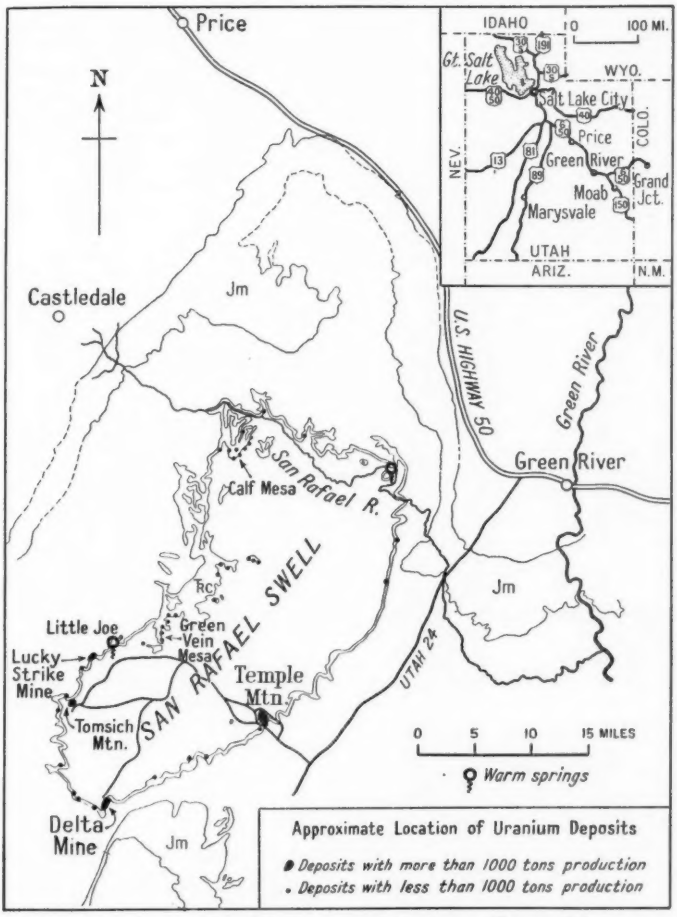


FIGURE 1.—SKETCH MAP SHOWING THE LOCATION OF TEMPLE MOUNTAIN
Warm springs occur in the vicinity of producing uranium mines.

deposits occur in a number of places on the San Rafael Swell, at Elk Ridge in eastern Utah, in New Mexico, at Placerville, Colorado, and probably elsewhere. At Temple Mountain, most of the ores are concentrated in the Moss Back Member of the Chinle Formation and are distributed throughout an area of about a square mile. Isolated ore patches in several horizons establish a vertical spread of approximately 1500 feet from the Triassic Wingate to the Permian Kaibab. The zone of widespread vertical distribution of ore is accompanied by alteration and lies close to the Temple Mountain collapse (Kerr, Kelley, Bodine, and Keys, 1955; Kerr, Bodine, Kelley, and Keys, 1957) where great blocks of down-dropped strata lie partly buried in consolidated debris.

A study of the Temple Mountain mining district began in 1954. A preliminary report on the mechanism of emplacement of the ore (Kelley and Kerr, 1956) is herein revised and expanded. A brief discussion of phases involved in the mechanism of ore emplacement has been published (Kerr and Kelley, 1956).

Temple Mountain lies along the southeastern side of the San Rafael Swell in Emery County, Utah, 44 miles southwest of Green River (Fig. 1). A description of Temple Mountain and the San Rafael Swell in general is furnished in the report on the collapse features cited above (Kerr, Bodine, Kelley, and Keys, 1957). A columnar section (Fig. 2), cross section (Fig. 5), and a diagram showing the distribution of the ore in the mining district (Fig. 6) indicate the geologic setting.

Two major types of organic material are as-

sociated with the organic ore: plant detritus and petroliferous residue.

Plant debris and fossilized logs are found in the Moss Back Sandstone and sparsely through

Tar seeps occur in many places, and porous sandstones from the Coconino through Wingate formations are locally oil-stained. Oil staining extends through Moss Back strata for several

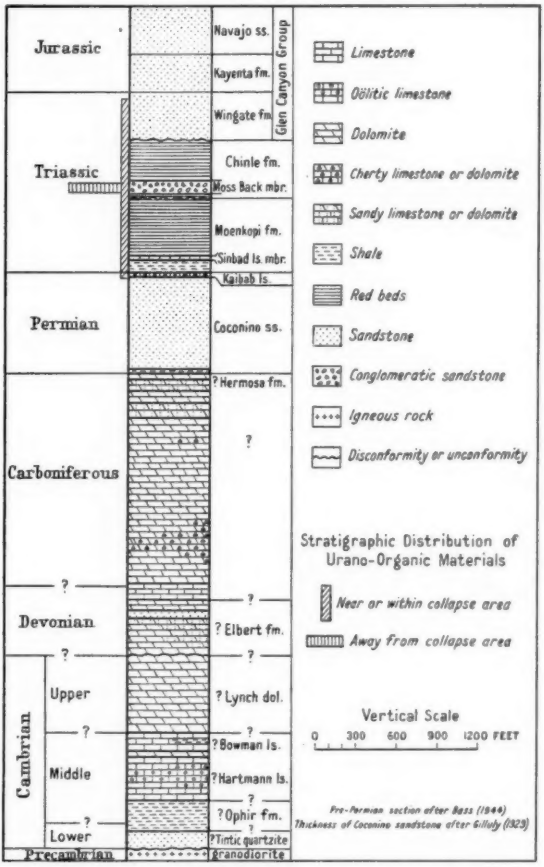


FIGURE 2.—COLUMNAR SECTION OF FORMATIONS IN THE VICINITY OF TEMPLE MOUNTAIN

the rest of the Chinle. At the Delta mine, near the southeastern corner of the swell, logs and carbonaceous trash have been replaced by pitchblende. No urano-organic ore or petroliferous material have been reported from this locality. Calf Mesa, at the north end of the swell, contains deposits of urano-organic materials. As at Temple Mountain, the coalified plant fragments associated with the ore are essentially unmineralized. Elsewhere on the swell, particularly along the western side, urano-organic ore is associated with both nonuranium- and uranium-bearing plant remains.

miles east of Temple Mountain. Similar staining also occurs in a number of localities elsewhere in the swell in Coconino, Moenkopi, and Chinle siltstones and sandstones. An asphaltic material similar physically to asphaltite is present in minor amounts in much of the Temple Mountain collapse. Locally, mixtures of petroliferous materials and coalified wood may be recognized.

Since the strata exposed at the surface do not generate oil the source of the petroleum lies either at depth or to one side of the swell in older Paleozoic rocks. The existence of petro-

liferous sands in the general region has long been known. Prommel and Crum (1927) recognized petroliferous strata in the vicinity of the Colorado and Green rivers; Gilluly (1929), Baker (1946), and Wengard and Strickland (1954) confirmed the presence of oil in the vicinity of the San Rafael Swell, particularly to the south, east, and north. Oil and gas showings have been reported from the subsurface of the Pennsylvanian Hermosa-Paradox sequence of sediments to the Glen Canyon Group of Triassic-Jurassic age.

## Acknowledgments

The writers wish to express their gratitude to Dr. H. D. Glass of the Illinois Geological Survey and Dr. H. S. Yoder of the Geophysical Laboratory for discussions that have aided this study. Appreciation is expressed to Miss P. K. Hamilton of the Department of Geology, Columbia University, for useful suggestions and assistance, and to Mr. Samuel Kamhi for electron photomicrography of the ores.

This study has been made possible through the assistance of the Division of Research and the Division of Raw Materials of the U. S. Atomic Energy Commission. The co-operation of Dr. Daniel R. Miller, Mr. Robert D. Nininger, Mr. Ernest Gordon, Mr. Hiram Wood, and their associates is greatly appreciated.

## Techniques of Investigation

### *General Statement*

Study of the uranium-bearing organic ore included a survey of physical properties and the interpretation of the mechanism of emplacement. The principal methods used have been X-ray diffraction, X-ray spectrographic analysis, microscopic examination of polished surfaces and thin sections, fragment immersion, microhardness determination, and differential thermal analysis.

The greatest handicap in the study of natural organic materials at Temple Mountain may be attributed to the finely mixed nature of the materials. Various contaminant mineral grains in the insoluble urano-organic ore range from a millimeter in diameter to submicroscopic dimensions and are irregularly distributed in size and area. Destructive techniques for obtaining pure organic material were avoided, since the resulting organic substance might be so altered that the determination of the original physical properties would be irrelevant. The best samples of material separated for physical testing contained about 10 to 15 per cent microscopically visible contaminants. Although the presence of fine-grained matter decreases the reproducibility and accuracy of experiments, the results of studies show that variations are restricted, and valid and significant interpretations are possible.

Various techniques have been used to isolate and identify the small contaminant mineral particles. Single minerals and mineral mixtures were separated from the ore by hand picking, elutriation, settling in tetrabromethane, and by the use of the Frantz Isodynamic Separator. The resulting small quantities of material were subjected to X-ray-diffraction study, X-ray spectrographic analysis, microscopic examination, and qualitative chemical tests.

Descriptive data on color and streak are based on Ridgway Color Standards (1912). Qualitative estimates of relative solubilities of organic material refer to powder immersed in carbon tetrachloride for 10 minutes at room temperature. Specific-gravity determinations were made, with a Roller-Smith Precision Berman Balance, on fragments weighing between 5 and 17 milligrams. All fragments were visibly free from contaminants under low magnification.

### *Microhardness*

A Tukon Microhardness Tester, Model MO, manufactured by the Wilson Mechanical Instrument Division of the American Chain and Cable Company, was used to determine microhardness (Kopp, 1955, M.A. Thesis, Columbia Univ.). The Knoop Indenter was used, and hardnesses are recorded in Knoop numbers. Indentations were made in areas visibly free from contamination under microscopic observation. All materials were tested more than four times. Distinguishable ranges of hardness were obtained for various types of organic substances.

### *Differential Thermal Analysis*

Differential thermal analyses were undertaken with the multiple apparatus described by Kerr and Kulp (1948). The rate of temperature increase was 12½° per minute to 1020° C. All materials were ground to approximately 0.07 mm, and similar packing and quantities were used.

Glass (1954) summarized attempts at differential thermal analyses of coals. By using conventional equipment with a nickel sample cover, he has been able to differentiate ranks.

Variability reflects plasticity and to some degree the amount of weathering, particularly in low-rank coals. Differential thermal analyses of naturally occurring carbonaceous material are not reproducible with the precision obtained in many cases with inorganic substances. Differential thermal analyses of organic materials in air, without covering, have little significance, because of dominant oxidation (exothermic).

In order to reproduce experimental conditions used by Glass (1954), runs were made varying the weight and fit of the sample cover.

Results obtained with a heavy cover are used in this report and are considered generally comparable to the study of coals by Glass. Forms of the curves for the same sample are reproducible, and similar samples are, in general, alike. However, variation occurs in the maximum temperatures of endothermic dehydration, endothermic devolatilization, and exothermic oxidation reactions. Reproducibility of high-temperature reactions has not been consistent; hence comparisons of curves of the different organic substances studied may be made only for the lower-temperature reactions. The variations are believed to be the result of:

(1) Contaminant reactions differentially produced by slight variations in the rate of oxidation, because of differences in total amount and packing of the material
(2) Minor reactions characteristic of the organic material but differentially masked
(3) Varying volatile partial pressures caused by differing rates of volatile escape between samples in the covered multiple sample head

About 45 thermal analyses have been made of coals and indurated hydrocarbons; the significant examples are included.

### *X-ray Spectrographic Analysis*

The theory and method of using internal standards for semiquantitative determinations of elements have been outlined by Stevenson (1954) for columbian ores.

X-ray spectrographic analysis of the organic materials was used, not only to determine associated metallic elements, but also for the semiquantitative determination of uranium equivalent to $U_3O_8$. A North American Philips X-ray Spectrograph was used. Samples were run in air, and the fluorescent spectra were diffracted by a lithium fluoride crystal. To guard against the unpredictable effect of variable amounts of contaminant elements, an internal standard was used. Bismuth was selected, since it has not been detected in the organic materials at Temple Mountain, because the wave lengths of the emission lines are relatively close to those of uranium, and the other elements present should have little effect on the standard-calibration reference lines. Standards were prepared, using approximately 4 per cent bismuth, pure silica as a diluent, and a range from 0.1 to 10.0 per cent $U_3O_8$. The resulting calibration curve was used for the semiquantitative determination of per cent $U_3O_8$ in the organic materials tested (Fig. 3). Small quantities of organic materials were mixed with the internal standard to total 2 grams. Mixing was accomplished by grinding. Identically sized sample holders were used, and grinding and packing were essentially uniform.

The approximate content of elements other than uranium could be estimated by comparison with the uranium standards and 1, 5, and 10 per cent standards of Cr, Fe, and Zn. Accuracy by comparison yields an order of magnitude of .x, x., and xx. per cent.

All runs were made under identical conditions, so that the minimum lower limit of element detection was kept constant. Total mechanical error is estimated at 6.5 per cent of the $U_3O_8$ determination. Under the established experimental conditions, the minimum lower limit of uranium detection was equivalent to 0.3 per cent $U_3O_8$.

### *X-ray Diffraction*

X-ray-diffractometer, powder-camera, and X-ray-microcamera techniques were used to identify minerals associated with the organic materials. Young (1954), in a preliminary investigation of solid hydrocarbons, described one- and two-ring powder patterns. X-ray patterns of the organic materials at Temple Mountain have not revealed significant ring characteristics. X-ray-diffraction patterns show that the major graphite spacing (002) is present as a warp in coals as low in rank as high-volatile bituminous (Sievert, 1952). The presence of prographite spacings in the organic materials at Temple Mountain has not been demonstrated. Other less definitive X-ray-diffraction spacings noted for various natural organic substances (Dietrich, 1956) are either absent or masked by contaminant mineral particles. Most of the lines from patterns of organic materials may be attributed to included contaminant grains, although the possibility exists that some un-

assigned lines may be due to one or more organic or metal-organic substances crystalline enough to give a pattern.

Standard tests were used in thin section and polished surface analyses (Larsen, 1921; Short, 1940), and a few autoradiographs were made of polished surfaces of ore samples.

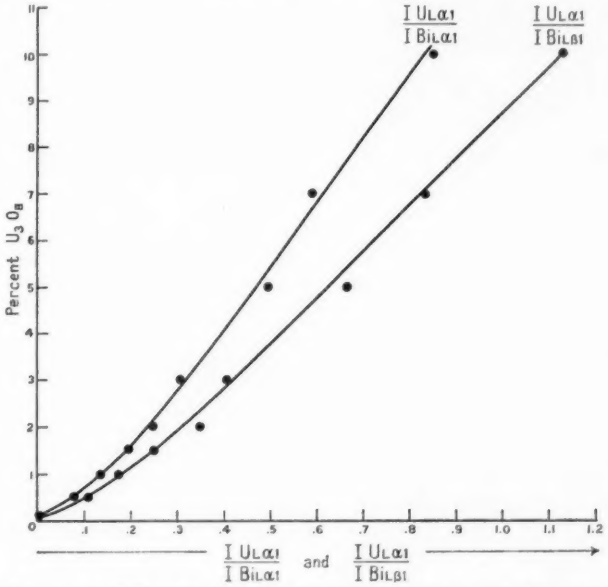


FIGURE 3.—X-RAY SPECTROGRAPH CALIBRATION CURVE FOR URANIUM
Bismuth is the internal standard

## ORGANIC MATERIALS

### *General Statement*

Several forms of organic material have been reported at Temple Mountain (Kerr, Bodine, Kelley, and Keys, 1957). These show a range in color, luster, hardness, microscopic appearance, radioactivity, chemical content, association, and field occurrence. The field occurrences recognized are:

Relics of vegetation
  Silicified logs
  Trash: vitrain, fusain, and clarain and durain
Organic material of petroliferous origin
  Fluid and semifluid tar
  Dry oil impregnating sandstones
  Asphaltic material
Urano-organic materials

### *Relics of Vegetation*

*Range in uranium content.*—The uranium content of fossil plant debris in general is limited to trace amounts (Gott, Wyant, and Beroni, 1952). Almost no uranium has been reported in the major coal fields of the Appalachian and Mid-Continent regions of the United States. Apparently, only in the Rocky Mountain region do certain large deposits of coal carry uranium (Vine, 1955). However, up to 10 per cent uranium occurs locally in lignitic units in the Dakotas.

Many of the uranium mines and prospects on the Colorado Plateau show an association of uranium with relict organic materials. Plant debris and logs may be replaced by pitchblende; some excellent replacements are found in the Delta mine at the southern end of the San Rafael Swell. Although replacements by the pitchblende may occur, the plant material in many cases retains microscopically the appropriate wood structure (Miller, 1955a).

Preliminary experiments show that coals and comparable substances can remove uranium from solution under laboratory conditions. The extraction of uranium by peats, lignites, and sub-bituminous coals may amount to between

98 and 99.9 per cent of the uranium present in solution (Moore, 1954). Uranium found in subbituminous coals and lignites is apparently associated with the humic components of coal, probably as a urano-organic compound (Breger, Deul, and Rubinstein, 1955; Breger, Deul, and Meyrowitz, 1955). Miller (1955b) believes that the formation of pitchblende associated with plant remains resulted from the reaction of ore solutions containing uranium (as a complex uranyl carbonate or uranyl hydroxide ion) with organic sulfur or pyritic sulfur genetically associated with the plant remains. Pitchblende also could be precipitated from reduction of uranium in solution by the organic materials. In the laboratory, uraninite has been precipitated between 25° C. and 260° C. Crystallite study by Croft (1954) suggests that coarser crystals result at the higher temperatures.

Although uranium ore is concentrated in wood replacements in the Colorado Plateau, plant detritus in the Temple Mountain uranium district yields little if any ore. Plant remains, both removed from and intimately associated with the urano-organic ore, yield no uranium above the lower limits of X-ray spectrographic detection (plus 0.3 per cent $U_3O_8$). In general, the usual types of plant remains characteristic of basal Chinle sandstones of the Plateau region appear to be present at Temple Mountain. These types include silicified logs and coalified wood trash. The Temple Mountain coalified fragments appear to be low-rank bituminous coal or lignite. Plant detritus is abundant in the Moss Back Sandstone but may also occur in upper Chinle and the lower Monitor Butte members.

*Silicified logs.*—Fossil logs are in many cases silicified, but a few have a ½- to 1½-inch rim of vitrain. Pyrite replaces the rim in many cases, and desiccation cracks in the outer portion of the logs are also filled with organic materials, detrital grains, pyrite, or secondary hydrous iron minerals. Cell texture is in many cases clearly outlined by the silica replacement. Association and content suggest that the organic rim may be in part impregnated with petroliferous material.

*Coalified wood trash.*—Coalified wood fragments constituting trash zones, in most places are restricted to bedding planes, have microscopic and physical properties characteristic of organic materials of the coal rock types vitrain, fusain, and possibly minor clarain and durain (Hacquebard, 1950; Marshall, 1955). In a few places pyrite is associated with the trash zones.

VITRAIN: The woody parts of original vegetation, composed predominantly of anthraxylon, represent the vitrain. The organic rims of silicified logs are made up mainly of this material. Trash fragments are commonly vitreous and black. In thin section, the material is weakly translucent, either deep red or reddish brown (Pl. 2, fig. 1; Pl. 3, fig. 2). Cell structure is uncommon. On polished surfaces, the material is gray and smooth (Pl. 2, fig. 2). X-ray spectrographic analyses reveal x. per cent Fe and traces of Zn, As, and V (0.x to x. per cent). Microhardness ranges between 26.0 and 32.1 Knoops (Moh's 2), typical of coals (Table 1).

FUSAIN: Commonly, the trash zones contain fusain that is dull and brown to brownish black. It is predominantly opaque in thin section and variably gray on polished surface. On polished surfaces, cell structure is common (Pl. 2, fig. 3). X-ray spectrographic analyses reveal x. per cent Fe, with a few traces of Zn and As (0.x per cent). The microhardness is

PLATE 1.—TEXTURES OBSERVED IN HAND SPECIMENS

FIGURE 1. Tar-soaked sandstone. A Moss Back core fragment from the collapse area. Semifluid tar (black mass) and scattered spots are shown in the bordering unsaturated sandstone.

FIGURE 2. Ore-impregnated standstone. Rounded, partially spherical masses of urano-organic ore (Uo) in the Moss Back Sandstone are surrounded by a zone of pyrite replaced sandstone (Py). Calyx area. (The vertical mark is a hardness indentation.)

FIGURE 3. Ore-impregnated sandstone penetrated by nonuranium-bearing asphalt. Asphaltic material (black) lies at the bottom of the view. It follows bedding in the Moss Back Sandstone in a specimen from Flat Top Mesa.

FIGURE 4. Nonuranium-bearing asphaltic material in mineralized sandstone. Asphalt (Asp)-filled fracture in low-grade urano-organic ore (Uo)-impregnated sandstone. Core fragment from the collapse area equivalent to upper Coconino or Kaibab.

FIGURE 5. Silicification along fracture. Sandstone along one side of a fracture is completely silicified (Si) and contains coatings of realgar and orpiment (Or). The other side of the fracture is composed of argillized sandstone (ss). Core fragment is from the breccia zone in the collapse area.

FIGURE 6. Marcasite in the collapse area. Bands of marcasite parallel and subparallel to bedding in silty mudstone. Core fragment is from the breccia zone in the collapse area.

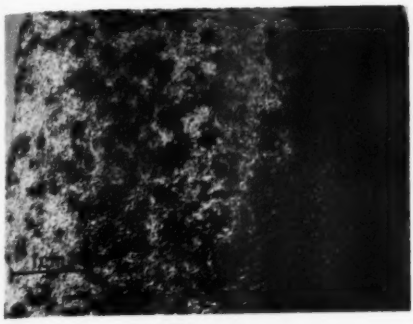

FIGURE 1

FIGURE 2

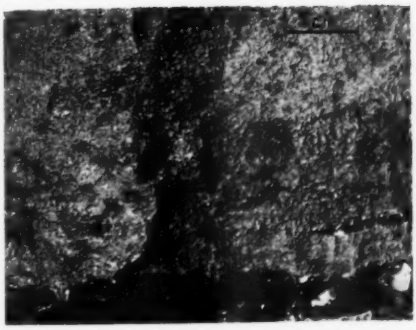

FIGURE 3

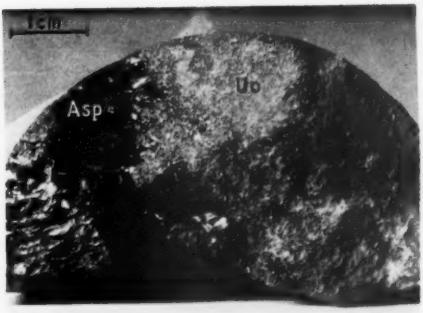


FIGURE 4

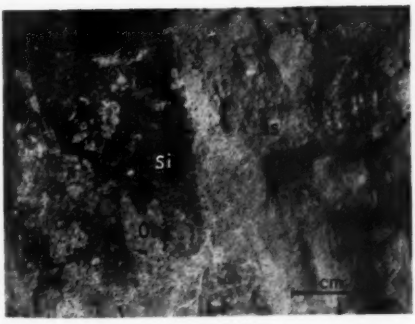


FIGURE 5

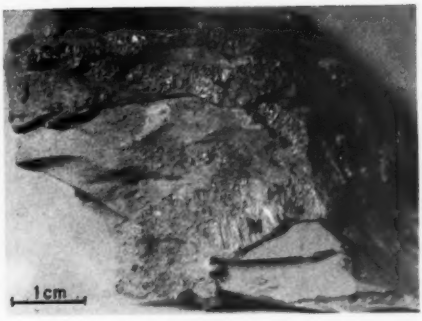


FIGURE 6

TEXTURES OBSERVED IN HAND SPECIMENS

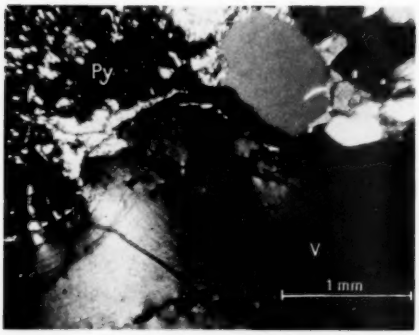


FIGURE 1

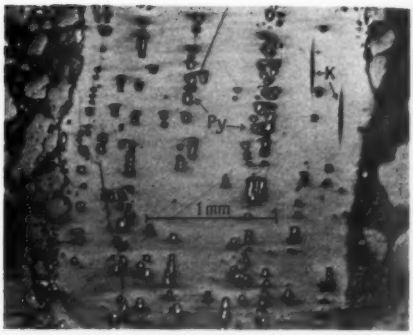


FIGURE 2

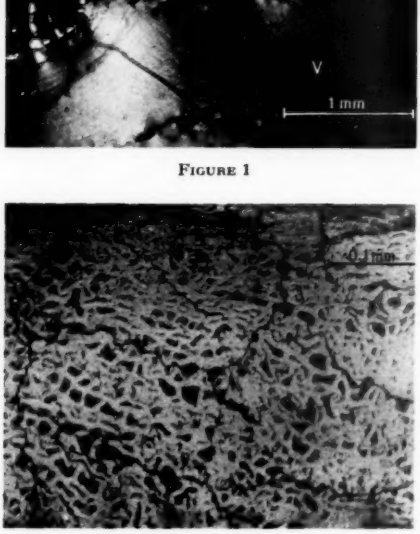


FIGURE 3

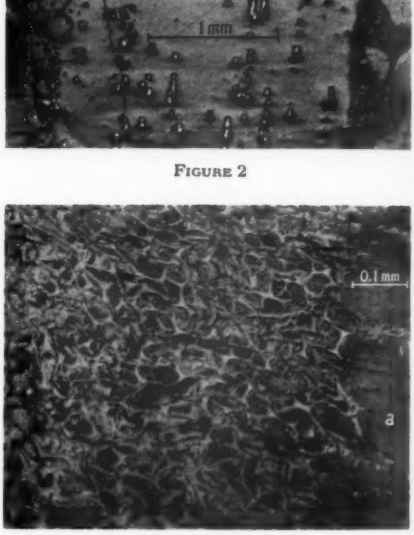


FIGURE 4

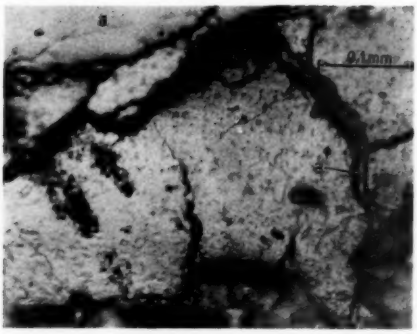


FIGURE 5

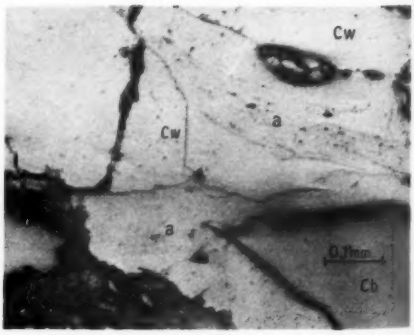


FIGURE 6

PHOTOMICROGRAPHS: SOME TEXTURES IN NONURANIUM-BEARING ORGANIC MATERIALS

approximately 24 Knoops (Moh's 2), typical for coals (Table 1).

CLARAIN AND DURAIN: Although most of the coalified wood fragments contain fusain or vitrain, some of the associated carbonaceous matter reveals in thin section small patches of granular or amorphous opaque material (opaque attritus or micrinite) and, rarely, translucent attritus. Sufficient amounts of these materials are not present to identify the constituents. The terms clarain and durain are tentatively applied to these attrital materials.

The larger fossil plant remains are generally silicified, whereas the smaller fragments are still organic. Possibly the species of fossil wood, as well as the type of woody material, influences its receptivity to replacement by mineralizing solutions. Most of the remains show compression, implying either soft vegetation or the existence of a considerable thickness of sediments on top of the Moss Back before silicification and pyritization.

### *Organic Material of Petroliferous Origin*

*Range in uranium content.*—Organic material of petroliferous origin is found along fault and fracture planes, along bedding planes, on contacts between lithologic units, and impregnating permeable strata.

Crude oil, in general, contains uranium in concentrations of less than 0.02 ppm (Erickson, Myers, and Horr, 1954). Indurated hydrocarbons, however, generally contain slightly more uranium; the amount varies considerably with the type of material and locality. Three types of nonradioactive petroliferous materials are recognized at Temple Mountain: fluid or semifluid tar, dry oil impregnating sandstones, and asphalt.

*Fluid and semifluid tar.*—Black to dark-brown viscous tar is common. It has been found in the Moss Back ore horizon (Marshbank Incline and Calyx Hole mines no.'s 3, 6, and 9, for example), in the Sinbad Member of the Moenkopi at the northern edge of collapse no. 4, in upper Chinle-lower Wingate dolomite near the collapse, in the Temple Mountain collapse (Pl. 1, fig. 1), in drill holes lower in the structure east of Temple Mountain, and along South Temple Mountain Wash. The tar forms seeps and viscous impregnations along bedding planes, fractures, and faults. In places it seeps over ore and plant debris. It is soluble in most organic solvents. It is present interstitially as thin coatings on the detrital grains and has no corrosive or replacement effect on the host rock.

Semiquantitative spectrographic analyses of the ash of two samples of "viscous asphalt" by Erickson, Myers, and Horr (1954) indicate that the uranium content is below 50 ppm (0.005 per cent) and that traces of the metallic elements common to petroliferous materials are present (Table 7). X-ray spectrographic analyses reveal .x per cent Fe and in a few samples traces of As and Ni (0.x per cent). An X-ray spectrographic analysis of the ash of one sample at approximately 1000° C. indicated only iron, since the arsenic was probably volatilized during calcination.

*Dry oil impregnating sandstones.*—Sediments impregnated with dry oil are conspicuous in the area. Bleaching, within and bordering the Temple Mountain collapse, may be attributed in part to the reduction of iron by petroleum.

---

PLATE 2.—PHOTOMICROGRAPHS: SOME TEXTURES IN NONURANIUM-BEARING ORGANIC MATERIALS

FIGURE 1. Vitrain, distorted with wavy extinction. Translucent fragment of vitrain (V) surrounded by pyrite (Py). From the Moss Back Sandstone in the calyx area. Thin section, crossed nicols.

FIGURE 2. Pyrite particles in vitrain follow partly destroyed cell structure. Pyrite is aligned along scattered cells in a fragment of vitrain. From the Moss Back Sandstone of the calyx area. Microhardness indentations (K) are shown. Polished surface.

FIGURE 3. Coalified wood fragment impregnated with asphalt. Distorted cell walls of fusain (?) are white. Asphaltic cell filling is dark gray. From the Moss Back Sandstone bordering the collapse area. Polished surface.

FIGURE 4. Distortion of coalified wood material by asphalt. White cell wall materials have been broken, distorted, and partially displaced by dark-gray asphalt (a). From the Moss Back Sandstone bordering the collapse area. Polished surface.

FIGURE 5. An intimate mixture of coalified wood and asphalt. The texture of the white cell walls of a coalified fragment is barely discernible. Dark-gray asphalt (a) appears as scattered patches and follows small fractures in the fossil wood. From the Moss Back Sandstone bordering the collapse area. Polished surface.

FIGURE 6. Mixed coalified wood and asphalt. Cell texture is absent. Asphalt (a) occurs surrounding, and as streaks within, coalified wood (Cw). Canada balsam cement appears darker gray (Cb). From the Moss Back Sandstone bordering the collapse area. Polished surface.

Moenkopi sandstones and siltstones are locally oil-impregnated, particularly adjacent to fractures, faults, and collapse structures. The Moss Back and Wingate sandstones are commonly saturated. Some Chinle sandstones and siltstones are locally bleached adjacent to faults. Most of the section of Moss Back northeast of Temple Mountain is impregnated. The Coconino Formation is petroliferous northeast of collapse no. 4, along Straight Wash to the northeast, and where encountered in drill holes in the Temple Mountain collapse area. Throughout the swell, many other localities are similarly impregnated.

Though Temple Mountain is an outlier, and the Wingate cap is not connected with Wingate strata to the east, possibly the distribution of the dry oil before erosion assumed the form of a cone, with the apex in the Wingate or even higher on Temple Mountain, and with a slope decreasing away from this center. However, distribution of the oil depended largely on the permeability of strata.

Spectrographic analyses of the ash of four samples of hydrocarbons extracted from "petroliferous rocks" by Erickson, Myers, and Horr (1954) show traces of metallic elements in the ash corresponding to viscous asphalts (Table 7). Uranium content ranges between 0.2 ppm and 67 ppm (less than 0.006 per cent).

The impregnated fresh rock is light brown, and the oil forms a thin coating on detrital grains, without corrosive effect. The organic material represents a stage in the normal oxidation of petroleum.

Dry oil, because of its uniform nature and wide distribution, is independent of the uranium mineralization. It both predates and postdates the ore. In places, oil-impregnated sediments are cut by fractures filled with ore and indurated hydrocarbons. Petroleum impregnation after ores were deposited is shown by the low concentration of uranium in dry oil, the lack of replacement of the host rock, and the lack of induration even where associated with the ore.

*Asphalt.*—A hardened, brittle, black, lustrous nonuranium-bearing petroliferous material, asphalt,[1] occurs in fractures in dolomitized, sideritized, and goethite-bearing masses on and near Temple Mountain (Pl. 3, fig. 1). It fills small fractures in core fragments in ore at a depth of 777 feet in hole V-5 (Pl. 1, fig. 4). It is present as coatings on calcite-filled fractures in upper Chinle strata along the south edge of South Temple Mountain.

The asphalt appears to form within and near the collapse areas. It fills vugs and fractures in the Sinbad northwest of collapse no. 4 and is present along bedding planes and fractures in ore-impregnated Moss Back Sandstone at the north end of Flat Top Mesa (Pl. 1, fig. 3), and locally in the calyx area.

DESCRIPTION: The physical characteristics of the asphalt (Table 5), are somewhat variable. In general, the hardness values agree with those of asphaltites and asphaltic pyrobitumens (Table 1). The material is softer and more elastic than coals and ore. Microhardness indentations in asphalts are more poorly developed than in coalified wood and ore.

Erickson, Myers, and Horr (1954) recorded spectrographic analyses of the ash of two samples of asphalt from the San Rafael Swell. Metallic elements in the ash are essentially the same as those found in the ash of viscous asphalts and hydrocarbons extracted from petroliferous rocks in the swell (Table 7). X-ray spectrographic analysis of the asphalt reveals 0.x to x. per cent Fe and a few traces of As, Cu and Ni (0.x per cent), similar to X-ray spectrographic analyses of semifluid tars (Table 8). However, the ash of an asphalt yielded only iron. As in the semifluid tars, the arsenic appears to have volatilized during ashing.

If one allows for the ordinary variations to which differential thermal analyses of organic materials are subject, particularly at higher temperatures, the asphalt at Temple Mountain appears to correspond to uintaite—a variety of gilsonite from eastern Utah (Fig. 4). Major endothermic dehydration occurs between 160° C. and 185° C. A secondary water loss apparently occurs between 195° C. and 245° C. Exothermic oxidation reactions occur as two peaks separated by the major endothermic devolatilization reaction between 430° C. and 445° C. The first oxidation peak is broad, between 350° C. and 400° C., and the secondary peak occurs between 540° C. and 550° C. Following the oxidation reactions, a small subsidiary endothermic devolatilization peak occurs between 600° C. and 620° C. The higher-temperature reactions are variable. The exothermic reaction in the vicinity of 865° C. and 880° C. may represent a structural change similar to the condensation of hexagonal carbon planes following volatile loss, as proposed by Glass (1954) for coals. The presence of secondary water loss and the temperature ranges of

[1] In physical properties, the material is similar to asphaltite, but chemically it corresponds to an asphalt or mineral wax.

oxidation, as well as volatilization reactions, distinguish the curves of the asphalts from the general variable patterns of other asphaltites, asphaltic pyrobitumens, urano-organic materials, and low-rank coals (Figs. 9, 10, 11).

TABLE 1.—MICROHARDNESS OF SOME ORGANIC MATERIALS

| Material | Range in hardness (Knoop) | Average hardness (Knoop) | Equivalent Moh's hardness |
|---|---|---|---|
| Indurated hydrocarbons* | 1.9–15.9 | 9.5 | −1 to 1.5 |
| Asphaltites* | 6.8–15.9 | 12.6 | 1 to 1.5 |
| Grahamite | 15.3–15.9 | 15.6 | ... |
| Gilsonite (var. uintaite) | 6.8–11.8 | 9.5 | ... |
| Asphaltic pyrobitumens* | 1.9–10.3 | 6.5 | −1 to 1 |
| Wurtzilite | 1.9–3.9 | 2.9 | ... |
| Albertite | 9.5–10.3 | 10.0 | ... |
| "Asphaltum" | 8.6–10.4 | 9.4 | ... |
| Temple Mountain asphalts | 3.1–15.0 | 8.4 | 1 to 1.5 |
| Some coals* | 22.3–62.3 | 43.0 | 2 to 2.5 |
| Lignite | 34.3–60.5 | 46.7 | ... |
| Bituminous | 22.3–29.0 | 25.0 | ... |
| Anthracite | 53.8–62.3 | 57.4 | ... |
| Temple Mountain coalified fragments | 24.2–32.6 | 28.5 | 2 |
| Thucholite | 52.0–89.7 | 65.5 | 2 to 3 |
| Elk Ridge, Utah urano-organic materials | 37.2–62.3 | 54.2 | 2 to 2.5 |
| San Rafael Swell urano-organic materials* | 31.1–129.4 | 67.7 | 2 to 3 |
| Temple Mountain | 31.1–129.4 | 71.9 | ... |
| Elsewhere | 55.3–76.4 | 63.5 | ... |
| Uraninite*† | 412.0–624.6 | 505.7 | 5.5 to 7 |
| Elk Ridge, Utah | 465.4–624.6 | 532.8 | ... |
| Happy Jack Mine, Utah | 412.0–562.0 | 478.6 | ... |

* Recorded range and average hardness include all types listed under this category.
† Palache *et al.* (1944) gives Moh's hardness of 5.5 for uraninite.

The physical characteristics of this material are those of asphaltites, particularly uintaite. However, chemically, the asphaltic material at Temple Mountain differs from asphaltites in having a lower percentage of fixed carbon and more oxygen (Tables 3, 4). In concentration of fixed carbon, it corresponds closely to mineral wax, such as ozokerite, which occurs as vein or fissure fillings in Utah (Abraham, 1920). The greater concentration of oxygen in the Temple Mountain material, compared with any of the indurated hydrocarbons, suggests oxidation subsequent to deposition. Iron sulfates are in many places associated with the material in fractures.

The writers consider that the Temple Mountain asphaltic material represents a product of induration and oxidation of a petroleum that has reached a stage between asphalt and asphaltite.

ASSOCIATIONS: Mineral fragments plucked from surrounding rocks by the asphalt yield X-ray-diffraction lines (Table 10, lower Wingate asphalt). In order of decreasing relative abundance, these are quartz, illite, dolomite, a little pyrite, and one or more additional substances, depending on the sample. Asphalt from fractures in dolomitic Wingate contains primarily quartz and dolomite, whereas asphalt from clay-bearing sediments, to a great extent, contains quartz and illite.

A sequence in deposition appears in asphalt-filled fractures where hematite and goethite cement lower Wingate Sandstone (Pl. 3, fig. 1). From the outside of the fracture inward the relationships are:

(1) A thin outer zone of massive goethite
(2) An intermediate zone of thin discontinuous stringers—dominantly magnesite, with minor intermixed calcite
(3) Massive asphalt which fills the center of the fracture

These relationships indicate that initially goethite and hematite replaced the lower Wingate Sandstone, fracturing and secondary deposition of goethite followed, and petroleum impregnation occurred along fractures. Finally, believed to be impregnated with asphaltic material.

Near the collapse, at the Camp Bird mines, polished surfaces of sandstone surrounding ore show two types of organic substances, neither

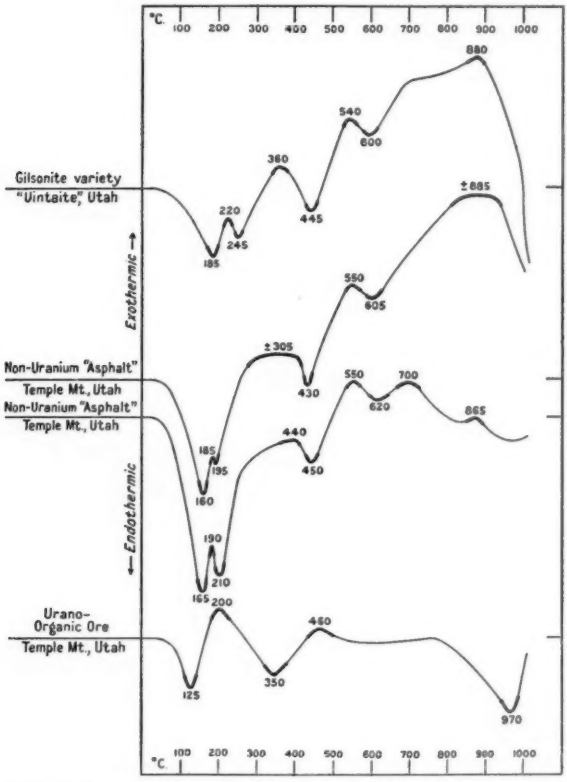


FIGURE 4.—DIFFERENTIAL THERMAL ANALYSIS OF TEMPLE MOUNTAIN "ASPHALT"
Heavy cover

the petroleum became indurated, shrinkage occurred, and magnesite and calcite were deposited in contraction cracks along the edge and through the asphalt. The goethite is not corroded by the asphalt and little corroded by the carbonate.

In places asphalt has directly filled fractures in the dolomite masses and in ore-impregnated sandstones. Asphalts fill fractures that cut carbonate, clay, iron-altered sediments, and ore, indicating introduction subsequent to the major period of alteration and mineralization (Pl. 1, figs. 3, 4).

COALIFIED WOOD IMPREGNATED WITH ASPHALT: A few fragments of coalified wood are of which contains uranium. The first is light gray, relatively free from foreign particles, and exhibits woody cell-wall texture. The second is darker gray, turbid with foreign particles, and forms as mobile impregnations having no woody texture.

A sequence of intimate textural relations shown with the microscope indicates that coalified wood distorted by compression along bedding planes was infiltrated by a hydrocarbon. The cells were first filled with the hydrocarbon (Pl. 2, fig. 3). Distortion of the cell walls and moderate destruction of the woody texture followed (Pl. 2, fig. 5). Finally, the two materials, although still retaining their identity,

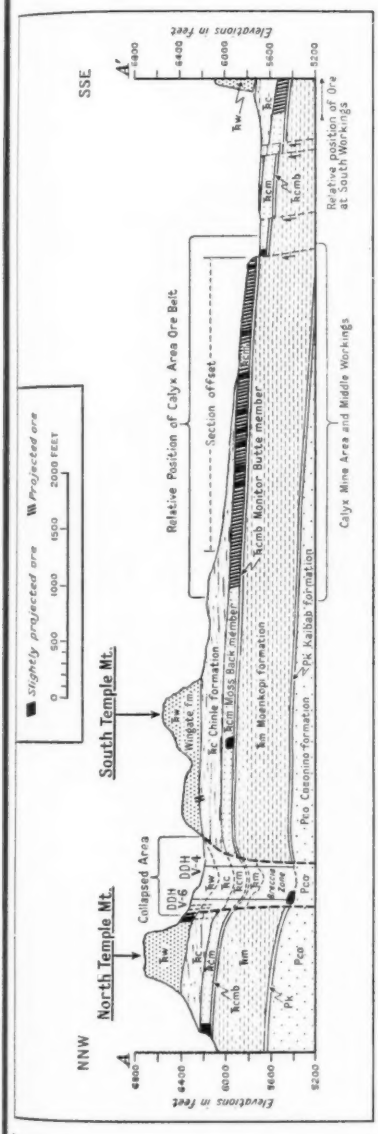


FIGURE 5.—SCHEMATIC CROSS-SECTION THROUGH TEMPLE MOUNTAIN MINING DISTRICT
See figure 6 for location of A-A' and for identification of symbols.

became so intimately mixed that the original cell structure was obliterated (Pl. 2, fig. 6). In a few cases, nodular forms of organic material represent distorted cell structure (Pl. 2, fig. 4). The microhardness of these mixtures (24–29 Knoops, Moh's 2) is similar to coalified wood fragments (24–33 Knoops, Moh's 2), harder than indurated hydrocarbons (2–16 Knoops, Moh's 1).

The mobilization of cell-wall components of the fossil plant debris is apparently localized near the original site of the wood and is restricted to destruction of woody texture. The microscopic relationships indicate an accompanying introduction of a hydrocarbon.

### *Urano-Organic Materials*

*Distribution.*—Uranium-bearing organic materials constitute the uranium ore in the Temple Mountain mining district. Near or within the collapse, these materials occur at scattered intervals in strata where surface pits, adits, and drill cores show a vertical range of approximately 1300 feet from Coconino through Wingate (Fig. 5). The ore is most abundant in the Moss Back but occurs in Wingate, Chinle, upper Moenkopi, and Kaibab or Coconino units.

In the major mining area away from the collapse, the ore is found in the Moss Back Sandstone, where deposits are small and most are discontinuous; their abundance and proximity make the district productive. Small ore bodies are characterized by predominantly lithologically controlled streaks of high-grade ore, with encircling halos of disseminated low-grade ore. Adjacent halos join in a few places and make a low-grade ore connection between the high-grade cores. However, many more halos are separated by barren to weakly mineralized sandstone. In a few places ore-impregnating sandstones cut across sedimentary structures and form ore rolls. Two levels of ore-impregnated Moss Back are represented at Calyx Hole mine no. 8, the South workings, and part of the Camp Bird workings. The lower level is close to the base of the Moss Back; the upper level is 25–30 feet above, toward the top of the sandstone. The greatest production of ore has been from the lower horizon.

Ore bodies in the calyx mining area, about half a mile southeast of the collapse, form a belt approximately a mile long and up to half a mile wide, trending northeast (Fig. 6). Near the collapse, deposits decrease in size and number.

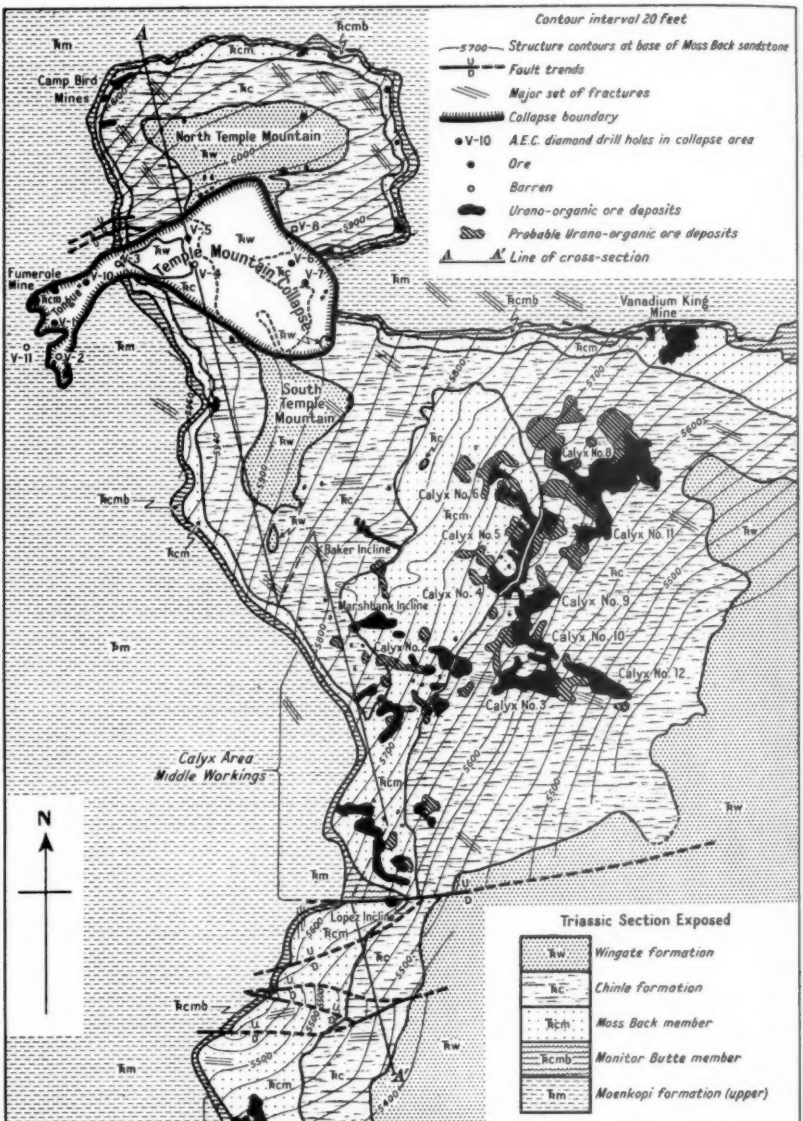


FIGURE 6.—DISTRIBUTION OF URANO-ORGANIC ORE, TEMPLE MOUNTAIN MINING DISTRICT

A thick cover of Wingate to the southeast necessitates deeper exploratory drilling. However, drilling has developed ore in places in the Moss Back where canyons cut into the Wingate. Thus the width of the ore belt is probably greater than shown in Figure 6.

Erosion removed the sediments above the Moenkopi, north and west of Temple Moun-

tain. Thus, the mining area represents a remnant of a Moss Back belt of ore which before erosion probably encircled the collapse. The alignment of the belt that remains with regional the local direction of flow and perhaps the sites of concentrations. The terrain nearest the source may also have been more porous from the effects of deformation and early alteration. The

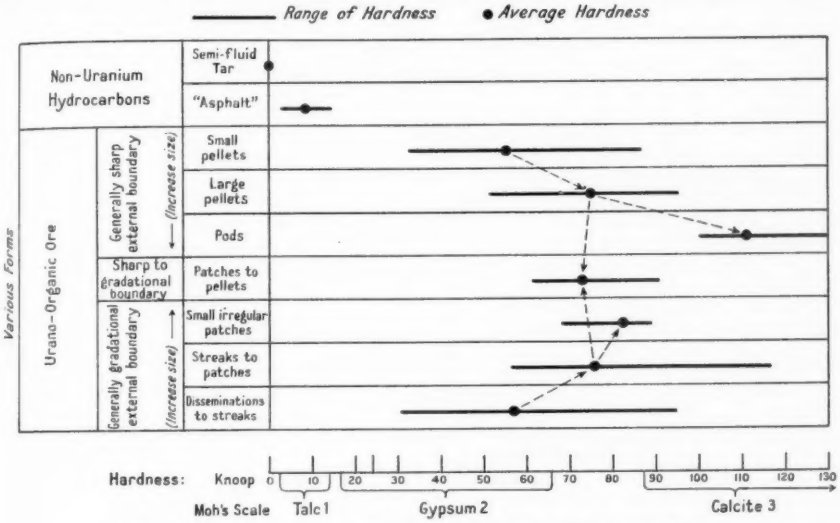


FIGURE 7.—HARDNESS OF TEMPLE MOUNTAIN URANO-ORGANIC ORE

structure led Keys and White (1956) to suggest a broad contour-level ore control.

The calyx area is inclined at 4°–6°, but the regional dip increases southeast of the ore belt. Local patterns suggest a rough east to southeast elongation and alignment of individual ore bodies. This trend roughly corresponds to the strike direction of major faults, including the direction of elongation of the collapse, and to the direction of sedimentation in the Moss Back, as indicated by cross-bedding, ripple marks, and channel structures. The influence of sedimentary trends would be expected, in view of the strong lithologic control of ore distribution.

The presence of the ore in some fractures and faults and the widespread vertical distribution near and within the collapse indicate a vertical influx of ore fluids along the collapse conduit, as well as along fractures and faults. Lateral migration proceeded outward from these local centers, mainly into the permeable Moss Back. To a lesser extent, emplacement occurred in the overlying Wingate and possibly some strata below. Channels of least resistance, earlier used by the fluid organic material, were followed by the mineralizing and rock-altering solutions. Sedimentary structures and textures influenced site of concentration of the organic material, either in a zonal band around the source or as a belt down-dip from the source, was determined by a combination of several factors. These included an increase in viscosity of the organic material, relative impermeability of the sediments outward from the broken source area, the volume, pressure, and distribution of ore fluids, temperature, and regional anticlinal structure.

*Description.*—The physical characteristics of the urano-organic ore are outlined in Table 5. The comparative insolubility of the ore has been noted. In determining uranium extractability, O'Brien (1953) lists 12 solvents, 9 organic and 3 inorganic. He states (p. 4), "The only effective solvents seem to be basic substances with the possible exception of xylene." In insolubility, the ore is similar to coals, asphaltic pyrobitumens (Abraham, 1920), and thucholite.

The urano-organic materials are harder, on the average, than coals (Table 1). They are also considerably harder than Temple Mountain asphalt and the indurated hydrocarbons (asphaltites and asphaltic pyrobitumens). A slight increase in hardness appears with increased size of the ore mass (Fig. 7). Where both hardness and uranium content were determined, it

appears that hardness increases slightly with an increase in uranium content (Fig. 8). Among such specimens, the hardness fails to increase with an increase in metallic elements other than uranium.

FIGURE 8.—COMPARISON OF HARDNESS AND EQUIVALENT PER CENT $U_3O_8$ OF URANO-ORGANIC MATERIALS

Differential thermal-analysis curves of organic materials range to such an extent that differentiation of indurated hydrocarbons (with the possible exception of uintaite) from low-rank coals is uncertain. The general forms of curves of indurated hydrocarbons (Fig. 9) and low-rank coals (Fig. 10) have been compared with urano-organic ore. A summary of low-temperature reactions for a number of curves is given at bottom of this page.

In general, oxidation and devolatilization reactions occur at a slightly lower temperature in indurated hydrocarbons than in lignites, but the difference is small, considering the temperature ranges.

The ore reveals the reactions shown in Figure 9. Endothermic dehydration occurs between 120° C. and 160° C. Exothermic oxidation is generally represented by two peaks, separated by a variable intense endothermic devolatilization reaction between 320° C. and 400° C. The first and major oxidation peak occurs between 200° C. and 280° C., and the secondary peak between 440° C. and 490° C. A few small endothermic peaks in the vicinity of 560° C. probably represent the inversion of quartz present as a contaminant. In some cases the devolatilization peak is small and poorly developed, so that oxidation appears nearly continuous between 200° C. and 500° C. The presence of either a poorly developed endothermic reaction or the presence of two oxidation peaks constitutes a difference between the ore and indurated hydrocarbons and low-rank coals. Most samples of ore reveal a variable intense endothermic reaction between 970° C. and 1010° C., which may represent the evolution of hydrogen. Corresponding reactions oc-

| *Material* | *Dehydration, endothermic* | *Oxidation, exothermic* | *Devolatilization, endothermic* |
|---|---|---|---|
| Lignites | 120°–170° C. | 240°–440° C. | 445°–515° C. |
| Asphaltic pyrobitumens | 120°–160° C. | 210°–265° C. | 420°–440° C. |
| Asphaltites | 140°–170° C. | 235°–265° C. | 385°–410° C. |
| Urano-organic ore | 120°–160° C. | 200°–280° C. | 320°–400° C. |

curring at this temperature in other materials are not reproducible.

Uraninite occurs as minute particles in the ore. Differential thermal analyses of uraninite in air give variable results, and the effect due to small amounts of uraninite in the organic material has not been determined.

Figure 11 is a diagram summarizing the reaction temperature ranges of several organic materials. Ultimately, it may be possible to demonstrate a sequence in the reactions of the indurated hydrocarbons, such as has been demonstrated for the ranks of coal, but at present it does not appear feasible to establish on the basis of differential thermal analysis alone whether a particular organic ore sample is more closely allied to low-rank coals or to petroliferous materials.

In thin section, the urano-organic materials are nearly always opaque, except for a few small, variably translucent patches along the edges of ore masses and, rarely, within the mass (Fig. 18; Pl. 5, fig. 1). The translucence results from (1) smearing and extra thinning of the organic material near the edge of a slide or between the organic material and harder minerals, during preparation of the thin section, (2) rare impregnation by nonradioactive asphalt, which may be variably translucent, and (3) intimate mixtures of ore and associated minerals. In polished surfaces, a rarely observed light-gray, clear ore is associated with the common darker-gray, turbid ore (Pl. 5, figs. 3–5). No difference appears between the two materials in microhardness, $U_3O_8$ content and radioactivity distribution, solubility, and other physical properties. The turbidity in the darker ore is caused by minute contaminant mineral particles and is the cause for the slight difference in appearance on polished surfaces.

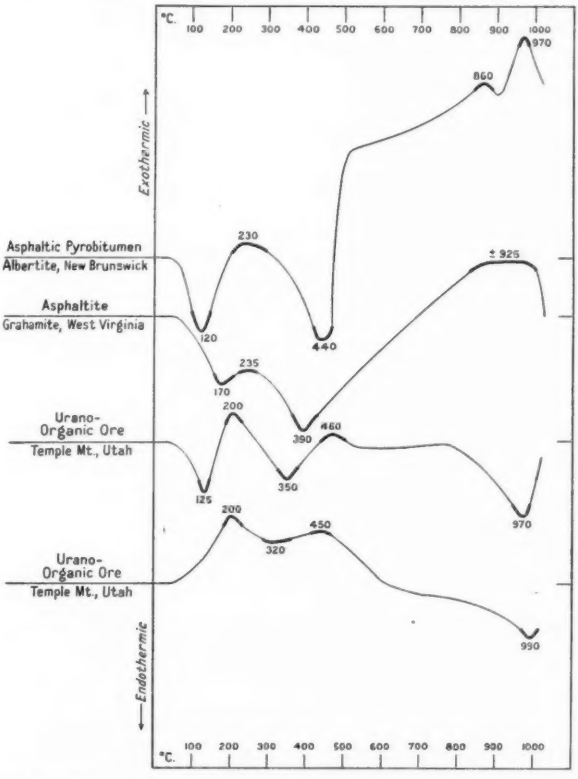


FIGURE 9.—DIFFERENTIAL THERMAL ANALYSIS, INDURATED HYDROCARBONS
Heavy cover

COALIFIED WOOD IMPREGNATED WITH ORGANIC ORE: On the basis of physical characteristics radioactive plant remains appear to be mixtures of unmineralized fossil wood and urano-organic ore. An example of this may be observed at North Mesa No. 9 mine, where a black, organic-appearing silicified log is highly radioactive (Fig. 12). Dull and vitreous black organic materials and pyrite form streaks and patches in fractures and also outline woody texture in streaks parallel to the log structure. Small amounts of nonradioactive asphalt coat some of the fractures. X-ray spectrographic analysis shows that the radioactive organic material contains 6.9 per cent $U_3O_8$.

In thin section, the organic material is seen to consist of two textureless substances, one red brown translucent and the other opaque. These may occur either as separated masses or gradationally mixed. Either may be found in fracture fillings and also in streaks outlining silica-filled wood cells and parallel to the log structure.

On polished surfaces, the translucent material is generally light gray and shows scattered collapsed wood cells. The microhardness (19.3 to 36.3 Knoops, Moh's 2) is similar to coal. The sharpness of the indentation is also similar to coal. Microscopically and physically, this material appears identical to vitrain elsewhere on Temple Mountain. X-ray spectrographic analysis of the vitrain, however, yields less than 0.5 per cent $U_3O_8$ and traces of Fe, As, and V.

The opaque material is generally light gray, clear to turbid, and exhibits no woody texture on polished surfaces. The microhardness (88.4 to 107.8 Knoops, Moh's 2½ to 3) is similar to that of the urano-organic ore containing up to 12.1 per cent $U_3O_8$ and impregnating the sandstone along bedding adjacent to the log (63.0 to 111.4 Knoops, Moh's 2½ to 3). The hardness indentations are less well developed than for

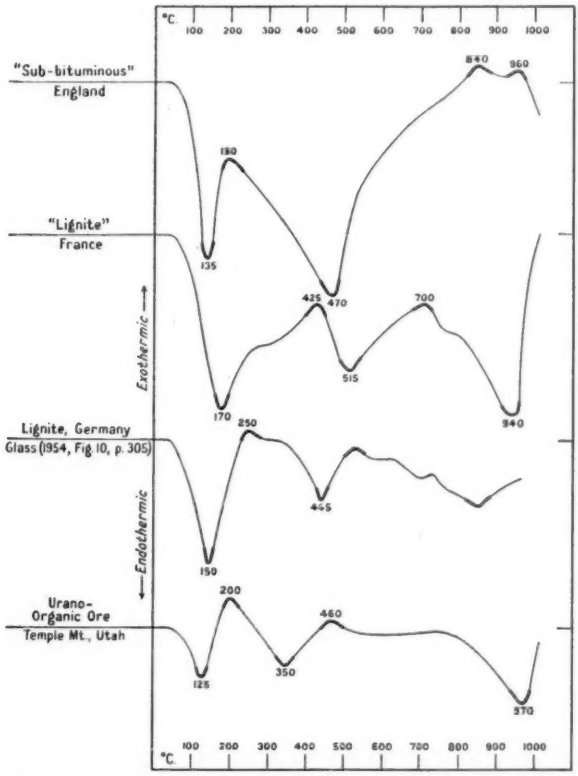


FIGURE 10.—DIFFERENTIAL THERMAL ANALYSIS, LOW-RANK COALS AND URANO-ORGANIC ORE
Heavy cover

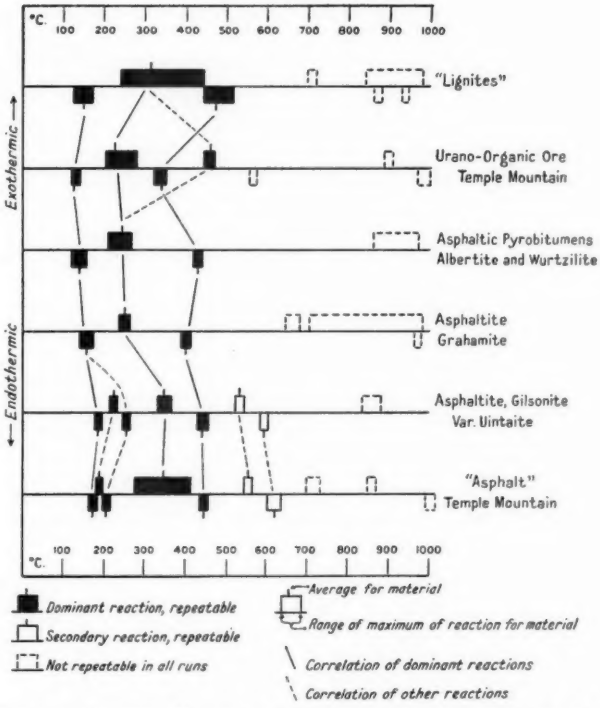


FIGURE 11.—RANGE OF REACTION MAXIMA OF DIFFERENTIAL THERMAL ANALYSES OF REPRESENTATIVE ORGANIC MATERIALS

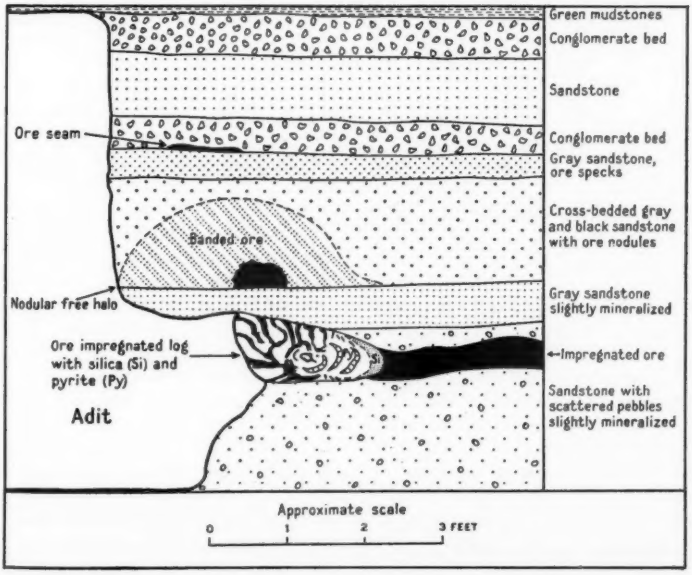


FIGURE 12.—URANO-ORGANIC ORE-IMPREGNATED LOG

TABLE 2.—LOSS OF WEIGHT ON HEATING OF HYDROCARBONS

(In per cent)

Original weight recalculated = loss of weight recalculated as 100 per cent at 1000° C.

| Temperature °C. | Tar | | Asphalt | | Urano-organic ore | |
|---|---|---|---|---|---|---|
| | Loss of weight | Loss of weight recalculated | Loss of weight | Loss of weight recalculated | Loss of weight | Loss of weight recalculated |
| 200 | 1.27 | 1.31 | 3.51 | 2.50 | 2.25 | 3.83 |
| | increased viscosity | | black, granular | | no visible change | |
| 400 | 94.98 | 97.60 | 94.50 | 96.66 | 39.01 | 66.42 |
| | gray-black flakes, masses, fibers | | mottled brown orange, granular | | grayish, no change in form | |
| 600 | 97.29 | 99.97 | 97.22 | 99.44 | 58.39 | 99.41 |
| | brown yellow, granular | | red orange, granular | | yellow brown, no change in form | |
| 800 | 97.29 | 99.97 | 97.62 | 99.72 | 58.62 | 99.80 |
| | brown yellow, granular | | mottled orange, brown, granular | | orange brown, granular | |
| 1000 | 97.32 | 100 | *900°* 97.76 | 100 | 58.73 | 100 |
| | brown yellow, granular | | as above | | purple brown, granular | |
| Original weight | 7.4150 g | | 0.1472 g | | 1.5376 g | |

| Temperature interval °C. | Loss of weight (recalculated) | | |
|---|---|---|---|
| | Tar loss | Asphalt loss | Urano-organic loss |
| 25–200 | 1.31 | 2.50 | 3.83 |
| 200–400 | 96.29 | 94.16 | 62.59 |
| 400–600 | 2.37 | 2.78 | 32.99 |
| 600–800 | 0.00 | 0.28 | 0.39 |
| 800–1000 | 0.03 | *800°–900°C.:* 0.23 | 0.20 |
| Total | 100.00 | 99.95 | 100.00 |

coals, a feature typical of urano-organic materials. Sufficient material for X-ray spectrographic analysis has not been satisfactorily separated, but microscopically and physically this material corresponds to urano-organic ore.

The microscopic relationships indicate that urano-organic material impregnated the log along fractures, filling voids in coalified and silicified woody material, as well as replacing included sedimentary and alteration minerals. The vitrain intimately mixed with the ore is neither mobilized nor mineralized above 0.5 per cent $U_3O_8$. Subsequently, a nonuranium-bearing hydrocarbon impregnated the log along the same paths and formed, upon induration, the asphalt fracture coatings.

A few vermicular remnants of organic material, similar to the cell-wall substance described under asphalt-impregnated coalified wood, are included in some of the ore masses near the collapse (Pl. 5, fig. 4). Woody texture is not observable, and there is no difference in microhardness, trace metallic-element content, and distribution of radioactivity, as revealed by

nuclear-track plates, between the remnants and the surrounding ore. The existence of these remnants as mobilized coalified wood-cell wall material was not established. However, coalified wood intimately mixed with urano-organic ore elsewhere neither contains vermicular remnants nor shows any evidence of mobilization.

CHEMICAL NATURE OF THE URANO-ORGANIC MATERIALS: The loss of volatile constituents in a high-temperature oven differs significantly for organic ore, tar, or asphalt (Table 2; Fig. 13, *A*). Powdered samples of semifluid tar, asphalt, and ore were each heated to arbitrary intervals of 200°, 400°, 800°, and 1000° C. (The sample of asphalt was heated to only 900° C.) To insure temperature equilibrium, though not loss of volatile equilibrium, the samples were allowed to remain at each temperature for 1 hour before weighing. The per cent loss of weight was calculated directly and also recalculated to 100 per cent at 900° C. or 1000° C., assuming that the remaining material at that temperature represented nonvolatile constituents in the range studied.

The tar (96.29 per cent) and the asphalt (94.16 per cent) suffered major loss in the 200°–400° C. range. The ore loss (62.59 per cent) in the same range was substantially less. Volatile constituents amounting to 32.99 per cent in the ore required a 400°–600° C. temperature range for removal. The greater resistance of the ore to heat suggests a more highly polymerized material.

The pine-splint test for porphyrins in the organic ore and the petroliferous material at Temple Mountain is negative, but negative

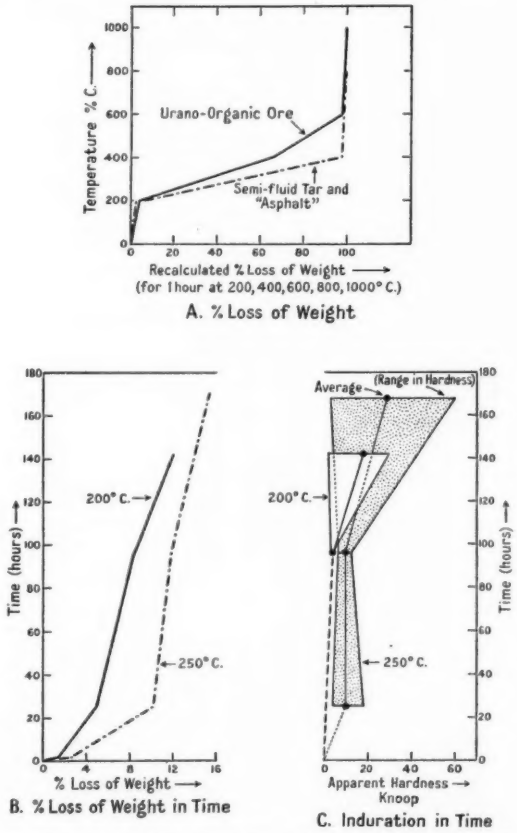


FIGURE 13.—LOSS OF WEIGHT AND HARDNESS UPON HEATING TEMPLE MOUNTAIN HYDROCARBONS

TABLE 3.—ANALYSIS OF TEMPLE MOUNTAIN ASPHALT AND URANO-ORGANIC ORE

(In per cent)

Analyst: W. C. Bowden, Ledoux & Company, Teaneck, New Jersey, May 22, 1956.

| | Asphalt* | Urano-organic ore† | |
|---|---|---|---|
| Volatile matter | | | |
| Total carbon | 75.30 | | 34.90 |
| Fixed carbon | 1.04 | | 34.20 |
| Hydrogen | 8.82 | | 2.80 |
| Oxygen | 6.02 | | 7.41 |
| Sulfur | 4.54 | | 4.48 |
| Nitrogen | 0.84 | | 0.18 |
| Arsenic | 0.06 | | 0.03 |
| Halogens | −0.01 | | −0.01 |
| Water at 105° C. | 0.59 | | 2.10 |
| Total | 96.17 | | 51.90 |
| Nonvolatile matter spectrographic examination | 0.70 | Chemical determination | 45.26 |
| Aluminum | 1–10 | Alumina | 4.15 |
| Calcium | 1–10 | Chromium | Trace |
| Copper | 0.1–1 | $Fe_2O_3$ | 1.66 |
| Iron | 0.1–1 | Magnesia | Trace |
| Lead | −0.1 | Silica | 63.86 |
| Magnesium | 1–10 | $TiO_2$ | 0.15 |
| Manganese | 0.1–1 | $U_3O_8$ | 8.30 |
| Nickel | 0.1–1 | $V_2O_5$ | 19.33 |
| Silica | 10–100 | Zinc | Trace |
| Titanium | −0.1 | Unaccounted for | 2.55 |
| Vanadium | 0.1–1 | | |
| Total | 100.00 | | 100.00 |
| Unaccounted for | 3.13 | | 2.84 |
| Total | 100.00 | | 100.00 |

* Sample no. 735910. Nonuranium-bearing asphalt from fracture in dolomite replaced lower Wingate Sandstone. Collapse area.

† Sample no. 735909. Urano-organic ore pod from Moss Back Sandstone, Calyx Hole mine No. 8.

results do not necessarily establish the absence of porphyrins.

O'Brien (1953) considered that the ore at Temple Mountain has an unusually high acid content.

Analyses have been published of soluble asphalts, asphaltites, and relatively insoluble asphaltic pyrobitumens by Abraham (1920), Crawford (1949), and Hunt, Stewart, and Dickey (1954); thucholites by Ellsworth (1928), Spence (1930), Davidson and Bowie (1951), Barthauer, Rulfs, and Pearce (1953), and Bowie (1955); and the urano-organic materials at Temple Mountain by O'Brien (1953) and Breger and Deul (1955). Since many of the published analyses are incomplete, comparison of the materials is difficult. In thucholites and urano-organic ores, ash content is considerably influenced by contaminant material.

One sample of nonuranium-bearing asphaltic material and one sample of urano-organic ore have been analyzed (Table 3). Although the ore sample was selected to be as free from impurities as possible by hand picking, contaminant mineral particles account for the high ash. The two materials differ chemically to a considerable degree, since the organic material containing uranium yields greater fixed carbon, water, oxygen, and less hydrogen than the asphaltic material.

Elemental analyses of some indurated hydrocarbons, thucholite, low-rank coals, and organic

ore, on an ash-free and moisture-free basis, are compared in Table 4. The ore contains more hydrogen than thucholite but less than the asphalts. Fixed carbon and oxygen in the ore exceed the asphalts. The sulfur content of ore and thucholite are reasonably comparable. A similarity in volatile concentrations exists between the ore and low-rank coals.

TABLE 4.—ASH- AND MOISTURE-FREE ELEMENTAL ANALYSES OF SOME ORGANIC MATERIALS

(In per cent)

| Element | Indurated hydrocarbons* | | | Temple Mountain† | | Thucholite** | Coals†† | |
|---|---|---|---|---|---|---|---|---|
| | Asphalt "tabbyite" | Asphaltite gilsonite | Asphaltic pyrobitumen albertite | Asphalt | Uranoorganic material | | Lignite | Bituminous |
| Total carbon | 84 | 88 | 85 | 79 | 70 | 79 | 60 | 84 |
| Fixed carbon | 9 | 15 | 38 | 1 | 69 | 78 | (up to approximately 78) | |
| Hydrogen | 11 | 9 | 11 | 9 | 6 | 2 | 6 | 5 |
| Oxygen | ? | 1 | 1 | 6 | 15 | 11 | 31 | 9 |
| Sulfur | 2 | 2 | 1 | 5 | 9 | 8 | 2 | <1 |
| Nitrogen | 3 | <1 | 2 | 1 | <1 | | 1 | 2 |
| Total | 100 | 100 | 100 | 100 | 100 | 100 | 100 | 100 |

Data recalculated from:
*Abraham (1920)
†Table 2
**Barthauer *et al.* (1953)
††Ries (1949)

*Origin of urano-organic constituents.*—The writers applied two interpretations in seeking the source of the organic material in the ore. One involves interaction of solutions with petroliferous material, the other organic extraction from coal.

Drill-hole records show that oil exists in almost all porous sediments of the San Rafael Swell. The organic ore at Temple Mountain is associated with semifluid tar, petroleum-impregnated sediments, and asphaltic material. Under such circumstances it is reasonable to consider petroliferous material as a possible source of organic substances.

Logs and other forms of plant detritus are abundant in the Moss Back Formation. On the basis of differential thermal curves and chemical analyses, Breger and Deul (1955) suggest that the ore represents an organic extract from coals of sub-bituminous and lignitic rank. They state (p. 19):

> "... aqueous solutions carrying organic material extracted from low-rank coals in the region, along with uranium and vanadium, may have saturated the pores of the sandstone. Eventually the organic matter was devolatilized and converted to its present insoluble state, perhaps radiochemically"

With regard to uranium-bearing "carbonaceous pellets," they indicate the following trends (p. 20):

> "... 1) ash rises with specific gravity; 2) carbon and hydrogen both decrease with specific gravity; and 3) the total of oxygen, nitrogen, and sulfur rises regularly with specific gravity. There does not appear to be any specific relationship between uranium and any of the other components or properties of the pellets"

Breger and Deul conclude that the compositions of the pellets show similarities with low-rank coals. A survey of their data leads them to interpret "a non-marine and, therefore, a non-petroliferous origin for the pellets" (p. 24).

Similarities in volatile concentrations are insufficient to support a coal-extract origin. A wide range exists in volatile compositions for the various ranks of coal. As shown in Table 4 the organic ore at Temple Mountain might be assumed to be similar to coal. However, other possibilities exist.

The chemical structure of the organic ore is unknown. Infrared and chromatographic analy-

ses are unobtainable because of the relative insolubility of the material. Coals and indurate hydrocarbons, containing as their essential components carbon, hydrogen, and oxygen, will have at least some structural similarities which are reflected in part by similarities in some of the physical and chemical characteristics.

The lack of division between oil and coal has been emphasized by Dietrich (1956, p. 663) who states:

"Further, it would appear that the data presented here may suggest that contentions of workers like Schopf (18) and Berl (2) that there is no real division between oil and coal, that all suggested divisions are arbitrary, and that all these materials may be derived from essentially the same material are correct. Certainly all high rank materials (the end products?) have quite similar properties"

In consideration of the problem of classifying naturally occurring organic materials Schopf (1956) states:

"The distinction.. (of coals).. from asphaltic rocks must be based largely on origin. In many instances this distinction is clear, but in other instances the origin of the carbonaceous material is obscure." (p. 522) . . . "For purposes of definition the demonstrable plant origin of organic matter in coal serves as a most convenient basis for distinguishing coal from asphaltic and certain kinds of graphitic rocks." (p. 526).

It has not been possible to demonstrate a plant origin for the organic matter in the urano-organic ore. In addition, it does not appear that the organic ore represents a coal extract, for the following reasons:

(1) Approximately 99 per cent of the carbon in the ore is fixed. Only in coals of rank greater than medium volatile bituminous will more than 90 per cent of the carbon be fixed. Asphaltic pyrobitumens contain up to 85 per cent fixed carbon (impsonite, Abraham, 1920).
(2) The X-ray spectrographic trace elements Cr, Ni, and Mn, which do not have a zonal distribution in the ore, are characteristic of both petroliferous substances and, locally, coals.
(3) Differential thermal analyses of indurated hydrocarbons, low-rank coals, and the ore are not sufficiently characteristic to base a conclusion on analytical data alone.
(4) A similarity of the indurated ore to low-rank coals, even if demonstrated, does not necessarily mean that the organic material was a coal extract at the time of emplacement and before induration. A petroliferous material could have undergone a metamorphism involving devolatilization and polymerization that would result in an organic compound similar chemically to low-rank coals.
(5) It is doubtful that extraction of organic materials from relatively insoluble carbonaceous compounds, after millions of years involving at least some leaching by ground water, will suddenly occur under unusual conditions that leave no evidence.
(6) The sediments in the San Rafael Swell show essentially no metamorphism away from the collapse, the hydrothermal solutions were only moderate in temperature, and were not particularly concentrated in elements or complexes.
(7) The sediments below the Chinle are essentially devoid of plant remains. Those of the Chinle, specifically the Moss Back within the ore deposits, are similar in all visible respects to plant remains outside of the mineralized area, which suggests no such unusual removal.
(8) Coals in the Mancos shale and other overlying strata surrounding the San Rafael Swell represent typical low-rank coals.
(9) The present remains of carbonaceous materials in the Chinle indicate that not enough organic material existed to form the large quantities of ore, particularly if there was some loss of volume on induration.
(10) It is doubtful that a coal extract derived from the Chinle or above could be transported downward while the hydrothermal solutions were rising from depth to form ore in the Kaibab or equivalent.

The organic material could have orginated by fractionation of a kerogen under the influence of heat and pressure, perhaps catalyzed by certain minerals and associated petroleum, as proposed by Crawford (1949) for gilsonite. However, this origin for the gilsonite in northeastern Utah, even though it is associated with the Green River shales, is not universally accepted. Some believe the gilsonite represents inspissation of petroleum (Murray, 1950). Hunt, Stewart, and Dickey (1954) demonstrated that the various indurated hydrocarbons of the Uinta Basin resulted from variations in the environment at the site of deposition.

The name thucholite was applied by Ellsworth (1928) to a primary hydrocarbon mineral from Parry Sound, Ontario; it is characterized by high percentages of uranium, thorium, and rare earths. The name has been extended subsequently to such uranium-bearing hydrocarbons as described by Barthauer, Rulfs, and Pearce (1953) from the Benser Mine, Ontario; Davidson and Bowie (1951) for several foreign localities; Joubin (1954) for the Blind River area, Canada; Robinson (1950) for the Goldfields

District, Saskatchewan; Kerr, Rasor, and Hamilton (1951) for Placerville, Colorado.

It is uncertain whether the ores at Temple Mountain and elsewhere are chemically similar to each other, or a thucholite type. There are similarities in volatile concentrations (Table 4) and physical properties (Table 5) between the ore and thucholite. At least, thucholite and the ore represent a group of materials harder and denser than the insoluble petroliferous substances, asphaltic pyrobitumens. The increase in fixed carbon in the uranium-bearing organic material may be indicative of greater polymerization or devolatilization, which would account for the increase in hardness and specific gravity. This is also analogous to an increase in ranks of coal resulting from metamorphism.

Table 5.—Comparison of Physical Properties of Some Organic Materials

| Property | Temple Mountain asphalt | Urano-organic ore | Thucholite | Asphaltic pyrobitumen |
|---|---|---|---|---|
| Form | Massive to partially spherical fragments | Massive to pisolitic | Massive | Massive |
| Fracture | Uneven to subconchoidal | Uneven to subconchoidal | Subconchoidal to conchoidal | Hackly to conchoidal |
| Color | Black | Black | Black | Black |
| Luster | Vitreous | Subvitreous to vitreous | Subvitreous to vitreous | Vitreous |
| Streak | Fuscous | Fuscous, chaetura to fuscous black and chaetura black | Chaetura black | Brown to black |
| Specific gravity | 1.11–1.13 | 1.28–1.72 | 1.67–1.82 | 1.00–1.09 |
| Solubility in carbon tetrachloride | Soluble | Insoluble | Insoluble | Very slightly soluble |
| Hardness: | | | | |
| Range in Knoops | 3–15 | 31.1–129.4 | 52.0–89.7 | 1.9–10.3 |
| Average in Knoops | 8.15 | 71.9 | 65.5 | 6.5 |
| Moh's | −1 | 2–3 | 2–3 | −1 |

Laboratory data are neither conclusive nor exclusive, but field evidence supports a petroliferous source for the organic constituents of urano-organic ore.

*Extraction of uranium from solution.*—Widespread, essentially nonuranium-bearing, low-rank coalified wood fragments are scattered through the ore horizon. These indicate the absence of radioactive minerals before the introduction of the organic ore. Davidson and Bowie (1955) and Spence (1930) believe that a radioactive source to react with the hydrocarbon is a prerequisite for the formation of thucholite. At Elk Ridge, Utah, polished surfaces from two localities show veinlets of urano-organic ore bordered by pitchblende (Kerr, Kelley, Bodine, and Keys, 1955). Field evidence suggests that the organic material in the Westwater Canyon Member of the Salt Wash near Grants, New Mexico, was accumulated before the introduction of uranium solutions along small faults and fractures.

A small amount of uranium in carbonized plant remains may result from the absorption of post-ore supergene-leached uranium. Previous chemical changes shown in silicified and pyritized logs and plant trash may make organic remains unreceptive to absorption.

Moore (1954) has shown that low-rank coals extract between 98 and 99.9 per cent of the uranium from uranyl sulfate solutions and 21 per cent from oil shale. The coalified fragments at Temple Mountain are low rank, but the extraction by coals relative to oils is not known.

The writers made an experiment to ascertain whether a uranium-saturated tar, when heated, might physically simulate the indurated urano-organic ore at Temple Mountain. A weight of 40.3 grams of natural semifluid tar from Temple Mountain was refluxed at 104° C. for 18 hours with 250 ml of 0.1844 molar acid uranyl sulfate

solution. After thorough washing and draining, the tar was heated for 96 hours at 250° C. Change in pH, concentration of the solution, and loss of weight were not determined in this experiment; its primary purpose was to determine whether the resulting asphaltic material contained uranium and became indurated. X-ray spectrographic analysis of the powdered asphalt yielded 1.05 per cent equivalent $U_3O_8$ and .x per cent Ni. The microhardness was between 2.5 and 26.0 Knoops (Moh's 1), and the indentation was more reliable than for heated nonuranium-bearing tar. Most of the "asphalt" dissolved in carbon tetrachloride at room temperature in a few minutes, but a small residue was insoluble after it was left in solution for a week. Differential thermal analysis revealed a similarity to the Temple Mountain asphalt. No crystalline compounds were revealed by X-ray diffraction. Some of the powdered material was leached for 20 hours in both concentrated nitric acid and ammonium hydroxide. X-ray spectrographic analysis of the leached material revealed 0.60 per cent equivalent $U_3O_8$. The leached material was only slightly soluble in carbon tetrachloride at room temperature. Apparently at an elevated temperature the Temple Mountain tar will extract uranium from a uranyl sulfate solution, and washing and leaching by strong acids and bases will not remove all the uranium absorbed or chemically combined with the organic material.

The development of the San Rafael Swell, which furnished the impetus for the petroleum migration, is considered to have taken place in post-Mancos time, probably post-Cretaceous, early Tertiary (Gilluly, 1929). Thus the folding probably occurred about 80 million years ago, the age of the "asphaltic type" ore at Camp Bird No. 13 Mine (Stieff, Stern, and Milkey, 1953), and probably during the period of the initial introduction of the petroleum. Only the early premineralization petroleum in contact with the ore solutions became urano-organic ore. Most of the nonuranium-bearing petroliferous materials at Temple Mountain were introduced after mineralization. The low uranium content of these materials in a few places may be attributed to absorption of post-ore supergene-leached uranium.

*Induration of the organic ore.*—Induration of the urano-organic materials accompanying emplacement of the uranium could have been accomplished by: (1) polymerization, (2) oxidation-devolatilization, or (3) a combination of the two. Davidson and Bowie (1951) and others proposed radioactive polymerization for the induration of thucholite. However, this would not account for accompanying argillic alteration, carbonate replacement, and associated metallic mineralization.

In a summary of the problem of sulfate reduction in deep subsurface waters, Ginter (1934) outlined two methods of reduction of sulfate in solution, with attendant oxidation of hydrocarbon or carbonaceous material. The first is the reduction of sulfate to sulfide by the hydrocarbons, which in turn are oxidized to carbonate. In the absence of oxygen, this reaction would probably occur only at high temperatures. The second assumes that anaerobic micro-organisms cause sulfate reduction and oxidize hydrocarbons. Although sulfate-reducing anaerobes have been found in deep subsurface waters, the significance of the biochemical reactions has not been established.

Induration of petroleum may occur through long exposure to oxidizing conditions. Much of the nonuranium-bearing petroliferous material abundant on the San Rafael Swell was indurated in this way. However, it is much less indurated than the ore.

Hydrothermal conditions prevailed during the formation of thucholite, as indicated by Ellsworth (1928). Davidson and Bowie (1951) considered that thucholite belongs to a late hydrothermal stage. Kerr, Rasor, and Hamilton (1951) conclude that the urano-organic mineralization at Placerville, Colorado is hydrothermal. Abraham (1920) and others consider the formation of asphaltites and asphaltic pyrobitumens as the gradual conversion of petroleum under the influence of time, heat, and pressure.

Oil, air-blown in the vicinity of 145° C., will become indurated (Dr. G. Skaperdoes, Kellogg Corporation, personal communication). The semifluid tar at Temple Mountain will become indurated in time upon heating in an oxidizing atmosphere at temperatures of 200° C. and 250° C. In the experiments, the tar was heated in an oven at the given temperatures for consecutive arbitrary intervals (Table 6; Fig. 13, *B*). Temperatures were controlled to within 1° C. The greatest per cent loss of weight per hour at both temperatures occurred within the first hour and subsequently decreased with increased time of heating. Equilibrium was not established in 142 hours at 200° C. or 168 hours at 250° C. The per cent loss of weight was greater at any time at 250° C. than at 200° C. Physical changes occurred in the tar through time at both temperatures. It first became more viscous and then became indurated. Induration occurred earlier at 250° C. than at 200° C. The

TABLE 6.—PERCENTAGE LOSS OF WEIGHT IN TIME FROM HEATING SEMIFLUID TAR

Hardness is apparent. Comparison is relative. All indentations partially closed over after testing loss of weight in per cent.

| Time (hours) Accumulative | At 200°C. | | | | At 250°C. | | | |
|---|---|---|---|---|---|---|---|---|
| | Loss of weight | | Apparent hardness (Knoop) | | Loss of weight | | Apparent hardness (Knoop) | |
| | Accumulative | Per hour | Range | Average | Accumulative | Per hour | Range | Average |
| 1 | 1.27 | 1.27 | viscous | | 2.43 | 2.43 | viscous | |
| 25 | 5.24 | 0.21 | very viscous | | 10.26 | 0.41 | 4.2–18.6 | 11.2 |
| 96 | 8.66 | 0.09 | 2.4–4.4 | 3.4 | 11.74 | 0.12 | 7.8–13.3 | 10.4 |
| 142 | 12.01 | 0.08 | 1.5–29.6 | 10.7 | ... | ... | ... | ... |
| 168 | ... | ... | ... | ... | 12.77 | 0.08 | 2.6–59.0 | 20.4 |

TABLE 7.—METALLIC ELEMENTS IN THE ASH OF PETROLIFEROUS MATERIALS, SAN RAFAEL SWELL

After Erickson, Myers, and Horr (1954)

| Material | Per cent ash | U* PPM | Partial metallic composition of ash | | | | | | | |
|---|---|---|---|---|---|---|---|---|---|---|
| | | | Fe | As | V | Cr | Zn | Ni | Cu | Pb |
| Viscous asphalt | 1.23– 2.92 | 0.2–50 | .x-x. | .... | .x | .x | .0x | .x | .0x | .00x |
| Petroliferous rocks | 0.79– 4.86 | 0.2–67 | x. | .... | .x | .0x-.x | .0x-.x | .0x-.x | .0x-.x | .0x |
| Asphalt | 2.32–13.61 | 30.0–1,137 | .x-x. | .x | .x | .00x-.x | .0x | .0x | .x | .0x |
| Uraniferous asphaltite | 17.0–62.0 | n.d. | x.-x. | x. | .0x-.00x | .0x-.00x | .... | .0x-.x | x. | .x |

*Recalculated from: $\frac{\text{Per cent ash} \times \text{per cent U in ash}}{10{,}000}$

Viscous asphalt: Two samples from the Moss Back at Temple Mountain and Flat Top Mesa.

Petroliferous rocks: Four samples from Temple Mountain and Flat Top Mesa. Two samples from the Moenkopi of Temple Mountain with a uranium content between 0.2 – 0.5 ppm. One sample from the Wingate at Temple Mountain; one sample from a slump block at collapse no. 1, Flat Top Mesa, with uranium content between 32 – 67 ppm.

Asphalt: Two samples from the Sinbad Limestone Member of the Moenkopi and the Moss Back Sandstone at Temple Mountain.

Uraniferous asphaltite: Two samples from Emery County, Utah.

indurated "asphalt" fractured conchoidally. In general appearance, the "asphalt" resembled the nonuranium asphalt material that naturally occurs at Temple Mountain. Microhardness tests of the artificial "asphalts" are not comparable to naturally occurring organic materials because of partial closure of the indentation after testing. However, they are relative, and comparison of hardness of the artificial materials may be made. There appears to be an increase in relative hardness with increased time of heating at both temperatures (Table 6; Fig. 13, *C*). The relative hardness was greater for any specific time at 250° C. than at 200° C. The minimum temperature of induration has not been established, since the hardening is related in part to time.

The induration of the urano-organic material probably occurred under the influence of heat and the action of solutions rather than by radioactive polymerization. Whether the hardening resulted from oxidation-devolatilization, polymerization, or both processes together is unknown.

*Metallic-element suite.*—Erickson, Myers, and Horr (1954, p. 2213) report emission spectrographic analyses for the ash of two "uraniferous asphaltites" from the swell (Table 7), as characterized by high U, As, Cu, and Mo, and relatively low V. Among the metallic elements listed, there is a slight but noticeable increase of Fe, As, Cu, and Pb and a decrease in V in the ash of the ore compared with the ash of viscous asphalts, oil extracted from petroliferous rocks, and asphalts.

X-ray spectrographic analyses of 12 samples

TABLE 8.—METALLIC TRACE ELEMENTS

Blank spaces and 0 indicate element not detected. Lower limit is approximately 0.1–0.3 per cent

A. Comparison of X-Ray Spectrographic Indications of Metallic Elements in Some Organic Substances

| Substance (and number of samples) | Per cent $U_3O_8$ | Per cent Semiquantitative | | | | | | | | | |
|---|---|---|---|---|---|---|---|---|---|---|---|
| | | Fe | Zn | As | V | Cr | Ni | Mn | Co | Se | Cu |
| Temple Mountain | | .x | | −.x | | | −.x | | | | |
| Semifluid tar (1) | | | | | | | | | | | |
| "Asphalt" (4) | | .x–x. | | 0–x. | | 0–.x | 0–.x | | | | |
| Urano-organic (12) | 1.8–15.0 | .x–x. | .x–x. | 0–x. | 0–x. | 0–.x | 0–.x | 0–x. | 0–.x | 0–x. | |
| Coalified plants (5) (in ore zones) | | x. | 0–x. | .x | 0–.x | | | | | | |
| Thucholite (1) | 1.2 | x. | | (Plus thorium, manganese, and rare earths) | | | | | | | |
| Indurated hydrocarbons | | | | | | | | | | | |
| Asphaltites (3) | | .x–x. | | | | | 0–.x | | | | 0–.x |
| Asphaltic pyrobitumens (3) | | .x–x. | | | | | 0–.x | | | | 0–.x |
| Some coals (4) (lignite to anthracite) | | .x–x. | 0–.x | | | 0–.x | 0–.x | | 0–.x | | 0–.x |
| Ash (Temple Mountain) | | | | | | | | | | | |
| Semifluid tar (1) | | x. | | | | | | | | | |
| "Asphalt" (1) | | x. | | | | | .x | | | | |
| Urano-organic (1) | 15.5 | x. | .x | x. | x. | | | | | | |

B. Analysis of X-Ray Spectrographic Indications of Metallic Elements in Temple Mountain Urano-Organic Ore

| Element | Per cent of samples having metallic element in: | |
|---|---|---|
| | .x per cent or less | x. per cent |
| Present in all samples | | |
| Fe | 33 | 67 |
| Zn | 75 | 25 |
| Present in over 90 per cent | | |
| As | 45 | 55 |
| V | 91 | 9 |
| Cr | 100 | ... |
| Present between 25–90 per cent | | |
| Ni | 100 | ... |
| Occasionally present (less than 25 per cent) | | |
| Mn | 67 | 33 |
| Co | 100 | ... |
| Se | 33 | 67 |

from 9 ore localities show a range in concentration of Fe, Zn, As, V, and Cr (Table 8). Nickel was found in half of the samples, and Mn, Co, and Se were noted in a few. Uranium concentration in the specimens selected ranged between 1.8 and 15.0 per cent equivalent $U_3O_8$.

TABLE 9.—X-RAY SPECTROGRAPHIC DISTRIBUTION WITH RELATION TO THE COLLAPSE AREA

| Element | Average concentration of elements (per cent) | | |
|---|---|---|---|
| | Calyx area | Bordering collapse | Collapse area |
| As* | 2.0 | 3.7 | 5.0 |
| $U_3O_8$ | 5.4 | 3.5 | 3.0 |
| V* | 2.0 | 0.5 | 0.5 |
| Zn* | 2.8 | 0.5 | 0.5 |

*Average concentration: considering for each sample .x per cent = 0.5 per cent and x. per cent = 5.0 per cent. Uranium is recorded as average per cent equivalent $U_3O_8$.

The ash of one specimen revealed the same suite, with the exception of chromium. There was some loss on ashing. However, 97.5 per cent equivalent $U_3O_8$ in nonashed material was present in the ash.

Emission spectrographic analyses of the ash (Erickson, Myers, and Horr, 1954) and X-ray spectrographic analyses of the nonashed ore differ somewhat, because of differences in the technique and sensitivity of the two methods, as well as either loss or concentration of elements upon ashing. Copper has not been detected with the X-ray spectrograph, but contamination by the equipment may mask small amounts of this element. Copper minerals are rarely present in the mining district. Molybdenum may be present in amounts less than approximately 0.2 per cent, the lower sensitivity of the experimental method used. Vanadium is characteristic of the metallic-element suite, but most of the vanadium is probably volatilized on ashing.

ZONAL DISTRIBUTION OF ELEMENTS: Variations in concentration of some of the metallic elements appear to reflect a zonal distribution with relation to the collapse area. Cobalt, selenium, and high-arsenic concentrations are found near or within the collapse and possibly locally along some faults. Cobalt has been detected from two of the nine localities tested. One of these is at the eastern edge of the collapse, and the other is in a fault zone in the calyx area (Lopez Incline). Selenium has been detected from the locality at the eastern edge of the collapse. Both of these elements may be present in the ore in concentrations below the sensitivity of the experimental method, as indicated by the presence of cobalt bloom in several mines and the widespread occurrence of the selenium indicator plant *Astragalus*. Cannon and Stillman (1952, *in* Keys and White, 1956) report high selenium content of the organic ores. Arsenic is present in more than 90 per cent of the samples. Ore from the calyx area yields concentrations generally of the order of .x per cent. A few yield x. per cent. Samples of ore from the collapse and surrounding area yield concentrations generally on the order of x. per cent; a few show .x per cent (Table 9).

In contrast, the average amounts of uranium, vanadium, and zinc seem to increase away from the collapse (Table 9). It had previously been reported that vanadium is more concentrated in the collapse (Keys, 1955; Keys and White, 1956). The concentrations of Fe, Cr, Ni, and Mn are irregularly distributed.

SOURCE OF METALLIC ELEMENTS: Erickson, Myers and Horr (1954) report trace-element analyses, as well as chemical determinations of uranium and other metals in petroliferous materials from many localities. Analytical data are given for 78 samples described as crude oil, petroliferous rock, asphalt, and asphaltite. The ash from asphalt and oil extracted from petroliferous rocks contains a nearly constant suite of metals: U, Co, Cr, Cu, Mn, Mo, Ni, Pb, V, and Zn. Ash from petroleum shows that V and Ni are the most abundant metallic elements, although Ag, W, As, Sn, and Au may be present. Crude oils from various localities are characterized by an abundance of particular elements. These metals are thought to be concentrated in the asphaltic fraction of petroleum.

The collapse and, to a lesser extent, faults represent the major channels for hydrothermal solutions, as indicated by the spatial distribution of alteration in the area (Kerr, Bodine, Kelley, and Keys, 1957) and argillic alteration in the ore horizon (Kelley and Kerr, 1957). Elements showing a zonal distribution with relation to the collapse are As, Co, Se, U, V, and Zn. Of these elements, only As and Se are not characteristic of the metallic suite of the ash of most petroliferous materials. Thus, with the exception of As and Se, the above metallic elements could have been derived from the organic materials present in the district by some mechanism of concentration. Erickson, Myers, and Horr (1954, p. 2216–2217) state:

TABLE 10.—X-RAY DIFFRACTION OF SOME ORGANIC MATERIALS FROM TEMPLE MOUNTAIN

All patterns are X-ray diffractometer except Lower Wingate asphalt which is powder camera. Cu/Ni. Intensities recalculated to 10 maximum for strongest line of each pattern

| Asphalts | | | | Urano-organic ore | | | | | | | | Thucholite Canada | | Possibility* |
|---|---|---|---|---|---|---|---|---|---|---|---|---|---|---|
| Collapse | | | | Collapse | | Calyx area | | | | | | | | |
| | | | | | | Moss Back | | | | | | | | |
| Lower Wingate | | ?Kaibab D.D.H. V-5:777 feet | | ?Kaibab D.D.H. V-1:370 feet | | Large pod | | Streak | | Nodules | | | | |
| d(Å) | I | d(Å) | I | d(Å) | I | d(Å) | I | d(Å) | I | d(Å) | I | d(Å) | I | |
| | | | | | | 9.35 | 5 | | | | | | | |
| 7.3 | 9 | 7.39 | 5 | 7.3 | 6 | | | | | | | | | Kaolinite |
| | | 5.049 | 5 | 4.993 | 3 | | | | | | | | | |
| | | | | 4.403 | 4 | | | | | | | | | Kaolinite |
| 4.277 | 10 | 4.271 | 6 | 4.247 | 4 | 4.263 | 8 | | | 4.208 | 5 | | | Quartz |
| | | 3.922 | 6 | 3.974 | 5 | | | | | | | | | |
| 3.791 | 1 | | | | | | | | | | | | | |
| | | 3.625 | 6 | 3.608 | 10 | | | | | | | | | Kaolinite |
| | | 3.528 | 5 | 3.507 | 5 | | | | | | | | | |
| | | 3.448 | 5 | | | | | 3.437 | 3 | | | | | |
| 3.336 | 5 | 3.350 | 10 | 3.340 | 8 | 3.339 | 10 | 3.317 | 10 | 3.315 | 10 | | | Quartz |
| | | | | 3.302 | 6 | | | | | | | | | |
| | | 3.184 | 3 | | | | | 3.216 | 2 | | | 3.184 | 8 | |
| | | | | 3.121 | 4 | 3.121 | 5 | 3.151 | 3 | 3.104 | 2 | 3.142 | 10 | Pitchblende, sphalerite |
| 3.066 | 6 | 3.094 | 4 | 3.051 | 4 | | | 3.097 | 9 | | | 3.081 | 8 | Pyrite |
| 2.885 | 9 | | | | | | | | | | | 2.871 | 7† | Dolomite |
| | | 2.729 | 3 | | | | | | | | | | | |
| | | | | 2.712 | 3 | 2.708 | 3 | 2.688 | 5 | 2.690 | 1 | 2.702 | 6 | Pitchblende, pyrite, sphalerite |
| 2.675 | 5 | | | | | | | | | 2.678 | 1 | | | Dolomite |
| | | 2.623 | 3 | 2.633 | 2 | 2.636 | 3 | 2.621 | 2 | 2.621 | 1 | | | Pyrite |
| | | | | 2.555 | 2 | | | | | | | | | Kaolinite |
| | | 2.471 | 3 | | | 2.454 | 4 | | | 2.440 | 2 | | | Quartz |
| | | 2.397 | 3 | 2.397 | 3 | | | 2.406 | 2 | | | | | Kaolinite, pyrite |
| | | 2.285 | 3 | | | 2.279 | 3 | | | 2.267 | 2 | | | Quartz |
| | | | | | | 2.235 | 2 | | | 2.221 | 1 | | | Quartz |
| 2.189 | 6 | | | | | | | 2.194 | 2 | | | | | Dolomite, pyrite |
| | | 2.118 | 4 | | | 2.129 | 3 | | | 2.115 | 2 | | | Quartz |
| 2.074 | 4 | 2.056 | 3 | | | | | | | | | | | Dolomite |
| 2.007 | 1 | 1.990 | 3 | 1.978 | 3 | 1.979 | 4 | | | 1.969 | 1 | | | Quartz, dolomite |
| | | 1.954 | 3 | | | | | | | | | | | |
| | | | | 1.908 | 3 | 1.919 | 3 | 1.902 | 7 | 1.906 | 1 | 1.911 | 6 | Pitchblende, pyrite, sphalerite |
| 1.882 | 1 | 1.855 | 3 | 1.854 | 3 | | | 1.899 | 7 | | | | | Pyrite |
| | | 1.819 | 3 | 1.819 | 3 | 1.815 | 4 | | | | | | | Quartz |
| 1.792 | 4 | | | 1.793 | 3 | | | 1.806 | 3 | 1.808 | 4 | | | Quartz |
| | | 1.673 | 3 | | | | | | | | | | | |

TABLE 10.—*Continued*

| Asphalts | | | | Urano-organic ore | | | | | | | | | | Thucholite Canada | | Possibility |
|---|---|---|---|---|---|---|---|---|---|---|---|---|---|---|---|---|
| Collapse | | | | Collapse | | Calyx area | | | | | | | | | | |
| | | | | | | Moss back | | | | | | | | | | |
| Lower Wingate | | ?Kaibab D.D.H. V-5 777 feet | | ?Kaibab D.D.H. V-1 370 feet | | Large pod | | Streak | | Nodules | | | | | | |
| (dÅ) | I | d(Å) | I | d(Å) | I | d(Å) | I | d(Å) | I | d(Å) | I | | | d(Å) | I | |
| 1.656 | 1 | 1.661 | 3 | | | | | | | 1.661 | 1 | | | | | Quartz |
| | | | | | | | | | | 1.647 | 1 | | | | | |
| | | | | 1.631 | 3 | 1.633 | 3 | 1.625 | 7 | 1.627 | 1 | | | 1.633 | 6 | Pitchblende, pyrite, sphalerite |
| | | | | | | | | 1.623 | 8 | | | | | | | Pyrite |
| 1.613 | 2 | 1.597 | 2 | | | | | | | | | | | | | Pyrite |
| 1.542 | 2 | 1.542 | 2 | 1.539 | 2 | 1.540 | 5 | | | 1.535 | 3 | | | | | Quartz |
| | | | | | | | | | | 1.446 | 1 | | | | | Quartz |
| | | | | | | | | | | 1.442 | 1 | | | | | Pyrite |
| | | 1.418 | 2 | | | | | | | | | | | | | |
| | | 1.382 | 2 | | | 1.381 | 2 | | | 1.377 | 1 | | | | | Quartz |
| | | 1.374 | 2 | | | 1.372 | 2 | | | 1.370 | 3 | | | | | Quartz |

* Blank spaces represent unassigned lines of unknown crystalline compounds.

† Does not represent dolomite.

"... the concentration of uranium, vanadium, copper, and arsenic, in the ash of oil extracted from petroliferous beds in the Moenkopi, Shinarump, and Wingate formations in the San Rafael Swell district, Emery County, Utah, is similar to the concentration of these metals in the uraniferous asphaltite deposits around the flanks of this structure ... The evidence suggests that the uraniferous asphaltite was derived through volatilization, oxidation, and polymerization of a petroleum whose ash was enriched in uranium, vanadium, copper, arsenic, molybdenum, and nickel."

The highest uranium content of crude oil is given as 0.02 ppm, and the lowest as 0.00001 ppm. There is a wide range in intermediate values. However, crude oil does not contain uranium in ore-bearing concentrations. In general, the nonuraniferous hydrocarbons in the vicinity of Temple Mountain show a concentration of uranium between 1500 and 3000 times the highest concentration of uranium in crude oil, whereas the uraniferous hydrocarbons show a concentration of uranium of more than 500,000 times. An average urano-organic ore sample would represent a concentration of 2,000,000 times that in crude oil. Seven gilsonite specimens show variations of 0.015 to 3 ppm uranium, representing a concentration difference of only 200 times.

The irregular increase in uranium in indurated hydrocarbons indicates that the element has been added to the petroliferous material locally. The hydrocarbons containing relatively large amounts of uranium are not apt to result wholly from the concentration by inspissation of a petroleum containing as low a concentration of uranium as 0.02 ppm or from a petroleum uniformly enriched.

The same argument would apply to the concentrations of As, Co, Se, V, and Zn. The uniform properties of the urano-organic material, in contrast to the zonal distribution of the contained metallic elements and representative metallic minerals, point to the local hydrothermal source responsible for the alteration associated with the occurrence of the organic ore. The concentration of the elements As, V, Zn, and U may be attributed to a concentration of submicroscopic and microscopic particles of native arsenic, montroseite, sphalerite, and uraninite that are known to exist intimately associated with the ore. Thus, the concentration of these elements may not be characteristic of the organic material but would

be representative of the minute included metallic minerals formed by the action of the original material on hydrothermal solutions carrying these elements.

The irregular distribution of low concentrations of Ni and Mn, which are not represented by primary minerals and are elements characteristic of organic materials, may indicate a source from the organic materials. Although the irregular distribution of low concentrations of Cr in the ore may also indicate an organic source for this element, the localized distribution of chromium mica clay (Kerr and Hamilton, 1958) in faults and near or within the collapse also may reflect transportation by late hydrothermal solutions. The widespread distribution of moderate concentrations of iron and the various generations of pyrite are indicative of a multiple source for that element.

TABLE 11.—X-RAY DIFFRACTION OF NATIVE ARSENIC

X-ray diffractometer, Cu/Ni

| Collapse border Camp Bird Mine No. 7 | | | | Collapse Fumarole Claim? | | Echizen Province Japan† | |
|---|---|---|---|---|---|---|---|
| Nodule | | Disseminated in ore* | | Band in nodule† | | | |
| d(Å) | I | d(Å) | I | d(Å) | I | d(Å) | I |
| | | 4.247q | 15 | | | | |
| 3.504 | 74 | 3.504 | 22 | 3.516 | 13.4 | 3.516 | 18 |
| 3.330q | 6 | 3.336q | 85 | 3.336q | 11.2 | | |
| | | | | | | 3.198c | 10.0 |
| 3.108 | 7 | 3.097 | 19 | 3.108 | 6.4 | 3.108 | 3.6 |
| 3.066c | 4 | | | | | 3.066c | 1.2 |
| 2.769 | 100 | 2.761r | 100 | 2.776 | 100 | 2.776 | 100 |
| | | | | | | 2.540c | 3.5 |
| 2.045 | 53 | 2.043r | 42 | 2.047 | 19.6 | 2.047 | 26.3 |
| | | | | | | 1.959c | 1.6 |
| 1.875 | 44 | 1.871r | 39 | 1.876 | 22.5 | 1.878 | 24.5 |
| 1.763 | 18 | 1.763 | 14 | 1.766 | 7.8 | 1.769 | 9.3 |
| 1.653 | 8 | 1.653 | 12 | 1.656 | 5.3 | 1.656 | 5.5 |
| 1.550 | 21 | 1.549r | 17 | 1.552 | 8.5 | 1.553 | 11.1 |

c = contaminant impurities unidentified, q = quartz, r = realgar.

* Separated from ore by tetrabromethane settling and Frantz Isodynamic Separator. Partical size is 60–120 mesh. Associated realgar lines are removed.

† From Kerr and Lapham (1954).

## METALLIC MINERALS OF THE ORE

### *General Statement*

Two types of mineral assemblages occur in the ore. The first consists of host-rock particles, chiefly nonmetallic sedimentary and alteration minerals, such as quartz, illite, kaolinite, and a few particles of carbonates and sulfates. The second group represents metallic-mineral particles, such as pyrite, arsenic, sphalerite, uraninite, and montroseite, with secondary alteration products, realgar, orpiment, and jarosite. The two most abundant contaminants are quartz and pyrite.

X-ray powder-camera patterns of the ore are generally indistinct. However, X-ray-diffractometer patterns of the urano-organic material yield lines corresponding to uraninite or sphalerite or both (Table 10). Pyrite is usually present. The spacings and intensities are such that many of the pyrite lines can be separated from those of uraninite-sphalerite. Sphalerite and uraninite concentrations of less than 1 or 2 per cent are not detected by the X-ray-diffraction technique used; however, the stronger X-ray reflections that could correspond to either of the two minerals are present everywhere in the ore. Uranium was present in more than 1.8 per cent equivalent $U_3O_8$ in samples, but zinc concentrations ranged from .X to X. per cent. Probably at least some

finely microscopic and submicroscopic uraninite is present in all the ore. Such lines are also present in thucholite from Besner Mine, Ontario, in which zinc was not detected by the X-ray spectrograph.

TABLE 12.—X-RAY MEASUREMENTS FOR HEAVY-MINERAL MIXTURE
Camp Bird Mines

Separated from ore by tetrabromethane and Frantz Isodynamic Separator. X-ray diffractometer, Cu/Ni. Black grains which yield on X-ray spectrographic analysis xx. per cent Fe and As, x. per cent Zn and V, and 0.x per cent U, Ni, Mn, and Cr. vb = very broad line.

| d(Å) | I | Possibilities |
|---|---|---|
| 8.42 | 4 | Unknown |
| Very weak lines | | |
| 3.34 | 9vb | Quartz |
| 3.12 | 8 | Pyrite, sphalerite |
| 2.94 | 3 | Loellingite |
| 2.88 | 2 | Loellingite |
| 2.76 | 5 | Native arsenic |
| 2.70 | 7 | Pyrite |
| 2.60 | 3 | Loellingite |
| 2.34 | 10 | Loellingite, pyrite |
| Very weak lines | | |
| 2.04 | 1 | Native arsenic, loellingite |
| Very weak lines | | |
| 1.88 | 2 | Native arsenic, loellingite, sphalerite, pyrite |
| 1.81 | 1 | Unknown |
| 1.65 | 1 | Unknown |
| 1.62 | 3 | Pyrite, sphalerite, loellingite |
| 1.59 | 2 | Loellingite |

The identified metallic minerals may be discussed on the basis of the significant metallic elements.

### *Arsenic Minerals*

Kerr and Lapham (1954) originally identified native arsenic in a band from a nodule taken from the collapse (Fig. 18, *G*). Native arsenic is relatively abundant in the ore zone at the Camp Bird mines north of the western collapse area. The arsenic not only forms as clusters of microscopic crystals (Pl. 3, figs. 3, 4) but as nearly solid nodules with dimensions up to 1 cm (Fig. 18, *H*, *I*) and as thin stringers and irregular patches. Minor native arsenic is present also in the heavy minerals separated from organic material in drill cores taken at depth in the collapse area. Alteration of the arsenic resulted in coatings of realgar and orpiment. Partial X-ray-diffraction patterns of native arsenic are shown in Table 11.

Native arsenic has been found at a number of localities in the United States (Palache, Berman, and Frondel, 1944). Periodic deposition of the metal is common. Examples would be the reniform masses in Arizona (Warren, 1903) and concentric layered deposits near Montreal, Canada (Evans, 1903). Both of these occurrences are considered the result of "fumarole action." In general, native arsenic is believed to be deposited from hydrothermal solutions.

Sedimentary rocks range in average arsenic content from 1 to 2 ppm for limestones and sandstones and up to 10 ppm for shales (Onishi and Sandell, 1955). Arsenic increases with organic content; some organic shales contain as much as 59 ppm. Some pyrite contains up to 450 ppm. The distribution of arsenic in sedimentary rocks is believed to reflect arsenic carried up from depth by thermal springs and volcanic exhalations, probably in the form of a chloride or oxide (Onishi and Sandell, 1955). Spectrographic analyses of the ash of various petroliferous materials yield arsenic contents ranging between .x and x. per cent on the average (Erickson, Myers, and Horr, 1954). The possibility exists that the arsenic at Temple Mountain may have been derived from the organic materials. However, the zonal distribution of the element in the ore and the restriction of occurrences of native arsenic near the collpase favor hydrothermal solutions.

The abundance of pyrite and the presence of other sulfides associated with the ore suggest the system Fe-As-S. The presence of an iron arsenic mineral is suggested by X-ray-diffraction measurements of metallic mixtures separated from high-arsenic-bearing ore. One such pattern is shown in Table 12. X-ray spectrographic analysis of this heavy black-mineral aggregate yielded iron and arsenic concentrations on the order of xx. per cent. Sulfur is present qualitatively. Native arsenic and pyrite are present in the ore from which this material was separated. A number of the X-ray spacings suggest loellingite-leucopyrite. Similarly, arsenopyrite has not been conclusively identified, although suggestive X-ray patterns have been obtained. X-ray spectrographic analyses of pyrite from ore zones yield arsenic on the order of .x per cent. Possibly the arsenic

is in solid solution. The assemblage pyrite-arsenic-arsenopyrite suggests temperatures between 320° C., the melting point of realgar, and 675° C., the melting point of arsenopyrite at 1 atmosphere pressure. In nature, however, increased pressure from the load of overlying sediments and the effects of water on the system would lower this temperature range somewhat.

The native arsenic at Temple Mountain is believed to have been derived from the ore solutions under elevated temperatures, inferred from other occurrences of the metal and the probable conditions of deposition in the presence of iron and sulfur.

TABLE 13.—PARTIAL X-RAY-DIFFRACTION MEASUREMENTS OF IRON SULFIDES

| Pyrite* | | Marcasite† | |
|---|---|---|---|
| Range in spacing d(Å) | Range in intensity I | Range in spacing d(Å) | Range in intensity I |
| 3.11–3.12 | 26–34 | 3.42–3.48 | 50 |
| 2.70 | 100 | 2.69–2.71 | 100 |
| 2.42 | 59–78 | 2.41–2.43 | 30–40 |
| 2.20–2.21 | 41–45 | 2.31–2.33 | 30–40 |
| 1.91 | 38–47 | 1.91–1.92 | 30–40 |
| 1.80–1.84** | 3–6 | 1.76–1.77 | 90 |
| 1.63 | 70–99 | 1.72–1.73 | 10 |
| 1.56 | 6–12 | 1.70 | 10–20 |
| 1.50 | 10–18 | 1.67–1.68 | 10 |
| 1.44–1.45 | 16–22 | 1.59–1.60 | 20–30 |
| 1.24 | 6–12 | (very faint lines) | |
| 1.20–1.21 | 6–12 | 1.43–1.44 | 10–30 |
| 1.18†† | 6–12 | 1.37–1.38 | 5–10 |
| | | 1.23 | 10 |
| | | 1.17 | 20 |

* X-ray diffractometer, Cu/Ni

† X-ray powder film, Cu/Ni

** Contaminant present in all patterns

†† hkl (421) used for estimate of unit cell dimensions. Actual measurements for four pyrites were 1.179, 1.180, 1.181, and 1.182 Å.

### *Iron Minerals*

Pyrite, the most abundant metallic mineral associated with the ore, appears in three generations. An earlier, pre-ore pyrite is associated with organic materials, particularly coalified wood (Pl. 2, figs. 1, 2; Pl. 3, fig. 2). The pyrite core of nodules, about which clay minerals and urano-organic materials have accumulated (Fig. 18), may also be of pre-ore age but later than that associated with the wood. The second generation of pyrite is that deposited during uranium mineralization and forms in zoned pods and pisolites containing ore and as crystals disseminated in the ore (Fig. 18; Pl. 1, fig. 2; Pl. 3, fig. 6). A third generation of post-ore pyrite is represented by a few streaks cutting ore masses.

Small amounts of marcasite may be present throughout the mining district, but the most noticeable occurrences are near or within the collapse. Bands of marcasite up to half an inch thick are present in fractures in cores from the collapse (Pl. 1, fig. 6). These are not associated with the ore. Marcasite is mixed with pyrite in ore-bearing nodules from the collapse (Fig. 18, *D*). Away from the collapse, it forms small radial clusters within pyrite-replaced coalified wood.

X-ray-diffraction measurements of some pyrite and marcasite from Temple Mountain are shown in Table 13. Pyrite associated with the ore contains arsenic in quantities ranging between .x and x. per cent. The lattice constant $a_0$ determined on the basis of hkl (421) averages 5.413 Å and ranges from 5.408 Å to 5.417 Å for four pyrites. The lattice constants for two pyrites listed on the ASTM Index Cards are 5.4046 Å and 5.407 Å. Kerr, Holmes, and Knox (1945) give the lattice constant $a_0$ for pyrite from Leadville as 5.40667 ± .00007 Å. The pyrite from Temple Mountain has slightly larger cell dimensions. This may result from the presence of arsenic in the lattice. According to a summary of the occurrence of minor elements in some sulfide minerals (Fleischer, 1955), the average arsenic content of sedimentary pyrites is 600–900 ppm and of hydrothermal pyrites 400–700 ppm. There is more arsenic in low-temperature vein pyrite than in higher-temperature vein pyrite. Neuhaus (*in* Fleischer, 1955) reported 5 per cent arsenic in pyrite with a unit cell of 5.442 Å. The general belief is that the arsenic is present in true solid solution and causes the increase in cell dimension.

Both marcasite and pyrite are found in many sedimentary deposits. From a study of the effect of temperature and acidity on the formation of marcasite and wurtzite, Allen, Crenshaw, and Merwin (1914, p. 430–431) concluded that the unstable forms, marcasite and wurtzite, formed from acid solutions. However, they were usually mixed with the corresponding stable forms, pyrite and sphalerite. The higher the maximum temperature

of the experiment, if other conditions remain unchanged, the greater the quantity of the stable forms. The higher the acidity, if other conditions remain unchanged, the greater the quantity of the unstable forms. Acid concentration necessary to give rise to pure marcasite falls with the temperature and is close to neutrality at ordinary temperatures. Marcasite, therefore, may be expected to be deposited srom acid solutions, or conversely, "... it becomes evident that the alkaline nature of fhe water, irrespective of the temperature, its sufficient to condition the formation of pyrite" (Allen, Crenshaw, and Merwin, p. 428). The temperature of formation of a specimen of natural marcasite from Obira, Japan, has been recorded as 279° C. on the basis of liquid inclusions (Ingerson, 1955).

TABLE 14.—X-RAY DIFFRACTION MEASUREMENTS OF TWO VARIETIES OF URANO-ORGANIC MATERIAL

From small amounts picked from a polished surface. Angles of reflection of galena followed by their intensities are from Swanson and Fuyat (1953).

| Clear gray | | Turbid gray | | Possibilities |
|---|---|---|---|---|
| d(Å) | I | d(Å) | I | |
| 5.25 | 6 | | | Unknown |
| | | 3.44 | 7 | Galena (3.429–84) |
| 3.34 | 1 | | | Unknown (?quartz) |
| 3.13 | 1 | 3.13 | 4 | Uraninite, sphalerite |
| | | 2.99 | 4 | Galena (2.969–100) |
| 2.73 | 1 | 2.72 | 1 | Uraninite |
| | | 2.11 | 5 | Galena (2.099–57) |
| 1.92 | 1 | 1.92 | 1 | Uraninite, sphalerite |
| | | 1.80 | 2 | Galena (1.790–35) |
| 1.65 | 1 | 1.64 | 1 | Uraninite, sphalerite |

The alternation of bands of pyrite and marcasite in a nodule from the collapse may indicate local changes in pH. Bernauer (1935) noted that marcasite altering with pyrite resulted from volcanic exhalations. If the temperature of the ore solutions was slightly elevated, the pH of the solutions at the time of deposition was neutral to slightly acidic, rather than alkaline. This interpretation would agree with the solution of carbonate below the Moss Back.

### *Lead Minerals*

Lead has not been determined by X-ray spectrographic analyses of the ore. The presence of galena, however, may be indicated in the calyx area on the basis of X-ray diffraction of some turbid urano-organic material (Table 14). Galena occurs in small crystals and nodular-like clusters of crystals found in drill cores from the upper Coconino and possibly Kaibab in the collapse. However, ore has not been found in association with these occurrences.

TABLE 15.—X-RAY-DIFFRACTION MEASUREMENTS OF MONTROSEITE

| Montroseite Temple Mountain* | | Montroseite Weeks *et al.* (1953) | |
|---|---|---|---|
| d(Å) | I | d(Å) | I |
| | | 4.75 | VF |
| 4.29q | 4 | 4.31 | S |
| 3.37q | 10b | 3.38 | M |
| 2.95u | 2 | | |
| 2.63 | 9 | 2.644 | S |
| 2.47 | 4 | 2.495 | M |
| 2.41 | 1 | 2.423 | W |
| 2.20 | 3 | 2.217 | M |
| 2.15 | 2 | 2.151 | F |
| 1.96 | 1 | 1.965 | W |
| 1.93 | 1 | 1.918 | W |
| | | 1.841 | Fb |
| | | 1.731 | W |
| | | 1.689 | W |
| 1.62 | 1 | 1.605 | W |
| 1.50 | 1 | 1.512 | M |
| 1.47 | 1 | 1.467 | W |
| 1.41 | 1 | 1.391 | W |
| | | 1.302 | F |
| | | 1.282 | F |

* X-ray diffractometer, Cu/Ni. q = quartz contamination, u = unknown, b = broad line.

Separated from ore. Black grains, opaque with submetallic luster and black streak. X-ray spectrograph yields xx. per cent V and x. per cent Fe.

### *Uranium Minerals*

Uraninite (var. pitchblende) is present in small amounts throughout most of the ore at Temple Mountain. It generally occurs as small crystals and irregular grains scattered at random throughout masses of ore (Fig. 18, *E*). These small particles furnish radioactive centers for autoradiographic reactions on polished surfaces. Radiation emanates from small light-gray hard grains. If nuclear-track plates are used, black reactions indicate particles of uraninite; elsewhere the tracks are irregularly scattered and in a few places ir-

regularly concentrated throughout the urano-organic material. Large masses of this mineral have not been noted. Only rarely have grains been identified on the order of 1 or 2 mm in diameter.

Although uraninite is well known as a replacement of fossil wood elsewhere, all uraninite identified from specimens examined is restricted to the urano-organic ore that shows no cell structure and has a texture indicative of a fluid or semifluid state at the time of deposition.

TABLE 16.—X-RAY-DIFFRACTION MEASUREMENTS OF SPHALERITE

| Sphalerite Temple Mountain* | | Sphalerite A.S.T.M. index card 5-0566 | |
|---|---|---|---|
| d(Å) | I | d(Å) | I |
| 3.343q | 2 | | |
| 3.124p | 10 | 3.123 | 100 |
| 2.708p | 3 | 2.705 | 10 |
| 2.415p | 1 | | |
| 2.209p | 1 | | |
| 1.911 | 8 | 1.912 | 51 |
| 1.629p | 5 | 1.633 | 30 |
| 1.559 | 1 | 1.561 | 2 |
| 1.443p | ½ | | |
| 1.348 | ½ | 1.351 | 6 |
| 1.241 | 1 | 1.240 | 9 |
| | | 1.209 | 2 |
| 1.1040 | 1 | 1.1034 | 9 |
| 1.0412 | 1 | 1.0403 | 5 |
| 0.9567 | ½ | 0.9557 | 3 |
| 0.9139 | ½ | 0.9138 | 3 |

* X-ray powder film, Cu/Ni. Contaminants are q = quartz, p = pyrite.

### *Vanadium Minerals*

The source of secondary vanadium minerals appears to be in part from montroseite, which has been identified by Weeks, Cisney, and Sherwood (1953) from the Rex No. 2 mine and from Calyx Hole mine No. 8 (Table 15). At the latter locality, it occurs mixed with the urano-organic ore. Separation of the heavy-mineral fraction and subsequent purification with the Frantz Isodynamic Separator yields material satisfactory for identification. Examination of the heavy minerals separated from the ore at other Calyx-South Workings localities may reveal that montroseite is more common than is here noted.

"Montroseite is the least oxidized vanadium mineral thus far found in the Colorado Plateau uranium-vanadium ores, and it is thought to be a primary mineral" (Weeks, Cisney, and Sherwood, 1953, p. 1241). Garrels (1953) considers $V_2O_3$ (or its hydrate) the lowest-valent vanadium oxide expected. It should occur under reducing conditions common in nature and oxidize to the next-higher-valent vanadium oxide at about the same potential necessary to convert sulfide ion to sulfate. It would be represented in the "... original montroseite-pyrite-pitchblende type of ore" (Garrels, 1953, p. 1265).

### *Zinc Minerals*

Kerr and Lapham (1954) found sphalerite in an arsenic-bearing nodule, disseminated in quartz and pyrite (Fig. 18). It forms small crystals and irregularly shaped particles scattered through the ore. Ore containing relatively abundant sphalerite particles contains Zn in concentration on the order of x. per cent. Rarely, stringers of sphalerite cut pyrite that has replaced rims of silicified logs. In a few cases, sufficient material can be isolated from these occurrences for X-ray diffraction (Table 16). Optical, etch (Short, 1940), and microhardness properties are similar to disseminated particles of sphalerite found in the ore (Pl. 3, fig. 6). Zinc is concentrated on the order of xx. per cent. Determinations of the lattice constants are approximate because of quartz and pyrite lines in the patterns. However, on the basis of one X-ray pattern, the (hkl) spacing (531) gives $a_0$ 5.407 Å.

Attempts at separation and purification of the small quantities of sphalerite were abandoned because of the fine size, sporadic distribution, and, in many samples, mixture with fine particles of quartz and pyrite. Sufficient material was not found for flotation and froth separations. Thus sphalerite has not been used as a geological thermometer (Kullerud, 1953). The FeS content on the basis of the lattice constant given above would be on the order of 25 per cent. This would yield an anomalous temperature.

Sphalerite reported in the presence of excess iron sulfide (pyrite) at the Happy Jack mine in White Canyon, Utah, and the Hidden Splendor mine (Delta mine) in the San Rafael Swell results in temperature determinations of less than 138° C. (Coleman, 1957).

Recently, some doubt has been expressed concerning the accuracy of the Kullerud

method, and the question of the effect of water and other components on the FeS-ZnS system is discussed in the literature (Fryklund and Fletcher, 1956; Kullerud, 1956). Even if purification of the Temple Mountain sphalerite is possible, it is doubtful that the resulting determination of FeS content and temperature would be reliable. Pyrite is the only mineral on which the presumption may be made that FeS saturation existed during deposition of the sphalerite. Whether pyrite is as reliable an indicator as pyrrhotite has not been established, although it is being used on the Colorado Plateau (Coleman, 1957). The pyrite at Temple Mountain occurs in several generations and probably cannot be used.

TABLE 17.—HEAVY METALLIC MINERALS SEPARATED FROM SELECTED ORE ZONES

Particle size was between 60–120 mesh. Separation was by tetrabromethane settling and Frantz Isodynamic Separator. Identification was by X-ray diffraction.

| Locality | Metallic minerals | Metallic-element concentration of separations (average)* | | |
|---|---|---|---|---|
| | | xx. | x. | .x |
| Collapse (DDH V-5; 777 feet) | Arsenic†, marcasite†, pyrite†, unknown | Fe | As | Cu, Mn, Sr, Zn |
| Collapse border (Camp Bird Mine No. 7) | Arsenic†, (realgar)†, pyrite†, sphalerite-uraninite, unknowns | As, Fe | Zn, V | Cr, Mn, Ni, U |
| Calyx Mine area (Calyx Mine No. 8) | Montroseite†, pyrite†, sphalerite-uraninite | V, Fe | | As, Cu, Mn, Ni, U, Zn |
| Flat Top Mesa (north end) | Arsenic, pyrite, sphalerite-uraninite, unknowns | Fe | As | Cu, Mn, Ni, U, V, Zn |

* Metallic-element concentration was by X-ray spectrograph.
† Most abundant.

### *Distribution of Metallic Minerals*

Arsenic, uraninite, sphalerite, and montroseite occur in and near urano-organic ore masses. Arsenic occurs in cores at depth as indicated by arsenic sulfides assumed to represent oxidation of the native metal. A common origin is indicated for As, Zn, V, and U, and an affinity for the organic material in representative metallic minerals is found.

Pyrite and marcasite may occur independently or associated with the ore. Various methods of deposition explain pyrite distribution. Most marcasite not associated with ore occurs near or within the collapse, particularly at depth. It does not appear to be influenced in deposition by organic material.

Galena from the upper part of the Coconino has been obtained in drill cores in the collapse. It may be present locally in minor amounts in the ore horizon. Deposition probably occurred accompanying the introduction of the other metallic elements.

ZONING: Ores with a relatively high concentration of metallic elements generally exhibit metal-bearing minerals. Lateral zoning by metallic elements is reflected in the mineral content of the ore (Table 17). Vanadium, which increases in the ore away from the collapse, yields occurrences of montroseite in the Calyx area. Uraninite and sphalerite are widely distributed in the ore, both near and away from the collapse. The increase in uranium and zinc in the ore away from the collapse reflects the concentration of the urano-organic material in the calyx area (Fig. 6). Arsenic, which increases in concentration in the ore toward the collapse, appears as native arsenic. No primary minerals of cobalt and selenium have been identified.

Data are inadequate to establish vertical zoning. Galena is found at depth in the collapse, whereas native arsenic, marcasite, and pyrite occur with mineralized organic material from the Kaibab or equivalent depth. The three are also present in the ore horizon.

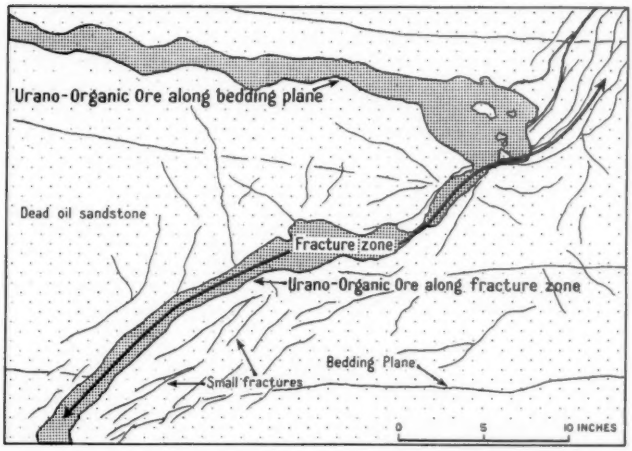


FIGURE 14.—URANO-ORGANIC ORE ALONG BEDDING AND FRACTURE

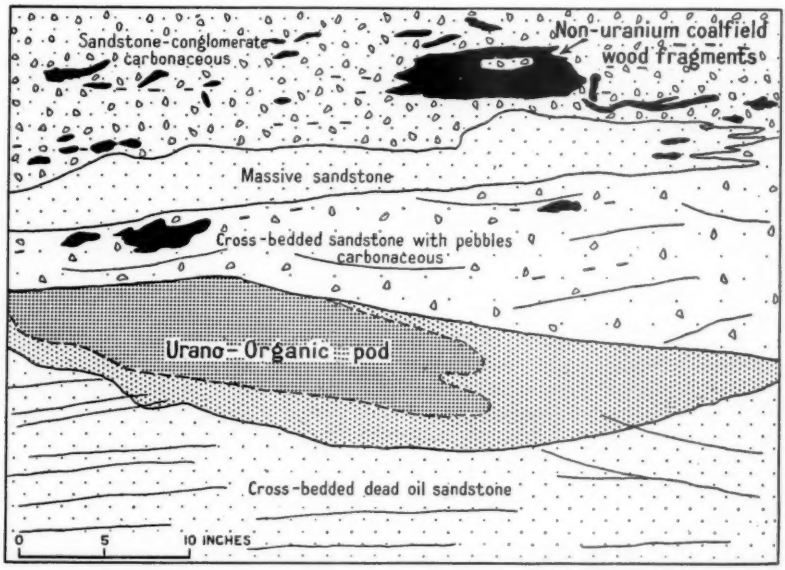


FIGURE 15.—URANO-ORGANIC ORE POD ALONG LITHOLOGIC CONTACT

## ORE AGGREGATES

### *General Statement*

The urano-organic materials occur as interstitial disseminations, pisolites, masses, streaks, and bands. Distribution occurs along bedding planes, lithologic contacts, in porous beds, on fractures, and along faults (Figs. 14–16). The greatest concentrations occur in permeable horizons and along lithologic contacts.

Two common ore forms occur in about equal abundance. The first consists of irregularly shaped masses which range from disseminated particles 0.2 mm thick to replacement masses several feet across. Ore also occurs in pisolites that are elliptical to spherical and range from minute spherules a millimeter in diameter to pods more than a foot across.

Pisolitic forms identical to those of the San Rafael Swell are found at Elk Ridge, Utah, in urano-organic materials (Kelley, D. R., Oertell, E., and Wichtner, J., 1953, unpub. U.S.A.E.C. Project Rept.), and Erickson, Myers, and Horr (1954) mention solid "asphaltite pellets", containing as much as 1.6 per cent uranium, found by the U. S. Geological Survey in well cuttings from the Panhandle gas field near Amarillo, Texas. The writers recognize the following sequence in the development of large ore masses.

(1) Initial replacement occurs at the expense of the interstitial clay cement and extends to detrital grains. The mineralization develops principally parallel to bedding along more permeable zones, or secondarily along fracture or fault trends. It forms with relatively sharp as well as irregular external boundaries. In the initial replacement, either small pellets less than a few millimeters in diameter form with sharp boundaries (Fig. 17, *A*) or irregular interstitial streaks and disseminations form irregular boundaries (Fig. 17, *B*).

(2) Further replacement occurs at the expense of the detrital grains. During this stage, the smaller pellets and interstitial streaks coalesce to form pellet groups or larger single pellets and larger streaks or irregular patches of up to 2 cm in diameter. The outlines of the forms of the first stage are generally preserved (Fig. 17, *D*).

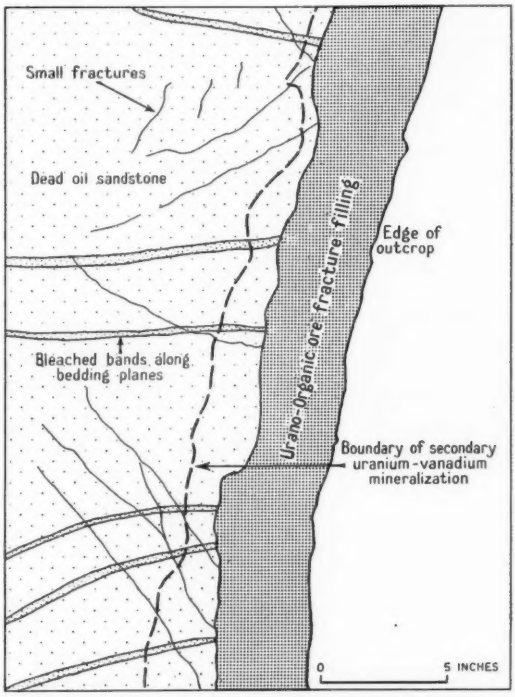


FIGURE 16.—URANO-ORGANIC ORE ALONG FRACTURE
Lower Wingate, South Temple Mountain

(3) A final stage is represented by large pellets, pods, patches, and streaks of more than a few centimeters in diameter, in which the detrital grains consist of a few scattered, corroded remnants. The outline of the smaller forms may be preserved by stringers of carbonate or clay that fill contraction fractures developed around the relict boundaries (Fig. 17, *E*). However, a massive body of urano-organic material generally results (Fig. 17, *F*).

Concentric development of pisolites is common. Massive and crystalline pyrite and, to a lesser extent, clay may form the nucleus of a nodule (Fig. 18, *B*, *E*). Subsequent alteration during the last stages of hydrothermal activity may convert the sulfide to the sulfate, jarosite (Fig. 18, *F*). The clay and pyrite cores are slowly replaced as the organic material accumulates. Nodules may be composed of one type of organic material (Fig. 18, *A*),

or they may show concentric bands of slightly different organic materials, in part translucent, in part opaque (Fig. 18, *B*). Concentric banding is seen in some larger disseminated ore masses.

Nodules composed of metallic minerals in which the ore is either absent or constitutes a minor portion are much less common. Pyrite nodules in which organic material and other

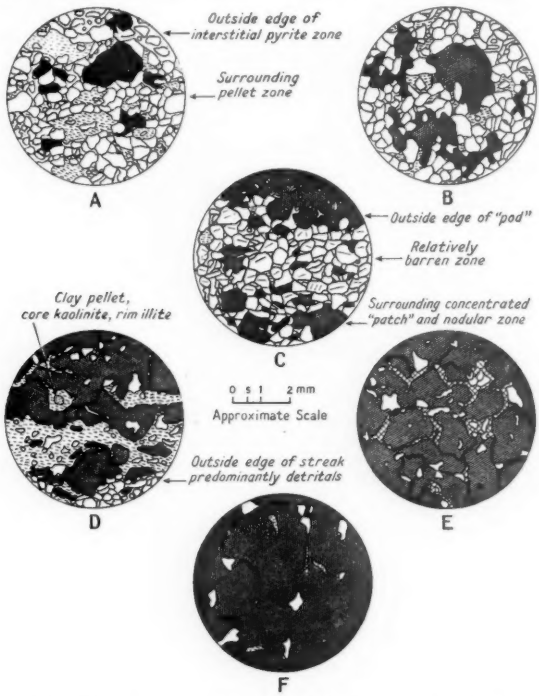


FIGURE 17.—DIAGRAMMATIC DEVELOPMENT OF MASSES OF URANO-ORGANIC MATERIAL
Moss Back Sandstone of Temple Mountain

A. Zone of scattered nodules of urano-organic material surrounding a large interstitial pyrite saturated body. Cement is dominantly intermixed kaolinite and illite.

B. Irregular interstitial patches of urano-organic material replacing clay cement

C. Border of large urano-organic pod showing narrow barren zone separating the edge of pod made up of coalescing nodules and the surrounding thin zone of patches and nodules of organic material

D. Coalescing of urano-organic patches and a few nodules to form streaks of ore along bedding planes. Ore associated with strong illitization.

E. Almost complete coalescing of patches and nodules to form masses of urano-organic material. Thin stringers of carbonate outline and in a few places penetrate small bodies of ore.

F. Massive ore with remnants of detrital grains and thin stringers of clay

No attempt was made to represent minute amounts of metallic minerals. Urano-organic material is dark stippling. Pyrite is lighter stippling. Clays are dashed (dominantly illite). Carbonates are cross-hatched. Detrital grains are outlined.

The ore mass may be surrounded by accretions of pisolitic or irregular forms, or a single zone of isolated pellets, or small interstitial streaks or patches. In some cases, a relatively barren zone of a few millimeters may separate the pod from the surrounding aggregate pellet zone (Fig. 17, *C*). In a few cases a partially spherical zone of scattered pellets and patches may be surrounded by a zone of interstitial pyrite (Fig. 17, *A*).

metallic minerals are absent are scattered throughout the district. Other metallic nodules in which the ore occurs as scattered inclusions and in a few places as rims are the least common and seem to be restricted to the collapse and immediate surroundings (Fig. 18, *D*, *E*, *H*, *I*). Cyclic deposition, as indicated by repetition of concentric mineral bands, is shown in the arsenic-bearing nodule described by Kerr and Lapham (1954) (Fig. 18, *G*), in which two

generations of pyrite-sphalerite occur, and by the alteration of pyrite and marcasite in nodule 4 (Fig. 18). The concentric banding and cyclic deposition reflect local changes in the intensity, any theory of detrital origin. In general, the presence of pyrite, clay, or silica core, particularly in the larger forms, and the spherical shape suggest the necessity of a nucleus for the

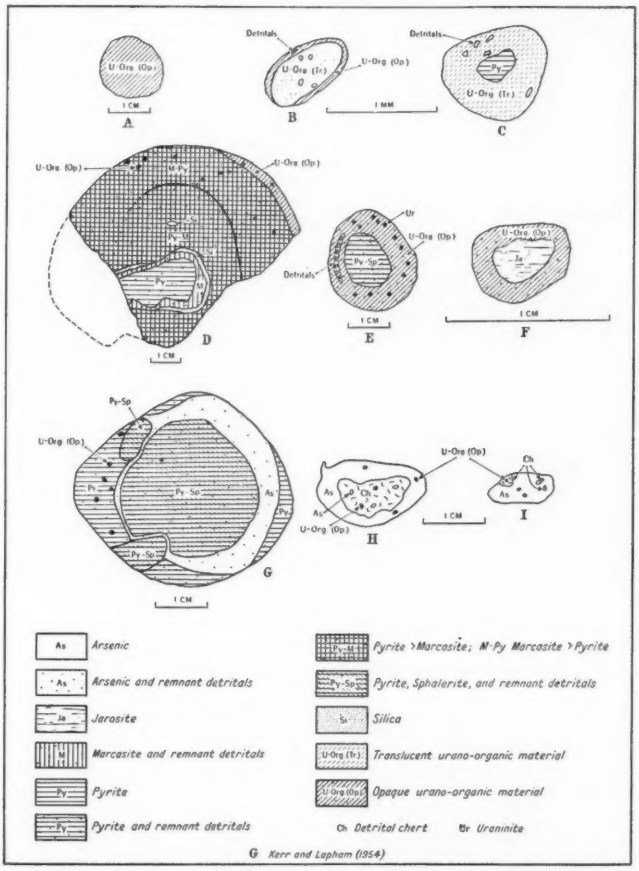


FIGURE 18.—SOME ORE-BEARING NODULES
Temple Mountain, Utah

composition, and quantity of the hydrothermal solutions. Urano-organic materials, and rarely uraninite, as disseminated inclusions and rims, appear to be restricted to the outer portion of nodules containing iron- and zinc sulfide (Fig. 18, *D*, *E*, *G*), but in a few cases are found as inclusions throughout nearly pure arsenic nodules (Fig. 18, *H*, *I*).

The pisolitic forms at Temple Mountain contain remnant sedimentary quartz grains, which are indicative of replacement. This texture, together with the mechanism of development of large masses of ore, eliminates precipitation and localization of some of the ore and associated metallic minerals.

Refluxing Temple Mountain semifluid tar in water shows that the tar may be circulated in solution as irregular spherical masses. These flocculate to form larger spherical masses, which in turn redisperse to smaller bodies during agitation of the solution. The margins of semifluid petroleum-impregnated sandstones contain irregular spherical bodies of viscous oil (Pl. 1, fig. 1). Similarly, the margins of massive ore patches contain pisolitic forms (Pl. 1, fig. 2). Upon emplacement or flocculation

of the emulsoid, the greater surface tension of the more viscous substance results in spherical forms similar to those produced from colloidal suspensions (Bastin, 1950). The contraction cracks developed during the shrinkage of colloidal material after deposition are similar to those produced during syneresis from the loss, or reorganization, of organic components upon induration and polymerization of a petroliferous material. Thus the texture of the urano-organic ore is indicative of semifluid or fluid material and reflects the probable petroliferous origin of the ore.

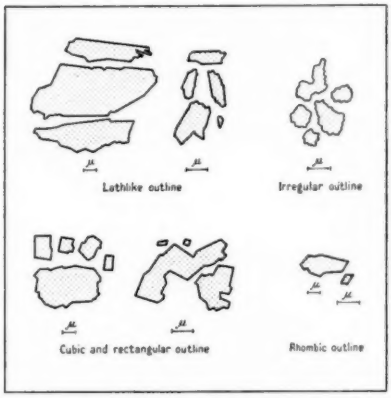


FIGURE 19.—COMPOSITE ELECTRON MICROGRAPHS OF URANO-ORGANIC ORE
Lower Wingate, South Temple Mountain

The spherical forms of the metallic nodules, however, are indicative of replacement and deposition about a nucleus rather than deposition of a colloid. No contraction fractures have been observed in these nodules.

### *Included Metallic Minerals*

Pods of irregularly disseminated pyrite are found up to 10 inches in diameter. However, electron photomicrographs show submicroscopic particles ranging in size from less than a micron to more than 10 microns in diameter. Most of these particles are irregularly shaped (Fig. 19; Pl. 4) and represent organic material, aggregate crystallites of pitchblende (Sciacca, 1954), or other mineral inclusions. Lathlike, cubic, rectangular, or rhombic outlines indicate fine crystals. Some correspond in shape to synthetic pitchblende, others to pyrite, clay, and carbonates.

With the exception of pyrite and the metallic nodules, the metallic minerals are generally submicroscopic or microscopic. Where microscopically visible, they range from minute irregular particles to crystals and are scattered at random, clustered, or occur as irregular concentrations in a matrix of urano-organic material (Pl. 3, fig. 5). Radioactivity intensity, as revealed by autoradiographs of polished surfaces, is irregularly distributed throughout the ore. However, in many cases the radioactivity is not correlative with microscopically visible particles.

Where two types of urano-organic material can be distinguished on a polished surface, a preferential orientation is noted in a few cases for the contaminant inclusions. The clear light-gray ore contains no microscopically

PLATE 3.—PHOTOMICROGRAPHS: SOME MINERALS ASSOCIATED WITH THE ORGANIC MATERIALS

FIGURE 1. Asphalt filling fracture in goethite vein penetrating lower Wingate Sandstone. Massive secondary goethite (g) lies along the fracture wall; massive asphalt (a) fills the center of the fracture. Magnesite and minor calcite (m) fill shrinkage cracks in and around the asphalt. Thin section, using both transmitted and reflected light. Adjacent to collapse area.

FIGURE 2. Partially spherical mass of pyrite in vitrain. Pyrite (black) crystallizing in fragment of vitrain causes distortion of the woody texture. From the Moss Back Sandstone of the calyx area. Thin section.

FIGURE 3. Arsenic and orpiment in turbid urano-organic ore. Small crystals of native arsenic (As) are grouped near the edge of urano-organic ore mass (Uo). Secondary massive orpiment (Or) is interstitial to the corroded detrital quartz fragments (shown as variable gray). From the Moss Back Sandstone bordering the collapse area. Polished surface.

FIGURE 4. Arsenic and orpiment in turbid urano-organic ore. Euhedral and subhedral native arsenic crystals (As) being oxidized to orpiment (Or) in massive urano-organic ore (Uo). From the Moss Back Sandstone bordering the collapse area. Polished surface.

FIGURE 5. Turbid urano-organic ore under high magnification. Minute contaminant mineral particles scattered in massive urano-organic ore cause the turbidity. From the Moss Back Sandstone of the calyx area. Polished surface.

FIGURE 6. Pyrite and sphalerite in the urano-organic ore. Small subhedral particles of pyrite (Py) and sphalerite (Sp) with remnant corroded quartz fragments (dark gray) in massive urano-organic ore (Uo). From the Moss Back Sandstone of the calyx area. Polished surface.

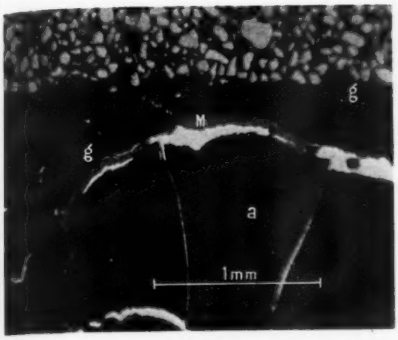


FIGURE 1

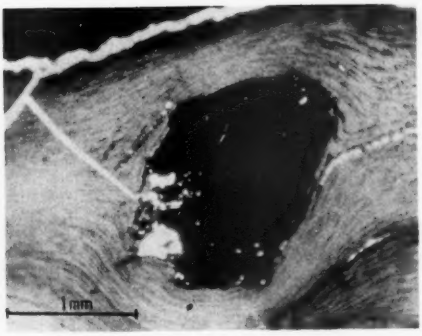


FIGURE 2

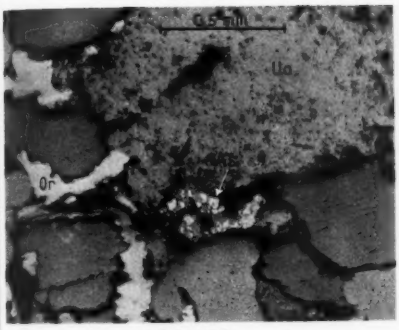


FIGURE 3

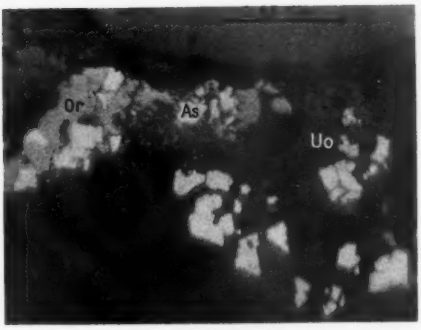


FIGURE 4

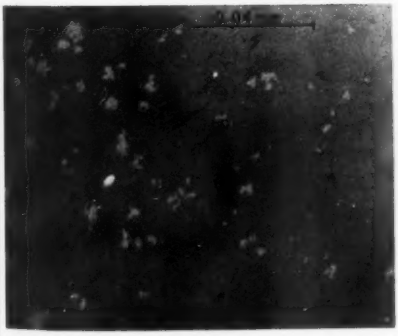

FIGURE 5

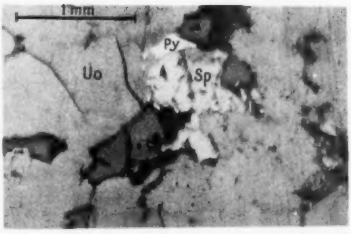


FIGURE 6

PHOTOMICROGRAPHS: SOME MINERALS ASSOCIATED WITH THE ORGANIC MATERIALS

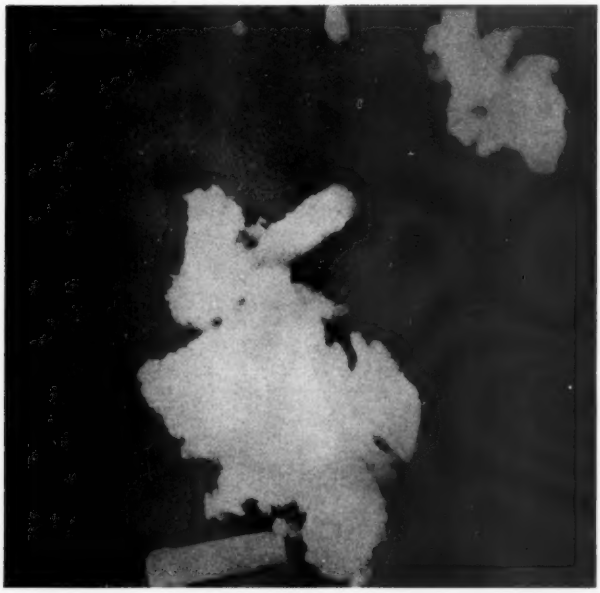

FIGURE 1

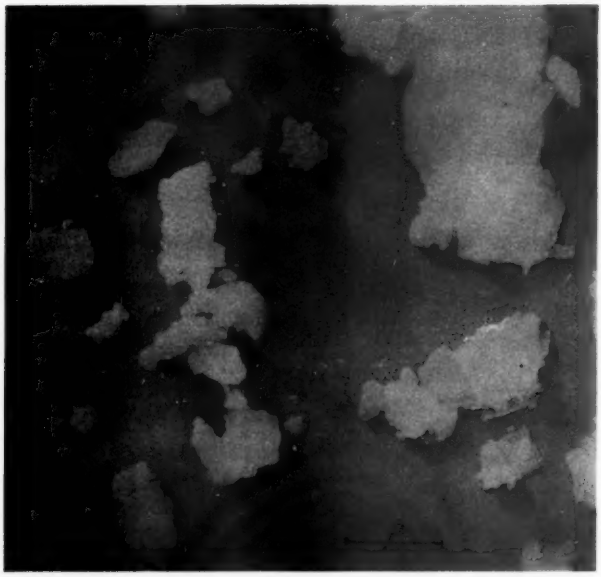

FIGURE 2

ELECTRON PHOTOMICROGRAPHS OF URANO-ORGANIC ORE
(PALLADIUM SHADOWED AT AN ANGLE OF 30°)

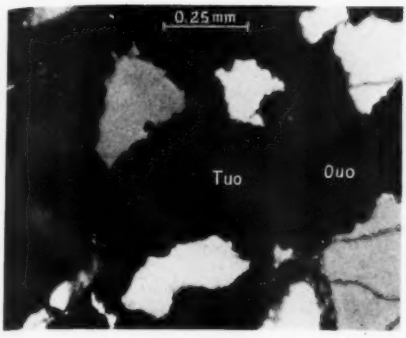


FIGURE 1

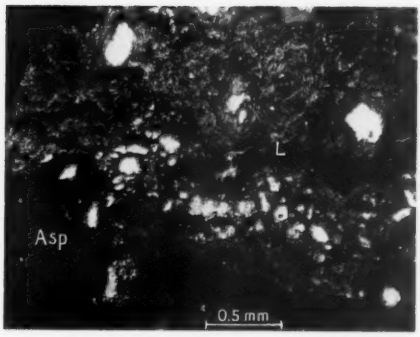


FIGURE 2

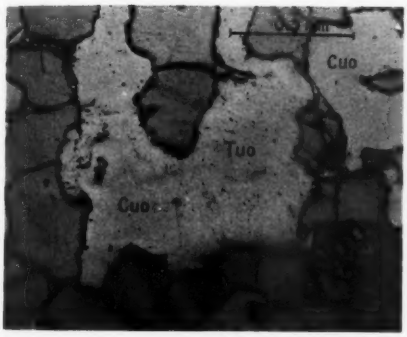


FIGURE 3

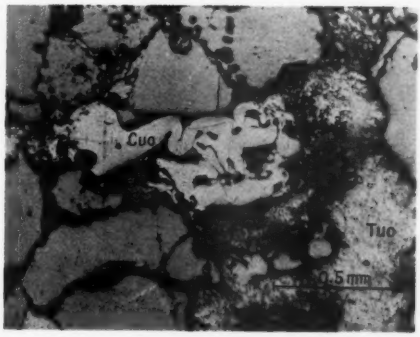


FIGURE 4

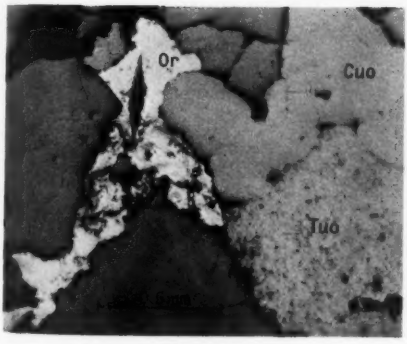


FIGURE 5

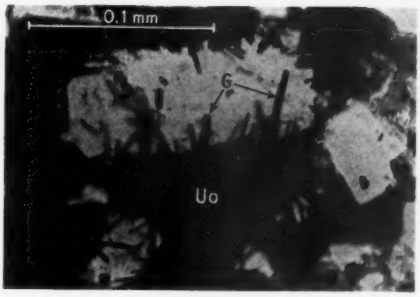


FIGURE 6

PHOTOMICROGRAPHS: URANO-ORGANIC ORE

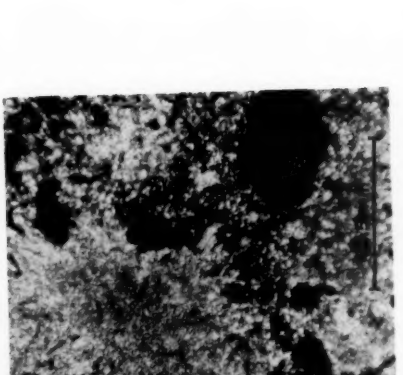

FIGURE 2

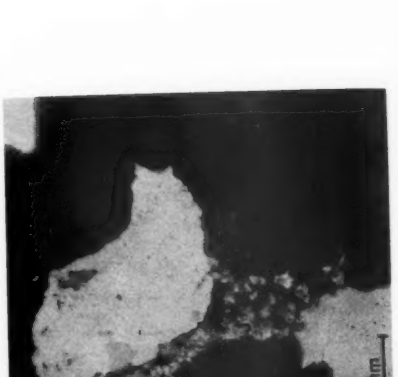


FIGURE 4

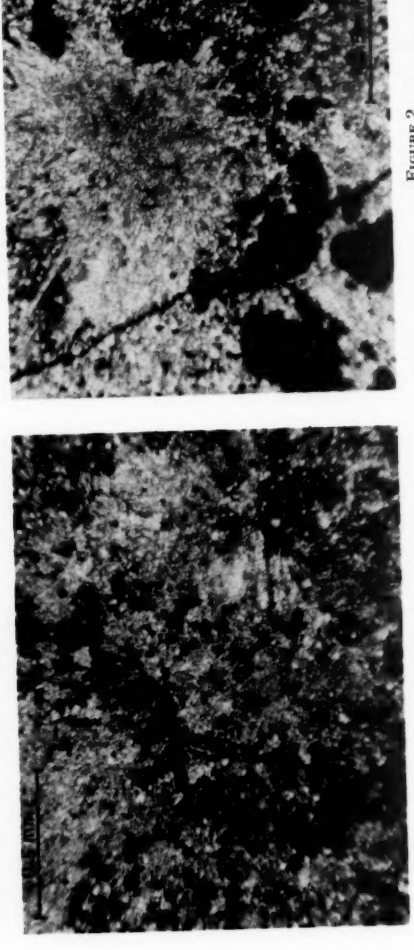

FIGURE 1

FIGURE 3

PHOTOMICROGRAPHS: SILICIFICATION AND JAROSITE

visible contaminants and in many cases is located interstitial to patches of remnant detrital grains (Pl. 5, figs. 3, 4, 5). The turbidity of the darker-gray ore, which generally makes up the mass of urano-organic material, is caused by minute contaminants (Pl. 3, fig. 5).

The irregular distribution would be unlikely to result before the emplacement of the organic material while it was fluid; otherwise, an alignment of particles should be noticed. Therefore, the crystallite particles apparently formed during or after emplacement.

On polished surfaces, in some cases particles of pyrite and carbonate are arranged in cubic and rhombic patterns. These relict outlines, plus the presence of corroded quartz fragments, plus inclusions of other sedimentary minerals as well as alteration minerals, indicate replacement of these contaminants during emplacement of the organic material.

Some minute particles of arsenic, sphalerite, and uraninite, which are essentially restricted in occurrence to masses of ore, show crystal form, which suggests direct crystallization. The distribution through the ore, rather than along the periphery, suggests two possibilities: (1) that the particles formed from the organic material during emplacement or induration, or (2) they were precipitated from the ore solutions by the organic material during emplacement but before induration.

The occurrence of small amounts of sphalerite and uraninite throughout most of the ore indicates that the Zn and U content of the ores is not wholly represented by metallo-organic complexes. Considering that the contaminant particles are submicroscopic as well as microscopic, possibly little of either Zn or U may be present as a metallo-organic compound. Fine grinding of the ore "... indicates that most of the uranium is not now chemically associated with the organic matter" (Breger and Deul, 1955). Whether the elements As, Co, Se, and V are tied up as discrete mineral particles or metallo-organic complexes is less certain. The metallic minerals of these elements are not universally found through the ore.

### *Other Ore Textures*

There is a strong corrosion of the sedimentary and alteration minerals by the organic ore—considerably more corrosion than occurs with either pyrite or the carbonates. The non-uranium-bearing organic materials of either petroliferous or carbonaceous origin show no corrosive effect on the sediments. The corrosive properties of the ore are, therefore,

PLATE 5.—PHOTOMICROGRAPHS: URANO-ORGANIC ORE

FIGURE 1. Translucent and opaque urano-organic ore. Patches of variably translucent ore (Tuo) in opaque ore (Ouo) are not sharply outlined. From the Moss Back Sandstone of the calyx area. Thin section. The translucency is caused by intimate mixture of the ore with particles of other minerals.

FIGURE 2. Diffusion, band of low-grade urano-organic ore. A diffusion band (L) of low-grade urano-organic material in mineralized asphaltic (Asp) impregnated Moss Back Siltstone from the calyx area. Thin section.

FIGURE 3. Interstitial turbid urano-organic ore (Tuo) and clear urano-organic ore (Cuo) in the Moss Back Sandstone from the calyx area. Polished surface.

FIGURE 4. Vermicular patch of clear urano-organic ore (Cuo) in interstitial mass of turbid urano-organic ore (Tuo) in the Moss Back Sandstone of the calyx area. Polished surface.

FIGURE 5. Orpiment associated with clear and turbid ore. Interstitial patch of orpiment (Or) along the edge of mass of clear (Cuo) and turbid (Tuo) urano-organic ore. Knoop microhardness indentation can be noticed in the orpiment. From the Moss Back Sandstone bordering the collapse. Polished surface.

FIGURE 6. Goethite associated with urano-organic ore. Minute needles of goethite (G) are shown penetrating corroded quartz grains from interstitial masses of urano-organic ore (Uo). From the Moss Back Sandstone of the calyx area. Thin section.

PLATE 6.—PHOTOMICROGRAPHS: SILICIFICATION AND JAROSITE

FIGURE 1. Chalcedony along the basal Moss Back contact. An aggregate of chalcedony contains disseminated particles and streaks of urano-organic ore (black). From the calyx area. Thin section, crossed nicols.

FIGURE 2. Chalcedony spherule. A chalcedony spherule (Cs) in aggregate chalcedony along the basal Moss Back contact. Irregular masses of ore (black) are scattered through the silicified zone. From the calyx area. Thin section, crossed nicols.

FIGURE 3. Chalcedony from the collapse area. A chalcedony band (Ch) associated with pyrite (Py) has developed in the argillized breccia zone in the collapse. From a core fragment. Thin section, crossed nicols.

FIGURE 4. An aggregate of jarosite. Jarosite (J) is peripheral to interstitial urano-organic ore masses (black) in the Moss Back Sandstone bordering the collapse. Thin section, crossed nicols.

attributed to the metallic components of the ore, or, more likely, their associated solutions. Consequently, emplacement of the ore must have occurred during the time the organic material was in association with the metallic components or with the ore solution.

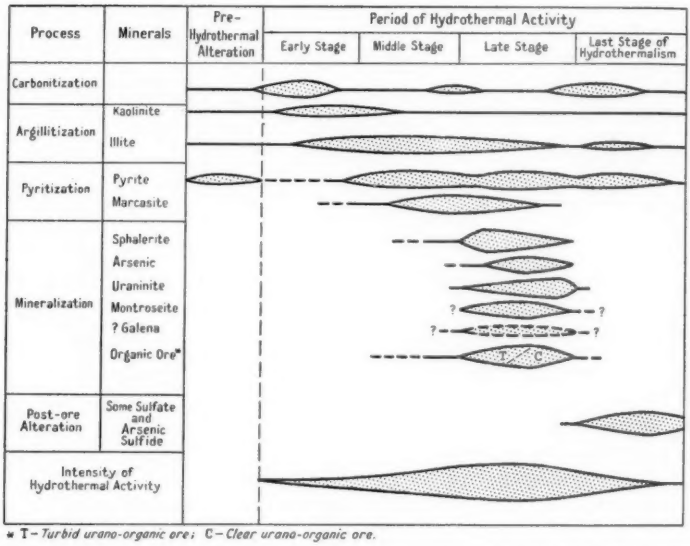


* T—*Turbid urano-organic ore*; C—*Clear urano-organic ore.*

FIGURE 20.—PARAGENESIS OF ALTERATION AND MINERALIZATION OF THE MOSS BACK SANDSTONE

There is evidence that local distribution of the ore was influenced by tectonic preparation of the sediments. Detrital grains are minutely fractured in many specimens (Fig. 17, *C*). These fractures may be aligned, and a few are filled with alteration clay minerals. Such fractures do not extend into patches of ore or correspond to syneresis fractures. Many of the masses of urano-organic material are irregularly elongated parallel to these fractures.

Thin rings of low-grade urano-organic material, similar in form to Liesegang rings, indicate some diffusion of aqueous-organic solutions and further illustrate the original fluid nature of the organic ore (Pl. 5, fig. 2).

### *Mineral Sequence*

Figure 20 is a diagrammatic representation of the paragenesis of the various minerals deposited during hydrothermal alteration and mineralization of the Moss Back ore horizon at the Temple Mountain uranium mining district. The time relationships between the metallic minerals are tentative, and differences are slight. Galena present at depth is included as a product of hydrothermal mineralization.

The individual replacement sequences represent surges rather than a clean-cut progression of minerals ending in the emplacement of the ore. Repetition of certain minerals occurs with maximum periods of emplacement at particular times. The emplacement of uranium apparently culminated in a single epoch of mineralization. An early stage was dominated by argillization and minor carbonitization, a middle stage by pyritization, and a final stage by the emplacement of the urano-organic materials and associated metallic elements. The earlier stages were not completed when the emplacement of the ore occurred.

## ALTERATION ASSOCIATED WITH MINERALIZATION

### *Hypogene Alteration*

Although more detailed study of the alteration is in progress (Bodine, 1956) a summary of alteration features is included here to complete the discussion of mineralization.

Three major alteration effects have been recognized at Temple Mountain (Kerr, Bodine, Kelley, and Keys, 1956; Bodine, 1956):

(1) The early argillization of upper Moenkopi and lower Chinle near the collapse and of lower

Chinle near ore deposits removed from the collapse

(2) A later carbonate stage involving emplacement of dolomite with some calcite at the expense of detrital silicates of upper Chinle and Wingate near the collapse

(3) The final stage of siderite and hematite formation in upper Chinle and Wingate near the collapse

The distribution of the three alteration effects may be outlined as in Figure 21.

The writers believe that removal of carbonate and iron from Kaibab and Moenkopi sediments at depth occurred as a result of ascending mineralizing solutions acidic in nature. Concentration of the carbonate ion increased as the solutions moved upward through carbonate-

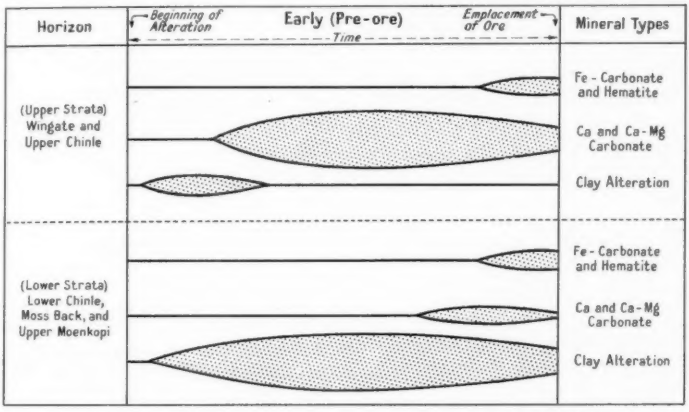


FIGURE 21.—PRE-ORE ALTERATION IN UPPER AND LOWER STRATA

In general, this sequence applies to individual stratigraphic units, yet the three stages occurred essentially contemporaneously, because of significant changes in the ascending hydrothermal solutions and original differences of lithic composition of the various strata. This is shown by the following:

(1) Field examination of the Moss Back Sandstone indicates that clay alteration continued up to the time of maximum ore emplacement.

(2) Most of the clay-forming elements were derived from the sediments being altered.

(3) Where clay minerals formed, carbonitization is negligible.

(4) Carbonitization occurs in upper Chinle and Wingate, where argillization is a minor feature.

(5) Adequate feldspars and sedimentary clay minerals occur in the lower Chinle, Moss Back, and upper Moenkopi and yield alteration clays.

(6) Clay-forming elements are less concentrated in the massive sandstones of the Wingate and upper Chinle.

(7) Argillization was facilitated in the lower horizons and hindered in the upper horizons (5 and 6) by the presence or absence of clay-forming elements.

(8) Solution of carbonates in lower horizons and deposition of carbonates in upper horizons reflect a vertical change in the character of the solutions.

bearing Moenkopi. As a result, acidity decreased. Neutralization was possibly aided by reaction with the alkali elements in dominantly argillaceous strata. Deposition and reconstitution of clays occurred through upper Moenkopi and lower Chinle; the solutions became essentially neutral in the lower Chinle. The pH continued to rise with further removal of carbonate and reaction with alkalies in the Chinle sediments. Concurrently, deposition of masses of Ca, Ca-Mg, and Fe carbonate occurred at the expense of upper Chinle and Wingate sediments. The silica of the sediments, removed by this replacement, remained in solution and was carried away, except for minor amounts resulting from replacement of the Moss Back Sandstone, which was precipitated near the base.

ALTERATION OF THE MOSS BACK ORE HORIZON: Argillic alteration occurs in the interstices between grains in the Moss Back Sandstone (Kelley and Kerr, 1957). Near collapse features and close to ore zones, kaolinite and mica clay (illite) become more abundant. Mixtures of 1M and $2M_1$ mica polymorphs are typical. The $2M_1$ mica polymorph becomes a more abundant constituent of the mixtures, and aggregate birefringence and particle size appear to increase. Near collapse areas, micro-

TABLE 18.—METALLIC-ELEMENT DISTRIBUTION IN ARGILLIC ALTERATION ASSOCIATED WITH URANO-ORGANIC MATERIALS

(In per cent on basis of X-ray spectrographic data)

A. Moss Back Sandstone east side of Temple Mountain collapse

| | Wall rock Sandstone | Fault Silty mudstone | Fault Urano-organic ore |
|---|---|---|---|
| $U_3O_8$ | | | 1.8 |
| Co | — | — | .x |
| Ni | — | — | x. |
| Mn | — | —.x | —.x |
| Se | — | — | x. |
| As | — | .x | x. |
| V | —.x | .x | —.x |
| Cr | .x | —.x | .x |
| Zn | —.x | — | — |
| Fe | .x | x. | .x |

B. Lopez Incline, South Workings, Calyx Mine area

| | Fault Altered sand-stone | Fault Urano-organic ore | Wall rock* Altered sand-stone | Wall rock Urano-organic ore |
|---|---|---|---|---|
| $U_3O_8$ | 0.37 | 4.19 | | 2.48 |
| Co | — | — | — | .x |
| Ni | — | — | — | —.x |
| Mn | — | — | — | —.x |
| Se | — | — | — | — |
| As | — | —.x | —.x | — |
| V | .x | — | — | — |
| Cr | .x | .x | .x | .x |
| Zn | — | — | — | .x |
| Fe | .x | .x | .x | .x |

* Contains chromium mica clay

vermicular aggregate growths of kaolinite become common. In unaltered and nonore-bearing sediments, the $2M_1$ mica-clay polymorph has not been observed, and $2M_1$ detrital muscovite flakes found along bedding appear to be breaking down to a 1M structure. The mica clay at Temple Mountain, which contains the $2M_1$ polymorph, is believed to have been deposited by hydrothermal solutions accompanying urano-organic ore deposition, on the basis of the hydrothermal synthesis of mica polymorphs by Yoder and Eugster (1955). The transition of 1M to $2M_1$ mica polymorphs appears to occur between 200° C. and 350° C. at 15,000 p.s.i. water pressure. The source of the clay-forming elements is probably not only the original interstitial material but also includes detrital feldspar replaced during the development of ore masses.

Increased crystallinity of clays in nonore-bearing lower Chinle toward the collapse areas appears to be associated with an increase in iron, as shown by the X-ray spectrograph. Argillic alteration associated with ore in the Moss Back Sandstone may show a concentration of metallic elements locally characteristic of urano-organic ore (Table 18). The concentration may be attributed to either of two processes:

(1) Leaching of the ore and metallic elements subsequent to deposition of both the ore and clays.
(2) "Absorption" of the metallic elements by the clays and precipitation accompanying the deposition during hydrothermal mineralization.

Both leaching and absorption with precipitation may have been active in the Temple Mountain mining district. In some localities, the presence of sulfates intermixed with the clays, sulfate replacement of pyrite, and physical characteristics of the ore indicate that leaching was responsible for the concentration of ore elements in the clays (Table 18, *A*). However, in other localities there is no direct evidence of significant leaching of the ore and associated metallic elements (Table 18, *B*).

SILICATE REPLACEMENT: Silicification of logs is a common feature in the Chinle of the Colorado Plateau. However, this silicification occurred before the alteration accompanying mineralization of the Moss Back Sandstone. Silicification of the Moss Back Sandstone along the contact with the underlying Monitor Butte Member of the Chinle and within this member also occurs at a number of localities on the San Rafael Swell.

At Temple Mountain, silicification along the lower contact of the Moss Back has been observed at the Vanadium King claims, Calyx Hole Mine No. 3, and near North Mesa No. 9. It probably occurs in other places not noted. The silica occurs as chalcedony and forms veinlets and nodular masses associated with concentration of urano-organic materials. Urano-organic materials are found as irregular disseminations, nodular patches, and concentrations in poorly defined and noncontinuous bands in the chalcedony (Pl. 6, figs. 1, 2). Most of the ore is later than the chalcedony, but it may be in part contemporaneous. The

TABLE 19.—MINERALS OF THE TEMPLE MOUNTAIN URANIUM AREA

Unless otherwise indicated the minerals have been identified in this study.

HYPOGENE MINERALIZATION

| Metallic mineralization | | Alteration | |
|---|---|---|---|
| Urano-organic material | Uranium hydrocarbon | Kaolinite | $Al_2O_3 \cdot 2SiO_2 \cdot 2H_2O$ |
| Uraninite | $UO_2$ | Illite | |
| Pyrite | $FeS_2$ | Chrome-bearing mica clay | |
| Marcasite | $FeS_2$ | Calcite | $CaCO_3$ |
| Sphalerite | ZnS | Dolomite | $CaMg(CO_3)_2$ |
| Native arsenic | As | Siderite | $FeCO_3$ |
| (?) Arsenopyrite | FeAsS | Hematitie | $Fe_2O_3$ |
| (?) Loellingite | $FeAs_2$ | Jarosite | $K_2Fe_6(OH)_{12}(SO_4)_4$ |
| Montroseite | $V_2O_3 \cdot H_2O$ | Adularia | $KAlSi_3O_8$ |
| Galena | PbS | Alunite | $K_2Al_6(OH)_{12}(SO_4)_4$ |
| (?) Chalcopyrite | $CuFeS_2$ | Opal | $SiO_2 \cdot nH_2O$ |
| (?) Covellite | CuS (Gruner and Gardiner, 1952) | Chalcedony | $SiO_2$ |
| (?) Bornite | $Cu_5FeS_4$ (Gruner and Gardiner, 1952) | | |

SUPERGENE MINERALIZATION

| | | |
|---|---|---|
| Metatorbernite | $Cu(UO_2)_2(PO_4)_2 \cdot 6\text{–}8H_2O$ | Gruner and Gardiner, 1952 |
| Zeunerite | $Cu(UO_2)_2(AsO_4)_2 \cdot 8\text{–}10H_2O$ | Gruner and Gardiner, 1952 |
| Carnotite | $K_2O \cdot 2UO_3 \cdot V_2O_5 \cdot 3H_2O$ | Gruner and Gardiner, 1952 |
| Tyuyamunite | $CaO \cdot 2UO_3 \cdot V_2O_5 \cdot 3H_2O$ | Gruner and Gardiner, 1952 |
| Abernathyite | $K_2(UO_2)_2(AsO_4)_2 \cdot 10\text{–}12H_2O$ | Thompson *et al.*, 1956 |
| Uvanite | $2UO_3 \cdot 3V_2O_5 \cdot 15H_2O$ | Weeks and Thompson, 1954 |
| Rauvite | $CaO \cdot 2UO_3 \cdot 5V_2O_5 \cdot 16H_2O$ | Gruner, 1952 |
| (?) Uranospinite | $Ca(UO_2)_2(AsO_4)_2 \cdot 8\text{–}10H_2O$ | |
| Corvusite | $V_2O_4 \cdot 6V_2O_5 \cdot nH_2O$ | Gruner and Gardiner, 1952 |
| Metahewettite | $CaO \cdot 3V_2O_5 \cdot 11H_2O$ | Gruner and Gardiner, 1952 |
| Pascoite | $2CaO \cdot 3V_2O_5 \cdot 11H_2O$ | Hess, 1922 |
| Pintadoite | $2CaO \cdot V_2O_5 \cdot 9H_2O$ | Hess, 1922 |
| Erythrite | $Co_3(AsO_4)_2 \cdot 8H_2O$ | Gruner and Gardiner, 1952 |
| Realgar | $As_2S_2$ | |
| Orpiment | $As_2S_3$ | |
| Gypsum | $CaSO_4 \cdot 2H_2O$ | |
| Jarosite | $K_2Fe_6(OH)_{12}(SO_4)_4$ | |
| Alunite | $K_2Al_6(OH)_{12}(SO_4)_4$ | |
| Copiapite | $Fe_4(OH)_2(SO_4)_5$ | Hess, 1922 |
| Halotrichite | $FeSO_4 \cdot (Al_2SO_4)_3 \cdot 24H_2O$ | Hess, 1922 |
| Celadonite | Fe, Mg, K silicate | Hess, 1922 |
| Brochantite | $CuSO_4 \cdot 3Cu(OH)_2$ | Gruner and Gardiner, 1952 |
| Kaolinite | $Al_2O_3 \cdot 2SiO_2 \cdot 2H_2O$ | |
| Illite | | |
| Calcite | $CaCO_3$ | |
| Magnesite | $MgCO_3$ | |
| Goethite | FeO(OH) | |
| Limonite | $Fe(O, OH) \cdot 2H_2O$ | |
| Sulfur | S | Hess, 1922 |

chalcedony replaces early interstitial alteration clays. The silica is believed to have been derived from detrital quartz replaced by urano-organic materials and alteration clays.

*Supergene Alteration*

Oxidation of the ore and associated metallic minerals produced a large suite of secondary

TABLE 20.—X-RAY DIFFRACTION OF JAROSITE FROM THE CAMP BIRD MINES (Cu/Ni)

| Associated with alteration about carbonaceous trash (diffractometer) | | Associated with alteration about ore pod (microcamera*) | | Jarosite U.S.N.M.-R6299 Warshaw (1956) | |
|---|---|---|---|---|---|
| d(Å) | I† | d(Å) | I† | d(Å) | I |
| 5.90 | 4 | 5.88 | 7 | 5.94 | 3 |
| 5.71 | 6 | | | 5.74 | 2 |
| 5.06 | 10 | 5.08 | 8 | 5.09 | 4 |
| | | 4.41 | ½ | | |
| 4.247 | 5** | | | | |
| 3.646 | 1 | 3.62 | ½ | 3.65 | 1 |
| 3.34 | 13** | | | | |
| 3.103 | 12 | | | 3.11 | 6 |
| 3.07 | 16 | 3.06 | 10 | 3.08 | 10 |
| 2.96 | 3 | | | 2.97 | 1 |
| 2.864 | 5 | 2.84 | 1 | 2.87 | 2 |
| 2.546 | 3 | 2.54 | 3 | 2.547 | 3 |
| 2.453 | 1** | | | | |
| 2.287 | 5** | 2.302 | 4 | 2.292 | 5 |
| 2.246 | 2** | | | | |
| 1.975 | 6** | 1.97 | 4 | 1.978 | 5 |
| | | | | 1.941 | 2 |
| | | | | 1.913 | 1 |
| 1.825 | 5** | 1.86 | 3 | 1.823 | 5 |
| 1.688 | 2** | | | | |
| 1.535 | 3** | | | 1.539 | 3 |
| 1.509 | 2 | | | 1.512 | 3 |
| 1.482 | 1 | | | 1.484 | 1 |
| 1.373 | 2** | | | | |

* Separation of interstitial material gave strong ferric iron and sulfate tests chemically
† Intensities relative
** Quartz

Small, irregular, nodularlike masses of opal and bands of chalcedony (Pl. 6, fig. 3) are found in a few places in interstitial material in the collapse. Similarly, a concentric band of silica from replaced quartz is present in ore-bearing nodules (Fig. 18, *D*). Silicification along fractures in the collapse may extend several inches into the bordering sediments (Pl. 1, fig. 5).

Small aggregate patches of carbonate are locally scattered through and mixed with the clay minerals in the Moss Back. Carbonate alteration is essentially insignificant in the ore horizon.

minerals (Table 19). These minerals reflect the metallic composition of the ores and, in part, the distribution of metallic components.

Hydrous oxides of uranium and vanadium are present throughout the mining district. Carnotite and tyuyamunite are the most abundant. The others are present only in minor amounts locally. Concentrations of the secondary vanadium minerals in the ore horizon are more noticeable away from the collapse in the calyx mining area, particularly the South Workings. Above the ore horizon, the hydrous vanadium oxides are associated with ore in

TABLE 21.—X-RAY DIFFRACTION OF JAROSITE, TEMPLE MOUNTAIN
(Diffractometer Cu/Ni)

| Temple Mountain | | Jarosite U.S.N.M. R6299 | | Karphosiderite U.S.N.M. R6266† | |
|---|---|---|---|---|---|
| d(Å) | I | d(Å) | I | d(Å) | I |
| 5.92 | 2 | 5.94 | 3 | 5.93 | 3 |
| 5.676 | 2b | 5.74 | 2 | .... | |
| 5.562 | 1 | .... | | 5.56 | 3 |
| 5.063 | 5 | 5.09 | 4 | 5.05 | 4 |
| 4.247x | 2b | .... | | .... | |
| 3.660 | 1b | 3.65 | 1 | 3.66 | 1 |
| 3.424 | 1 | .... | | 3.48 | 1 |
| 3.333x | 10 | .... | | .... | |
| 3.104 | 8 | 3.11 | 6 | 3.11 | 8 |
| 3.067 | 10 | 3.08 | 10 | 3.06 | 8 |
| 2.958 | 2b | 2.97 | 1 | 2.96 | 2 |
| 2.837 | 2 | 2.870 | 2 | 2.778 | 2 |
| 2.540 | 3 | 2.547 | 3 | 2.526 | 2 |
| 2.456x | 2b | .... | | .... | |
| 2.327 | 1b | .... | | .... | |
| 2.277x | 3b | 2.292 | 5 | 2.228 | 3 |
| 2.125x | 1b | | | | |
| 1.977 | 4b | 1.978 | 5 | 1.975 | 4 |
| 1.931 | 1 | 1.941 | 2 | .... | |
| 1.921 | 1 | 1.913 | 1 | .... | |
| 1.893 | 1b | | | 1.905 | 1 |
| 1.826 | 4 | 1.823 | 5 | 1.830 | 4 |
| 1.819x | 2 | | | | |
| 1.744 | 1 | "Several weak lines" | | | |
| 1.717 | 1 | .... | .. | .... | .. |
| 1.703 | 1 | .... | .. | .... | .. |
| 1.648 | 1 | .... | .. | .... | .. |
| 1.539x | 2 | .... | .. | .... | .. |
| 1.535 | 2 | 1.539 | 3 | 1.529 | 1 |

..... Not Continued .....

* Jarosite, Meadow Valley Mine, Pioche, Nevada. $KFe_3(SO_4)_2(OH)_6$ (Warshaw, 1956)

† Karphosiderite, Greenland. $Fe_3(SO_4)_2(OH)_5(H_2O)$ (Warshaw, 1956)

x—Quartz

b—Broad

the Wingate Sandstone. Uranium arsenates appear to be more abundant near or adjacent to the collapse area. Abernathyite, a new mineral, has been identified from the tongue of the collapse (Thompson *et al.*, 1956). The writers tentatively identified uranospinite, a hydrous calcium uranium arsenate, near the collapse at the Camp Bird mines on the basis of optical properties and X-ray diffraction.

Occurrences of erythrite, realgar, and orpiment are scattered but seem to occur in greatest concentration near or within the collapse and faults. Considerable amounts of realgar and orpiment can be found at the Camp Bird mines.

POSSIBLE LATE HYDROTHERMAL ALTERATION: Although paragenetic relations indicate that alunitization and jarositization occurred later than the ore, the distribution, particularly of jarosite, suggests deposition before other typical supergene minerals.

Jarosite may be found in intimate mixture with the interstitial alteration clays bordering or within the collapse features and faults, or as nearly pure masses and veinlets associated with carbonized wood fragments and urano-organic materials near or within the collapse (Pl. 6, fig. 4). The occurrence with clays is similar to that noted for jarosite in California Tertiary argillites and sandstones (Briggs, 1951) and for jarosite in Pennsylvania underclays (Warshaw, 1956), where the extreme small size and mixture with other materials make mechanical separation and optical identification unreliable. However, X-ray-diffractometer patterns of the clays at Temple Mountain in a few cases show spacings representative of jarosite, and qualitative chemical tests of these clays yield strong ferric iron and sulfate. X-ray microcamera patterns confirm the identification of jarosite (Table 20).

X-ray-diffractometer patterns of the purer material (Table 21) associated with organic substances indicate that the sulfate consists of a mixture of jarosite ("high" potassium-iron sulfate) and either karphosiderite ("low" potassium-iron sulfate) or natrojarosite, the sodic analogue of jarosite (Warshaw, 1956). X-ray-diffraction patterns of natrojarosite are similar to karphosiderite. The agreement of some spacings with karphosiderite and the presence of abundant iron qualitatively suggest karphosiderite rather than natrojarosite, particularly where the associated clays are high in potassium, not sodium.

At the Camp Bird mines, slightly altered interstitial clays surrounding pyritized wood fragments contain few, if any, sulfates, whereas the extensively altered clays surrounding nonpyritized wood contain abundant mixed sulfate. In many cases pyrite constitutes the core of urano-organic nodules. Within the Moss Back collapse, where considerable al-

TABLE 22.—X-RAY-DIFFRACTION MEASUREMENTS OF FAINTLY TRANSLUCENT MATERIAL ASSOCIATED WITH ORGANIC MATERIALS (Cu/Ni)

| Ore pod* Powder camera | | Ore pod† Micro-camera | | Organic material in alteration about ore pod** (nonore) Micro-camera | | Mineral possibilities |
|---|---|---|---|---|---|---|
| d(Å) | I | d(Å) | I | d(Å) | I | |
| | | 10.4 | 1 | | | Mica |
| | | 7.36 | 1 | 7.1 | 1 | Kaolinite |
| | | | | 6.1 | 5 | Jarosite |
| 5.38 | 7 | | | 5.0 | 2 | Jarosite |
| 4.82 | 8 | 4.81 | 10 | | | Orpiment |
| | | | | 4.45 | 2 | Kaolinite |
| | | 4.33 | 1 | | | Mica |
| 4.25 | 6 | | | | | Quartz |
| 3.98 | 1 | 3.97 | 5 | | | Orpiment |
| | | 3.63 | 5 | 3.63 | 1 | Jarosite, kaolinite, hematite |
| 3.40 | 10 | | | | | Quartz |
| | | | | 3.35 | 6 | Jarosite |
| 3.15 | 5 | 3.16 | 2 | | | Orpiment |
| 3.04 | 1 | 3.04 | 1 | 3.07 | 6 | Jarosite, orpiment |
| 2.94 | 2 | 2.97 | 1 | | | Arsenic |
| | | 2.842 | 5 | | | Orpiment |
| 2.746 | 3 | 2.779 | 6 | | | Arsenic |
| 2.690 | 3 | 2.695 | 7 | | | Orpiment, hematite |
| 2.570 | 1 | 2.555 | 1 | 2.55 | 5 | Jarosite, orpiment, hematite |
| 2.441 | 2 | 2.435 | 7 | | | Quartz, orpiment |
| | | 2.350 | 1 | | | Unknown |
| | | 2.300 | 1 | | | Orpiment |
| 2.269 | 2 | | | | | Quartz |
| | | 2.202 | 1 | | | Jarosite, hematite |
| 2.120 | 1 | 2.118 | 1 | | | Orpiment |
| | | 2.073 | 2 | | | Orpiment, hematite |
| 1.968 | 1 | 2.012 | 1 | | | Orpiment, quartz |
| | | 1.910 | 2 | | | Orpiment |
| 1.811 | 1 | | | | | Quartz |
| 1.674 | 1 | | | | | Quartz |
| 1.537 | 1 | | | | | Quartz |
| 1.371 | 2 | | | | | Quartz |

teration is evident, nearly pure jarosite makes up the core of nodules. Petrographic study indicates that the iron and sulfate were derived from the pyrite associated with the organic materials in these cases. Near or within the collapse, the concentration of mixed jarosite increases where there is an increase in concentration of alteration clays toward the ore zones.

The mechanism for the production of jarosite at Temple Mountain is similar to that proposed for the jarosite in the underclays of Pennsylvania (Warshaw, 1956). Oxidation of pyrite associated with organic materials under acidic conditions took place locally near collapse features and faults. The solutions were most acid near the sulfide concentrations (Merwin and Posnjak, 1937). Away from the oxidizing pyrite, the acidity was lowered by dilution and reaction of the acid solutions with alkalies, particularly illite. Deposition of the basic ferric sulfate occurred within the clay masses. Development of the gossan zone (Kerr, Bodine, Kelley, and Keys, 1957) in upper Chinle and lower Wingate at the collapse may represent the final stage in the oxidation of pyrite concentrations. Under alkaline conditions, final deposition of iron in the form of limonitic goethite occurred.

Jarosite is present in only minor amounts outside of the collapse, and these occurrences are generally near or within faults. However, pyrite is nearly as abundant outside of the collapse as within it. The abundance of jarosite bordering and within the collapse suggests that the mineral formed during the last stages of hydrothermal alteration after deposition of ore and associated metallic elements. Hutton and Bowen (1950, p. 560–561), for example, consider that the jarosite in pneumatolytically altered volcanic rocks in California "...may represent the very latest or hydrothermal phase of the long and varied sequence of crystallization and metasomatism..."

Goethite replacement of the lower Wingate is common near the collapse. Tentatively identified goethite, intimately associated with the Moss Back ore near or within the collapse, may have formed during the period of development of jarosite from oxidation of iron in the urano-organic material (Pl. 5, fig. 6).

* Ore pod: Mostly orpiment and quartz, minor jarosite or alunite and arsenic.

† Ore pod: Mostly orpiment with minor jarosite, kaolinite, mica, arsenic, and possibly hematite.

** Nonradioactive mobile organic material: Mostly jarosite and kaolinite.

INTIMATE MINERAL MIXTURES ASSOCIATED WITH THE ORE: Many small, poorly defined patches along the edges of masses of organic material are composed of intimate mixtures of secondary minerals. These mixtures are most prevalent near the collapse area. In thin section, these areas are irregularly and faintly translucent. On polished surfaces, they may be distinguished from the opaque gray organic ore by irregular faint anisotropism and in a few cases by slight yellowish to reddish-brown internal reflections. X-ray-diffraction patterns of patches associated with the ore at the Camp Bird mines contain fine mixtures of orpiment with minor amounts of jarosite, kaolinite, mica, arsenic, and possibly hematite (Table 22, footnote 2). Patches associated with nonuranium-bearing petroliferous materials lack the arsenic compounds and are composed of fine mixtures of jarosite and kaolinite (Table 22, footnote 3).

The abundance of these mixtures near the collapse and their association with considerable jarositization in the vicinity of the collapse area suggest that they represent post-mineralization hydrothermal activity.

In summary, most of the jarosite and some of the secondary arsenic sulfides, alunite, and clays may represent a late hydrothermal phase after deposition of the ore. Late weathering and downward percolating ground water, however, yielded the large suite of supergene minerals; the source of the metallic elements was the urano-organic ore and associated metallic minerals.

## CONCLUSION

The writers believe that evidence favors the emplacement of uranium ore at Temple Mountain by hydrothermal solutions:

(1) A rough zonal relation in the Moss Back involves metallic trace elements in the ore, metallic minerals, and alteration. Arsenic, cobalt, and selenium are present near or within the collapse (or certain faults), whereas uranium, zinc, and vanadium appear to increase away from the collapse.
(2) The greatest known vertical spread of mineralization occurs at the collapse area.
(3) The sediments are most highly altered around the collapse.
(4) The solution of carbonate at depth and redeposition in large masses of dolomite above, coupled with the increase in marcasite at depth near and within the collapse, indicate a change in the rising solutions. Neutral to slightly acidic conditions prevailed from the lower Chinle downward, and neutral to slightly alkaline conditions prevailed from upper Chinle upward.

In addition to the migration pattern of the mineralizing solutions, the mineralogy of the ores suggests temperatures in the vicinity of 200°C. Considering a geothermal gradient of about 5°C. per 1000 feet of sediments under an approximate load of 10,000 to 12,000 feet, an estimated minimum of 50°C. above normal surface temperatures should have existed. An upper limit would probably be established by the argillic alteration of about 350°C. to 400°C. In determining a likely temperature within this range, several features indicate temperatures above those normally attributed to circulating ground waters:

(1) Native arsenic apparently would be deposited at elevated temperatures about 300° C. Recorded occurrences and the probable conditions of deposition in the presence of iron and sulfur confirm this conclusion.
(2) The abundance of the $2M_1$ mica polymorph in alteration mica clays toward the collapse and deposits of ore in the Moss Back (Kelley and Kerr, 1957) suggest temperatures in the vicinity of 200° C., on the basis of synthetic mica experiments (Yoder and Eugster, 1955).
(3) The deposition of large replacement masses of replacement dolomite near the collapse would probably result from solutions having elevated temperatures (Bodine, 1956).
(4) The writers believe that induration of the organic material occurred under the influence of heat and the action of solutions rather than by radioactive polymerization.

Field observation and laboratory data suggest a progressive development of ore masses. Initially weak mineralizing solutions infiltrated permeable sediments. The interstices between sand grains were filled and the cement was replaced. This was accompanied by extraction of uranium from solution and coagulation of the immiscible hydrocarbon present as an interstitial film. The hydrocarbon formed either as small stringers and interstitial disseminations or as nodules. As the strength of the mineralization increased, more uranium was extracted, and coagulation increased; the hydrocarbons coalesced to form larger nodules and patches, which in turn eventually formed large patches of massive ore. Replacement of the sedimentary grains and previous interstitial alteration products occurred. Pyrite present was slowly replaced. Some concentric banding of the hydrocarbons and

associated metallic elements developed as the intensity, composition, and quantity of the mineralizing solutions varied through time. Coagulation of colloidally dispersed minor amounts of precipitating pitchblende and other metallic minerals accounts for their irregular distribution in the uranium hydrocarbon. Finally, induration of the hydrocarbon occurred, accompanied by some volume loss compensated by contraction fissures which were later filled by alteration products.

Miller's study of the chemical environment of pitchblende (1955b) suggests that sulfur, in the form of sulfide or sulfite, may be important as a precipitant of pitchblende. The association of pre-ore pyrite with the ore at Temple Mountain suggests that sulfur may have facilitated the extraction of uranium from mineralizing solutions and perhaps determined in part the distribution of the immiscible coagulating hydrocarbon. Possibly some of the contemporaneous and post-ore sulfide (pyrite) represents reduction of sulfate solutions and attendant oxidation of the hydrocarbons, as postulated by Ginter (1934). It is reasonable to infer that warm, slightly acid sulfate solutions carrying uranyl-ion decarbonitized the Chinle and lower sediments; when it came in contact with hydrocarbons and sulfides, the uranium was extracted from the solution, the sulfate oxidized the hydrocarbons in part to carbonate and in turn was reduced to sulfide. The reduction that attended oxidation of the hydrocarbons resulted in the formation of the native arsenic, montroseite, sphalerite, and uraninite associated with the ore. The induration of the hydrocarbons was accomplished by polymerization and oxidation of the hydrocarbon by heated solutions.

Heat and oxidation conditions must have persisted after completion of the alteration and mineralization cycle to cause induration of the initial post-ore hydrocarbons, to form the asphalt of Temple Mountain, and to produce abundant jarosite and some minor arsenic sulfides near the collapse area.

The lack of variety and scarcity of the metallic elements in the ores at Temple Mountain is a feature of the relatively barren uppermost (hot-spring) portion of hydrothermal vein systems in general. The pattern of alteration surrounding the collapse corresponds to that proposed by Schmitt (1950a; 1950b) for epithermal mineral deposits based on hot-spring areas. It consists of a basal $CO_2$ leaching phase, medial potassic and sodic phases, and an upper sulfide-sulfate phase. In view of the location of argillic alteration with respect to the main ore at Temple Mountain, Schmitt's (1950b, p. 199) statement is significant: "It may be found that 'epithermal' ore deposition is usually just above (or to one side of) the hypogene clay zone and presumably associated with a sericitic-quartz or potassic phase." The peculiar collapse and the form of this structure are similar to the conelike or wedge-like upward flares of channel structures in hot-spring areas.

Most of the metallic elements associated with the ore at Temple Mountain have been found in minor amounts locally in hot-spring areas. Arsenic and jarosite deposits associated with hot springs have recently been summarized by White (1955). In general, the Temple Mountain collapse is suggestive of a fossil hot-spring region. The considerable amount of silica dissolved during the carbonate replacement of Wingate must have made siliceous deposits above the Wingate of extent comparable to those at hot springs. A warm-spring area bordering the San Rafael River in the northeast portion of the swell has been reported to have above normal concentrations of uranium in solution, which is not only depositing siliceous sinter and sulfates but appears to be carrying hydrocarbons.

At the Little Joe Claims along the west side of the swell, urano-organic ore is localized along a large fault zone which has an associated collapse structure and a radioactive warm spring. Near the small urano-organic ore deposits at Calf Mesa at the north end of the swell is a nonuranium-bearing fossil hot-spring deposit in the Moss Back Sandstone, containing sulfide pipes. Small crystals of sulfur are scattered in hydrocarbon-sulfate saturated sandstones above the pipes. In the ore at Calf Mesa, somewhat similar sulfide pipes are locally present and contain urano-organic material. The considerable amount of sulfides associated with the ore have formed, upon leaching, an unusual occurrence of secondary iron minerals.

In speaking of epithermal quicksilver deposits associated with many hot springs, Lindgren (1933, 464) states:

"A scant association of ore minerals characterizes these deposits. Besides cinnabar and a few secondary minerals, they contain almost invariably pyrite or marcasite. . . Among gangue minerals we have predominatingly opal, chalcedony, and quartz, also calcite and dolomite. . . Replacements of adjoining country rock by dolomitic carbonates or by opal are common. . . Hydrocarbons are frequent."

In conclusion, the urano-organic ore at Temple Mountain is considered to have resulted from epithermal mineralization of hot-spring type. Solutions were introduced into the ore horizon at the collapse, and to a lesser extent, along faults or fractures. Away from these channels, evidence of hydrothermal activity diminishes. The principles of carbonate alteration (Bodine, 1956) and the features of argillization (Kelley and Kerr, 1957), together with the occurrence of sulfates and zonal elemental distribution, may be widely applicable to the determination of centers of uranium mineralization elsewhere on the Colorado Plateau. It is significant that uranium mineralization is relatively sparse at these centers but may be more abundant near by.

## References Cited


Abraham, H., 1920, Asphalts and allied substances: N. Y., D. Van Nostrand Co., 608 p.

Allen, E. T., Crenshaw, J. L., and Merwin H. E., 1914, Effect of temperature and acidity in the formation of marcasite ($FeS_2$) and wurtzite (ZnS): Am. Jour. Sci., 4th ser., v. 38, p. 393–431

Baker, A. A., 1946, Geology of the Green River Desert-Cataract Canyon region, Emery, Wayne, and Garfield counties, Utah: U.S. Geol. Survey Bull. 951, 122 p.

Barthauer, G. L., Rulfs, C. L., and Pearce, D. W., 1953, Investigations of thucholite: Am. Mineralogist, v. 38, p. 802–814

Bastin, E. S., 1950, Interpretation of ore textures: Geol. Soc. America Mem. 45, 100 p.

Bass, N. W., 1944, Correlations of basal Permian and older rocks in southwestern Colorado, northwestern New Mexico, northeastern Arizona, and southeastern Utah, 1944: U.S. Geol. Survey Oil and Gas Invs. Prelim. Chart no. 7, accompanied by paper on Paleozoic stratigraphy as revealed by deep wells in parts of southwestern Colorado, northwestern New Mexico, northeastern Arizona, and southeastern Utah, 20 p.

Bernauer, F., 1935, Rezente Erzbildung auf der Insel Vulcana, Teil I: Neues Jahrb. für Min. Geol. und Paläontologie Abh., Beil. 64, Abt. A., p. 60–92

Bowie, S. H. U., 1955, Thucholite and hisingerite-pitchblende complexes from Nicholson Mine, Saskatchewan, Canada: Geol. Survey Gt. Britain Bull. 10, p. 45–57

Breger, I. A., and Deul, M., 1955, The association of uranium with carbonaceous materials on the Colorado Plateau: U.S. Atomic Energy Comm., TEIR-539, p. 1–35

Breger, I. A., Deul, M., and Meyrowitz, R., 1955, Geochemistry and mineralogy of a uraniferous subbituminous coal: Econ. Geology, v. 50, p. 610–624

Breger, I. A., Deul, M., and Rubinstein, S., 1955, Geochemistry and mineralogy of a uraniferous lignite: Econ. Geology, v. 50, p. 206–226

Briggs, L. I., 1951, Jarosite from the California Tertiary: Am. Mineralogist, v. 36, p. 902–906

Coleman, R. G., 1957, Mineralogical evidence on the temperature of formation of the Colorado Plateau uranium deposits: Econ. Geology, v. 52, p. 1–4

Crawford, A. L., 1949, Gilsonite and related hydrocarbons of the Uinta Basin, Utah, p. 235–260 *in* Hansen, G. H., and Bell, M. M., The oil and gas possibilities of Utah: Utah Geol. Mineralog. Survey, 341 p.

Croft, W. J., 1954, An X-ray line study of uraninite: U.S. Atomic Energy Comm., Ann. Rept. (pt 11), RME-3096, p. 7–71

Davidson, C. F., and Bowie, S. H. U., 1951, Related hydro-carbon-uraninite complexes: Geol. Survey Gt. Britain Bull. 3, p. 1–19

Dietrich, R. V., 1956, Is anthraxolite related genetically to coal or to oil?: Econ. Geology, v. 51, p. 649–664

Ellsworth, R. V., 1928, Thucholite from the vicinity of Parry Sound, Ontario: Am. Mineralogist, v. 13, p. 419–442

Erickson, R. L., Myers, A. T., and Horr, C. A., 1954, Association of uranium and other metals with crude oil, asphalt, and petroliferous rock: Am. Assoc. Petroleum Geologists Bull., v. 38, p. 2200–2218

Evans, N. N., 1903, Native arsenic from Montreal: Am. Jour. Sci., 4th ser., v. 15, p. 92–93

Fleischer, M., 1955, Minor elements in some sulfide minerals: Econ. Geology, 50th Anniversary Volume, p. 970–1024

Fryklund, V. C., and Fletcher, J. D., 1956, Geochemistry of sphalerite from the Star mine, Coeur d'Alene District, Idaho: Econ. Geology, v. 51, p. 223–247

Garrels, R. M., 1953, Some thermodynamic relations among the vanadium oxides, and their relations to the oxidation state of the uranium ores of the Colorado Plateaus: Am. Mineralogist v. 38, p. 1251–1265

Gilluly, J., 1929, Geology and oil and gas prospects of part of the San Rafael Swell, Utah: U.S. Geol. Survey Bull. 806, p. 69–130

Ginter, R. L., 1934, Sulphate reduction in deep subsurface waters: Am. Assoc. Petroleum Geologists, Problems of Petroleum Geology (Sidney Powers Memorial Volume), p. 907–925

Glass, H. D., 1954, Investigation of rank in coal by differential thermal analyses: Econ. Geology, v. 49, p. 294–309

Gott, G. B., Wyant, D. G., and Beroni, E. P., 1952, Uranium in black shales, lignites, and limestones in the United States: U.S. Geol. Survey Circ. 220, p. 31–35

Gruner, J. W., and Gardiner, L., 1952, Mineral associations in the uranium deposits of the Colorado Plateau and adjacent region with special emphasis on those in the Shinarump formation: U.S. Atomic Energy Comm., Ann. Rept., July 1, 1951, to June 30, 1952 (pt. III), p. 1–41

Hacquebard, P. H., 1950, The nomenclature and classification of coal petrography: Nova Scotia Dept. Mines, Conf. on Origin and Constitution of Coal, p. 8–48

Hess, F. L., 1922, Uranium-bearing asphaltite sediments of Utah: Eng. and Min. Jour., v. 114, p. 272–276

Hunt, J. M., Stewart, F., and Dickey, P. A., 1954, Origin of Hydrocarbons of Uinta Basin, Utah: Am. Assoc. Petroleum Geologists Bull. v. 38 (pt. 2), p. 1671–1698

Hutton, C. O., and Bowen, O. E., 1950, An occurrence of jarosite in altered volcanic rocks of Stoddard Mountain, San Bernardino County, California: Am. Mineralogist, v. 35, p. 556–561

Ingerson, E., 1955, Methods and problems of geologic thermometry: Econ. Geology, 50th Anniversary Volume, p. 341–410

Joubin, F. R., 1954, Uranium deposits of the Algoma district, Ontario: Can. Inst. Min. Met. Trans., v. 58, p. 431–437

Kelley, D. R., and Kerr, P. F., 1956, Emplacement of uraniferous hydrocarbons at Temple Mountain, Utah: U.S. Atomic Energy Comm., Ann. Rept. for June 30, 1955, to April 1, 1956, p. 1–79

—— 1957, Clay alteration and ore, Temple Mountain, Utah: Geol. Soc. America Bull., v. 68, p. 1101–1116

Kerr, P. F., and Hamilton, P. K., 1958, Chrome mica-clay, Temple Mountain, Utah: Am. Mineralogist, v. 43, p. 34–47

Kerr, P. F., and Kelley, D. R., 1956, Urano-organic ores of the San Rafael Swell, Utah: Econ. Geology, v. 51, p. 386–391

Kerr, P. F., and Kulp, J. L., 1948, Multiple differential thermal analysis: Am. Mineralogist, v. 33, p. 387–419

Kerr, P. F., and Lapham, D. M., 1954, Report on a nodule from Temple Mountain, Utah: U.S. Atomic Energy Comm., RME-3096 (pt. 1), p. 7–15

Kerr, P. F., Holmes, R. J., and Knox, M. S., 1945, Lattice constants in the pyrite group: Am. Mineralogist, v. 30, p. 498–504

Kerr, P. F., Rasor, C. A., and Hamilton, P. K., 1951, Uranium in Black King Prospect, Placerville, Colorado: U.S. Atomic Energy Comm., Ann. Rept., RMO-797, p. 25–43

Kerr, P. F., Bodine, M. W., Kelley, D. R., and Keys, W. S., 1957, Collapse features, Temple Mountain uranium area, Utah: Geol. Soc. America Bull., v. 68, p. 933–982

Kerr, P. F., Kelley, D. R., Bodine, M. W., and Keys, W. S., 1955, Collapse features, Temple Mountain uranium area, Utah: U.S. Atomic Energy Comm., RME-3110 (pt. 3), p. 1–138

Keys, W. S., 1955, Deep drilling in the Temple Mountain Collapse, San Rafael Swell, Utah: United Nations, Geneva Conf. on Peaceful Uses of Atomic Energy, Proc., v. 6, p. 371–378

Keys, W. S., and White, R. L., 1956, Investigation at the Temple Mountain collapse and associated features, San Rafael Swell, Emery County, Utah: U.S. Geol. Survey Prof. Paper 300, p. 285–298

Kullerud, G., 1953, The FeS-ZnS system a geological thermometer: Saertrykk av Norsk Geologisk Tidsskrift, b. 32, h. 2–4, p. 61–147

—— 1956, Geochemistry of sphalerite from the Star Mine, Coeur d'Alene District, Idaho: Econ. Geology, v. 51, p. 828–830

Larsen, E. S., 1921, The microscopic determination of nonopaque minerals: U.S. Geol. Survey Bull. 697, p. 1–294

Lindgren, W., 1933, Mineral deposits: N. Y., McGraw Hill Book Co., 930 p.

Marshall, C. E., 1955, Coal petrology: Econ. Geology, 50th Anniversary Volume, p. 757–834

Merwin, H. E., and Posnjak, E., 1937, Sulphate incrustations in the Copper Queen Mine, Bisbee, Arizona: Am. Mineralogist, v. 22, p. 567–571

Miller, L. J., 1955a, Uranium ore controls of the Happy Jack Deposit, White Canyon, San Juan County, Utah: Econ. Geology, v. 50, no. 2, p. 156–169

—— 1955b, The chemical environment of pitchblende: U.S. Atomic Energy Comm., RME-3110 (pt. 1), p. 1–49

Moore, G. W., 1954, Extraction of uranium from aqueous solution by coal and some other materials: Econ. Geology, v. 49, p. 652–658

Murray, A. N., 1950, The gilsonite deposits of the Uinta Basin, Utah, p. 115–118 *in* Eardley, A. J., *Editor*, Petroleum geology of the Uinta Basin: Guidebook to the Geology of Utah, no. 5, 152 p.

O'Brien, T. C., 1953, Uranium occurrence in asphaltites: U.S. Atomic Energy Comm., RME-3040, p. 1–6

Onishi, H., and Sandell, E. B., 1955, Geochemistry of arsenic: Geochim. et Cosmochim. Acta, v. 7, p. 1–33

Palache, C., Berman, H., and Frondel, C., 1944, Dana's system of mineralogy: v. 1, 7th Ed., N. Y., John Wiley & Sons, 834 p.

Prommel, H. W. C., and Crum, H. E., 1927, Salt domes of Permian and Pennsylvanian age in southeastern Utah and their influence on oil accumulation: Am. Assoc. Petroleum Geologists Bull., v. 11, p. 373–393

Ridgway, R., 1912, Color standards and color nomenclature: Published by author, Washington, D. C., 43 p., 53 pls.

Ries, H., 1949, Economic geology: 7th Ed., N. Y., John Wiley & Sons, Inc., 720 p.

Robinson, S. C., 1950, Mineralogy of the Goldfields District, Saskatchewan (Interim Account): Geol. Survey Canada Paper 50-16, 38 p.

Schmitt, H., 1950a, The fumarolic-hot spring and "epithermal" mineral deposit environment, *in* Applied Geology, a symposium: Colo. School Mines Quart. v. 45, no. 1B, p. 209–229

—— 1950b, Origin of the epithermal mineral deposits: Econ. Geology, v. 45, p. 191–197

Schopf, J. M., 1956, A definition of coal: Econ. Geology, v. 51, p. 521–527

Sciacca, T. P., 1954, Electron micrographs of synthetic pitchblende precipitates: U.S. Atomic Energy Comm., RME-3096 (pt. 2), p. 93–99

Short, M. N., 1940, Microscopic determination of the ore minerals: U. S. Geol. Survey Bull. 914, p. 1–314

Siever, R., 1952, X-ray diffraction study of rank increase in coal: Nova Scotia Dept. Mines, 2nd Conf. on Origin and Constitution of Coal, p. 341–362

Spence, H. S., 1930, A remarkable occurrence of thucholite and oil in a pegmatite dyke, Parry Sound, Ontario: Am. Mineralogist, v. 15, no. 11, p. 499–520

Stevenson, J. S., 1954, Determination of columbium in ores by X-ray fluorescence: Am. Mineralogist, v. 39, no. 5–6, p. 436–443

Stieff, L. R., Stern, J. W., and Milkey, R. G., 1953, A preliminary determination of the age

of some uranium ores of the Colorado Plateaus by the lead-uranium method: U. S. Geol. Survey Circ. 271, 19 p.

Swanson, H. E., and Fuyat, R. K., 1953, Standard x-ray diffraction powder patterns: N.B.S. Circ. 539, v. II, p. 19

Thompson, M. E., Ingram, B., and Gross, E. B., 1956, Abernathyite, a new uranium mineral of the metatorbernite group: Am. Mineralogist, v. 41, no. 1–2, p. 82–90

Vine, J. D., 1955, Uranium bearing coal in the United States: United Nations Conf. Paper 55, v. 6, p. 452–457

Warren, C. H., 1903, Native arsenic from Arizona: Am. Jour. Sci., 4th Ser., v. 16, p. 337–339

Warshaw, C. M., 1956, The occurrence of jarosite in underclays: Am. Mineralogist, v. 41, no. 3–4, p. 288–296

Weeks, A. D., Thompson, M. E., 1954, Identification and occurrence of uranium and vanadium minerals from the Colorado Plateaus: U. S. Geol. Survey Bull. 1009–B, 62 p.

Weeks, A. D., Cisney, E. A., and Sherwood, A. M., 1953, Montroseite, a new vanadium oxide from the Colorado Plateaus: Am. Mineralogist, v. 38, p. 1235–1241

Wengard, S. A., and Strickland, J. W., 1954, Pennsylvanian stratigraphy of the Paradox Salt Basin, Four Corners region, Colorado and Utah: Am. Assoc. Petroleum Geologists Bull., v. 38, p. 2157–2199

White, D. E., 1955, Thermal springs and epithermal ore deposits: Econ. Geology, 50th Anniversary Volume, p. 99–154

Yoder, H. S., and Eugster, H. P., 1955, Synthetic and natural muscovites: Geochim. et Cosmochim. Acta, v. 8, no. 5/6, p. 225–280

Young, R. S., 1954, Preliminary X-ray investigation of solid hydrocarbons: Am. Assoc. Petroleum Geologists Bull., v. 38, no. 9, p. 2017 2020

Department of Geology, Columbia University, New York 27, N. Y.

Manuscript Received by the Secretary of the Society, May 14, 1957

BULLETIN OF THE GEOLOGICAL SOCIETY OF AMERICA
VOL. 69, PP. 757-774, 2 FIGS. JUNE 1958

# PRECAMBRIAN CLASSIFICATION AND CORRELATION IN THE CANADIAN SHIELD

BY M. E. WILSON

## ABSTRACT

Grout *et al.* (1951) concluded that the Precambrian formations of Minnesota were deposited during three eras which they named Earlier, Medial, and Later; and James (1955) proposed Lower, Middle, and Upper divisions for the Precambrian of northern Michigan. These threefold classifications apparently are meant to replace the dual classification so long in use in the Lake Superior region and although possibly not so intended imply by the use of the word Precambrian that they are applicable to the whole Canadian Shield. Although there is much too little information as yet for certainty, probably not more than one recognizable major unconformity is sufficiently extensive in the shield to permit the division of Precambrian time into more than two eras by means of stratigraphical investigation.

Only a tentative dual classification of the rocks of the shield according to their relationship to the great unconformity beneath the (Huronian) Cobalt Series on Lake Timiskaming has been attempted. Formations beneath this unconformity in the Timiskaming and Grenville subprovinces and less positively in the north or northwest subprovince are classed as Archean (Early Precambrian), those above as Proterozoic (Late Precambrian). Rocks in the northern part of the shield are either assigned on lithological and structural evidence to the Archean or Proterozoic or are unclassified under the designation Archean and/or Proterozoic. In places, the Archean classification of formations has been confirmed by physicochemical age determinations of minerals.

The Canadian Shield is divided by geographical and geological barriers into provinces and subprovinces. The subprovinces delimit the territory to which direct serial correlations can be extended with reasonable certainty. At the present the use of most serial names in more than one subprovince is unwarranted.

## CONTENTS

### TEXT

| | Page |
|---|---|
| Introduction | 758 |
| Determination of age by physicochemical methods | 758 |
| Classification of formations in the Canadian Shield | 759 |
| Classifications proposed | 759 |
| Pre-Cobalt Series unconformity | 760 |
| General statement | 760 |
| Age of the Grenville Series | 760 |
| Pre-Cobalt Series unconformity in the Timiskaming and southern subprovinces | 761 |
| Pre-Cobalt Series unconformity in the northwestern subprovince and northern parts of the Canadian Shield | 763 |
| Limitations of serial and group correlation | 766 |
| Major divisions of the Precambrian in the Canadian Shield | 767 |
| General statement | 767 |
| Keweenawan and Animikie types | 768 |
| Timiskaming and pre-Timiskaming types | 768 |
| Grenville, Kisseynew, and Great Slave types | 769 |
| Conclusions | 769 |
| Bibliography | 770 |

### ILLUSTRATIONS

| Figure | Page |
|---|---|
| 1. Geological provinces of the Canadian Shield | 766 |
| 2. Subprovinces of the St. Lawrence geological province | 767 |

### TABLES

| Table | Page |
|---|---|
| 1. Age of uraninite in the Grenville subprovince from chemical analyses | 761 |
| 2. Age of uraninite or uranoan thorianite in the Grenville subprovince from lead-isotope, lead-isotope-uranium, or lead-isotope-thorium ratios | 762 |
| 3. Age of uraninite in pegmatite in northwest subprovince and in northern parts of the Canadian Shield from lead-isotope, or lead-isotope-uranium ratios | 763 |

## Introduction

This paper is a discussion of two major problems: (1) into how many divisions according to age can the formations of the Canadian Shield, as a whole, be best classified; and (2) over what extent of territory can Precambrian rock series be correlated with reasonable certainty? Because most Precambrian sediments and volcanic rocks are highly folded, and because most geological mapping has been too general for the determination of structure, much of the information for the final answers to these questions is not known; yet the answers must be based on reasonably certain data, and they must be practicable. Although most of the folded surficial rocks of the shield have structures from which the tops of beds or lava flows can be determined, structural mapping by means of these requires such detailed work that it will be many years, even in the more easily accessible southern part of the shield, before the succession of formations will be fully known.

## Determinations of Age by Physicochemical Methods

Age determinations of minerals by physicochemical methods may eventually be of considerable assistance in the classification of rocks in the Canadian Shield, but at present they confront the geologist with the following problems:

(1) Some of the methods of age determination proposed have scarcely passed beyond the speculative stage. Geologists, therefore, except where the determination conflicts with the geology, are compelled to distinguish between those methods that are hypothetical and those that seem to be scientifically established.

(2) With the possible exception of sediments containing glauconite (Cormier, 1957), a mineral uncommon in the Precambrian, the methods of age determination so far proposed are assumed to indicate not the time of deposition of surficial rocks but the dates of formation of minerals, most of which are believed to be related in origin to mountain building. For this reason, physiocochemical datings may supplement but not replace stratigraphy in determining the major geological divisions of the Canadian Shield.

(3) In Paleozoic and later rocks, presumably because of the effect of uplift on the extent of the continental shelf, a relationship exists between orogeny and major changes in fossil life. In the Precambrian the absence of fossils makes structural unconformities and related mountain building of even greater importance in classification. Reliable age determinations of mountain building in the Canadian Shield could, therefore, be of great assistance in correlation.

(4) In many parts of the shield conglomerate containing granitic boulders is intruded by granite and in a few places (Lawson, 1913, p. 4; Henderson, 1937, p. 13–18; Lord, 1942, p. 17) rests unconformably on granite; these relations prove the existence of two ages of mountain building separated by prolonged erosion. In such places the last mountain building may destroy the physicochemical evidence of the older uplift, so that only the age of the later orogeny can be determined. For this reason some of the Early Precambrian rocks of the shield are possibly much older than the oldest age determinations. This situation exists on the Huron Claim in southeast Manitoba, where uraninite-bearing pegmatite intrudes andesite (De Lury and Ellsworth, 1931, p. 569) of the Rice Lake Series (Moore, 1912, p. 264) which also contains beds of conglomerate including boulders of granite (J. F. Wright, 1932, p. 11–12; Stockwell, personal communication).

Another item related to problem (4) is the time interval indicated by intertectonic erosion. In folded belts of post-Precambrian age, as noted by Gilluly (1949, p. 561–574), mountain building may recur at relatively short intervals. In contrast with this, however, regions that intervene between folded belts, as for example the interior plains and the Canadian Shield of North America, are underlain in most places by unfolded Paleozoic and later formations or by Proterozoic rocks that have not been mountain built. Where granitic intrusions associated with belts of folding occur in separate regions as those related to the Taconic (Alcock, 1947, p. 132), Acadian (Alcock, 1947, p. 133; 1948, p. 8–9; Billings, 1945, p. 55–56), and Appalachian (Barrell, 1915, p. 33–34; Billings, 1946, p. 1277) revolutions, their difference in age is determined by the fossils of the rocks they intrude; in the Precambrian, where fossil are absent, the different age of the intrusions would not be evident, and they would all be classed together as parts of a single orogeny.

## Classification of Formations in the Canadian Shield

### *Classifications Proposed*

Classifications into two, three, or four major subdivisions have been proposed locally for the formations of the shield, but only the dual classification has been attempted for the shield as a whole. The names of the eras, systems, or major divisions used are as follows:

(1) Laurentian and Huronian (Logan and Hunt, 1855): This classification was not based, as some erroneously have assumed, on the succession of formations on the north shore of Lake Huron but on Logan's observations on Lake Timiskaming, where unfolded (Huronian) "slate conglomerate", now called Cobalt Series, rests with great unconformity on granite (Logan, 1863, p. 50).

(2) Archean and Algonkian: Irving (1888, p. 450) suggested that the name Archean (Dana, 1872, p. 253), which up to that time had included all the Precambrian, be restricted to the Laurentian "gneissic basic terrane", and that an "entirely new term of equal rank with Palaeozoic and Archean be introduced to cover the formations between the gneissic series and the Cambrian". Following this proposal of Irving the geologists of the United States Geological Survey chose the term Algonkian (Powell, 1890, p. 66) for the new era (Wilmarth, 1924, p. 103).

(3) Loganian, Temiskamian, Animikean, and Keweenawan: Miller and Knight (1913, p. 126) proposed these names for a fourfold classification of the Precambrian rocks of Ontario and the adjacent parts of Manitoba and Quebec. They concluded that three major unconformities—the pre-Temiskaming, the pre-Animikie, and the pre-Keweenawan—extended throughout this region.

(4) Archean and Proterozoic: The attempt to identify the Laurentian and Huronian of Logan on Lake Timiskaming throughout the Canadian Shield during the exploratory period that continued to 1903, when the silver-bearing veins of Cobalt were discovered, went so far amiss (Van Hise, 1908, p. 6–7; M. E. Wilson, 1939, p. 294–295) that these names were almost abandoned in Canada, and for more than 30 years major time divisions were omitted from the legends of most Precambrian maps published by the Geological Survey of Canada. Commencing in 1913, however, the writer divided the rocks of the Grenville region into Early and Late Precambrian parts, and in 1917 (p. 23) W. H. Collins in the Lake Huron-Lake Timiskaming region used Huronian and pre-Huronian. The rocks of the shield were also divided into Early and Late Precambrian in the 1924 edition of the geological map of Canada (Young, 1924). In 1934, a committee of the Royal Society of Canada on stratigraphical nomenclature recommended that Precambrian time be divided into two eras and that the names of the eras by Archean and Proterozoic (Alcock, 1934, p. 119; Van Hise and Leith, 1909, p. 20). These recommendations were adopted at meetings of the Precambrian geologists of the Canadian Survey on January 30 and February 2,[1] 1935; since that time the dual classification has been used in the legends of most geological maps issued by the Geological Survey of Canada, but up to 1942, Early and Late Precambrian were added in brackets after Archean and Proterozoic, respectively. In the third report of the American Commission on Stratigraphic Nomenclature (Harrison, 1955), "it is recommended that the major divisions of Precambrian time, approximately equivalent to eras, be known simply as Early and Late Precambrian". In the comments of the commissioners that follow, however, Stockwell advocates the retention of the names Archean and Proterozoic.

(5) Earlier, Medial, and Later Precambrian eras: These time divisions of the Precambrian were suggested by Grout *et al.* (1951, p. 1021) for the Precambrian of Minnesota. The rocks assigned to the three eras were:

Earlier Precambrian—Keewatin volcanic rocks, Soudan Iron Formation Member, and pre-Knife Lake batholithic intrusive rocks

Medial Precambrian—Knife Lake Group and Algoman batholithic intrusive rocks

Later Precambrian—Animikie and Keweenawan

(6) Lower Precambrian, Middle Precambrian, and Upper Precambrian: These major classification titles recently put forward by James (1955, p. 1459) for the pre-Huronian, Huronian, and Keweenawan of northern Michigan, although almost the same as those of Grout *et al.*, are, in part at least, according to the usual correlations between the two regions, differently applied.

James and Grout *et al.* presumably propose the substitution of a threefold classification

[1] The writer is indebted to T. L. Tanton for the exact dates.

for the dual names, Archean and Algonkian, so long in use in the Lake Superior region (Van Hise and Leith, 1911, p. 598).

### *Pre-Cobalt Series Unconformity*

*General statement.*—The standard of reference for the dual classification of the rocks of the shield is the rock succession on Lake Timiskaming where the Huronian of Logan, the Cobalt Series, rests with great unconformity on granite (G. A. Young, personal communication, 1934). The immensity of this unconformity is indicated by: (1) the structural contrast between the normally almost flat Cobalt sediments and the underlying highly folded Timiskaming and older formations; and (2) the great areal extent of granite beneath the unconformity indicating deep erosion.

*Age of Grenville Series.*—Except for some igneous intrusions all the rocks occurring in the Grenville subprovince are assigned to the Archean. The relationship of the Grenville Series to the pre-Cobalt Series unconformity has recently been described by the the writer (1956, p. 1423), and only three items are mentioned here: (1) The discovery of abundant boulders of granite in conglomerate of the Hastings Series near Kaladar, Ontario, by Harding (1942, p. 65–66) shows that mountain building and granitic intrusion followed by deep erosion intervened between the Hastings and pre-Hastings rocks. (2) In the Lake Kipawa-Lake Timiskaming region, metamorphosed sediments of the Grenville, or possibly the younger Hastings Series, are intruded by potassic granite overlain unconformably by conglomerate of the Cobalt Series. (3) The igneous intrusions of Proterozoic age in the Grenville subprovince include a mass and dikes of lamprophyre in the Buckingham district, Quebec (M. E. Wilson, 1913, p. 205; Dresser and Denis, 1944, p. 180); dikes of diabase or gabbro, notably in a parallel swarm adjoining the north side of the lower Ottawa River, in Quebec (M. E. Wilson, 1925, p. 397); stocklike masses of granite, syenite, and quartz syenite porphyry, at Grenville, Quebec (Logan, 1853, p. 29–33; M. E. Wilson, 1917, p. 22–23; 1925, p. 397; Osborne, 1934), and at Rigaud, Ontario (LeRoy, 1901; Osborne, 1934); and possibly the Killarney granite north of Lake Huron (Collins, 1916; M. E. Wilson, 1956, p. 1422).

Uranium-bearing minerals occur in widely scattered localities in the Grenville subprovince, but the most common of these, and possibly the most reliable for age determination, are uraninite and uranoan thorianite found either in pegmatite or pegmatitic contact zones. In the western part of the subprovince, uraninite or uranoan thorianite has been discovered in 12 districts within a belt extending for more than 200 miles from the east shore of Georgian Bay to Villeneuve Township, in the Laurentian highlands of Quebec north of Ottawa. Uraninite in pegmatite also occurs at Lac Pied des Monts, near Murray Bay, Quebec, and in the McLear pegmatite, near Richville Station, St. Lawrence County, New York.

The age of the uraninite from six occurrences in the western part of the Grenville subprovince as determined from chemical analyses prior to 1939, ranged from 985 to 1204 million years. The average age was 1088 million years (Table 1). For these it was assumed that the amount of common lead present was negligible. The age of the uraninite or uranoan thorianite from eight districts in the same western zone, determined since 1939 using the mass spectrograph to ascertain the content of the lead isotopes, range from 960 to 1310 million years, but the average age, 1094 million years, is practically the same as that determined by the older method using chemical analyses only (Table 2). The single exception to the average age of 1094 million years for the uraninite in the western part of the Grenville subprovince is that of the Besner property, in Henvey Township, Parry Sound district at the northeast extremity of Lake Huron. Three chemical analyses of this uraninite by Ellsworth (1932, p. 105) gave it an average age of 806 million years. Later determinations from lead isotopes or from lead isotopes combined with chemical analyses indicate that the uraninite has a maximum age of 940 and an average age of 843 million years (Table 2). Ellsworth stated (1931, p. 578; 1932, p. 103; personal communication), however, that the uraninite is altered. There are therefore two possible explanations for its apparent younger age: (1) the pegmatite in which the uraninite occurs is a Late Precambrian intrusion, or (2) the age determinations of the uraninite because of alteration are geologically erroneous. The preponderance of evidence favors the last alternative.

The average age of more than 1050 million years for the uraninite in the western part of the Grenville subprovince is presumably also the approximate age of both the pegmatite

in which it occurs and the post-Hastings or Ottawa mountain building to which the pegmatite is probably related, but it is not the age of the Hastings or the rocks that have been called Grenville Series, for these may have been deposited hundreds of millions of years before the mountain building occurred. The ages of the uraninite so far discovered in the Grenville subprovince indicate that all these occurrences are probably related to a single late Archean orogeny. The presence of abundant boulders of granite in the basal Hastings conglomerate shows, however, that an earlier pre-Hastings orogeny followed by deep erosion also occurred in the region.

TABLE 1.—AGE OF URANINITE IN THE GRENVILLE SUBPROVINCE FROM CHEMICAL ANALYSES

| Locality | Ages | References | Averages |
|---|---|---|---|
| Conger Township, Ontario | 1077 1077 1019 | Ellsworth (1932, p. 105) | 1057 |
| Butt Township, Ontario | 1045 1037 1045 985 | Ellsworth (1932, p. 105) | 1028 |
| Cardiff Township, Ontario | 1100 1195 | Ellsworth (1932, p. 105) | .... |
| | 1050 | Todd (*in* Walker 1924, p. 43–44) | .... |
| | 1127 | Wells (*in* Baxter and Bliss, 1930) | .... |
| | 1204 1110 | Hecht and Rohrig (*in* Shaub, 1940, p. 484) | .... |
| | 1116 1100 | Alter and Kipp (1936, p. 126) | .... |
| | 1137 1142 | Hecht and Kroupa (1937, p. 56) | 1128 |
| March Township, Ontario | 1150 | Ellsworth (1932, p. 106) | 1150 |
| Derry Township, Quebec | 1057 | Ellsworth (1932, p. 105) | 1057 |
| Villeneuve Township, Quebec | 1100 | Hillebrand (1891, p. 390) | .... |
| | 1100 1117 | Ellsworth (1932, p. 105) | 1108 |
| Average | | | 1088 |
| Lac Pied des Monts, Saguenay district, Quebec | 1130 | Ellsworth and Osborne (1934, p. 424) | 1130 |
| Richville Station, St. Lawrence County, New York | 1094 | Shaub (1940, p. 485) | 1094 |
| Henvey Township, Ontario | 835 792 792 | Ellsworth (1932, p. 105) | 806 |

*Pre-Cobalt Series unconformity in the Timiskaming and Southern subprovinces.*—The original Cobalt Series in the Lake Timiskaming region, except where faulted, lies horizontally or with low angles of dip upon the highly folded older formations and the igneous rocks by which these are intruded. This pre-Cobalt Series unconformity has been correlated with that beneath the Chibougamau Series 300 miles northeast (Barlow *et al.*, 1911, p. 121–122; Retty, 1929, p. 57–58; Mawdsley and Norman, 1935, p. 41–48). In the territory southwest from Lake Timiskaming, W. H. Collins (1937) concluded that the rocks north of Lake Huron mapped as Huronian by Murray (1847) form two sedimentary groups, the Bruce Series and the Cobalt Series, separated by an erosional unconformity. He also concluded that the Bruce Series thins out toward the northeast, so that the pre-Cobalt Series erosion interval in the Timiskaming region represents a union of two unconformities; but the pre-Bruce (pre-Huronian of Murray) unconformity many years before had been correlated (Irving, 1887, p. 214–216; Pumpelly and Van Hise, 1892, p. 226–231) with that below the Marquette and similar Huronian groups in the region south of Lake Superior. Thus it seemed to be established that the pre-Cobalt Series unconformity extends for more than 900 miles from the Penokee district in the southern subprovince to Lake Chibougamau at the northeast end of the Timiskaming subprovince. The recent work of Thomson (1953, p. 18) in the Sudbury district, however, indicates a possible change in the succession of formations in the region north of Lake Huron, for fol-

lowing a detailed examination of Baldwin Township, southwest of Sudbury, he suggests that the rocks of that area resemble the Timiskaming and concludes that "This study has shown that Collins' stratigraphic sequence in the eastern part of the north shore of Lake Huron is open to question because it is incorrect in one of the key townships along this sedimentary belt". Notwithstanding the possible changes that may result from the new, more detailed work of Thomson and his associates, it is reasonably certain that the pre-Cobalt erosion interval is present somewhere in the Precambrian succession of the Lake Huron-Sudbury area and in the region south of Lake Superior.

A considerable number of physicochemical age determinations of pitchblende (C. B. Collins *et al.*, 1954, p. 9), galena (Cumming *et al.*, 1955, p. 59–62; Shillibeer and Cumming, 1956, p. 66–70), uraninite-bearing ores (Stieff *et al.*, 1956), and micas (Wetherill *et al.*, 1957) in the Timiskaming subprovince have been recorded in recent years, but so many of these are variable for mineral occurrences of the same type or are so much at variance with geological evidence (Lang, 1952, p. 23) or are designated anomalous that their reliability is doubtful. In western Quebec east of the Quebec-Ontario boundary, the post-Hastings (post-Grenville) potassic granite is so nearly continuous with the post-Timis-

TABLE 2.—AGE OF URANINITE OR URANOAN THORIANITE IN THE GRENVILLE SUBPROVINCE FROM LEAD-ISOTOPE, LEAD-ISOTOPE-URANIUM, OR LEAD-ISOTOPE-THORIUM RATIOS

| Locality | Ages | | | References | Average |
|---|---|---|---|---|---|
| Conger Township, Ontario | 1003 | 1030 | | Nier *et al.* (1941, p. 113) | .... |
| | 993 | 995 | 1000 | Wasserburg *et al.* (*in* Faul, 1954, p. 274) | .... |
| | 1050 | | | Shillibeer and Cumming (1956, p. 60) | 1012 |
| Butt Township, Ontario | 960 | 980 | 1020 | Shillibeer and Cumming (1956, p. 59) | |
| | 1150 | | | | 1027 |
| Cardiff-Monmouth Townships, Ontario (Wilberforce) | 1035 | 1077 | | Nier (1939b, p. 159) | .... |
| | 1025 | 1032 | 1090 | Collins *et al.* (1952, p. 23) | .... |
| | 1040 | 1100 | | Collins *et al.* (1954, p. 10) | .... |
| | 1002 | 1020 | 1026 | Wasserburg and Hayden (*in* Faul, 1954 p. 274) | .... |
| | 1045 | | | Wanless (Personal communication) | .... |
| | | | | Robinson and Sabine (1955, p. 631) | 1045 |
| Faraday Township, Ontario | 1045 | | | Wanless (Personal communication) | .... |
| | | | | Robinson and Sabine (1955, p. 631) | 1045 |
| Dungannon Township, Ontario | 1045 | | | Wanless (Personal communication) | .... |
| | | | | Robinson and Sabine (1955, p. 631) | 1045 |
| Bathurst Township, Ontario | 1310 | | | Cumming *et al.* (1955, p. 51) | .... |
| | 1080 | | | Shillibeer and Cumming (1956, p. 58) | 1195 |
| Huddersfield Township, Quebec | 1190 | | | Wanless (Personal communication) | .... |
| | | | | Robinson and Sabine (1955, p. 631) | 1190 |
| Wakefield Township, Quebec | 1090* | | | Wanless (Personal communication) | .... |
| | | | | Robinson and Sabine (1955, p. 631) | 1090 |
| Average | | | | | 1094 |
| Lac Pied des Monts, Saguenay District, Quebec | 920 | | | Muench (1939, p. 2742) | .... |
| | 882 | 905 | | Nier (1939b, p. 159) | .... |
| | 950 | 970 | 1000 | Cumming *et al.* (1955, p. 56) | 938 |
| Henvey Township, Ontario (Besner mine) | 765 | 825 | 787 | Nier (1939b, p. 159) | .... |
| | 860 | 770 | 800 | Cumming *et al.* (1955, p. 52) | 824 |
| | 845 | 940 | | | |

* Not corrected for $Pb^{204}$

kaming potassic granite farther north that both were probably intruded as part of the same mountain-building revolution. The Timiskaming Series, however, was probably deposited earlier in the preceding intertectonic interval than the rocks classed as Grenville beneath the Animikie in the region northwest of Lake Superior is equivalent to that beneath the Cobalt Series on Lake Timiskaming. The northern Precambrian rocks are then classified according to their lithological and structural similarity to those in the southern

TABLE 3.—AGE OF URANINITE IN PEGMATITE IN NORTHWEST SUBPROVINCE AND IN NORTHERN PARTS OF CANADIAN SHIELD FROM LEAD-ISOTOPE OR LEAD-ISOTOPE-URANIUM RATIOS

| Locality | Ages | | | | References | Average |
|---|---|---|---|---|---|---|
| Huron claim, southeast Manitoba | 2200 | 2468 | 1564 | 1985 | Nier (1939b, p. 158–159) | 2054 |
| | | | | | Collins *et al.* (1954, p. 19) | .... |
| | 2535 | 2580 | | | Cumming *et al.* (1955, p. 64) | 2557 |
| | 1860 | 2170 | 2505 | 1360 | Kulp and Eckelmann (1957, p. 162) | 1974 |
| Viking Lake, Saskatchewan | 1850 | 1880 | | | Wasserburg and Hayden (1955, p. 56) | 1865 |
| | 1525 | 1720 | 1870 | (445) | Kulp and Eckelmann (1957, p. 157) | 1705 |
| Charlebois Lake, Saskatchewan | 1780 | 1800 | | | Russell *et al.* (1953, p. 1224) | 1790 |
| Lee Lake, Lac La Ronge | 1740 | | | | Russell *et al.* (1953, p. 1224) | 1740 |
| | (565) | (868) | 1750 | | Kulp and Eckelmann (1957, p. 162) | 1750 |

Series (M. E. Wilson, 1956, p. 1423). No age of uraninite in pegmatite has been reported to date (May 31, 1957) from this region. The presence of granitic boulders in the Timiskaming conglomerate indicates that an earlier pre-Timiskaming orogeny also occurred in the Timiskaming subprovince. Tyler *et al.* (1940) investigated the bearing of the accessory-mineral content of igneous and sedimentary rocks on the relationship of the Precambrian formations of the regions northwest and south of Lake Superior in considerable detail, and Marsden (1955) extended this investigation to the territory north of Lake Huron. The full significance of these studies will not be known until the detailed examination of the Lake Huron-Sudbury region is completed. A pebble of granite from the Timiskaming Series in western Quebec submitted to Tyler by the writer, as might be anticipated, contained the "hyacinth" variety of zircon characteristic of the pre-Huronian granites of the southern subprovince.

*Pre-Cobalt Series unconformity in the northwestern subprovince and northern parts of the Canadian Shield.*—The classification of the rocks in the northern parts of the shield begins with the assumption that the unconformity part. Thus the folded lavas and sediments resembling the Keewatin or pre-Timiskaming and Timiskaming are placed in the Archean, an assignment confirmed in places by physicochemical age determinations (Table 3). The three types of rock assemblage that follow are classed as Proterozoic: (1) the Coppermine River (O'Neill, 1924, p. 23–24; Jenny, 1954), Athabasca (Tyrrell, 1895, p. 17–18), Et-Then (Stockwell, 1932, p. 59), and Dubawnt (Tyrrell, 1896, p. 171–174; Lord, 1953, p. 5–6; Wright, 1955, p. 8–11, 1956, p. 12–14) groups in the western and northern parts of the shield; (2) the Belcher Islands (Moore, 1918; Young, 1921), Nastapoka Islands (Low, 1900b, p. 8–13), Richmond Gulf (Low 1900a, p. 72–80; Leith, 1910), Mistassini (Neale, 1952; Wahl, 1953; Neilson, 1953), Labrador-Quebec (Gill *et al.*, 1937; Retty and Moss 1951; Harrison, 1952; Auger, 1954), and similar groups in the eastern part of the shield; and (3) the Epworth (O'Neill, 1924, p. 21–22; Jenny, 1954, p. 16), Goulburn (O'Neill, 1924, p. 23; Wright, 1956, p. 10–11), Great Slave (Stockwell, 1932, p. 55–58), Nonacho (Henderson, 1937, p. 6–17), and Snare (Lord, 1942, p. 17–23) groups in the Northwest Territories. In addition, immense areas of rock in the

shield are designated Archean and/or Proterozoic.

Some of the most noteworthy features of the formations in the northern part of the shield shown as Proterozoic on the geological map of Canada are:

(1) Almost all include interbedded lava flows of basic composition and are intruded by dikes, sills, or masses of gabbro or diabase.

(2) The rocks of the Coppermine River type (class 1) resemble the Keweenawan Series of the Lake Superior region. Except for a zone of folded and faulted rocks on the north shore of Lake Athabasca mapped as Athabasca Series or Group (Alcock, 1936, p. 23–24; Christie, 1953, p. 48–55; Tremblay, 1955; Blake, 1955, p. 6–10), they are mainly flat-lying or gently dipping.

(3) The Proterozoic Nastapoka, Labrador-Quebec, and similar rock groups (class 2), like the Animikie Series of the region northwest of Lake Superior, include iron formation and concentric, Cryptozoon-like structures in limestone or dolomite. They have been subjected to widely varying degrees of deformation. The Nastapoka Islands and Richmond Gulf groups, along the west coast of Hudson Bay, strike north and dip gently west (Low, 1900b, p. 13; 1900a, p. 88). The strata of the Belcher Islands Group farther west also strike north but are folded. They "in general have comparatively low angles of dip in the axial areas, whereas on the limbs of folds high angles of dip up to vertical are common" (Young, 1921, p. 16). The rocks of the Labrador-Quebec belt strike northwest to north in the middle and northern parts of the belt but bend westward at its south end. Along the western border the strata dip gently east but are folded and thrust to the west with increasing intensity eastward (Harrison, 1952, p. 15–17; Auger, 1954, p. 531). In the Wabush Lake and Mount Wright areas at the south end, they have been recrystallized and intruded by granite (S. Duffell, personal communication). The sediments of the Mistassini group, which lie about 100 miles southwest of Mount Wright, throughout most of their area dip gently southeast. They are moderately folded and faulted, however, along their southeast margin. It is possible that this deformation is the southwesterly attenuated end of the Labrador-Quebec orogeny. The Cape Smith Group of lavas and sediments which extends across the northern end of the Ungava peninsula are highly folded and intruded by diorite and granite. Gunning (1933, p. 154) concluded that they were probably Early Precambrian. Possibly they are a part of the Labrador-Quebec Group and are Proterozoic (Harrison, personal communication).

(4) The rocks of the Great Slave type (class 3) are intermediate in character between the Coppermine River and Animikie-like groups. They consist mainly of clastic sediments interbedded with limestone and dolomite in which concentric, Cryptozoon-like forms occur in places. They include little or no iron formation and are separated from the Coppermine River strata by an unconformity.

The ages of a considerable number of rocks in the region northwest of Lake Superior and the northern parts of the shield have been estimated by physicochemical methods. In the northwest subprovince, age determinations of uraninite (Table 3) and lepidolite in pegmatite along the Winnipeg River in southeast Manitoba (Davis and Aldrich, 1953, p. 380; Ahrens, 1955, p. 156; Aldrich, L. T., 1956, p. 121) range from 1564 to 3300 million years, but most of these are more than 2200 million years. In Minnesota age determinations of biotite in granite or muscovite in pegmatite (Goldrich *et al.*, 1956) suggest that granitic rocks 2400 to 2500 and 1600 to 1800 million years old respectively exist in this region. The presence of granites of two ages in northern Minnesota and the adjacent parts of Ontario to the north is in accord with geological observations (Lawson, 1913, p. 4), but the classification of the Vermilion Granite in Minnesota as old from the potassium-argon ratio of its biotite conflicts with its relationships as described by geologists.

In the northern parts of the shield physicochemical age determinations by five methods have been reported to date (May 31, 1957). The most numerous of these have been from pitchblende deposits occurring in the Goldfields belt on the north shore of Lake Athabasca, Saskatchewan, and in the Great Bear, Hottah, Contact, and Beaver Lodge lakes region in the Northwest Territories. In the Goldfields area Robinson (1955, p. 83, 86–92) concluded from 27 older and 30 new age determinations that "the earliest introduction of uranium in epigemetic deposits probably occurred between 1500 and 1600 million years ago", and "marked grouping of ages suggests that there may have been well-defined periods of mineralization. . . .1400–1600, 850–950, and 230–350 millions of years ago". Additional determinations by Eckelmann and Kulp (1956, p. 35–45) show that the apparent ages

of the pitchblende at Goldfields range from 220 to 1860 million years. But the deposits occur in part in relatively unmetamorphosed rocks classed as Athabasca group (Alcock, 1936, p. 21–24; Christie 1953, p. 48–55; Tremblay, 1955) believed to be of late Proterozoic age. It must be concluded, therefore, that (1) the rocks mapped as Athabasca Group at Goldfields are older than the undeformed original Athabasca south of Lake Athabasca (McConnell, 1893, p. 51); or (2) the rocks of the Athabasca Group are much older than their geological relations seem to indicate; or (3) the physicochemical age determinations, although possibly right for the pitchblende, are geologically erroneous. The second possibility implies that the Athabasca, Dubawnt, Coppermine River, and Et-Then groups are all older than the similar Keweenawan of the Lake Superior region, and, except for the moderate deformation in the Goldfields area, no mountain building has occurred in the western part of the Canadian Shield for more than 1600 million years.

Physicochemical age determinations of pitchblende in the Great Bear Lake area range from 1015 to 1500 million years (Nier, 1939b, p. 159; Collins *et al.*, 1954, p. 6; Cumming *et al.*, 1955, p. 74–77; Kulp and Eckelmann, 1955). Pitchblende deposits at Contact, Beaver Lodge, and Hottah lakes, on the other hand, have ages ranging from 330 to 879 million years (Kulp *et al.*, 1953, p. 21; Collins *et al.*, 1954, p. 6, 8); Cumming *et al.*, 1955, p. 73–74). The pitchblende-bearing veins cut across dikes of massive gabbro or diabase that intrude the folded lavas and sediments of the Echo Bay and Snare groups and the little-disturbed Hornby sediments, all classed as Proterozoic (Kidd, 1932, p. 4; Murphy, 1948, p. 261; Henderson, personal communication). The pitchblende was, therefore, almost certainly deposited after all mountain building in the area and probably during the late Precambrian (Henderson 1948, p. 48–54).

Other physicochemical age determinations in the northern parts of the shields have been recorded from uraninite, feldspar, mica, and galena. Uraninite in pre-Great Slave Group diorite (Barnes, 1952, p. 5–8; Lang, 1952, p. 63–64) at Stark Lake on the south side of the northeast arm of Great Slave Lake has been determined to be 1860 million years old (Cumming *et al.*, 1955, p. 70). Most uraninite in pegmatite intruding either the Tazin Group or post-Tazin Group granite at Viking, Charlebois, and Lee lakes in Saskatchewan is estimated to be from 1525 to 1880 million years old (Table 3). These determinations are possibly in accord with the Archean age to which the pegmatite has been assigned by geologists, but they conflict in part with the older ages of the pitchblende of the Goldfields belt (Collins *et al.*, 1952, p. 21–22; Christie, 1953, p. 9; Robinson, 1955, p. 86–87; Eckelmann and Kulp, 1956, p. 44). Physicochemical age determinations of feldspar from four localities in northern Saskatchewan by the potassium-argon method range from 1160 to 1950 million years (Shillibeer and Russell, 1954, p. 690; Wasserburg and Hayden, 1955, p. 55; Mawdsley and Farquhar, 1955, p. 41; Cumming *et al.*, 1955, p. 67–71). Three of these ages do not differ greatly from that of uraninite in the same pegmatite dikes (Table 3), but the 1150 and 1470 potassium-argon age determinations of feldspar in pegmatite at Foster Lake are considerably younger. Eight potassium-argon age determinations from seven localities (Folinsbee, 1955, p. 20; Folinsbee *et al.*, 1956, p. 62) have been reported from the Yellowknife subprovince (A. W. Jolliffe, 1948, p. 143) Most of these, however, were experimental, because: (1) the assumption of two decay constants for each determination resulted in age differences of 45 to 330 million years; (2) the determinations were made partly from unseparated rock (Reynolds, 1956, p. 141) and partly from one or more mineral constituents; and (3) Reynolds states (p. 143) "it would appear that work with separated micas offers the best possibility for reliable dating of rocks and minerals by the potassium-argon method", but only one of the eight determinations was from mica alone. Age determinations of galena from its lead isotopes have been recorded from widely scattered areas in the northern parts of the shield. Some of this galena is in rocks mapped indefinitely as either Archean or Proterozoic; its age in such cases cannot be checked by geological observation. Galena at Nesbitt Lake in the Goldfields belt on the north shore of Lake Athabasca has been determined to have about the same age as the oldest pitchblende in that area (Cumming *et al.*, 1955, p. 69); galena in pre-Great Slave Group diorite at Stark Lake has a physicochemical age of 1245 to 1300 million years compared with 1860 million years for uraninite from the same locality (Table 3). In the Yellowknife region galena in nine gold-bearing veins of quartz has been determined to range from 2130 to 2500 million

years (Cumming *et al.*, 1955 p. 71–72), whereas in two outlying veins at Indin and Indian Mountain lakes, the ages of the galena are 800 and 1335 million years (Cumming *et al.*, 1955, p. 68–69) respectively. Most of the geologists who have carried on geological work extensively in the Great Slave-Great Bear Lake region (Stockwell, 1932, p. 46c; Lord, 1941, p. 18; Henderson, 1948, p. 50; A. W. Jolliffe, 1948, p. 142) agree that granitic rocks of two widely different ages occur in that territory, but the galena-bearing veins occur in the lavas and sediments of the Yellowknife group, the oldest rocks in the district, and are therefore possibly related directly (Folinsbee *et al.*, 1956, p. 63) or indirectly (Boyle, 1954, p. 74–75) to the granitic intrusions of earlier age. Thus the nine lead-isotope age determinations of galena, within their range of 370 million years, are in accord with the known geology of the area. Nevertheless, so many of the galena-isotope ages in the southern part of the shield are designated anomalous or are contrary to geological evidence that there is doubt regarding the accuracy of this method of age determination.

FIGURE 1.—GEOLOGICAL PROVINCES OF THE CANADIAN SHIELD

*Limitations of Serial and Group Correlation*

The Canadian Shield has been divided into geological provinces and subprovinces on various bases. Van Hise and Leith (1911, p. 597–615) in their discussion of correlation called the regions northwest and south of Lake Superior the northern and southern subprovinces. The writer (1918b) proposed the names Timiskaming and Grenville for two additional subprovinces in the southeastern part of the shield and suggested that serial names such as Keewatin and Timis-

kaming be restricted to the subprovince in which they were originally proposed (Fig. 2), because: (1) much of the geological mapping in these regions had been lithological rather than structural and (2) geographical and geological barriers prevented direct correlation between them. The above-named subprovinces include most of the Precambrian parts of the St. Lawrence basin and therefore together can appropriately be called the St. Lawrence province. In 1939 (p. 237–239) and 1941 (p. 274–276) the writer pointed out that the Canadian Shield is divided naturally into five regions or provinces in which the relationships of formations because of their proximity to one another can be determined in greater detail than is possible for regions separated by wide stretches of water, by Paleozoic or later sediments, or by belts of complex gneisses (Fig. 1).

Gill (1949, p. 61–65) attempted to divide the Canadian Shield into provinces using the structural trends of formations as a standard, and J. T. Wilson (1949, p. 179–182; Umbgrove, 1947, p. 144–216; Cumming *et al.*, 1955, p. 46) proposed a division of the shield based on physicochemical age determinations which he believes support the hypothesis that the shield has grown by successively younger mountain building from its core outward. More recently Gill (1952, 1955) stated objections to widespread correlation that in part at least are the same as those cited by the writer in 1918. In the present state of knowledge the division of the Canadian Shield into provinces based on structural trends or scattered physicochemical age determination, in contrast with those of Figure 1, are speculative.

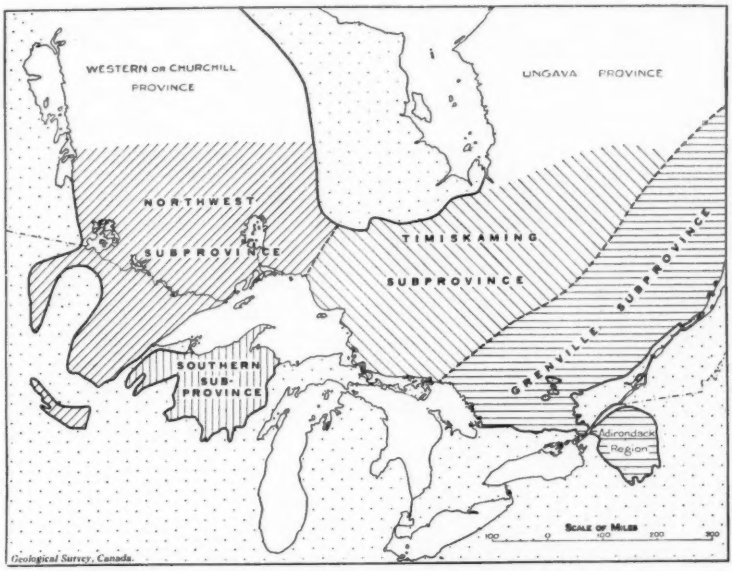


FIGURE 2.—SUBPROVINCES OF THE ST. LAWRENCE GEOLOGICAL PROVINCE

### *Major Divisions of the Precambrian in the Canadian Shield*

*General statement.*—Archean and Algonkian, as names for major divisions of the Precambrian, have been in use in the Lake Superior region since 1890, and the equivalent terms, Archean and Proterozoic, have been officially in use in Canada since 1935. The changes to Earlier, Medial, and Later Precambrian in the region northwest of Lake Superior by Grout *et al.* (1955) and to Lower, Middle and Upper Precambrian in northern Michigan by James (1955) presumably are proposed to replace the older dual names, but the word Precambrian in these divisional titles suggests that they are applicable to the whole Canadian Shield. If the threefold classification was intended to

apply locally, only local names would normally be used.

*Keweenawan and Animikie types.*—(1) The Coppermine River, Dubawnt, Et-Then, Athabasca, and similar groups in the western part of the shield resemble the Keweenawan in the following respects: (a) in most places they have the characteristics of terrestrial deposits (Van Hise and Leith, 1911, p. 414–418); (b) they rest, for the most part, on an eroded surface of low or moderate relief; (c) except for local moderate deformation, as in the Lake Athabasca and the Lake Superior basins, they have not been folded; (d) they lie at the top of the Precambrian succession in their respective localities. It is reasonably certain, therefore, that they are all of Late Precambrian age and were probably deposited during the same cycle of erosion and deposition (Stockwell, 1932, p. 59; Alcock, 1936, p. 10–13). According to Atwater and Clement (1935, p. 1684–1686) a structural unconformity separates the Keweenawan rocks from upper Cambrian sandstone, but this interval of erosion and deformation is probably not great enough (Grout *et al.*, 1951, p. 1063) for the Keweenawan Series to be more than 1600 million years old, as suggested by age determinations of pitchblende in rocks mapped as Athabasca group at Goldfields, Saskatchewan.

(2) The iron-bearing sediments of the Belcher Islands, Nastapoka Islands, Richmond Gulf, Labrador-Quebec, Mistassini, and similar groups occurring in the eastern part of the shield have certain features in common: (a) they rest with great structural unconformity on highly folded surficial rocks intruded by granite; (b) they are lithologically similar; (c) either they have not been mountain built, or where deformation occurs, as in the Labrador-Quebec group, it ranges in intensity from almost nil to complete recrystallization; (d) they closely resemble the Animikie of the Lake Superior region, which as noted by many geologists (Van Hise and Leith, 1911, p. 499–528; Gruner, 1922, p. 459–460; Gill, 1927, p. 726–728; H. R. Aldrich, 1929, p. 135–180; Moore and Maynard, 1929, p. 524–527; Leith, Lund, and Leith, 1935, p. 21–23) were deposited under special environmental conditions that apparently reached their climax in Late Precambrian time. Therefore, it is probable that they have been properly classified as Proterozoic on the geological map of Canada.

(3) Grout *et al.* (1951, p. 1021) place the Animikie and Keweenawan together in a Later Precambrian era, whereas James (1955, p. 1459) classifies only the Keweenawan as Upper Precambrian. If the Animikie is equivalent to part or all of the Huronian of Michigan (Leith, Lund, and Leith, 1935, p. 15; Grout *et al.*, 1951, p. 1069–1072) James' classification conflicts with that of the Minnesota geologists. The rocks of the Animikie and Keweenawan types in the shield considered as a whole with reasonable certainty belong structurally in the same major division or era as the Archean-Proterozoic dual classification assumes. Their widely separate distribution in opposite parts of the shield makes more restricted classification doubtful.

(4) The dual division of the Precambrian implies that the pre-Animikie unconformity extended over most of the Canadian Shield, an assumption that Gill recently (1955) questioned. Gill is almost certainly right in pointing out that mountain building did not occur simultaneously over the shield, but a widespread unconformity does not demand this. All that is required is a prolonged period of erosion and crustal stability, a condition that existed prior to the Paleozoic submergence and probably extended backward into Precambrian time, as shown by the nearly flat-lying attitude of rocks of the Animikie and Keweenawan types throughout so much of the shield.

*Timiskaming and pre-Timiskaming Types.*—The rocks at the base of the Precambrian succession in the Canadian Shield nearly everywhere consist of lava and graywacke or other clastic sediments and are overlain with structural unconformity in places by lithologically similar rock groups of the Timiskaming or Knife Lake types. The abundance of clastic sediments in these groups and the occurrence of pillow structure in the lavas indicate that they were probably laid down in the sea adjacent to mountains (Pettijohn, 1943, p. 963–968; M. E. Wilson, 1956, p. 1423–1426). The genetic similarity of these groups is not necessarily evidence that they were deposited similtaneously throughout the shield, but possibly it lends some support to their classification together as Early Precambrian or Archean. It is noteworthy, however, that (a) the Timiskaming Series of western Quebec and northeastern Ontario resembles the Knife Lake group of the northwest subprovince, and (b) the Knife Lake rocks are so different lithologically from the Huronian south of Lake Superior that their

correlation is doubtful. Possibly, therefore, the Middle Precambrian of James (1955) in Michigan is not the equivalent of the Medial Precambrian of the Minnesota geologists.

*Grenville, Kisseynew, and Great Slave types.*—(1) In addition to the rock groups already mentioned, folded sediments of the well-sorted or moderately well-sorted types occur in places in the shield. Examples of these classed as Archean on the geological map of Canada are: the Grenville or Hastings group, which occurs extensively in the southeastern part of the shield, the Kisseynew gneisses in Manitoba, and the Tazin Group in Saskatchewan. Examples mapped as Proterozoic are: the Great Slave and Snare groups in the Northwest Territories, and the Lower Huronian or Bruce Series on the north shore of Lake Huron. The sorted character of these sediments and the presence in them of limestone indicates that they are of marine origin and were presumably deposited on a continental shelf adjacent to land of low or moderate relief. However, the proportion of limestone in the Grenville or Hastings is much greater than in all the other groups of this class. It is scarcely possible for well-sorted sediments to be deposited in the sea contemporaneously near sediments of the piedmont type, of which those of the Timiskaming and pre-Timiskaming groups are typical examples, but simultaneous deposition could occur in widely separate localities.

(2) The relationship of the Lower Huronian or Bruce Series to the Cobalt Series (W. H. Collins, 1937, p. 1442–1444) and Grenville (Hasting?) Series has been recently discussed by the writer (1956, 1422–1423), and only three items are mentioned here: (a) The Cobalt Series on Lake Timiskaming rests unconformably on granite intruding the Grenville (Hastings?) Series. For this reason Quirke's suggestion (1926) that the Bruce and the Grenville are parts of the same series is not possible unless a major unconformity separates the Bruce Series from the Cobalt Series. (b) Wetherill *et al.* (1957) report that ages of biotite in Killarney granite at Wavy Lake south of Sudbury determined by the rubidium-strontium and potassium-argon methods are 1075 and 1025 million years respectively. If these are reliable, the Killarney granite has about the same age as the post-Grenville (Hastings?), pre-Cobalt granite to the northeast on Lake Timiskaming. (c) The rocks of the original Huronian (Cobalt Series) on Lake Timiskaming and northward, except where faulted, dip at low angles, are wholly clastic, and are believed to be of glacial or interglacial origin. The Huronian rocks on the north shore of Lake Huron, called Bruce and Cobalt Series by W. H. Collins (1914, p. 98–104), are highly to moderately folded (W. H. Collins, 1925, p. 99–101; Roscoe, 1956).

## Conclusions

(1) Only a small part of the folded surficial rocks of the Canadian Shield has been mapped in structural detail. Their positive classification, therefore, must await a more detailed investigation of their structural history. However, because such a large part of its formations belongs to either the very early or very late Precambrian, an approximately dual classification is possible.

(2) Attempts to divide the rocks of the shield into more than two divisions must introduce considerable error. The replacement of the dual classification so long in use both in United States and Canada is therefore scarcely warranted at present.

(3) The Canadian Shield is divided geologically and geographically into regions separated by extensive barriers of sea, lakes, or overlying Paleozoic or later strata, across which correlation by continuity or approximate continuity of outcrop is not possible. When the detailed succession of formations in various parts of the shield is more fully known, the similarities may be sufficient for correlation across intersubprovincial or even interprovincial barriers, but until that time, it is more scientific to use local nomenclatures within these areas.

(4) Numerous physicochemical age determinations of minerals occurring in the Canadian Shield have been published since the early work of Ellsworth (1931; 1932). These, within certain limitations, may eventually be of considerable assistance in the age classification of its rocks, but at their present stage, their reliability is uncertain, and a careful, objective evaluation of the various methods proposed is necessary before they can be accepted with assurance. Furthermore, when their reliability is established, thousands of age determinations covering all parts of the shield will be required before they can be fully utilized in shield rock classification. The limitations to the determinations are: (a) the possibility of chemical change or recrystallization is much greater for Precambrian minerals

than for those of later age; (b) most of the minerals used for age determination are related genetically to igneous intrusion or mountain building, and these may occur hundreds of millions of years after the deposition of the intruded or mountain-built surficial rocks; (c) because mountain building is usually local or linear (Gill, 1955; M. E. Wilson, 1918b, p. 331–332) the area of each age determination is restricted.

S. C. Robinson, who as chief of the Mineralogical Division of the Geological Survey of Canada supervises its mass spectrograph investigations, kindly read the physicochemical parts of this paper and gave the writer the following comment:

"For some minerals the ages are apparently correct, for most minerals the ages are of the correct order. The principal uncertainties are: (1) poor sampling; (2) use of grab samples taken without consideration of the degree of weathering or other alteration; and (3) lack of mineralogical and geological interpretation.

"It is essential that the reliability of the physicochemical ratio as resolved into an apparent age be fully evaluated, geologically, mineralogically, and physically before interpretation of its true geological significance can be established. Too often geologists send in poor samples, and too often physicists make unjustified assumptions in assessing the meaning of the ages they determine. A well disciplined team approach to the problem is imperative."

## Bibliography


Ahrens, L. H., 1955, Oldest rocks exposed, p. 155–168 *in* Poldervaart, Arie, *Editor*, Crust of the earth: Geol. Soc. America Special Paper 62, 762 p.

Alcock, F. J., 1920, The Athabasca Series: Am. Jour. Sci., 4th ser., v. 50, p. 25–32

——1934, Report of the national committee on stratigraphical nomenclature: Royal Soc. Canada Trans., 3rd ser., v. 28, sec. 4, p. 113–121

——1936, Geology of the Lake Athabasca region, Saskatchewan: Geol. Survey Canada, Mem. 196, 41 p.

——1947, Geology and economic minerals of Canada, 3rd ed.: Geol. Survey Canada, Economic Geology ser., no. 1, p. 98–155

——1948, Problems of New Brunswick geology: Royal Soc. Canada Trans., 3d. ser., v. 42, sec. 4, p. 1–15

Aldrich, H. R., 1929, The geology of the Gogebic iron range of Wisconsin: Wis. Geol. Nat. Hist. Survey Bull 71, 279 p.

Aldrich, L. T., 1956, Nuclear processes in geological settings: Nat. Acad. Sci.-Nat. Research Council Nuclear Sci. Ser. Rept. 19, p. 121

Aldrich, L. T., Davis, G. L., Tilton, G. R., Wetherill, G. W., and Jeffrey, P. M., 1956, Evaluation of mineral age measurements, I, Nuclear processes in geologic settings: Nat. Acad. Sci.-Nat. Research Council Nuclear Sci. ser. Rept. 19, p. 147–150

Alter, C. M., and Kipp, E. M., 1936, The variation of the lead-uranium-thorium ratio of a single crystal of Wilberforce, Ontario uraninite, Am. Jour. Sci., v. 32, p. 120–128

Atwater, G. I., and Clement, G. M., 1935, Precambrian and Cambrian relations in the upper Mississippi Valley: Geol. Soc. America Bull., v. 46, p. 1659–1686

Auger, P. E., 1954, The stratigraphy and structure of the northern Labrador trough, Ungava, New Quebec: Can. Min. Metall. Bull. 508, p. 529–532

Barlow, A. E., 1897, Report on the geology and natural resources of the area included by the Nipissing and Timiskaming map-sheets, comprising portions of the district of Nipissing, Ontario, and of Pontiac county, Quebec: Geol. Survey Canada Ann. Rept., v. 10, pt. i, 302 p. (1899)

Barlow, A. E., Gwillim, J. C., and Faribault, E. R., 1911, Report on the geology and mineral resources of the Chibougamau region, Quebec; Quebec Dept. Colonization, Mines, and Fisheries, 224 p.

Barnes, F. Q., 1952, McLean Bay map-area, District of Mackenzie, Northwest Territories: Geol. Survey Canada Paper 52–5, 25 p.

Barrell, J., 1915, Central Connecticut in the geological past: Conn. State Geol. and Nat. Hist. Survey Bull. 23, 44 p.

Baxter, G. F., and Bliss, A. D., 1930, The atomic weight of uraninite lead from Wilberforce, Ontario: Am. Chem. Soc. Jour., v. 52, p. 4851–4853

Billings, M. P., 1945, Mechanics of igneous intrusion in New Hampshire: Am. Jour. Sci., v. 243A, p. 40–68.

——1946, Some major problems of New England geology (Abstract): Geol. Soc. America Bull., v. 57, p. 1277–1278

Blake, 1955, Geological notes on the region south of Lake Athabasca and Blake Lake, Saskatchewan and Alberta: Geol. Survey Canada Paper 55–33, 12 p.

Boyle, R. W., 1954, The shear zone systems of the Yellowknife greenstone belt: Can. Min. Jour., v. 75, pt. 2, p. 69–75

——1955, The geochemistry and origin of the gold bearing quartz veins and lenses of the Yellowknife greenstone belt: Econ. Geology, v. 50, p. 51–66

Christie, A. M., 1953, Goldfields-Martin Lake map-area, Saskatchewan: Geol. Survey Canada Mem. 269, 126 p.

Collins, C. B., Farquhar, R. M., and Russell, R. D., 1954, Isotopic constitution of radiogenic leads and the measurement of geologic time: Geol. Soc. America Bull., v. 65, p. 1–21

Collins, C. B., Lang, A. H., Robinson, S. C., and Farquhar, R. M., 1952, Age determinations for some uranium deposits in the Canadian Shield: Geol. Assoc. Canada Proc., v. 5, p. 15–41

Collins, W. H., 1914, The Huronian formations of the Timiskaming region, Canada: Geol. Survey Canada Bull. 8, 27 p.

——1916, The age of the Killarney granite: Geol. Survey Canada Bull. 22, 12 p.

——1917, Onaping map-area: Geol. Survey Canada Mem. 95, 157 p.

Collins, W. H., 1925, North Shore of Lake Huron: Geol. Survey Canada Mem. 143, 160 p.
——1937, Timiskaming subprovince: Geol. Soc. America Bull., v. 48, p. 1427–1458
Cormier, R. F., 1957, Rubidium-strontium ages of the mineral glauconite and their application to the construction of a post-Precambrian time scale: Mass. Inst. Tech., Dept. Geology and Geophysics 4th Ann. Rept., 1956–1957, p. 1–23.
Cumming, G. L., Wilson, J. T., Farquhar, R. M., and Russell, R. D., 1955, Some dates and subdivisions of the Canadian Shield: Geol. Assoc. Canada Proc., v. 7, pt. 2, p. 27–79
Dana, J. D., 1872, Green Mountain geology; on the quartzite: Am. Jour. Sci., v. 3, p. 240–256
Davis, G. L., and Aldrich, L. T., 1953, Determination of the age of lepidolites by the method of isotope dilution: Geol. Soc. America Bull., v. 64, p. 379–380
De Lury, J. S., and Ellsworth, H. V., 1931, Uraninite from the Huron claim, Winnipeg River area, southeast Manitoba: Am. Mineralogist, v. 16, p. 569–575
Dresser, J. A., and Denis, T. C., 1944, Geology of Quebec. V. 2, Descriptive geology: Quebec Dept. Mines Geol. Rept. 20, 544 p.
Eckelmann, W. R., and Kulp, J. L., 1956, Uranium-lead method of age determination: Geol. Soc. America Bull., v. 67, p. 35–53
Ellsworth, H. V., 1931, Uraninite from Henvey Township, Parry Sound district, Ontario: Am. Mineralogist, v. 16, p. 576–579
——1932, Rare-element minerals of Canada: Geol. Survey Canada Econ. Geology Ser., no. 11, 272 p.
Ellsworth, H. V., and Osborne, F. F., 1934, Uraninite from Lac Pied des Mont, Saguenay district, Quebec: Am. Mineralogist v. 19, p. 421–425
Faul, H., 1954, *Editor*, Nuclear geology: N. Y. John Wiley & Sons, 414 p.
Folinsbee, R. E., 1955, Archean monazite in beach concentrates, Yellowknife geologic province, Northwest Territories, Canada: Royal Soc. Canada Trans., 3d ser., v. 49, sect. 4, p. 7–24
Folinsbee, R. E., Lipson, J., and Reynolds, J. H., 1956, Potassium-argon dating: Geochim. Cosmochim. Acta., v. 10, p. 60–68
Gill, J. E., 1927, Origin of the Gunflint iron-bearing formation: Econ. Geology, v. 22, p. 687–728
——1949, Natural divisions of the Canadian Shield: Royal Soc. Canada Trans., 3d ser., v. 43, sec. 4, p. 61–69
——1952, Early history of the Canadian Shield: Geol. Assoc. Canada Proc., v. 5, p. 57–68
——1955, Precambrian history of the Canadian Shield: Geol. Assoc. Canada Proc., v. 7, pt. 2, p. 117–124
Gill, J. E., Bannerman, H. M., and Tolman, C., 1937, Wapussakatoo Mountains, Labrador: Geol. Soc. America Bull., v. 48, p. 567–586
Gilluly, J., 1949, Distribution of mountain building in geologic time: Geol. Soc. America Bull., v. 60, p. 561–590
Goldich, S. S., Nier, A. O. C., Baadsgaard, H., and Hoffman, J. H., 1956, K40/A40 datings of the Precambrian rocks of Minnesota (Abstract): Geol. Soc. America Bull., v. 67, p. 1698–1699
Grout, F. F., 1929, Ages and differentiation series of the batholiths near the Minnesota-Ontario boundary: Geol. Soc. America Bull., v. 40, p. 791–809
Grout, F. F., Gruner, J. W., Schwartz, G. M., and Thiel, G. A., 1951, Precambrian stratigraphy of Minnesota: Geol. Soc. America Bull., v. 62, p. 1017–1078
Gruner, J. W., 1922, The origin of sedimentary iron formations: Econ. Geology, v. 17, p. 407–460
——1941, Structural geology of the Knife Lake area of northeastern Minnesota: Geol. Soc. America Bull., v. 52, p. 1577–1642
Gunning, H. C., 1933, Sulphide deposits at Cape Smith, east coast of Hudson Bay: Geol. Survey Canada Summary Rept., pt. D., p. 139–154
Harding, W. D., 1942, Geology of Kaladar and Kennebec townships: Ont. Dept. Mines 51st Ann. Rept., pt. 4, p. 51–74
Harrison, J. M., 1952, The Quebec-Labrador iron belt, Quebec and Newfoundland: Geol. Survey Canada Paper 52–20, 21 p.
——1953, Iron formations of Ungava Peninsula: 19th Internat. Geol. Cong., Algeria, C. R., Sec. 10, F 10, p. 19–33
——1955, Nature, usage, and nomenclature of time-stratigraphic and geologic-time units as applied to the Precambrian. Am. Assoc. Petroleum Geologists Bull., v. 39, p. 1859–1861
Hecht, F., and Kroupa, A., 1937, Report of the committee on the measurement of geologic time: Natl. Research Council, p. 53–58
Henderson, J. F., 1937, Nonacho Lake area, Northwest Territories: Geol. Survey Canada Paper 37–2, 22 p.
——1939, Beaulieu River area, Northwest Territories: Geol. Survey Canada Paper 39–1, 16 p.
——1948, Extent of Proterozoic granitic intrusion in the western part of the Canadian Shield: Royal Soc. Canada Trans., 3d ser., v. 42, sec. 4, p. 41–54
Hewitt, D. F., 1956, The Grenville region of Ontario: The Grenville problem, Royal Soc. Canada Special Pub. 1, p. 22–41
Hillebrand, W. F., 1891, New analysis of uraninite: Am. Jour. Sci., 3d ser., v. 42, p. 390–393
Irving, R. D., 1887, Is there a Huronian group?: Am. Jour. Sci., 3d ser., v. 34, p. 204–216, 249–263, 365–374
——1888, Classification of early Cambrian and Precambrian formations: U. S. Geol. Survey 7th Ann. Rept., p. 365–454
James, H. L., 1955, Zones of regional metamorphism in the Precambrian of northern Michigan: Geol. Soc. America Bull., v. 66, p. 1455–1487
Jenny, C. P., 1954, The Coppermine River area, Northwest Territories, Canada: Geol. Assoc. Canada Proc., v. 6, pt. 2, p. 11–26
Jolliffe, A. W., 1948, The northwestern part of the Canadian Shield: 18th Internat. Geol. Cong. London, Rept., pt. 13, p. 141–149
Jolliffe, F., 1936, Yellowknife River area, Northwest Territories: Geol. Survey Canada Paper 36–5, 10 p.
Kidd, D. F., 1932, Great Bear Lake area, Northwest Territories: Geol. Survey Canada Summary Rept., pt. C. p. 1–36
Knopf, A., 1955, Bathyliths in time, p. 685–702 *in* Poldervaart, Arie, *Editor*, Crust of the earth: Geol. Soc. America Special Paper 62, 762 p.
Kulp, J. L., 1955, Isotopic dating and the geologic time scale, p. 609–630 *in* Poldervaart, Arie,

*Editor*, Crust of the earth: Geol. Soc. America Special Paper 62, 762 p.

Kulp, J. L., and Eckelmann, W. R., 1955, Anomalus uranium-lead ages: Geol. Soc. America Bull., v. 66. p. 767–768

——1957, Discordant U-Pb ages and mineral type: Am. Mineralogist, v. 42, p. 154–164

Kulp, J. L., Broecker, W. S., and Eckelmann, W. R., 1953, Age determinations of uranium minerals by the $Pb^{210}$ method: Nucleonics, v. II, no. 8, p. 19–21

Lang, A. H., 1952, Canadian deposits of uranium and thorium: Geol. Survey Canada, Econ. Geology Ser., no. 16, 173 p.

Lawson, A. C., 1913, The Archean geology of Rainy Lake restudied: Geol. Survey Canada Mem. 40, 115 p.

Leith, C. K., 1910, An Algonkian basin in Hudson Bay; a comparison with the Lake Superior basin: Econ. Geology v. 5, p. 227–246

Leith, C. K., Lund, E. J., and Leith, A., 1935, Precambrian rocks of the Lake Superior region: U. S. Geol. Survey Prof. Paper 184, 34 p.

LeRoy, E. O., 1901, Geology of Rigaud Mountain, Canada: Geol. Soc. America Bull., v. 12, p. 377–394

Logan, W. E., 1857, On the geology of Argenteuil and Two Mountains counties, Quebec: Geol. Survey Canada Rept. Progress, 1853–1856, 494 p.

——1863, Geology of Canada: Geol. Surv. Canada Rept. Progress to 1863, 988 p.

Logan, W. E., and Hunt, T. S., 1855, Esquisse geologique du Canada . . . . a l'exposition universelle de Paris: Geol. Survey Canada, 100 p.

Lord, C. S., 1941, Mineral industry of the Northwest Territories: Geol. Survey Canada Mem. 230, 136 p.

——1942, Snare River and Ingray Lake map-area, Northwest Territories: Geol. Survey Canada Mem. 235, 55 p.

——1953, Geological notes on southern district of Keewatin, Northwest Territories, Geol. Survey Canada Paper 53–22, 11 p.

Low, A. P., 1900a, Report on an exploration of the east coast of Hudson Bay: Geol. Survey Canada Ann. Rept., v. 13, pt. D, 84 p.

——1900b, Report on the geology and physical Character of the Nastapoka Islands: Geol. Survey Canada Ann. Rept., v. 13, pt. DD, 31 p.

Marble, J. P., 1949, Accuracy of the lead method for the absolute measurement of geologic age (Abstract): Geol. Soc. America Bull., v. 60, p. 1907

Marsden, R. W., 1955, Precambrian correlations in the Lake Superior region in Michigan, Wisconsin, and Minnesota: Geol. Assoc. Canada Proc., v. 7, pt. 2, p. 107–116

Mawdsley, J. B., and Norman, G. W. H., 1935, Chibougamau Lake map-area: Geol. Survey Canada Mem. 185, 95 p.

Mawdsley, J. B., 1950, The geology of the Charlebois Lake area: Saskatchewan Geol. Survey Rept. 5, 32 p.

Mawdsley, J. B., and Farquhar, R. M., 1955, Report of the committee on Precambrian and related dating: Royal Soc. Canada, 3d ser., v. 49, sec. 4, p. 37–45

McConnell, R. G., 1893, Report on a portion of the district of Athabasca: Geol. Survey Canada Ann. Rept., v. 5, pt. D., 67 p.

Miller, W. G., and Knight, C. W., 1913, Correlation of the Precambrian rocks of Ontario, western Quebec, and southeastern Manitoba: Ont. Bur. Mines 22d Ann. Rept., pt. 2, p. 123–138

Moore, E. S., 1912, Region east of the south end of Lake Winnipeg: Geol. Survey Canada Summary Rept., p. 262–270

——1918, The iron formation on Belcher Islands, Hudson Bay, with special reference to its origin and its associated algal limestone: Jour. Geology, v. 26, p. 412–438

Moore, E. S., and Maynard, J. E., 1929, Solution, transportation, and precipitation of iron and silica: Econ. Geology v. 24, p. 272–303, 365–402, 506–527

Muench, O. B., 1939, Pied des Monts uraninite: Am. Chem. Soc. Jour., v. 61, p. 2742–2749

Murphy, R., 1948, Eldorado mine, p. 259–268 *in* Structural geology of Canadian ore deposits: Can. Inst. Mining Metallurgy, Geol. Div., 948 p.

Murray, A., 1847, Report on the geology of the Lake Huron region: Geol. Survey Canada Rept. Prog., 1847–1848, p. 93–124

Neale, E. R. W., 1952, Bethaulat Lake area, Mistassini territory: Quebec Dept. Mines Prelim. Rept. 264, 13 p.

Nielson, J. M., 1953, Albanel area, Mistassini territory: Quebec Dept. Mines Geol. Rept. 53, 35 p.

Nier, A. O., 1939a, The isotopic constitution of uranium and the halflives of the uranium isotopes: Phys. Rev., 2nd ser., v. 55, p. 150–153

——1939b, The isotopic constitution of radiogenic leads and the measurement of geologic time: Phys. Rev., 2nd ser., v. 55, p. 154–163

Nier, A. O., Thompson, R. W., and Murphy, B. F., 1941, The isotopic constitution of lead and the measurement of geologic time: Phys. Rev., 3d. ser., v. 60, p. 112–116

O'Neill, J. J., 1924, The geology of the Arctic coast of Canada, west of Kent Peninsula: Rept. Can. Arctic Exped., v. 11, pt. A., 107 p.

Osborne, F. F., 1934, The Chatham-Grenville composite stock, Quebec: Royal Soc. Canada Trans., 3d ser., v. 28, sec. 4, p. 49–54

Pettijohn, F. J., 1943, Archean sedimentation: Geol. Soc. America Bull., v. 54, p. 925–972

Powell, J. W., 1890, U. S. Geol. Survey 10th Ann. Rept., 1888–1889, pt. 1, 774 p.

Pumpelly, R., and Van Hise, C. R., 1892, Observation upon the structural relations of the Upper Huronian, Lower Huronian, and basement complex on the north shore of Lake Huron: Am. Jour. Sci., 3d ser., v. 43, p. 224–232

Quirke, T. T., 1926, Huronian Grenville relations: Am. Jour. Sci., 5th ser. v. 11, p. 165–173

Retty, J. A., 1929, Township of McKenzie, Chibougamau region: Quebec Bur. Mines Ann. Rept., pt. D., p. 41–72

Retty, J. A., and Moss, A. E., 1951, Iron ore deposits of new Quebec and Labrador (Abstract): Econ. Geology, v. 46, p. 799–800

Reynolds, J. H., 1956, Potassium-argon dating; Nuclear processes in geologic settings: Nat. Acad. Sci.-Nat. Research Council Nuclear Sci. ser. Rept. 19, p. 135–146

Robinson, S. C., 1955, Mineralogy of uranium deposits, Goldfields, Saskatchewan: Geol. Survey Canada Bull. 31, 128 p.
Robinson, S. C., and Sabine, A. P., 1955, Uraninite and thorianite from Ontario and Quebec: Am. Mineralogist, v. 40, p. 624–633
Roscoe, S. M., 1956, Geology and uranium deposits, Quirke Lake-Elliott Lake, Blind River Area, Ontario: Geol. Survey Canada Paper 56–7, 21 p.
Russell, R. D., 1956, Interpretation of lead isotope abundances, nuclear processes in geologic settings: Nat. Acad. Sci.-Nat. Research Council Nuclear Sci. ser. Rept. 19, p. 301–309
Russell, R. D., Farquhar, R. M., Cumming, G. L., and Wilson, J. T., 1954, Dating galenas by means of their isotopic constitutions: Am. Geophys. Union Trans., v. 35, p. 301–309
Russell, R. D., Schillibeer, H. A., Farquhar, R. M., and Mousuf, A. K., 1953, The branching ratios of potassium 40: Phys. Rev., v. 9, p. 1223–1224
Satterly, J. 1942, Mineral occurrences in Parry Sound District: Ont. Dept. Mines 51st Ann. Rept., pt. 2, 86 p.
Shaub, B. M., 1940, Age of the uraninite from McLear pegmatite near Richville station, St. Lawrence county, N. Y.: Am. Mineralogist, v. 25, p. 480–487
Shillibeer, H. A., and Cumming, G. L., 1956, The bearing of age determinations on the relation between the Keewatin and Grenville provinces: Royal Soc. Canada Special pub. 1, p. 54–73
Shillibeer, H. A., and Russell, R. D., 1954, Potassium-argon method of geological age determination: Can. Jour. Physics, v. 32, p. 681–693
Stieff, L. R., Stern, T. K., Cialella, C. M., and Warr, J. J., 1956, Preliminary age determinations of some uranium ores from the Blind River area, Algoma district Ontario, Canada (Abstract): Geol. Soc. America Bull., v. 67, p. 1736–1737
Stockwell, C. H., 1932, Great Slave Lake-Coppermine River area, Northwest Territories: Geol. Survey Canada Summary Rept., pt. C. p. 37–63
Thomson, J. E., 1953, Geology of Baldwin township: Ont. Dept. Mines 61st Ann. Rept., pt. 4, 33 p.
Tremblay, L. P., 1955, Uranium City, Saskatchewan, map with marginal notes: Geol. Survey Canada Paper 55–28
Tyler, S. A., Marsden, R. W., Grout, F. F., and Thiel, G. A., 1940, Studies of the Lake Superior Precambrian by accessory mineral methods: Geol. Soc. America Bull., v. 51, p. 1429–1538
Tyrrell, J. B., 1895, Report on the country between Athabasca Lake and Churchill River: Geol. Survey Canada Ann. Rept., v. 8, pt. D, 120 p.
——1896, Report on the Doobaunt, Kazan, and Ferguson Rivers and the northwest coast of Hudson Bay: Geol. Survey Canada Ann. Rept. v. 9, pt. F, 218 p.
Umbgrove, J. H. F., 1947, The pulse of the earth: 2d ed., The Hague, Martinus Nijhoff, 358 p.
Van Hise, C. R., 1908, Problems of the Precambrian: Geol. Soc. America Bull., v. 19, p. 1–28
Van Hise, C. R., and Leith, C. K., 1909, Precambrian geology of North America: U. S. Geol. Survey Bull. 360, 939 p.
—— 1911, The geology of the Lake Superior region: U. S. Geol. Survey Mem. 52, 641 p.
Wahl, W. G., 1953, Temiscamie River area: Quebec Dept. Mines Geol. Rept. 53, 38 p.
Walker, T. L., 1924, Uraninite from Cardiff township, Ontario: Toronto Univ. Studies, geol. ser., no. 17, p. 42–45
Wanless, R. K., and Trail, R. J., 1956, Age of uraninites from Blind River, Ontario: Nature, v. 178, p. 249–250.
Wasserburg, G. J., and Hayden, R. J., 1955, $A^{40}$-$K^{40}$ dating: Geochimica et Cosmochimica Acta, v. 7, p. 51–60
Wetherill, G. W., Davis, G. L., and Aldrich, L. T., 1957, Age measurements in rocks north of Lake Huron: Am. Geophys. Union Program, 28th Ann. Meeting, p. 39–40
Wetherill, G. W., Tilton, G. R., Davis, G. L., and Aldrich, L. T., 1956, Nuclear processes in geologic settings: Nat. Acad. Sci.-Nat. Research Council Nuclear-Sci. ser. Rept. 19, p. 151–156
Wilmarth, M. Grace, 1924, Geologic time classification of the United States Geological Survey compared with other classifications: U. S. Geol. Survey Bull. 769, 138 p.
Wilson, J. T., 1949, The origin of continents and Precambrian history: Royal Soc. Canada Trans., 3d ser., v. 43, sec. 4, p. 157–184
Wilson, M. E., 1913, Southeastern portion of Buckingham map-area; Quebec: Geol. Survey Canada Summary Rept., p. 196–208
——1917, Magnesite deposits of Grenville district, Argenteuil county, Quebec: Geol. Survey Canada Mem. 98, 88 p.
—— 1918a, Timiskaming county, Quebec: Geol. Survey Canada Mem. 103, 197 p.
——1918b, The subprovincial limitations of Precambrian nomenclature in the St. Lawrence Basin: Jour. Geology, v. 26, p. 325–333
——1920, Buckingham map-area, Hull and Labelle counties, Quebec: Geol. Survey Canada map
——1925, The Grenville Precambrian subprovince: Jour. Geology, v. 33, p. 389–407
——1939, The Canadian Shield: Geology of North America, p. 232–311 *in* Krenkel, Erich, Editor, Geologie der Erde, Berlin, Verlag von Gebrüder Borntrager, 643 p.
——1941, Precambrian, p. 271–305 *in* Fiftieth Anniversary Volume: Geol: Soc. America 578 p.
——1956, Early Precambrian rocks of the Timiskaming region, Quebec and Ontario: Geol. Soc. America Bull., v. 67, p. 1397–1430
Wright, G. M., 1955, Geological notes on central district of Keewatin, Northwest Territories: Geol. Survey Canada Paper 55–17, 17 p.
——1956, Geological Notes on eastern district of Mackenzie, Northwest Territories: Geol. Survey Canada Paper 56–10, 23 p.
Wright, J. F., Geology and mineral deposits of a part of southeastern Manitoba: Geol. Survey Canada Mem. 169, 150 p.
Young, G. A., 1921, Iron-bearing rocks of Belcher Islands, Hudson Bay: Geol. Survey Canada Summary Rept., pt. E, 61 p.
——1924, Geological map of the Dominion of Canada and Newfoundland, 3rd. ed.: Geol. Survey Canada

GEOLOGICAL SURVEY OF CANADA, OTTAWA, ONTARIO, CANADA

MANUSCRIPT RECEIVED BY THE SECRETARY OF THE SOCIETY, JULY 12, 1957

BULLETIN OF THE GEOLOGICAL SOCIETY OF AMERICA
VOL. 69, PP. 775–788, 2 FIGS. JUNE 1958

# GEOCHEMISTRY OF THE STERLING HILL ZINC DEPOSIT, SUSSEX COUNTY, NEW JERSEY

BY R. W. METSGER, C. B. TENNANT, AND J. L. RODDA

## ABSTRACT

The Sterling Hill ore body is mineralogically similar to its neighbor to the north in Franklin, N. J. It is an intricately folded, steeply plunging body in Precambrian graphitic, sparsely silicated, coarsely crystalline white marble. The marble is graphite-free within 5 feet of ore. The ore is wrapped around a central core of graphitic marble and an annular gneissic cylinder of mica, feldspar, hornblende, pyroxene, and garnet composition.

Ore minerals are willemite, franklinite, and zincite. Franklinite, tephroite, pyroxene, and biotite compose the leanly mineralized areas. The mineral distribution is zoned. Black willemite with magnetic franklinite forms a band of varying thickness that follows closely the convolutions of the upper surface of the brown willemite-franklinite body. Ore textures are identical with those of the areas of lean mineralization, and the transition is not sharply defined. A thin band of rhodonite is found at this boundary between pyroxenes and willemite.

Paragenetically, it appears that of the ore minerals, willemite formed first in the sequence, with tephroite, zincite, and franklinite following in undetermined order; tephroite and zincite may have been emplaced at the same time. There is abundant evidence of later generations of willemite, franklinite and zincite. Primary zincite has been observed only in the presence of tephroite. There is evidence that tephroite has replaced willemite. Manganese solutions possibly replaced the zinc in willemite to form tephroite and may have resulted in the formation of zincite.

The rock core of the ore body is altered to zinciferous clayey mud, locally containing hemimorphite. This alteration extends from the surface to a depth of 680 feet.

The variation in willemite color is due to color differences in <10 micron franklinite inclusions. Red franklinite is nonmagnetic with a unit cell dimension of nearly 8.51 Å. Black franklinite is magnetic with a unit cell dimension of about 8.42 Å. Macroscopic franklinite cell dimensions are intermediate. Origin of franklinite inclusions is attributed to willemite serpentinization, similar to that commonly observed in magnetite formation by serpentinization of olivine.

## CONTENTS

### TEXT

| | Page |
|---|---|
| Introduction and acknowledgments | 776 |
| Description of the Sterling Hill ore deposit | 776 |
| Geological environment | 776 |
| Outer zincite zone | 776 |
| Central zincite zone | 777 |
| Black willemite zone | 778 |
| Brown willemite zone | 778 |
| Pyroxene zones | 780 |
| Franklinite zone | 780 |
| Gneiss zone | 780 |
| Calamine-mud zone | 780 |
| Causes of variation in willemite physical properties | 781 |
| Color differences | 781 |
| Fluorescence | 781 |
| Microscopic franklinite inclusions | 781 |
| Serpentine inclusions | 782 |
| Spinel (franklinite) lattice measurements | 782 |
| Results of lattice measurements | 784 |
| Paragenesis of the macroscopic ore minerals | 785 |
| Genesis of inclusions | 785 |
| References cited | 787 |

### ILLUSTRATIONS

| Figure | Page |
|---|---|
| 1. Geologic map of the Sterling Hill ore body | 779 |
| 2. Ferrite lattice dimensions | 783 |

### TABLE

| Table | Page |
|---|---|
| 1. Chemical compositions of minerals discussed | 777 |

## Introduction and Acknowledgments

The Sterling Hill zinc deposit is one of a geologically unique pair of ore occurrences in Franklin and Ogdensburg boroughs of Sussex County, New Jersey. Innumerable papers have been written on their vast suite of minerals. The Franklin mine was recently (1954) shut down because of exhaustion of ore.

Most of the published works on these deposits describe individual minerals rather than their relationships to each other and to their host rock. The few papers concerned with the genesis of the ore bodies are, for the most part, speculative and are based on brief field observations. Ries and Bowen (1922) published the most detailed study of the ore bodies. Pinger (1950), Chief Geologist at Franklin from 1929 to 1950, summarized the important hypotheses of origin. He described the ore bodies only briefly. Ridge (1952) discussed at length solutions that may have formed the mineral deposits, on the assumption that they are a pyrometasomatic deposit. Hague *et al.* (1956) described the areal geology and structure of the area with particular emphasis on the gneisses.

The present paper is the result of a continuing study undertaken by the writers early in 1953. Recent work on the Sterling Mine is reported. It is hoped that continuation of the present work will find application in mining and exploration and in furnishing better geological understanding of processes associated with ore formation.

The work has been carried out co-operatively between the Exploration and Research departments of The New Jersey Zinc Company. A number of people from each department have contributed to the work in various ways. The authors are pleased to acknowledge their assistance. Also, the authors wish to express appreciation to The New Jersey Zinc Company for permission to publish this information.

## Description of the Sterling Hill Ore Deposit

### *Geological Environment*

The Sterling Hill ore body is structurally complex. It occupies an isoclinal syncline in white crystalline limestone. Its long east limb and shorter west limb dip eastward at 55°, This structure is complicated by a cross member, greatly thickened in its middle portion, which joins the middle of the west limb with the middle of the east limb. The ends of the two limbs, the keel of the syncline, the thickened part of the cross member, and the latter's junctions with the two limbs plunge roughly parallel at 45°, N.70E.

The ore distribution in plan is similar to its pattern in section, owing to the 45-degree plunge of the ore body.

The ore body occurs in a coarse crystalline white marble generally well banded with mica, amphibole, and chondrodite. Graphite is ubiquitous in the limestone except in and near ore and, in some cases, adjacent to pegmatite and gneiss. A marble zone 5 feet thick which envelopes the ore body is graphite-free but otherwise apparently identical with the country rock. The banding of the limestone appears to parallel the foliation of the adjacent gneisses and has been attributed to bedding. Locally, large masses of the limestone have been dolomitized. The dolomitized masses in the mine appear to be related to joints, faults, and breccia zones which are known to be post-Algonkian.

The Sterling Hill ore body lies within the White (Franklin) Limestone about 600 feet away from its contact with the Cork Hill gneiss. The Franklin ore body 3 miles to the north is only a few feet from the same contact. The well-annotated paper by Hague *et al.* (1956) should be referred to for specific geographical and stratigraphic location.

The ore body proper is distinctly zoned mineralogically, but, owing to extreme structural complexity, the distribution of the zones is imperfectly understood.

### *Outer Zincite Zone*

The outer zincite zone comprises the east and west limbs of the ore structure. The ore is composed typically of pale flesh to red willemite[1] and tephroite[2] (or a related olivine), nonmagnetic franklinite, and sparsely disseminated to locally abundant zincite (Table 1). These minerals are found in varying proportions, disseminated pepper-and-salt fashion in white limestone which generally displays a pink fluorescence, or as sheets or lenses with

[1] These willemite grains are fluorescent along fractures and in irregular zones, although to the naked eye they appear to fluoresce uniformly.

[2] Tephroite as used here is not a specific mineral name but refers to a series of olivine minerals not yet differentiated.

gneissic texture and essentially free of included limestone. In general, the franklinite comprises 40–60 per cent of the ore minerals in all zones.

The limestone is everywhere coarsely crystalline and highly twinned.

TABLE 1.—CHEMICAL COMPOSITIONS OF MINERALS DISCUSSED*

| Mineral | Composition |
|---|---|
| Franklinite | $(Zn,Fe,Mn)O \cdot Fe_2O_3$ |
| Willemite | $Zn_2SiO_4$ |
| Zincite | $ZnO$ |
| Tephroite | $Mn_2SiO_4$† |
| Serpentine | $H_4Mg_3Si_2O_9$ |
| Friedelite | $H_7(Mn,Cl)Mn_4Si_4O_{16}$ |
| Pyroxenes | Diopside—$CaMgSi_2O_6$ |
| | Augite—$Ca(MgFe)Si_2O_6$ |
| Rhodonite | $MnSiO_3$ |
| Garnet (var. Andradite) | $Ca_3Fe_2Si_3O_{12}$ |
| Gahnite | $ZnAl_2O_4$ |
| Calcite | $CaCO_3$ |
| Dolomite | $CaCO_3 \cdot MgCO_3$ |

* These formulae disregard elements that may be present in minor concentrations.

† As used in this report Mg can proxy for Mn.

In the disseminated ore the grain size of the willemite and franklinite are roughly comparable and are of the order of a quarter of an inch in diameter. In general, the grains are rounded and equidimensional but locally are euhedral. The tephroite, which closely resembles the willemite and occurs locally to the exclusion of willemite, appears in general as a peripheral replacement of individual willemite grains. The zincite is relatively fine-grained and sparsely disseminated through much of the ore but has not been observed in normal ore except in the presence of tephroite.

The gneissic type of ore, which in general occurs as sheets or lenses within the disseminated ore, is composed of willemite and franklinite grains slightly smaller in diameter than those in the disseminated variety. Zincite, as before, is generally sparsely disseminated. In this ore the willemite grains are elongated parallel to the crystallographic axis. L. A. Herrmann (Unpublished report) has shown that these willemite grains, as well as those from other zones, parallel the major structural elements of the ore body. The degree of orientation is inversely proportional to the amount of limestone present. Where limestone occurs within the gneissic bands, it appears as augen-like lenses 1–3 inches long oriented in the plane of the gneissic foliation, or as larger irregular masses.

An unusual feature of the ore is visible primarily in the west limb. In the hanging-wall half of the limb, the ore is of the normal disseminated variety. About midway between the hanging and foot walls, this pepper-and-salt ore contains sparsely distributed, generally rounded nodules of calcite-free willemite and franklinite, gneissic in texture. A few of these nodules on close inspection have revealed hexagonal outlines, suggesting that they are possibly "ghosts" of some pre-existing crystal. Toward the foot wall, these nodules become more and more abundant, until they coalesce to form a thick band of the gneissic ore described above.

The contacts between ore and rock are normally gradational. The ore minerals become coarser and more disseminated over distances of from 6 inches to a foot. Where they are very sparse (as in the hanging wall of the east limb) the willemite and franklinite crystals in many cases have diameters ranging from 1 inch to more than 2 inches. The crystals locally are well formed. This coarseness of texture is also observed where the minerals are sparsely disseminated in the local masses of limestone within the ore.

Within the ore band, generally within less than a foot of the hanging-wall contact in the case of the east limb, and the foot-wall contact in the case of the west limb, is a band of concentrated zincite roughly 6 inches thick. In many places the zincite occurs as irregularly shaped single crystals as much as 3 inches in diameter. These are invariably associated with similarly coarse crystals of silicate minerals, which until recently were erroneously called tephroite but are actually three or more phases of an unidentified olivine.

The ore band of the outer zincite zone varies considerably in thickness (Fig. 1) and feathers out by increasing dissemination at the north end of the east limb.

### *Central Zincite Zone*

Midway between the keel and the northern termination of the west limb, the ore branches off to the northeast to form a cross member which is greatly thickened in the middle and either joins or abuts (the structure is not yet clear) the east limb approximately midway

between its northernmost extremity and the keel.

Although it is continuous with and not greatly different mineralogically from the outer zincite zone, the western half of the cross member has been designated as the central zincite zone.

The zincite band in the outer zone has not been traced in the central zone, although disseminated zincite is present. The distribution of the magnetic franklinite is not yet well defined, but for the most part it appears to be confined to the eastern side of the zone near its contact with the black willemite zone.

A considerable amount of dull brownish-green, glassy, essentially nonfluorescent willemite is present in the middle of the thickened part of the central zincite zone, but it has not been observed in the outer zone.

Except for these differences, which may be more apparent than real, the ore of the central zone is similar to that of the outer zincite zone.

### *Black Willemite Zone*

Black willemite ore is radically different in appearance from all the other ore in the mine. Most of this ore is in the eastern half of the thickened part of the cross member and, where massive with little limestone, appears as a jet-black rock.

Mineralogically it is not very different from the red and brown willemite ores of the remainder of the ore body. The major constituents are willemite and franklinite in grain sizes comparable with those described for the outer zincite zone. In this zone, however, the willemite is jet black to grayish black to gray and in many cases is difficult to distinguish from franklinite in unpolished hand specimens. The metallic luster of the franklinite differentiates the two. As with all willemite, this material is transparent in thin section. The associated tephroite (roepperite) likewise is black. In polished section and thin section its appearance is similar to that of willemite. The franklinite differs from that of the outer zincite zone in that it is highly magnetic and black even in powdered form. The black willemite is sufficiently magnetic to make its separation from franklinite difficult.

Zincite has never been found in the black willemite zone.

As in the outer zone, the ore is disseminated, with a pepper-and-salt texture, and also in massive form with little limestone. This latter type is probably also gneissic, but foliation is obscured by the similarity in color of the ferrite and silicate minerals. The willemite grains are probably oriented parallel with the structure of the ore body, but no work has been done to prove this.

The black ore, until recently, was thought to occur only in the thick part of the cross member, as local masses or lenses in the midst of the pyroxene zone, and near the junction of the west limb and cross member. It has now been traced (Fig. 1) as a relatively thick mass at the north end of the west limb; it thins to a ±3-inch band of disseminated gray willemite and magnetic franklinite, which parallels the west limb about 2 feet above its hanging wall to another thick mass at the junction with the cross member. From there it again thins to ±3 inches and extends parallel with and 2 feet beneath the foot wall of the cross member to another thick mass north of the thick part of the central zincite zone. Its course from there to the main body of black ore has not been traced precisely and is indicated in Figure 1 as a dashed line. The writers' examination has not been extensive enough to determine whether or not this connection exists.

At all places where the black ore adjoins the red ore, there is a gradational zone of dark-brown ore.

### *Brown Willemite Zone*

About halfway between the thick part of the black willemite zone and the junction of the cross member and the east limb, the black ore thins and grades into a dark-brown to red-brown willemite-franklinite ore containing no zincite. The franklinite is magnetic and in general black in finest powdered form. Texturally, the ore is similar to all ore previously described. Also included in this zone are lenses of ore lying parallel with and close under the foot wall of the east limb. These lenses may be connected through thin low-grade bands with the ore of the cross member, and the latter may not actually join the east limb. More field study will be needed to prove or disprove this.

The margins of the brown willemite ore bands are typically of the pepper-and-salt variety, whereas their inner parts have a generally gneissic texture. There is a mineralogical gradation between this disseminated ore and the surrounding mineralization of the pyroxene zone, although the texture remains the same.

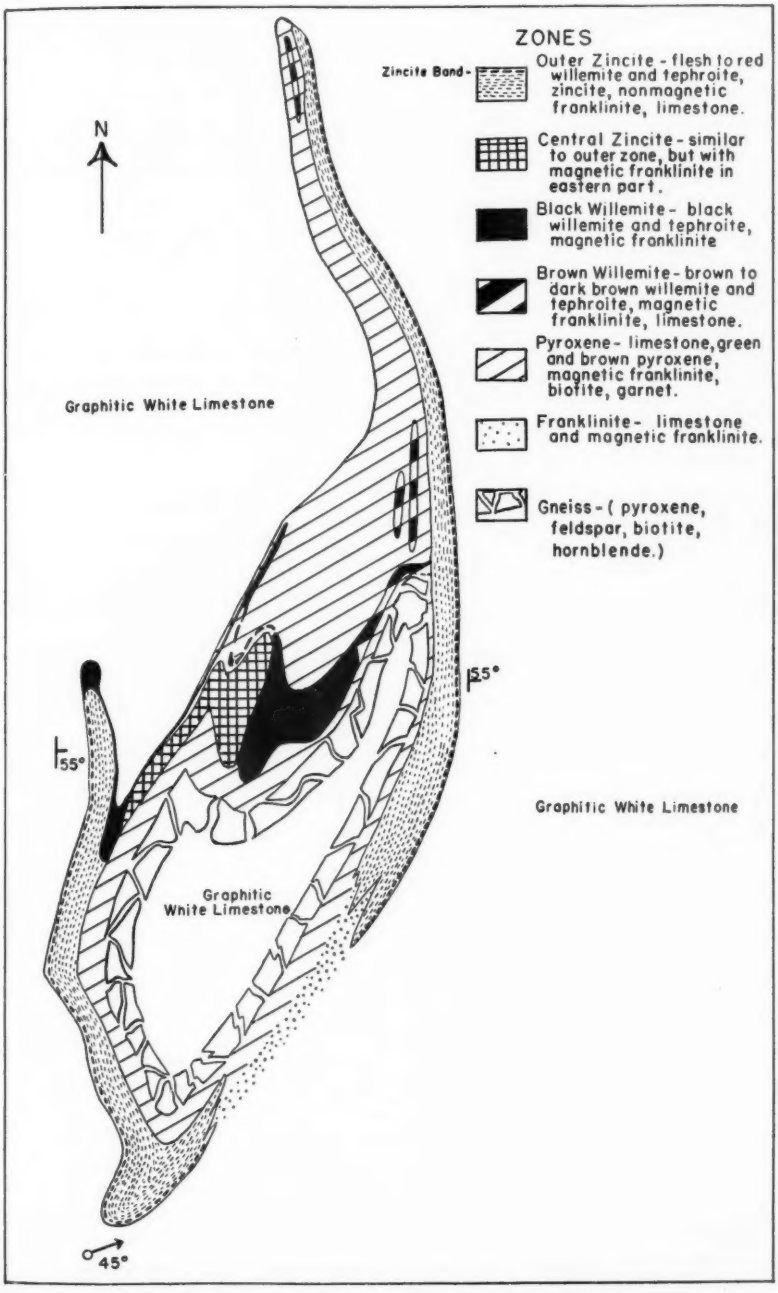
ZONES
Zincite Band-
Outer Zincite - flesh to red willemite and tephroite, zincite, nonmagnetic franklinite, limestone.
Central Zincite - similar to outer zone, but with magnetic franklinite in eastern part.
Black Willemite - black willemite and tephroite, magnetic franklinite
Brown Willemite - brown to dark brown willemite and tephroite, magnetic franklinite, limestone.
Pyroxene - limestone, green and brown pyroxene, magnetic franklinite, biotite, garnet.
Franklinite - limestone and magnetic franklinite.
Gneiss - ( pyroxene, feldspar, biotite, hornblende.)
N
Graphitic White Limestone
55°
55°
Graphitic White Limestone
Graphitic White Limestone
45°

FIGURE 1.—GEOLOGIC MAP OF THE STERLING HILL ORE BODY

### *Pyroxene Zones*

There are two pyroxene zones, mineralogically and texturally identical, but occupying different structural positions in the ore body. Because they are not considered to be of ore grade, there are few openings in them, and they are therefore the least-known parts of the ore body.

One of these zones extends northward from the thick part of the cross member beneath the foot wall of the east limb and pinches out near the northern end of that limb. It is composed of fluorescent limestone with green pyroxene (optically near diopside), brown pyroxene (optically near augite), magnetic franklinite of low zinc content, biotite, and relatively sparse garnet. These minerals are distributed in bands and closely resemble the banded, disseminated ore in texture. Data are insufficient to reveal whether or not these bands are tightly folded in the same manner as the black willemite ore.

This zone appears to be an important and integral part of the mineral deposit. The high magnesian content of the pyroxene phase (see Palache, 1935 for typical analysis) seems to contradict Ridge's (1952) suggestion that the ore fluids were low in magnesium content.

At the contact between this limestone pyroxene-franklinite rock and the ore of the brown willemite zones, particularly noticeable in the hanging wall of the lenses beneath the east limb, is a narrow zone (±1 inch thick) of rhodonite and franklinite. When seen from a distance underground, it is difficult to see where ore ends and rock begins. On close inspection it is obvious that the texture and the amount of franklinite remain the same, and the silicates range from willemite in the ore, through rhodonite, to pyroxene.

The second pyroxene zone forms a rough cylinder between the ore and the gneiss zone. Except at its contact with the gneiss, it is mineralogically the same as its counterpart to the north. At that contact, coarse garnet, pyroxene, biotite, and gahnite crystals are developed, products of the reaction between the limestone and adjacent sedimentary gneiss at the time of metamorphism. Such "skarn" minerals are typical of gneiss-limestone contact zones throughout the area.

### *Franklinite Zone*

This zone is composed of highly magnetic, low-zinc franklinite sparsely disseminated in limestone, in the east limb near the keel of the ore body. Its plunge is somewhat less than that of the ore body, so that near the surface it wraps around the keel and appears, in part, in the west limb. In depth this zone is entirely within the east limb (Fig. 1). More work is necessary to determine its relationship to the rest of the ore.

### *Gneiss Zone*

This zone is a band of pyroxene and/or hornblende-feldspar-mica gneiss, locally intruded with pegmatite, which lies between the pyroxene zone and the central core of the ore body. Because it is of no economic importance, it has not been studied in detail. The core of the ore body is normal graphitic white limestone.

### *Calamine-Mud Zone*

Replacing part of the limestone core as well as parts of the surrounding gneiss and pyroxene zones in the upper levels of the ore body is a huge cavity filled with mud. The cavity parallels the hanging wall of the west limb and that of the cross member south of its thickened part. It extends 680 feet beneath the surface. At the surface in plan it looks much like a pair of spectacles. The material filling the cavity appears to be transported in part and in part residual. It appears to be zinc bearing in some degree.

In the mine the roof of a cross cut appeared to be brown-stained, very coarsely crystalline marble containing disseminated franklinite. Blocks 3 feet in diameter and more, bounded by intersecting joints such as are common throughout the Franklin Limestone, displayed excellent diffusion rings, obviously controlled by the joints. Cleavage rhombs and twinning traces were clearly visible. On close inspection the "marble" proved to be claylike in consistency and, on drying, crumbled to dust. Chemical analysis of the material after removal of a small amount of franklinite showed only 0.54 per cent CaO and 1.71 per cent MgO. In the same cross cut a layer of hemimorphite several feet thick rests on the footwall of the cavity. The hemimorphite crystals contain mud inclusions, and mud is found interstitially in the porous mass. In some places the banding in the marble is retained in the mud, in others the mud appears to have been transported.

Other minerals composing the mud as identi-

fied by X ray are goethite, kaolinite, sericite type, and nontronitic type.

As yet there are few mine openings in the mud, and the distribution of the various minerals is not known well.

The problems posed by the existence of the mud zone are numerous, and too little is known to speculate on its origin. It is surrounded by mine workings in solid rock, and, until it was penetrated by diamond drilling from beneath, it appeared to be completely water tight. The zone bottoms about 50 feet below sea level. Circulating ground water is therefore an improbable agency of weathering.

Pinger (1950) suggested that sulfuric acid derived from blende acted in the formation of what was then known of the mud zone, *i.e.*, two pits at the surface outcrop of the ore. However, the authors have studied the unaltered marble directly beneath the zone on the 700 level, as well as in other places in the mine, and cannot find evidence of sufficient sulfides to account for such a massive corrosive attack.

## Causes of Variation in Willemite Physical Properties

### *Color Differences*

There are striking differences in the color and magnetic properties of the willemite. Because of the zoning of these properties in the ore body and the possible genetic significance of the variations, the writers attempted to discover their causes.

Willemite occurs in three colors, green, red, and black. The green variety predominated in the Franklin ore body, although considerable red willemite was taken from the upper parts of the mine near the keel in the early years of the mining operation. Black willemite, if present, was rare. At Sterling Hill the primary willemite is either red or black, and the only green willemite is secondary. About one-third of the willemite in the ore body is black.

### *Fluorescence*

The typical green color of willemite from the Franklin mine is apparently a green fluorescence induced by ultraviolet wave lengths in daylight and common artificial sources. When heated to a temperature just below incandescence, green willemite becomes grayish white, and there is no ultraviolet fluorescence. On cooling, the ultraviolet-induced fluorescence gradually returns, and then the green color returns.

### *Microscopic Franklinite Inclusions*

The black willemite and tephroite and red willemite and tephroite are colored by minute 1–10 micron inclusions. These inclusions have not been found in any of the pyroxenes, calcite, or other gangue minerals of the ore body.

Several sets of thin sections were prepared from samples collected in series across the contact zone between the black and brown to red willemite in the thickened part of the cross member. Although Ries and Bowen (1922, p. 543) attributed the color of black willemite to inclusions of franklinite, and that of red willemite to zincite, the authors found that both varieties were colored by franklinite inclusions.

Willemite, regardless of its apparent color in the hand specimen, is transparent and colorless in thin section. Black willemite, in thin section, is crowded with opaque black 1-to-10-micron inclusions, many of which display good octahedral form (although most are anhedral). These are thickly scattered in planes and, locally, in what appear to be irregular or curved, apparently healed cracks. At first, this distribution pattern was thought to indicate formation by exsolution from iron-bearing willemite. Accordingly, samples of coarse-grained Sterling black willemite (received from L. H. Bauer in 1947) were annealed in nitrogen as follows:

| Thin section number | Treatment |
|---|---|
| 2196 | Untreated |
| 2197-1 | 5 hours at 985°C. |
| 2197-2 | 5 hours at 985°C. |
| 2226 | 100 hours at 1050°C. |
| 2378 | 63 hours at 1300°–1350°C. |

Some slight change in the color of the inclusions may have taken place at the lower temperatures, but even at 1300°–1350°C., the inclusions had not dissolved but had grown. Exsolution, then, is probably not the source of the inclusions in black willemite.

Red willemite in thin section is seen to contain spinel (franklinite) inclusions distributed in the same fashion as those in the black. These spinels, however, are transparent and ruby, and although generally rounded, many display good octahedral form. These apparently are the inclusions mistaken by Ries and Bowen for zincite on the basis of color. Where zincite has been observed in such fine particles, it is yellow rather than red.

The brown willemite typical of regions of gradational contact contains a mixture of red and black spinel inclusions. Its shade depends on the relative proportions of black and red particles.

The color variations of tephroite (roepperite) are also due to these spinel inclusions distributed in fractures typical of the olivine group. A few slides showed concentrations of inclusions in the tephroite, whereas the associated willemite was free of inclusions. Such inclusion-free willemite in hand specimens appears as a glassy, dirty, brownish-green mineral.

Willemite and tephroite also occur in paler shades of gray and flesh pink. These shades are due to the sparse scattering of inclusions.

The foregoing description has considered only the equidimensional, rounded to octahedral inclusions. Other thin sections, from large single crystals of red and flesh-colored willemite, revealed isotropic transparent red rodlike inclusions 1–10 microns thick and of variable length. These are continuous with rods of a colorless mineral of lower index than the willemite. The two minerals contact in a featherlike manner. Further study proved that the red material is franklinite and the colorless mineral is chrysotile.

Thin-section work indicated that the inclusions were spinels; more specific identification necessitated the separation and concentration of the inclusions from the willemite. This was accomplished by dissolving the willemite in 5 per cent $HNO_3$ and centrifuging the residue. After repeated washing with distilled water and additional centrifuging, a residue clean enough for X-ray-diffraction studies was obtained.

In developing the method for separation and concentration, it was found that black inclusions suspended in liquid could be attracted by an Alnico hand magnet. The rounded and octahedral red inclusions were not attracted by the magnet. The rodlike red inclusions, however, possessed polarity, and, although they were not attracted by the magnet, their orientations could be altered by movement of the magnet.

Powder X-ray studies of the concentrated colored inclusions (all from willemite) proved that all, regardless of color or form, are franklinite.

### *Serpentine Inclusions*

In the course of the powder X-ray work on the inclusions, it was found that all were associated with serpentinelike minerals or friedelite. The friedelite patterns were identical with patterns obtained from known samples. The serpentinelike inclusions show one diffraction pattern, with recurring minor differences which indicate three members of the serpentine family. One of these patterns closely resembles the pattern obtained from a specimen of chrysotile from Thetford, Quebec. The remaining two patterns are like the first but less like the chrysotile.

The inclusions most like chrysotile were from one of the large pale-flesh willemite crystals. These inclusions were sufficiently large to afford optical data. These data, as reported by L. A. Herrmann, are as follows:

| 1 | 2 |
|---|---|
| Biaxial positive | Uniaxial or biaxial positive with small 2V |
| Length slow | Length slow |
| Fibrous | Fibrous |
| $n\beta$ Slightly greater than 1.56 | $n\beta$ Very slightly less than 1.54 |

The optical properties of chrysotile (Rogers and Kerr, 1942) follow:

Biaxial positive
2V = 0–50°
Length slow
Fibrous
$n\beta$ 1.504–1.550

These colorless inclusions have not been identified definitely because the authors do not have access to exactly comparable reference patterns, and the particles are, for the most part, too minute to permit optical determinations or to permit separation for chemical analysis. It is safe to say, however, that they are all members of the serpentine family.

In addition to the serpentine inclusions, inclusions of friedelite (a hydrous chlorosilicate of manganese) were identified in many of the franklinite concentrates from willemite. In some cases, this was present to the exclusion of serpentine varieties, and in others it was present with them.

## Spinel (Franklinite) Lattice Measurements

The method of determining the cell size of the ferrite samples was not elaborate. The $d$ values for the lines

(511) (731)
(333), (440), (533), and (553)

were measured from a metal scale made up for Cu radiation. No correction was made for film-length variation. Each of these $d$ values was used to calculate an $a_0$ value using $a_0 = d \cdot \sqrt{h^2 + k^2 + l^2}$. The arithmetic mean of the four $a_0$ values thus determined was used as the cell size. It was found that the standard deviation of this determination was 0.011Å. This value was determined from data on four samples, two run in duplicate and two in triplicate. More elaborate determination of the cell size was not warranted, since the quality of the X-ray patterns of these iron-bearing materials was poor, and the sampling procedures in some cases were not of high precision.

A synthetic 1-to-1 zinc-manganese ferrite sample ($ZnO \cdot MnO \cdot (Fe_2O_3)_2$) gave a sharper X-ray pattern than the others, and the lattice constant was determined by the extrapolation procedure described by Henry, Lipson, and Wooster (1951, p. 191). This result for $ZnO \cdot MnO \cdot (Fe_2O_3)_2$ (Fig. 2) compares satisfactorily with the value determined by the simpler procedure described above and used for routine cell-size determinations in this work.

Figure 2 lists the values for the lattice constants of several ferrite materials. The measured lattice dimensions have been plotted on a

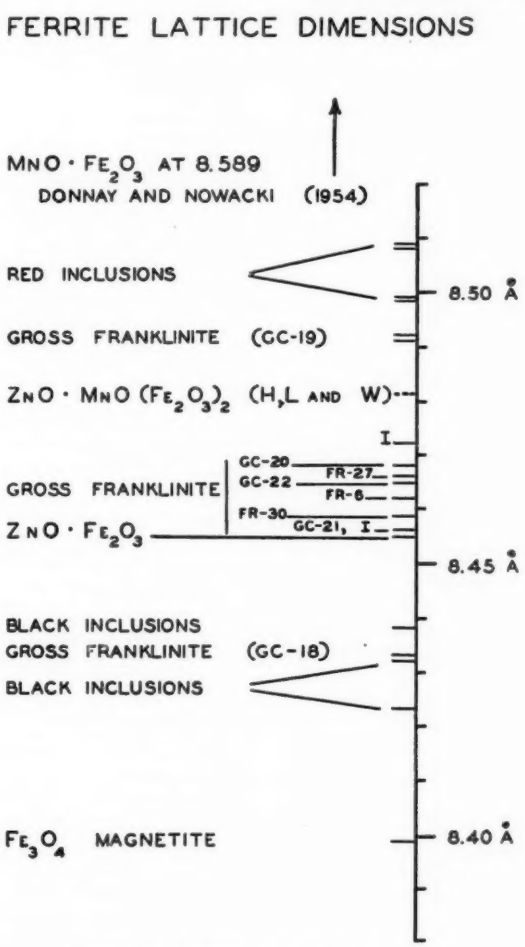


FIGURE 2.—FERRITE LATTICE DIMENSIONS

linear scale in angstrom units. Multiple listings on the plot are for different samples of the same type. Values shown on the plot include:

(1) Red inclusions recovered from willemite samples
(2) Black inclusions recovered from willemite samples
(3) Gross franklinite I—Large franklinite particles occurring adjacent to either red or black willemite. The inclusions from these willemite samples were recovered and measured.
(4) Gross franklinite GC or FR—Mine location of these samples not known. They are ore franklinite samples on which analytical data were available.
(5) $ZnOFe_2O_3$ (synthetic zinc ferrite)
$ZnO \cdot MnO \cdot (Fe_2O_3)_2$ (Synthetic 1-to-1 zinc-manganese ferrite)
$Fe_3O_4$ (Magnetite sample from the bottom of the north shaft, Sterling)
(6) $MnO \cdot Fe_2O_3$ Value obtained from Donnay and Nowacki (1954)

## Results of Lattice Measurements

The plotted cell-size data (Fig. 2) show a striking distribution. The magnetite standard has the smallest lattice dimensions. Somewhat larger, yet still close to magnetite, are the black microscopic inclusions from black willemite. The macroscopic franklinites are next in increasing size. The largest lattice dimensions are exhibited by the microscopic red inclusions from brown or red willemite.

The small spread in the cell size of the gross franklinite samples is remarkable when contrasted with the variations of the microscopic ferrite inclusions. The average dimension for gross franklinite is fixed in the range near 8.46Å.

The color and magnetic properties of the ferrite apparently correlate with the lattice changes. The darker, low-spaced samples are more magnetic, and the red, high-spaced materials are less magnetic.

A progressive increase in lattice dimension is observed in the measured values for the samples $FeO \cdot Fe_2O_3$, $ZnO \cdot Fe_2O_3$, $ZnO \cdot MnO \cdot (Fe_2O_3)_2$, and $MnO \cdot Fe_2O_3$ (Fig. 2). This suggests that the same composition variations cause lattice expansion in the natural materials from the mine. The lattice dimension probably increases as manganese or zinc progressively replaces iron in $Fe_3O_4$. The increase is greater for manganese substitution than for zinc. It follows that the lattice dimensions of samples will be determined by the interaction of all three ions, $Fe^{++}$, $Mn^{++}$, and $Zn^{++}$.

The transparency and redness of the inclusions with the largest cell sizes might be expected to correlate with increased zinc and manganese contents, since zinc chemicals are typically transparent, and manganese chemicals are typically pink or red. Increased transparency observed microscopically correlates with increasing zinc content of franklinite samples.

The ionic radii of these ions are $Fe^{++}$ = $Zn^{++}$ = 0.74 and $Mn^{++}$ = 0.80 (Green, 1953). The large value of $Mn^{++}$ is consistent with the indication that it results in larger cell sizes. The indicated increase by $Zn^{++}$ substitution for $Fe^{++}$ must be due to a larger effective ionic size of zinc in the spinel environment than that indicated by its listed equivalence to iron. This seems possible since the $Zn^{++}$ and $Fe^{++}$ occupy different lattice sites in the spinel in accordance with the inverse structure for $FeO \cdot Fe_2O_3$ and the normal structure observed for $ZnO \cdot Fe_2O_3$.

Analytical data and lattice dimensions were obtained for a series of gross franklinite samples (Fig. 2).

Calculations based on various assumptions have been made involving possible valence states, ionic radii, and structural considerations in spinel-type materials in an attempt to correlate composition and lattice dimensions. The proximity of Mn, Fe, and Zn in the periodic table and the resulting similarity in properties reduces the effectiveness of calculations, as does the lack of precision of the lattice-dimension measurements.

The microscopic inclusions recovered from willemite crystals were not pure enough or in sufficient quantity for chemical analysis. Hence, sampling was made of gross franklinite, on which analysis would be possible immediately adjacent to both red and black willemite. Lattice dimensions were determined for the gross franklinite samples and for the red and black inclusions from the willemite, with the hope that correlation of cell size of corresponding samples could be established, and hence some information might be indirectly obtained on inclusion composition. These values are designated as *I* on Figure 2. No correlation exists between lattice dimensions of such inclusions and adjacent large franklinite particles. These materials are in proximity in the mine, —that is, a gross franklinite grain might contact a willemite grain which could include the microscopic ferrite inclusions. The dimension variations observed are probably due to varia-

tions in chemical composition of the various ferrite samples.

These variations support the conclusion that the ferrite inclusions in willemite are a product of post-ore alteration, probably serpentinization.

## Paragenesis of the Macroscopic Ore Minerals

The determination of paragenesis of the ore minerals is complicated by the wide distribution of secondary occurrences. Thin sections of the massive or gneissic type of ore, in which all the ore minerals are in contact, have indicated that willemite precedes franklinite, tephroite, and zincite. This is in disagreement with Ries and Bowen (1922, p. 546) who say,

"In the very few sections where the two silicates (willemite and tephroite) were found in association, they occurred as granular intergrowths which indicated contemporaneous formation, though it is possible that the tephroite slightly antedated the willemite".

In the sections studied, the interstices of the rounded willemite grains are filled with franklinite and/or tephroite. The former tends to wedge in between the willemite grains; the latter, in many cases, peripherally replaces the willemite and may replace all but a few small remnants of a grain. Zincite, too, appears to be interstitial and has been observed thus far only in thin sections containing tephroite.

This association of zincite with tephroite, and the latter's relation to willemite suggests the possibility that manganese solutions, in replacing the zinc in willemite to form tephroite, resulted in the formation of zinc oxide which has been thrown down as zincite.

This paragenetic sequence applies only to primary ore minerals. There is at least one later generation of willemite, zincite, and franklinite. A hypothesis involving the formation of secondary zincite and franklinite follows.

## Genesis of Inclusions

Although the distribution of inclusions in willemite suggests origin by exsolution from the silicate lattice, this has been ruled out on both theoretical and experimental grounds. Theoretically, it is improbable that iron would exsolve from a silicate lattice as an oxide phase such as franklinite. Had ferrous iron exsolved from the willemite lattice, it more logically would have been thrown down as the silicate fayalite. If the ferrous iron had actually exsolved as an oxide, the annealing experiments should have resulted in its resolution into the willemite lattice.

It seems significant that the franklinite inclusions are confined primarily to the orthosilicate minerals, willemite and tephroite, and are not found in the pyroxenes. Also, they are missing in the calcite associated with those silicates. The distribution of the inclusions in fractures and cleavage planes of the silicates indicates that they are of more recent origin than the silicates. As the willemite is considered to have replaced calcite, if the inclusions existed before willemite, they should also be present in the calcite.

The apparently universal co-occurrence of the franklinite inclusions with inclusions of the hydrous silicates serpentine ($H_4Mg_3Si_2O_9$) and friedelite $H_7(Mn, Cl)\ Mn_4Si_4O_{16}$ suggests that these minerals are genetically related. Such a relationship is easily visualized.

Iron-bearing olivines when partially serpentinized are altered along their cleavage planes and fractures, and microscopic grains of magnetite-type material have been found disseminated in the serpentine within those zones. In some completely serpentinized minerals, it is possible to infer the nature of the original mineral by the pattern of distribution of the magnetite-type grains. The pattern of distribution of franklinite inclusions in tephroite is similar to the pattern of magnetite-type distribution in olivine. The pattern in willemite is less similar because of its crystallographic difference from olivine.

Bowen and Tuttle (1949) reported on experimental serpentinization of iron-bearing olivines. Some black, magnetic iron oxide was found. They concluded that this was not pure iron oxide but had the composition $(FeMg)O \cdot Fe_2O_3$.

This serpentinization (or a similar process producing friedelite) then seems to be a possible mechanism for the production of franklinite inclusions.

The authors believe the silicate ore minerals were formed at great depth and at high temperatures (whether deposited from hydrothermal solutions, or by metamorphism of a preexisting zinc-manganese-iron deposit). Phase studies on the serpentinization reaction reported in the literature indicate that serpentinization occurs only at relatively low temperatures. Also, since serpentine is a hydrate, the period of mineralization that produced the

inclusions of franklinite and serpentine and/or friedelite must be comparatively recent and must have occurred at temperatures and pressures below those prevailing during ore formation. The temperature and pressure must have remained low, or the serpentine would have been destroyed. This would place the period of inclusion formation in the late Precambrian or post-Algonkian, long after the folding of the ore body. A post-Algonkian period of magnesium mineralization which resulted in the dolomitization of the limestone may also have been responsible for the formation of the inclusions.

The inclusion-forming solutions were either simple magnesian solutions, or they contained magnesium, iron, manganese, and zinc.

The black willemite has been described as composing a band that varies greatly in thickness and is apparently intricately folded parallel with the structure of the west limb and the cross member. In all cases it lies within a few inches of, or in gradational contact with, the red or brown willemite of those structures.

If the inclusion-forming solutions contained all the metal ions necessary to produce franklinite, serpentine, and friedelite by reaction with the silicate minerals, it seems inconceivable that color variations in the ore would coincide with the folded structure of the ore body. It seems more likely, therefore, that the mineralizing solutions were of simple composition, perhaps containing only magnesium as the active metallic ion, and that the other metal ions were derived from the silicates themselves.

A reaction to produce serpentine from willemite would require simple magnesian solutions. The reaction might be written:

$$2Zn_2SiO_4 + 3Mg^{++} + 5H_2O \rightarrow 1H_4Mg_3Si_2O_9 + 4ZnO + 6H^+$$

The hydrogen ion would react with the carbonate of the host rock.

It is not presumed that the reactions were as simple as stated above. For example, willemite from Sterling Hill in general contains appreciable manganese in solid solution. It has been established experimentally from other unpublished work that willemite can also contain ferrous iron in solid solution. The presence of admixed franklinite, however, has made it impossible to determine whether or not iron is present in natural willemite. These impurities could complicate the reaction and result in formation of a mixed ferrite as the oxide product.

In the equation given, the volume of the products is far in excess of the volume of the initial minerals. This increase must be explained if the serpentinization has taken place on a large scale.

In spite of the probable complexity of the reactions in nature, a reaction similar to that described in the above equation may have taken place. In the Sterling Hill mine, there is a rather large mass of rock having the appearance and texture of normal red willemite-franklinite ore disseminated in limestone. However, in this case the red mineral is antigorite, colored by a more than normal abundance of red franklinite inclusions. The associated macroscopic franklinite is normal in appearance, and the limestone matrix is made up of interlocking grains of calcite and dolomite. At a distance of the order of 15–20 feet from the serpentinous mass is an unusually large irregular mass of fine granular zincite with franklinite, sparse willemite, and almost no carbonate. The rock is generally brecciated.

It is therefore suggested that the antigorite was originally willemite containing iron and manganese, which was acted upon by magnesian solutions. In the initial stages of the alteration, manganese and iron oxides and zinc were released. These combined to form the highly insoluble franklinite inclusions that remained within the grains. When all the manganese and iron in the willemite lattice had been removed, the remaining zinc, by far the most abundant metallic ion of the three, was released as ZnO (zincite), a stable form. Because it is much more soluble than franklinite in a carbonate environment, it was transported from the immediate vicinity and precipitated some distance away.

Total serpentinization of the willemite, accompanied by dolomitization of the limestone, implies that the circulation of magnesian solutions was sufficient to alter the silicates completely.

The hypothesis suggested to explain the formation of franklinite by the action of magnesian solution on willemite may be extended to explain the differences in the inclusions and the co-occurrence of black and red inclusions in the same crystal.

Magnesian solutions acting on willemite containing considerable iron and manganese in solid solution would, according to the proposed hypothesis, produce serpentine and franklinite. If the iron and manganese in the willemite vary in a regular fashion areally, the franklinite product of the serpentinization reaction would also vary in composition. As the serpentiniza-

tion proceeds, willemite crystals with a certain initial balance of manganese and iron could at first react to give ferrite crystal inclusions with a composition producing a dark color. As the reaction continues, the initial balance of iron and manganese in the willemite crystals may alter. This change in balance might then result in the production of ferrite inclusions of similarly altered composition of different color. This may explain the willemite peculiar to the brown-black contact zone where ferrite inclusions of both color types occur mixed in single crystals. It follows that, if such a composition variation did exist in the unaltered willemite in a gradational fashion across the willemite body, inclusions of only color, black or red, should be found on either side of the brown-black contact, as is the case.

If the serpentinizing process continues to a stage in which manganese and iron are no longer available in the willemite, then zincite rather than the ferrites begins to form in addition to the serpentine. Such zincite inclusions have been observed, but only in the pale flesh-colored to red willemites.

The variation in cell size of the inclusions with color as determined by powder X ray qualitatively supports this suggestion of varying composition.

The writers suggest that, in the case of willemite containing inclusions of franklinite and serpentine, the solutions were present in quantities and concentration sufficient only for partial serpentinization. In such a case, the reaction did not progress past the stage of franklinite formation and left the willemite essentially intact. If this is true, some masses of willemite should be unaltered. Such masses do exist, notably in the thickened part of the cross member. The willemite in these portions of the ore body is a dull brownish green.

The X-ray data on franklinite indicate a wide variation in lattice dimensions. The black magnetic inclusions have cell dimensions in the vicinity of 8.42–8.44Å and are only slightly larger than those of magnetite 8.40Å. The red nonmagnetic inclusions have cell dimensions in the vicinity of 8.50Å. Gross franklinite has been found with cell dimensions ranging from those of the black inclusions through about 8.47Å but this far have not been found to match the red inclusions.

The experimental measurement of the ferrites indicates that manganese, and zinc to a lesser extent, control the ferrite lattice variations. Accepting bivalent manganese as the controlling factor, there are two alternatives for further explanation. Either the manganese content of the inclusions is more or less uniform in all franklinites and the valence state differs, or there are varying concentrations of manganese. Impurity of the inclusion concentrates has prevented checking the latter. As to whether the valence of manganese varies in different franklinites, it seems impossible to check because of the co-occurrence of manganese and iron in the same mineral and the oxidation-reduction reaction that takes place between them when the mineral is dissolved in acid.

Friedelite has been detected as a common associate of franklinite inclusions, in places almost to the exclusion of serpentine. A reaction such as that described previously for the serpentinization of willemite could be written with manganese substituted for magnesium. The reaction would perhaps take place under similar environmental conditions, and the metallic oxide inclusion products would be the same. It is improbable, however, that both processes could have continued simultaneously. Thus far, insufficient facts are available to reconcile the two processes.

The foregoing generalized hypothesis can explain certain features of the ore that seemed irreconcilable. If the microscopic inclusions were considered to be emplaced in fractures of the silicate minerals at the time the macroscopic franklinite was formed and thereby to be directly related to it genetically, it was difficult to account for the discrepancies in lattice dimensions between gross franklinite and microscopic franklinite from the same hand specimen. It was even more difficult to explain the existence, side by side, of black and red franklinite, and in some cases, zincite, in the same willemite grain. The serpentine hypothesis seems to clarify the problem somewhat.

## References Cited

Bowen, N. L., and Tuttle, P. F., 1949, The system $MgO$-$SiO_2$-$H_2O$: Geol. Soc. America Bull. v. 60, p. 439–460

Donnay, J. D. H., and Nowacki, W., 1954, Crystal data: Geol. Soc. America Mem. 60, 719 p.

Green, J., 1953, Geochemical table of the elements for 1953: Geol. Soc. America Bull. v. 64, p. 1001–1012

Hague, J. M., Baum, J. L., Herrmann, L. A., and Pickering, R. J., 1956, Geology and structure of the Franklin-Sterling area, New Jersey: Geol. Soc. America Bull. v. 67, p. 435–474

Henry, N. F. M., Lipson, H., and Wooster, W. A., 1951, The interpretation of the X-ray diffraction photographs: New York, Macmillan and Company, 258 p.

Palache, C., 1935, The minerals of Franklin and Sterling Hill, Sussex County, New Jersey: U. S. Geol. Survey Prof. Paper 180, p. 1–135

Pinger, A. W., 1950, Geology of the Franklin-Sterling area, Sussex County, New Jersey, p. 77–87 *in* Dunham, K.C., *Editor*, Symposium on the geology, parageneses, and reserves of the ores of lead and zinc: 18th Internat. Geol. Congr., 1948, Great Britain, Rept. pt. 7, 400 p.

Ridge, J. D., 1952, Geochemistry of the ores of Franklin, N. J.: Econ. Geology, v. 47, p. 180–192

Ries, H., and Bowen, W. C., 1922, Origin of the zinc ores of Sussex County, New Jersey: Econ. Geol., v. XVII, p. 517–571

Rogers, A. F., and Kerr, P. F., 1942, Optical mineralogy: 2d. ed., New York, McGraw-Hill, 390 p.

THE NEW JERSEY ZINC COMPANY, FRANKLIN, NEW JERSEY; THE NEW JERSEY ZINC COMPANY, PALMERTON, PENNSYLVANIA; THE NEW JERSEY ZINC COMPANY, PALMERTON, PENNSYLVANIA

MANUSCRIPT RECEIVED BY THE SECRETARY OF THE SOCIETY APRIL 29, 1957

# Short Notes

BULLETIN OF THE GEOLOGICAL SOCIETY OF AMERICA
VOL. 69, PP. 789–790, 1 PL. JUNE 1958

## FORMATION OF BADLAND TOPOGRAPHY

BY MAX F. CARMAN, JR.

The detailed account of the formation of badland topography by S. A. Schumm (1956) serves as a background for study of the many varied forms of this feature. In the course of mapping in Lockwood Valley, California, the writer has observed in some detail the occurrence of a striking variety of badland topography. Lockwood Valley lies in a semiarid region south of Mount Pinos in Kern and Ventura counties in the northernmost Transverse Ranges. The feature to be described is mostly confined to the Caliente Formation which is part of a sequence of Tertiary continental sedimentary rocks exposed widely around the flanks of Mount Pinos in southeastern Cuyama Valley and extending eastward into Lockwood Valley.

The whole Tertiary sequence is characterized by the fine-textured drainage pattern commonly referred to as badland topography. A variety of this topography consists of narrow ridges, the sides of which are sculptured into delicate flutings, resulting in thin septumlike subridges with nearly vertical sides and distal terminations (Pl. 1, figs. 1, 2). This variety is characteristic of the Caliente Formation. It occurs only in rocks which range in texture from sandy to coarsely conglomeratic (Pl. 1, fig. 3) and which are peculiar in that the coarser material is set in a clay matrix which constitutes a major fraction of the rock.

The formation of this type of badland topography here appears to be due to several factors. The climate is winter-wet semiarid, with annual rainfall seldom exceeding 15 inches. Thus the sediments are dry most of the time. A second factor is very active headward erosion, for the unusual sculpturing appears chiefly at the heads of streams and subsidiary rivulets, and the scale depends on the size and activity of the streams involved. For example, where large streams have unusually steep headward gradients septa and flutings measure tens of feet in height (Pl. 1, fig. 1), but where smaller and less active streams are working on the beds the scale of the phenomenon is smaller, with ridges seldom more than 6 or 8 feet high and commonly much shorter (Pl. 1, fig. 3). A third factor that appears to be even more basic is the presence of clay mixed with coarser fragments. More well-sorted silts and clay interbedded with the fluted layers give smoother and less delicately carved slopes (Pl. 1, fig. 2). In adjoining formations coarse arkoses with predominantly calcareous cement form smooth slopes composed of loose sandy detritus when eroded under the same stream conditions. The fluted ridges, on the other hand, are armored with a hard veneer of sandy clay a few inches thick, which covers a softer inner layer and hard core, suggesting a zone of leaching immediately under the indurated outer layer. In times of rain the water does not soak in readily but moves rapidly into the troughs of the flutings. Its action on the clay-laden material in steep sides of the septa is much like that of surficial melting, wherein only a very thin layer softens and is washed away. Common occurrence of festooned ridgelets similar to those formed by paint that has run is evidence of such action. Ireland *et al.* (1939, p. 66–69) noted similar effects in gully erosion in South Carolina. In washing of gully walls they observed a "paintlike coating" of clay washed from an upper zone and covering a soft lower zone of deeply weathered gneissic bedrock. They further noted the "protective" effect of this coating in retarding removal of the soft material. In Lockwood Valley the protective covering has not washed from an upper zone, but develops from the badland layers themselves. In some places overlying beds are siltstone or arkose with very little clay. Also, the armored layer shows bedding by alignment of clasts which is continuous with bedding of the same nature in the hard core, and which is

concordant across badland ridges (Pl. 1, fig. 3). The cause of armoring is not clearly understood, and a more-detailed study of the septa and the nature of the clay throughout them is needed.

Schumm (1956, p. 632–634) has discussed the formation of rills in badland erosion, pointing out that they form from the channeling of water on steep slopes during rapid runoff. The flutings in the Caliente Formation apparently develop from rills of this type when they are accentuated as a result of a progressively increased ratio of downcutting in rill troughs to slopewash on their sides. Causes seem to be a combination of the armoring of ridge sides, making them resistant to slopewash, and a concentration of water in steep narrow runways containing an abundant supply of clastic particles for cutting. The clastic particles come from within the badland beds, and wash out of the ridges to accumulate in the channels of the flutings. Such cutting tools should materially facilitate downcutting in the channels, which are themselves very well indurated when dry.

Such fluting does not occur in a nearly pure clay which overlies the Caliente Formation; instead, the surface of the clay is composed of a loose granulose aggregate into which water soaks rather than collecting into rill-forming rivulets. The presence of the fluted variety of badland topography in Caliente beds but not in the pure clay suggests that the kind of clay may be a fourth factor in the development of badlands. It is not known whether the clay is different in each formation found in this area, however. X-ray-diffraction patterns from several samples of the pure clay and one of the matrix from the Caliente Formation indicate that most of the material is montmorillonite-type clay, but the fine-grained materials from the other formations have not been identified.

Whether fluting and septa could form in an environment that remains moist over long periods is questionable. If the clay were thoroughly soaked, slumping might prevent development of permanent narrow ridges. The rills and ridges described here showed no important seasonal changes. Though the area is subject to moderate frost action during the wet winter this does not cause disintegration of the ridges, as happens in the cases described by Schumm.

It appears that here we have an exception to Schumm's "Rill Cycle" in which the rills become permanent fluting and under favorable conditions develop the striking septumlike ridges. As noted above, these conditions would include semiarid climate, active headward erosion by streams in the area, and a bedrock composed of clastic particles set in a clay matrix. The nature of the clay in the matrix may also be important, but this point has not been established.

Mr. Schumm has made several helpful suggestions concerning this note. He points out that what is described herein is "probably the normal situation in most badlands", and that it may be concluded that his rill cycle is the exception rather than the rule in the West.

*References Cited*

Ireland, H. A., Sharpe, C. F. S., and Eargle, D. H., 1939, Principles of gully erosion in the piedmont of South Carolina: U. S. Dept. Agriculture Tech. Bull. 633, 142 p.

Schumm, S. A., 1956, Evolution of drainage systems and slopes in badlands at Perth Amboy, New Jersey: Geol. Soc. America Bull., v. 67, p. 597–646

PETROBRÁS CENAP - CURSO DE GEOLOGIA, AV. JOANNA ANGELICA 183, SALVADOR, BAHIA, BRASIL

MANUSCRIPT RECEIVED BY THE SECRETARY OF THE SOCIETY, NOVEMBER 26, 1957

PLATE 1.—BADLAND TOPOGRAPHY

FIGURE 1.—Large-scale fluting in conglomeratic Caliente beds. Fluted cliff is 150 feet high left of center. Mark above ridge line is meaningless.

FIGURE 2.—Small-scale fluting in beds of typical Caliente lithology with interbedded clay and overlying silt. Fault, left of center, has dropped stratigraphically higher arkose on left against badland beds on right. Barren ridge is 30 feet high.

FIGURE 3.—Shallow fluting in coarsely conglomeratic Caliente beds. Note accumulation of clastic fragments in bottoms of channels.

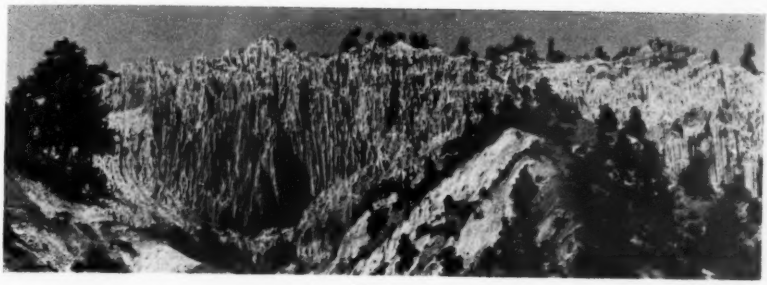

FIGURE 1

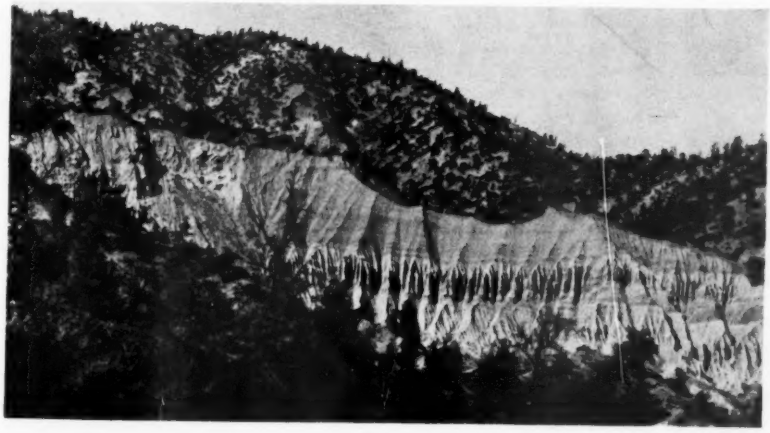

FIGURE 2

FIGURE 3

BADLAND TOPOGRAPHY

BULLETIN OF THE GEOLOGICAL SOCIETY OF AMERICA
VOL. 69, PP. 791–796, 4 FIGS. JUNE 1958

# CROSS-BEDDING IN PENNSYLVANIAN SANDSTONES OF CENTRAL PENNSYLVANIA: A PRELIMINARY STUDY

BY RICHARD P. NICKELSEN

## *Introduction*

Recent regional cross-bedding studies in lower Pennsylvanian sandstones of the Eastern Interior Basin (Potter and Siever, 1956) have stimulated interest in Pennsylvanian paleogeography and have shown the value of cross-bedding in indicating source areas for Pennsylvanian sediments. No cross-bedding studies have been completed on the Pennsylvanian rocks of the Appalachian Plateau.

This note presents information collected from a 600-square-mile area in Centre and Clearfield counties, Pennsylvania, on the type and dip directions of cross-bedding. During 1954–1956, while doing stratigraphic work on Pennsylvanian rocks, the writer recorded 440 cross-bedding dip directions, at 36 localities, in 7 stratigraphically different sandstones. Each cross-bedded sandstone encountered during stratigraphic work was sampled on a grid with stations commonly spaced 10 feet along the base and up the face of the exposure. No preliminary regional sampling was established at the beginning of work because correlation and extent of cross-bedded sandstone bodies were not known.

Financial support for stratigraphic work in central Pennsylvania was provided by the Department of Geology and Experiment Station of the College of Mineral Industries, The Pennsylvania State University. The writer thanks Eugene Williams for supplying cross-bedding data from the Clearfield area and for critically reading the manuscript. Francis J. Pettijohn read a preliminary draft of the manuscript and offered a number of helpful suggestions.

## *Stratigraphy*

A generalized section showing the stratigraphic position of coals and sandstones of the area is shown in Figure 3. The section below the Lower Kittanning coal was compiled by Williams and the writer (Williams and Nickelsen, In press) while the part above the Lower Kittanning coal was modified from Sisler (1926, p. 164). With few exceptions the sandstones are named for the coal which overlies them. Pennsylvanian rocks of the area occur in cyclic successions, consisting of sandstone, clay or claystone, coal, and shale in ascending order. The sandstone of the overlying cycle may occur in conformable sequence above the shale or may disconformably overlie any rock type in the preceding cycle. Most cross-bedding appears in thick, massive, disconformable sandstone occupying channels in the underlying rocks. Sandstones are irregular in thickness and distribution, and none, except possibly the Homewood, persist over the whole area. They either interfinger with shales or thin to a feather edge where surfaces of disconformity rise on the sides of channeled areas. Some, such as the Lower Kittanning sandstone in the region between Houtzdale and Philipsburg and the Middle Kittanning sandstone north of Philipsburg, are present over areas of 40 to 50 square miles, but others, such as the Upper Kittanning sandstone, are extremely local.

## *Cross-Bedding*

Figure 2 illustrates the type of cross-bedding most commonly observed in Pottsville and lower Allegheny sandstones. The vector sum of all cross-bedding dips at this locality is shown by the arrow. It is inferred that the average direction of current movement paralleled the arrow. The right face of the block is a section parallel to the average direction of current movement, and the left face is perpendicular to the average current direction.

Cross-bedding shown in Figure 2 is most like planar cross-stratification (McKee and Weir, 1953, p. 387) in which the lower bounding surface of cross-bedding sets are planar surfaces of erosion and sets are tabular or wedge-shaped. Trough cross-stratification, in which the lower bounding surfaces of sets are curved surfaces of erosion, is also shown in Figure 2, and all transitions between planar and trough cross-stratification probably exist. Whether a particular set is classified as trough or planar type depends upon radius of curvature of the erosional surface in relation to the size of the outcrop. Units of sedimentation containing cross-

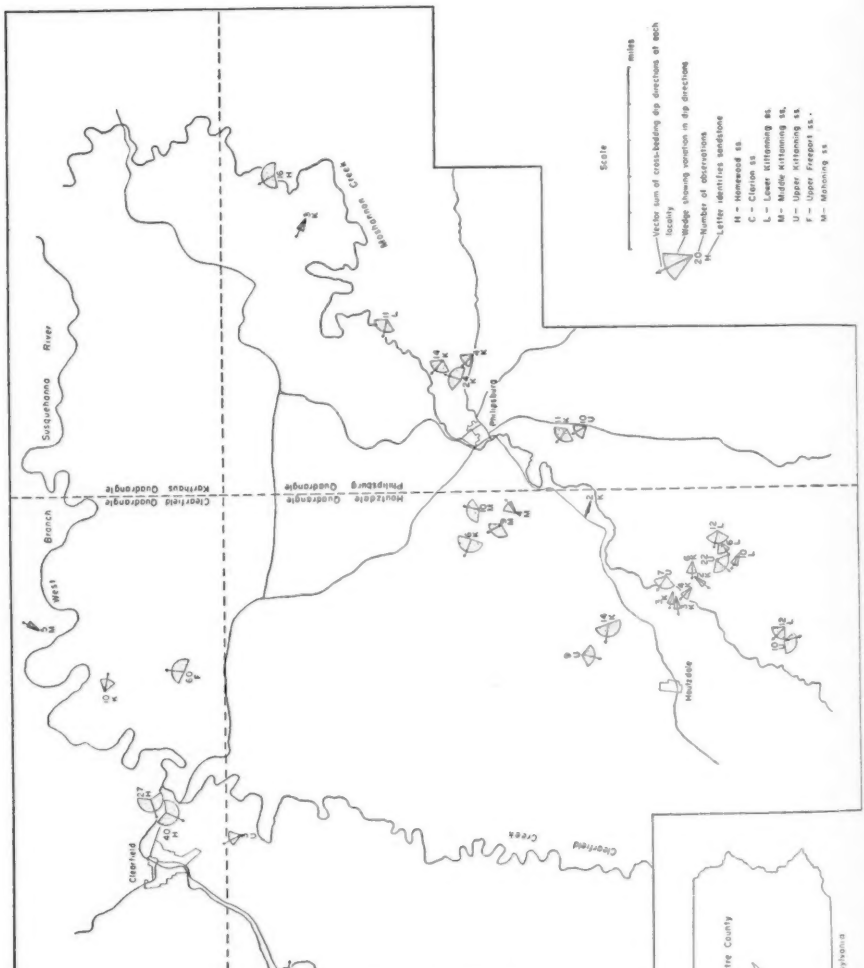


FIGURE 1.—MAP SHOWING CROSS-BEDDING LOCALITIES

bed sets are apparently elongated in the direction of current flow (*compare* right and left faces of Figure 2) and either lenticular or wedging tabular. The cross-bed unit diagrammatically shown by Potter and Siever (1956, Fig. 3) is similar to those inferred for this area

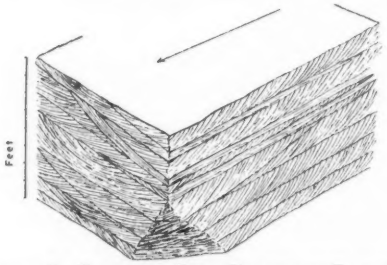


FIGURE 2.—SKETCH OF CROSS-BEDDING IN CLARION SANDSTONE AT BILGERS ROCKS, NORTHWEST OF CURWENSVILLE, PENNSYLVANIA
Arrow shows vector sum of all cross-bedding dips.

except that greater variation in strike of cross-bedding within sets was found in central Pennsylvania, and sets were not always concave in the direction of current flow. Tanner, (1955, p. 2473) compared the various statistical measures of central tendency as applied to cross-bedding and concluded that modes, vector sums, and minimum arrows are most useful for indicating paleocurrent trends. The writer has followed Tanner in using modes (circular histograms) and vector sums to present data.

Figures 1 and 4 summarize the observations on cross-bedding dip directions. Figure 1 shows localities where cross-bedding was measured. Vector sums were calculated graphically by vector addition. Figure 4 shows the frequency of occurrence of cross-bed dip directions in 10-degree classes for each sandstone.

*Discussion of Cross-Bedding Dip Orientation*

Vector sums of cross-bedding dips in the Homewood Sandstone at three localities fall in the northwest and southwest quadrants, and the histogram shows modes in the northwest, southwest, and southeast quadrants (Fig. 4*B*). Although data are meager, a westerly direction of transport is indicated. In sharp contrast, the trends of the Clarion Sandstone (Fig. 4*C*), which is well developed only in the western part of the area near Curwensville (Fig. 1), are to the northeast or southeast. This is the only sandstone in the area showing such an easterly trend. The Lower Kittanning Sandstone which was sampled only near Philipsburg and Houtzdale shows an equally strong development of westerly dips with a concentration of vector sums and modes in the northwest quadrant

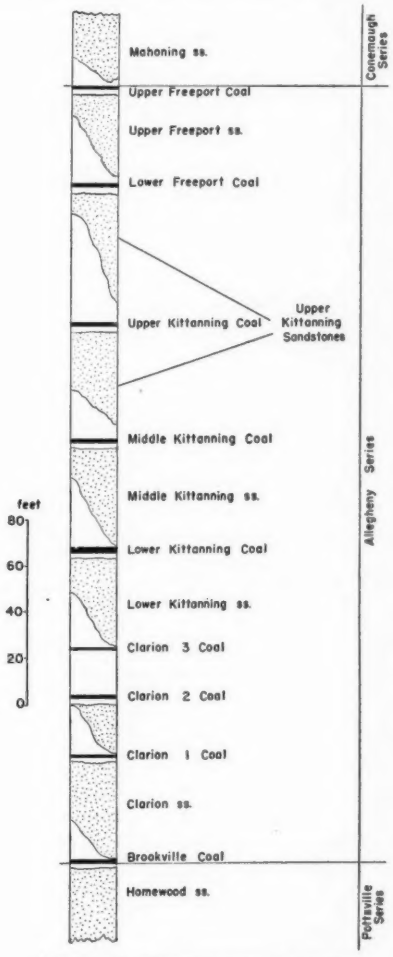


FIGURE 3.—GENERALIZED SECTION, PENNSYLVANIAN ROCKS OF CLEARFIELD AND CENTRE COUNTIES, PENNSYLVANIA

(Fig. 4*D*). The Middle Kittanning Sandstone was sampled more extensively than other sandstones because abundant exposures are provided by strip mining on the underlying Lower Kittanning coal. There is a high concentration of dips and vector sums in the western half of the diagram (Fig. 4*E*), but regional variations are present. Dips to the west and north are pre-

FIGURE 1.—MAP SHOWING CROSS-BEDDING LOCALITIES

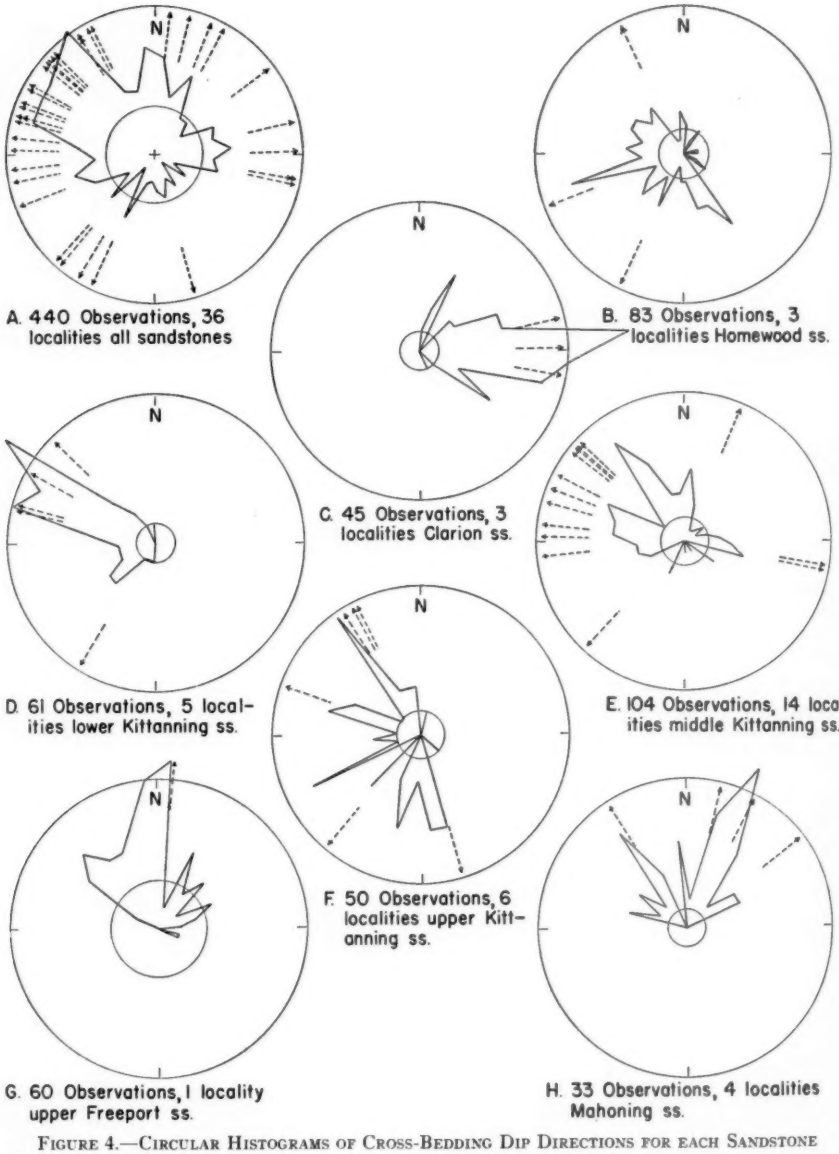
N
A. 440 Observations, 36 localities all sandstones
B. 83 Observations, 3 localities Homewood ss.
C. 45 Observations, 3 localities Clarion ss.
D. 61 Observations, 5 localities lower Kittanning ss.
E. 104 Observations, 14 localities middle Kittanning ss.
F. 50 Observations, 6 localities upper Kittanning ss.
G. 60 Observations, 1 locality upper Freeport ss.
H. 33 Observations, 4 localities Mahoning ss.

FIGURE 4.—CIRCULAR HISTOGRAMS OF CROSS-BEDDING DIP DIRECTIONS FOR EACH SANDSTONE

Radii of small circles equal 2 per cent of total cross-beds plotted in each diagram. Arrows are vector sums for each locality plotted on Figure 1.

dominant in the eastern part of the area in an extensive body of sandstone between Philipsburg and West Branch of the Susquehanna River. South of Philipsburg dips swing to the southwest. In the central and western part of the area, however, two localities show vector sums to the southeast. Cross-bedding from sandstones both above and below the Upper Kittanning coal has been plotted in Figure 4*F*. Both sandstones are local in development, and there is great variability in cross-bedding dip directions. Nevertheless there are few dips to

the east, and a westerly direction of current flow is suggested. Sandstones above both Freeport coals show a high frequency of northeasterly and northwesterly dips and similar vector sum directions (Fig. 4, *G* and *H*). Although only five localities in the central part of the area were sampled, a northerly direction of current flow is strongly indicated.

### *Interpretation*

Cross-bedding orientations over such a small area and including so few sampling localities cannot lead to major conclusions about the source of Pennsylvanian sediments. Studies by Potter and Olson (1954), Potter and Siever (1956), and Pettijohn (1957) have demonstrated the need for systematic coverage of a large area in order to exclude overemphasis on local vagaries in current direction. However, certain tentative interpretations can be made.

The Homewood, Lower Kittanning, Middle Kittanning, and Upper Kittanning sandstones are all marked by a predominance of cross-bed dips in the western quadrants of Figure 4, *B*, *D*, *E*, and *F*. Cross-bedding in these sandstones is largely responsible for the modal and vector sum concentrations in the northwest quadrant of Figure 4*A*. Each sandstone shows slight differences in dip direction within this pattern. Homewood and Upper Kittanning cross-beds vary around a southwesterly median, whereas Lower and Middle Kittanning dip directions are heavily concentrated in the north and northwest. It is plausible to suggest a source to the southeast or east for these sandstones. The predominance of easterly cross-bedding dips in the Clarion Sandstone of the Curwensville area has already been noted (Fig. 1, 4*C*). Only three outcrops of this sandstone were visited, but readings, if significant, indicate a direction of current flow greatly different from that of most other sandstones of the region. The Middle Kittanning sandstone also shows easterly dips at two localities in the western part of the region. Local easterly dips may result from a meander in the delta distributary or stream that deposited the sandstone or may indicate a different genesis for the sandstone (*e. g.*, sand bar). Less likely, they could mean a shift in the source of sediments to the west. A local source or local uplift within the area of sedimentation which served to deflect currents may also be suggested to explain these anomalous dips. Wanless (1946, p. 132) reports great Pennsylvanian thickness differences on opposite sides of several anticlines and fault zones in Kentucky, and Fettke (1954, p. 8) notes that "prominent folds on the southeastern side of the Appalachian basin are much more complex structurally at depth than had been anticipated from earlier surfaces studies." Thickening of Pennsylvanian sediments in synclinal troughs and thinning over anticlinal crests has been recognized in Clearfield and Centre counties, Pennsylvania (Williams and Nickelsen, In press). These observations indicate structural growth within the Appalachian Plateau before and during deposition of Pennsylvanian rocks. The Chestnut Ridge anticline, just west of the map area (Fig. 1), was perhaps growing at the time of sedimentation, and could have deflected regional current flow or been a local source, giving rise to the easterly cross-bedding dips. The La Salle anticline of Illinois may have acted similarly to deflect currents depositing the Mansfield Sandstone (Potter and Olson, 1954, p. 66).

Northerly cross-bedding dips in both the Upper Freeport and Mahoning sandstones are an example of variation in dip direction at different stratigraphic horizons. A southeasterly source is still indicated, but deflection of current flow northward has occurred, perhaps by sedimentary upbuilding south of the study area.

### *Summary*

Data indicate an east or southeast source for central Pennsylvania Upper Pottsville and Allegheny sediments. Problems for further work suggested by this preliminary study are:

(1) A study of cross-bedding in the lower Pottsville (Conoquenssing Sandstone and Olean Conglomerate) in central and west-central Pennsylvania to discover if a southeast source is indicated or if a northerly source, as suggested by Potter and Siever (1956) and Fuller (1955) for the lower Pottsville of Ohio, Illinois and Indiana, is more probable.

(2) A regional cross-bedding study of the Upper Freeport and Mahoning sandstones to bring out the reasons for the northerly dips found in the study area. Was there a shift in the regional slope from northwest to north at this time, or are the trends shown merely part of the fanning out of currents from a local area of sedimentary upbuilding?

(3) A study of the cross-bedding in a number of sandstones along both sides of Chestnut Ridge to test various hypotheses for the easterly cross-bedding dips in the Clarion and Middle Kittanning sandstones of this area.

*References Cited*

Fettke, C. R., 1954, Structure contour maps of the plateau region of north central and western Pennsylvania: Pa. Geol. Survey Bull. G 27, p. 1–23

Fuller, J. O., 1955, Sources of Sharon conglomerate of northeastern Ohio: Geol. Soc. America Bull., v. 66, p. 159–176

McKee, E. D., and Weir, G. W., 1953, Terminology for stratification and cross-stratification in sedimentary rocks: Geol. Soc. America Bull., v. 64, p. 381–390

Pettijohn, F. J., 1957, Paleocurrents of Lake Superior Precambrian quartzites: Geol. Soc. America Bull., v. 68, p. 469–480

Potter, P. E., and Olson, J. S., 1954, Variance components of cross-bedding direction in some basal Pennsylvanian sandstones of Eastern Interior Basin: Geological application Jou:r. Geology, v. 62, p. 26–49

Potter, P. E., and Siever, R., 1956, Sources of basal Pennsylvanian sediments in the Eastern Interior Basin, I. Cross-bedding: Jour. Geology, v. 64, p. 225–244

Sisler, J. D., 1926, Bituminous coal fields of Pennsylvania, Part II: Pa. Geol. Survey Bull. M 6, p. 1–511

Tanner, W. F., 1955, Paleogeographic reconstructions from cross-bedding studies: Am. Assoc. Petroleum Geologists Bull., v. 39, p. 2471–2483

Wanless, H. R., 1946, Pennsylvanian geology of part of the southern Appalachian coal field: Geol. Soc. America Mem. 13, p. 1–162

Williams, E., and Nickelsen, R. P., in press, Stratigraphy of the Pottsville- and lower Allegheny series in parts of Clearfield and Centre counties, Pennsylvania. Bulletin of the Mineral Industries Experiment Station, Mineral Conservation series, the Pennsylvania State University

Dept. of Geology, College of Mineral Industries, Pa. State University, University Park, Pa.

College of Mineral Industries Contribution Number 57-34

Manuscript Received by the Secretary of the Society, July 27, 1957

# INDEX TO VOLUME 69 (January–June)*


Age determination (*See also* Geochronology)
Potassium-argon dating of sedimentary rocks.
By G. H. Curtis and J. H. Reynolds ..... 151
By Joseph Lipson ..... 137
Precambrian classification and correlation in the Canadian Shield. By M. E. Wilson ..... 757
Time factor in formation of desert varnish. By C. G. Engel and R. P. Sharp ..... 487
† Age of the metamorphism of the rocks of the Manhattan Prong. By L. E. Long and J. L. Kulp ..... 603
Alaska
Basins in coastal foreland. By R. P. Sharp ..... 617
Malaspina Glacier. By. R. P. Sharp ..... 617
Alluvium
Geological geomorphology. By R. J. Russell ..... 1
Alteration
Urano-organic ore at Temple Mountain, Utah. By D. R. Kelley and P. F. Kerr ..... 701
**Alteration of clay minerals in Illinoian till by weathering.** By J. B. Droste and J. C. Tharin ..... 61
Analyses
Chemical
Asphalt and urano-organic ore, Temple Mountain, Utah. By D. R. Kelley and P. F. Kerr ..... 701
Desert varnish. By C. G. Engel and R. P. Sharp ..... 487
Water from Kapingamarangi Atoll, Caroline Islands. By E. D. McKee ..... 241
Dimensional
Fluvially eroded landforms. By A. N. Strahler 279
Modal
White Tank quartz monzonite, California. By J. J. W. Rogers ..... 449
Soil
Kapingamarangi Atoll, Caroline Islands. By E. D. McKee ..... 241
Spectrochemical
Feldspars, White Tank quartz monzonite, California. By J. J. W. Rogers ..... 449
Spectrographic
Desert varnish. By C. G. Engel and R. P. Sharp 487
Pumice from Kapingamarangi Atoll, Caroline Islands. By E. D. McKee ..... 241
Spectrometric
Potassium-argon dating of sedimentary rocks. By Joseph Lipson ..... 137
Appalachian Basin, Petrology of underclays of. By L. G. Schultz ..... 363

Bachman, G. O., and Hayes, P. T.: Stratigraphy of Upper Pennsylvanian and Lower Permian rocks in the Sand Canyon area, Otero County, New Mexico 689
Bellemin, G. J., and Merriam, Richard: Petrology and origin of the Poway conglomerate, San Diego County, California ..... 199
Biostratigraphical concepts. By Curt Teichert ..... 99
† Birch, Francis: Differentiation of the mantle ..... 483
Blue Ridge Mountains, Virginia, Infolded metasedimentary rocks near the axial zone of. By E. O. Gooch 569
Borehole data, Malaspina Glacier, Alaska. By R. P. Sharp ..... 617
† Bramlette, M. N.: Significance of coccolithophorids in calcium-carbonate deposition ..... 121

British Columbia, Canada, Geology of the Mount Garibaldi map-area, southwestern. By W. H. Mathews 161, 179

California
Chemical data on desert varnish. By C. G. Engel and R. P. Sharp ..... 487
Petrology and origin of the Poway conglomerate, San Diego County. By G. J. Bellemin and Richard Merriam ..... 199
Shallow submerged marine terraces of Southern. By K. O. Emery ..... 39
Textural and spectrochemical studies of the White Tank quartz monzonite. By J. J. W. Rogers ... 449
† Callaghan, Eugene (With G. T. Faust): Mineralogy and petrology of the Currant Creek magnesite deposits and associated rocks of Nevada ..... 353
Cambrian
Stratigraphy of the Cow Head region, western Newfoundland. By C. H. Kindle and H. B. Whittington ..... 315
—stratigraphy in northern Utah and southeastern Idaho, Lower and Middle. By G. B. Maxey ..... 647
Canada
Precambrian classification and correlation in the Canadian Shield. By M. E. Wilson ..... 757
Canadian Shield, Precambrian classification and correlation in. By M. E. Wilson ..... 757
† Carman, M. F., Jr.: Formation of badland topography 789
Caroline Islands, Geology of Kapingamarangi Atoll. By E. D. McKee ..... 241
Catoctin Mountain-Blue Ridge anticlinorium, Virginia, Infolded metasedimentary rocks near the axial zone of. By. E. O. Gooch ..... 569
Catoctin Mountains, Virginia, Infolded metasedimentary rocks near the axial zone of. By E. O. Gooch ..... 569
Chemical analyses
Asphalt and urano-organic ore, Temple Mountain, Utah. By D. R. Kelley and P. F. Kerr ..... 701
Desert varnish. By C. G. Engel and R. P. Sharp ..... 487
Water from Kapingamarangi Atoll, Caroline Islands. By E. D. McKee ..... 241
**Chemical data on desert varnish.** By C. G. Engel and R. P. Sharp ..... 487
Chromite
Geology and petrology of the Masinloc deposit, Zambales, Luzon, Philippine Islands. By W. C. Stoll 419
Clay minerals in Illinoian till
Alteration by weathering. By J. B. Droste and J. C. Tharin ..... 61
Coal geology
Petrology of underclays. By L. G. Schultz ..... 363
Colorado, Uranium deposits under conglomeratic sandstone of the Morrison formation in. By D. A. Phoenix 403
† Complex origin of silts in the vicinity of Fairbanks, Alaska. By Stephen Taber ..... 131
**Contribution to the petrography of the Tanner graywacke, by Reinhard Heimbold.** By F. B. Van Houten, Translator ..... 301
Coral reefs
Geology of Kapingamarangi Atoll, Caroline Islands. By E. D. McKee ..... 241
† Cormier, R. F. (With W. H. Pinson, Jr., and H. W. Fairbairn): Sr/Rb age measurements on hornblende and feldspar, and the age of syenite at Chicoutimi, Quebec, Canada ..... 599


*Full titles of papers are in **boldface** type.
† Indicates Short Note.

Coronas, Coronites from India and their bearing on the origin of. By M. V. N. Murthy ..... 23
**Coronites from India and their bearing on the origin of coronas.** By M. V. N. Murthy ..... 23
Correlation in the Canadian Shield, Precambrian. By M. E. Wilson ..... 757
Cow Head group (new name) (Cambrian-Ordovician), western Newfoundland. By C. H. Kindle and H. B. Whittington ..... 315
— —region of western Newfoundland, Stratigraphy of. By C. H. Kindle and H. B. Whittington ..... 315
† Cross-bedding in Pennsylvanian sandstones of central Pennsylvania: A preliminary study. By R. P. Nickelsen ..... 791
CURTIS, G. H., AND REYNOLDS, J. H.: Notes on the potassium-argon dating of sedimentary rocks ..... 151

Danley Ranch tongue, Abo sandstone (Pennsylvanian) (new name), New Mexico. By G. O. Bachman and P. T. Hayes ..... 689
Deformation in Wombeyan marble, Experimental. by M. S. Paterson ..... 465
Deltas
Geological geomorphology. By R. J. Russell ..... 1
Desert pavement, Varnished stones in. By C. G. Engel and R. P. Sharp ..... 487
—varnish, Chemical data on. By R. P. Sharp ..... 487
† Differentiation of the mantle. By Francis Birch ..... 483
**Dimensional analysis applied to fluvially eroded landforms.** By A. N. Strahler ..... 279
**Drainage evolution in northeastern Montana and northwestern North Dakota.** By A. D. Howard ..... 575
DREWES, HAROLD: Structural geology of the southern Snake Range, Nevada ..... 221
DROSTE, J. B., AND THARIN, J. C.: Alteration of clay minerals in Illinoian till by weathering ..... 61

Economic geology
Geochemistry of the Sterling Hill zinc deposit, Sussex County, New Jersey. By R. W. Metsger, C. B. Tennant, and J. L. Rodda ..... 775
Masinloc chromite deposit, Zambales, Luzon, Philippine Islands. By W. C. Stoll ..... 419
Petrology of underclays. By L. G. Schultz ..... 363
Uranium deposits under conglomeratic sandstone of the Morrison formation, Colorado and Utah. By D. A. Phoenix ..... 403
Urano-organic ore at Temple Mountain, Utah. By D. R. Kelley and P. F. Kerr ..... 701

EMERY, K. O.: Shallow submerged marine terraces of Southern California ..... 39
ENGEL, C. G., AND SHARP, R. P.: Chemical data on desert varnish ..... 487
Eocene
Poway conglomerate, San Diego County, California. By G. J. Bellemin and Richard Merriam ..... 199
Erosion
Dimensional analysis applied to fluvially eroded landforms. By A. N. Strahler ..... 279
—surfaces
Drainage evolution in northeastern Montana and northwestern North Dakota. By A. D. Howard ..... 575
**Experimental deformation and faulting in Wombeyan marble.** By M. S. Paterson ..... 465

† FAIRBAIRN, H. W. (WITH W. H. PINSON, JR., AND R. F. CORMIER): Sr/Rb age measurements on hornblende and feldspar, and the age of syenite at Chicoutimi, Quebec, Canada ..... 599

Faulting in Wombeyan marble, Experimental. By M. S. Paterson ..... 465
† FAUST, G. T., AND CALLAGHAN, EUGENE: Mineralogy and petrology of the Currant Creek magnesite deposits and associated rocks of Nevada. New data ..... 353
† Flowtill in southeastern Massachusetts. By J. H. Hartshorn ..... 477
† Formation of badland topography. By M. F. Carman, Jr. ..... 789

GAGE, MAXWELL, AND SUGGATE, R. P.: Glacial chronology of the New Zealand Pleistocene ..... 589
**Geochemistry of the Sterling Hill zinc deposit, Sussex County, New Jersey.** By R. W. Metsger, C. B. Tennant, and J. L. Rodda ..... 775
Geochronology (*See also* Age determination)
Some biostratigraphical concepts. By Curt Teichert ..... 99
**Geological geomorphology.** By R. J. Russell ..... 1
**Geology and petrology of the Masinloc chromite deposit, Zambales, Luzon, Philippine Islands.** By W. C. Stoll ..... 419
**Geology of the Kapingamarangi Atoll, Caroline Islands.** By E. D. McKee ..... 241
**Geology of the Mount Garibaldi map-area, southwestern British Columbia, Canada.** By W. H. Mathews
Part I ..... 161
Part II ..... 179
Geomorphology
Desert varnish in arid region. By C. G. Engel and R. P. Sharp ..... 487
Dimensional analysis applied to fluvially eroded landforms. By A. N. Strahler ..... 279
Geology of the Mount Garibaldi map-area, southwestern British Columbia, Canada. By W. H. Mathews ..... 161, 179
—, Geological. By R. J. Russell ..... 1
Geophysical exploration
Recent underwater surveys using low-frequency sound to locate shallow bedrock. By W. O. Smith ..... 69
Geophysics
Shallow submerged marine terraces of Southern California. By K. O. Emery ..... 39
† GIBSON, W. M.: Gulf of Alaska Trough parallels Aleutian Trench ..... 611
**Glacial chronology of the New Zealand Pleistocene.** By Maxwell Gage and R. P. Suggate ..... 589
—deposits
Alteration of clay minerals in Illinoian till by weathering. By J. B. Droste and J. C. Tharin ..... 61
Glaciation
Geology of the Mount Garibaldi map-area, southwestern British Columbia, Canada. By W. H. Mathews ..... 161, 179
Glacial chronology of the New Zealand Pleistocene. By Maxwell Gage and R. P. Suggate ..... 589
Glacier regimen, Malaspina-Seward system, Alaska. By R. P. Sharp ..... 617
Glaciology
Malaspina Glacier, Alaska. By R. P. Sharp ..... 617
GOOCH, E. O.: Infolded metasedimentary rocks near the axial zone of the Catoctin Mountain-Blue Ridge anticlinorium in Virginia ..... 509
Graywacke, Contribution to the petrography of Tanner, by Reinhard Helmbold. By F. B. Van Houten, Translator ..... 301
Ground water
Geology of Kapingamarangi Atoll, Caroline Islands. By E. D. McKee ..... 241
Uranium deposits under conglomeratic sandstone of

the Morrison formation, Colorado and Utah. By D. A. Phoenix ... 403
† Gulf of Alaska Trough parallels Aleutian Trench. By W. M. Gibson ... 611

† Hartshorn, J. H.: Flowtill in southeastern Massachusetts ... 477
Hayes, P. T. (With G. O. Bachman): Stratigraphy of Upper Pennsylvanian and Lower Permian rocks in the Sand Canyon area, Otero County, New Mexico ... 689
† Hospers, J., and van Wijnen, J. C.: Rock densities of the central Venezuelan Andes ... 359
Howard, A. D.: Drainage evolution in northeastern Montana and northwestern North Dakota ... 575
Hydrographic surveying
Recent underwater surveys using low-frequency sound to locate shallow bedrock. By W. O. Smith ... 69

Idaho, Lower and Middle Cambrian stratigraphy in southeastern. By G. B. Maxey ... 647
Igneous rocks
Geology and petrology of the Masinloc deposit, Zambales, Luzon, Philippine Islands. By W. C. Stoll ... 419
— of the Mount Garibaldi map-area, southwestern British Columbia, Canada. By W. H. Mathews 161, 179
Structural geology of the southern Snake Range, Nevada. By Harald Drewes ... 221
Textural and spectrochemical studies of the White Tank quartz monzonite, California. By J. J. W. Rogers ... 449
Illinoian till
Alteration of clay minerals by weathering. By J. B. Droste and J. C. Tharin ... 61
Illinois Basin, Petrology of underclays of. By L. G. Schultz ... 363
India, Coronites and their bearing on the origin of coronas. By M. V. N. Murthy ... 23
**Infolded metasedimentary rocks near the axial zone of the Catoctin Mountain-Blue Ridge anticlinorium in Virginia.** By E. O. Gooch ... 569

Joshua Tree National Monument, California, Textural and spectrochemical studies of the White Tank quartz monzonite. By J. J. W. Rogers ... 449

Kapingamarangi Atoll, Caroline Islands, Geology of. By E. D. McKee ... 241
Kelley, D. R., and Kerr, P. F.: Urano-organic ore at Temple Mountain, Utah ... 701
Kerr, P. F. (With D. R. Kelley): Urano-organic ore at Temple Mountain, Utah ... 701
Kindle, C. H., and Whittington, H. B.: Stratigraphy of the Cow Head region, western Newfoundland ... 315
† Konizeski, R. L.: Pliocene vertebrate fauna from the Bitterroot Valley, Montana, and its stratigraphic significance ... 345
† Kulp, J. L. (With L. E. Long): Age of the metamorphism of the rocks of the Manhattan Prong ... 603

Lee Ranch tongue, Abo sandstone (Pennsylvanian) (new name), New Mexico. By G. O. Bachman and P. T. Hayes ... 689
Lipson, Joseph: Potassium-argon dating of sedimentary rocks ... 137
Little Missouri River
Drainage evolution in northeastern Montana and northwestern North Dakota. By A. D. Howard ... 575
† Lochman, Christina: Lower Cambrian section of Vermont ... 127
† Long, L. E., and Kulp, J. L.: Age of the metamorphism of the rocks of the Manhattan Prong ... 603
**Lower and Middle Cambrian stratigraphy in northern Utah and southeastern Idaho.** By G. B. Maxey ... 647
† Lower Cambrian section of Vermont. By Christina Lochman ... 127
Luzon, Philippine Islands, Geology and petrology of the Masinloc deposit, Zambales. By W. C. Stoll ... 419

**Malaspina Glacier, Alaska.** By R. P. Sharp ... 617
Marble, Experimental deformation and faulting in Wombeyan. By M. S. Paterson ... 465
Masinloc chromite deposit, Zambales, Luzon, Philippine Islands, Geology and petrology of. By W. C. Stoll ... 419
Mathews, W. H.: Geology of the Mount Garibaldi map-area, southwestern British Columbia, Canada
Part I ... 161
Part II ... 179
Maxey, G. B.: Lower and Middle Cambrian stratigraphy in northern Utah and southeastern Idaho ... 647
McKee, E. D.: Geology of Kapingamarangi Atoll, Caroline Islands ... 241
Meandering
Geological geomorphology. By R. J. Russell ... 1
† Melton, M. A.: Use of punched cards to speed statistical analyses of geomorphic data ... 355
Merriam, Richard (With G. J. Bellemin): Petrology and origin of the Poway conglomerate, San Diego County, California ... 199
Metamorphic rocks
Geology of the Mount Garibaldi map-area, southwestern British Columbia, Canada. By W. H. Mathews ... 161, 179
Metamorphism
Infolded metasedimentary rocks near the axial zone of the Catoctin Mountain-Blue Ridge anticlinorium in Virginia. By E. O. Gooch ... 569
Water-deficient dolerites. By M. V. N. Murthy ... 23
Metsger, R. W., Tennant, C. B., and Rodda, J. L.: Geochemistry of the Sterling Hill zinc deposit, Sussex County, New Jersey ... 775
Mid-Continent Basin, Petrology of underclays of. By L. G. Schultz ... 363
† Military use of geologists in World War II. By R. L. Nace ... 615
Mineralogy
Coronites from India and their bearing on the origin of coronas. By M. V. N. Murthy ... 23
Geochemistry of the Sterling Hill zinc deposit, Sussex County, New Jersey, By R. W. Metsger, C. B. Tennant, and J. L. Rodda ... 775
Underclays. By L. G. Schultz ... 363
Urano-organic ore at Temple Mountain, Utah. By D. R. Kelley and P. F. Kerr ... 701
† Mineralogy and petrology of the Currant Creek magnesite deposits and associated rocks of Nevada. New data. By G. T. Faust and Eugene Callaghan ... 353
Missouri River
Drainage evolution in northeastern Montana and northwestern North Dakota. By A. D. Howard ... 575
Modal analyses
White Tank quartz monzonite, California. By J. J. W. Rogers ... 449
Mojave Desert, California, Chemical data on desert varnish. By C. G. Engel and R. P. Sharp ... 487
Montana, Drainage evolution in northeastern. By A. D. Howard ... 575
Monzonite, California, Textural and spectrochemical studies of the White Tank quartz. By J. J. W. Rogers 449

Morrison formation, Colorado and Utah, Uranium deposits under conglomeratic sandstone of. By D. A. Phoenix . . 403
Mount Garibaldi map-area, southwestern British Columbia, Canada. By W. H. Mathews . . . . . 161, 179
MURTHY, M. V. N.: Coronites from India and their bearing on coronas . . . . . 23

† NACE, R. L.: Military use of geologists in World War II . . . . . 615
Naomi Peak limestone member (new name), Langston formation (Cambrian). By G. B. Maxey . . . . . 647
Nevada, Structural geology of the southern Snake Range in. By Harald Drewes . . . . . 221
New Jersey, Geochemistry of the Sterling Hill zinc deposit, Sussex County, By. R. W. Metsger, C. B. Tennant, and J. R. Rodda . . . . . 775
New Mexico, Stratigraphy of Upper Pennsylvanian and Lower Permian rocks in the Sand Canyon area, Otero County. By G. O. Bachman and P. T. Hayes . . . . . 689
New South Wales
  Experimental deformation and faulting in Wombeyan marble. By M. S. Paterson . . . . . 465
New Zealand
  Glacial chronology of the Pleistocene. By Maxwell Gage and R. P. Suggate . . . . . 589
  Potassium-argon dating of sedimentary rocks. By Joseph Lipson . . . . . 137
Newfoundland, Stratigraphy of the Cow Head region in western. By C. H. Kindle and H. B. Whittington . . . 315
† NICKELSEN, R. P.: Cross-bedding in Pennsylvanian sandstones of central Pennsylvania: A preliminary study . . . . . 791
North Dakota, Drainage evolution in northwestern. By A. D. Howard . . . . . 575
**Notes on the potassium-argon dating of sedimentary rocks.** By G. H. Curtis and J. H. Reynolds . . . . . 151

† Olivine-spinel transition in fayalite. By A. E. Ringwood . . . . . 129
Ordovician
  Stratigraphy of the Cow Head Region, western Newfoundland. By C. H. Kindle and H. B. Whittington . . . . . 315
Ore deposits
  Geochemistry of the Sterling Hill zinc deposit, Sussex County, New Jersey. By R. W. Metsger, C. B. Tennant, and J. L. Rodda . . . . . 775
  Masinloc chromite deposit, Zambales, Luzon, Philippine Islands. By W. C. Stoll . . . . . 419
  Uranium deposits under conglomeratic sandstone of the Morrison formation, Colorado and Utah. By D. A. Phoenix . . . . . 403
Otero County, New Mexico, Stratigraphy of Upper Pennsylvanian and Lower Permian rocks in Sand Canyon area. By G. O. Bachman and P. T. Hayes . . . . . 689
Otero Mesa member, Yeso formation (Permian) (new name), New Mexico. By G. O. Bachman and P. T. Hayes . . . . . 689
Otiran glacial stage
  Glacial chronology of the New Zealand Pleistocene. By Maxwell Gage and R. P. Suggate . . . . . 589

Pacific Ocean
  Geology of Kapingamarangi Atoll, Caroline Islands. By E. D. McKee . . . . . 241
Paleogeography
  Lower and Middle Cambrian stratigraphy in northern Utah and southeastern Idaho. By G. B. Maxey . . . . 647
Paleontology
  Geology of Kapingamarangi Atoll, Caroline Islands. By E. D. McKee . . . . . 241
  Lower and Middle Cambrian stratigraphy in northern Utah and southeastern Idaho. By G. B Maxey . . 647
  Some biostratigraphical concepts. By Curt Teichert . . 99
  Stratigraphy and structure of the St. Albans area, northwestern Vermont. By A. B. Shaw . . . . . 519
Paleozoic
  Structural geology of the southern Snake Range, Nevada. By Harald Drewes . . . . . 221
PATERSON, M. S.: Experimental deformation and faulting in Wombeyan marble . . . . . 465
Pennsylvania, Alteration of clay minerals in Illinoian till in. By J. B. Droste and J. C. Tharin . . . . . 61
Pennsylvanian rocks in the Sand Canyon area, Otero County, New Mexico, Stratigraphy of Upper. By G. O. Bachman and P. T. Hayes . . . . . 689
Permian rocks in the Sand Canyon area, Otero County, New Mexico, Stratigraphy of Lower. By G. O. Bachman and P. T. Hayes . . . . . 689
Petrography
  Coronites from India and their bearing on the origin of coronas. By M. V. N. Murthy . . . . . 23
  Masinloc chromite deposit, Zambales, Luzon, Philippine Islands. By W. C. Stoll . . . . . 419
  Tanner graywacke, by Reinhard Helmbold. By F. B. Van Houten, Translator . . . . . 301
Petrology
  Coronites from India and their bearing on the origin of coronas. By M. V. N. Murthy . . . . . 23
  Masinloc chromite deposit, Zambales, Luzon, Philippine Islands. By W. C. Stoll . . . . . 419
  White Tank quartz monzonite, California. By J. J. W. Rogers . . . . . 449
**Petrology and origin of the Poway conglomerate, San Diego County, California.** By G. J. Bellemin and Richard Merriam . . . . . 199
**Petrology of underclays.** By L. G. Schultz . . . . . 363
Philippine Islands, Geology and petrology of the Masinloc chromite deposit, Zambales, Luzon. By W. C. Stoll . . 419
PHOENIX, D. A.: Uranium deposits under conglomeratic sandstone of the Morrison formation, Colorado and Utah . . . . . 403
Physiography
  Geological geomorphology. By R. J. Russell . . . . . 1
† PINSON, W. H., JR., FAIRBAIRN, H. W., AND CORMIER, R. F.: Sr/Rb age measurements on hornblende and feldspar, and the age of syenite at Chicoutimi, Quebec, Canada . . . . . 599
Pleistocene
  Drainage evolution in northeastern Montana and northwestern North Dakota. By A. D. Howard . . . . . 575
  Glacial chronology of New Zealand. By Maxwell Gage and R. P. Suggate . . . . . 589
† Pleistocene glaciation in northern Labrador. By E. P. Wheeler, 2nd . . . . . 343
† Pliocene vertebrate fauna from the Bitterroot Valley, Montana, and its stratigraphic significance. By R. L. Konizeski . . . . . 345
**Potassium-argon dating of sedimentary rocks.** By Joseph Lipson . . . . . 137
— — — — — Notes on. By G. H. Curtis and J. H. Reynolds . . . . . 151
Poway conglomerate, San Diego County, California, Petrology and origin of. By G. J. Bellemin and Richard Merriam . . . . . 199
**Precambrian classification and correlation in the Canadian Shield.** By M. E. Wilson . . . . . 757

Quartz monzonite, California, Textural and spectrochemical studies of the White Tank. By J. J. W. Rogers . . . . 449

Radioactivity, Dating by
Some biostratigraphical concepts. By Curt Teichert 99
Reaction rims
Coronites from India and their bearing on the origin of coronas. By M. V. N. Murthy 23
**Recent underwater surveys using low-frequency sound to locate shallow bedrock.** By W. O. Smith 69
REYNOLDS, J. H. (WITH G. H. CURTIS): Notes on the potassium-argon dating of sedimentary rocks 151
† RINGWOOD, A. E.: Olivine-spinel transition in fayalite 129
Rivers
Geological geomorphology. By R. J. Russell 1
† Rock densities of the central Venezuelan Andes. By J. Hospers and J. C. van Wijnen 359
RODDA, J. R. (WITH R. W. METSGER AND C. B. TENNANT): Geochemistry of the Sterling Hill zinc deposit, Sussex County, New Jersey 775
ROGERS, J. J. W.: Textural and spectrochemical studies of the White Tank quartz monzonite, California 449
Ross glacial stage
Glacial chronology of the New Zealand Pleistocene. By Maxwell Gage and R. P. Suggate 589
RUSSELL, R. J.: Geological geomorphology 1

St. Albans area, northwestern Vermont, Stratigraphy and structure of. By A. B. Shaw 519
Sand Canyon area, Otero County, New Mexico, Stratigraphy of Upper Pennsylvanian and Lower Permian rocks in. By G. O. Bachman and P. T. Hayes 689
San Diego County, California, Petrology and origin of the Poway conglomerate. By G. J. Bellemin and Richard Merriam 199
Sandstone of the Morrison formation, Colorado and Utah, Uranium deposits under. By D. A. Phoenix 403
SCHULTZ, L. G.: Petrology of underclays 363
Sedimentary rocks
Potassium-argon dating
By G. H. Curtis and J. H. Reynolds 151
By Joseph Lipson 137
Sedimentation
Geological geomorphology. By R. J. Russell 1
Geology of Kapingamarangi Atoll, Caroline Islands. By E. D. McKee 241
Lower and Middle Cambrian stratigraphy in northern Utah and southeastern Idaho. By G. B. Maxey 647
Sedimentology
Contribution to the petrography of the Tanner graywacke, by Reinhard Helmbold. By F. B. Van Houten, Translator 301
Recent underwater surveys using low-frequency sound to locate shallow bedrock. By W. O. Smith 69
Seward Glacier, Alaska. By R. P. Sharp 617
**Shallow submerged marine terraces of Southern California.** By K. O. Emery 39
SHARP, R. P.: Malaspina Glacier, Alaska 617
— (WITH C. G. ENGEL): Chemical data on desert varnish 487
SHAW, A. B.: Stratigraphy and structure of the St. Albans area, northwestern Vermont 519
† Significance of coccolithophorids in calcium-carbonate deposition. By M. N. Bramlette 121
Slickensides in experimental deformation of Wombeyan marble. By M. S. Paterson 465
SMITH, W. O.: Recent underwater surveys using low-frequency sound to locate shallow bedrock 69
Snake Range, Nevada, Structural geology of the southern. By Harald Drewes 221
Soil analyses
Geology of Kapingamarangi Atoll, Caroline Islands. By E. D. McKee 241
— studies
Alteration of clay minerals in Illinoian till. By J. B. Droste and J. C. Tharin 61
**Some biostratigraphical concepts.** By Curt Teichert 99
Sonar method of exploration
Recent underwater surveys using low-frequency sound to locate shallow bedrock. By W. O. Smith 69
† *Sonoraspis* and *Albertella* in the Inyo Mountains, California. By Alexander Stoyanow 347
Spectrochemical analyses
Feldspars, White Tank quartz monzonite, California. By J. J. W. Rogers 449
Spectrographic analyses
Desert varnish. By C. G. Engel and R. P. Sharp 487
Pumice from Kapingamarangi Atoll, Caroline Islands. By E. D. McKee 241
Spectrometer studies
Alteration of clay minerals in Illinoian till by weathering. By J. B. Droste and J. C. Tharin 61
Spectrometric analysis, Potassium-argon dating of sedimentary rocks by. By Joseph Lipson 137
† Sr/Rb measurements on hornblende and feldspar, and the age of syenite at Chicoutimi, Quebec, Canada. By W. H. Pinson, Jr., H. W. Fairbairn, and R. F. Cormier 599
Sterling Hill zinc deposit, Sussex County, New Jersey, Geochemistry of. By R. W. Metsger, C. B. Tennant, and J. R. Rodda 775
STOLL, W. C.: Geology and petrology of the Masinloc chromite deposit, Zambales, Luzon, Philippine Islands 419
† STOYANOW, ALEXANDER: *Sonoraspis* and *Albertella* in the Inyo Mountains, California 347
† —: Suture of *Acanthohoplites aschillaensis* (Anthula) 607
STRAHLER, A. N.: Dimensional analysis applied to fluvially eroded landforms 279
Stratigraphy
Cow Head region, western Newfoundland. By C. H. Kindle and H. B. Whittington 315
Infolded mestasedimentary rocks near the axial zone of the Catoctin Mountain-Blue Ridge anticlinorium in Virginia. By E. O. Gooch 569
Lower and Middle Cambrian stratigraphy in northern Utah and southeastern Idaho. By G. B. Maxey 647
Poway conglomerate, San Diego County, California. By G. J. Bellemin and Richard Merriam 199
Some biostratigraphical concepts. By Curt Teichert 99
Structural geology of the southern Snake Range, Nevada. By Harald Drewes 221
**Stratigraphy and structure of the St. Albans area, northwestern Vermont.** By A. B. Shaw 519
**Stratigraphy of the Cow Head region, western Newfoundland.** By C. H. Kindle and H. B. Whittington 315
**Stratigraphy of Upper Pennsylvanian and Lower Permian rocks in the Sand Canyon area, Otero County, New Mexico.** By G. O. Bachman and P. T. Hayes 689
**Structural geology of the southern Snake Range, Nevada.** By Harald Drewes 221
Structure
Experimental deformation and faulting in Wombeyan marble. By M. S. Paterson 465
Geology of the Mount Garibaldi map-area, southwestern British Columbia, Canada. By W. H. Mathews 161, 179
In ice, Malaspina Glacier, Alaska. By R. P. Sharp 617
Infolded metasedimentary rocks near the axial zone of the Catoctin Mountain-Blue Ridge anticlinorium in Virginia. By E. O. Gooch 569

Precambrian classification and correlation in the Canadian Shield. By M. E. Wilson ... 757
St. Albans area, northwestern Vermont. By A. B. Shaw ... 519
Southern Snake Range, Nevada. By Harald Drewes ... 221
Uranium deposits under conglomeratic sandstone of the Morrison formation, Colorado and Utah. By D. A. Phoenix ... 403
Submarine terraces of Southern California. By K. O. Emery ... 39
Submerged terraces of Southern California. By K. O. Emery ... 39
SUGGATE, R. P. (WITH MAXWELL GAGE): Glacial chronology of the New Zealand Pleistocene ... 589
Sussex County, New Jersey, Geochemistry of the Sterling Hill zinc deposit. By R. W. Metsger, C. B. Tennant, and J. R. Rodda ... 775
† Suture of *Acanthohoplites aschiltaensis* (Anthula). By Alexander Stoyanow ... 607

† TABER, STEPHEN: Complex origin of silts in the vicinity of Fairbanks, Alaska ... 131
Tanner graywacke, Petrography of, by Reinhard Helmbold. By F. B. Van Houten, Translator ... 301
TEICHERT, CURT: Some biostratigraphical concepts ... 99
Temple Mountain, Utah, Urano-organic ore at. By D. R. Kelley and P. F. Kerr ... 701
TENNANT, C. B. (WITH R. W. METSGER AND J. L. RODDA): Geochemistry of the Sterling Hill zinc deposit, Sussex County, New Jersey ... 775
Terraces of Southern California, Shallow submerged marine. By K. O. Emery ... 39
**Textural and spectrochemical studies of the White Tank quartz monzonite, California.** By J. J. W. Rogers ... 449
THARIN, J. C. (WITH J. B. DROSTE): Alteration of clay minerals in Illinoian till by weathering ... 61
Tidal fluctuations
Geology of Kapingamarangi Atoll, Caroline Islands. By E. D. McKee ... 241

Underclays, Petrology of. By L. G. Schultz ... 363
Uranium
Urano-organic ore at Temple Mountain, Utah. By D. R. Kelley and P. F. Kerr ... 701
**Uranium deposits under conglomeratic sandstone of the Morrison formation, Colorado and Utah.** By D. A. Phoenix ... 403
**Urano-organic ore at Temple Mountain, Utah.** By D. R. Kelley and P. F. Kerr ... 701
† Use of punched cards to speed statistical analyses of geomorphic data. By M. A. Melton ... 355
Utah
Lower and Middle Cambrian stratigraphy in northern. By G. B. Maxey ... 647
Uranium deposits under conglomeratic sandstone of the Morrison formation. By D. A. Phoenix ... 403
Urano-organic ore at Temple Mountain. By D. R. Kelley and P. F. Kerr ... 701

VAN HOUTEN, F. B., Translator: Contribution to the petrography of the Tanner graywacke, by Reinhard Helmbold ... 301
† VAN WIJNEN, J. C. (WITH J. HOSPERS): Rock densities of the central Venezuelan Andes ... 339
Varnish, Chemical data on desert. By C. G. Engel and R. P. Sharp ... 487
Vermont, Stratigraphy and structure of the St. Albans area, northwestern. By A. B. Shaw ... 519
Virginia, Infolded metasedimentary rocks near the axial zone of the Catoctin Mountain-Blue Ridge anticlinorium in. By E. O. Gooch ... 569
Volcanism
Geology of the Mount Garibaldi map-area, southwestern British Columbia, Canada. By W. H. Mathews ... 161, 179
Structural geology of the southern Snake Range, Nevada. By Harald Drewes ... 221

Waimaungan glacial stage
Glacial chronology of the New Zealand Pleistocene. By Maxwell Gage and R. P. Suggate ... 589
Weathering
Alteration of clay minerals in Illinoian till by. By J. B. Droste and J. C. Tharin ... 61
Chemical data on desert varnish. By C. G. Engel and R. P. Sharp ... 487
† WHEELER, E. P., 2nd: Pleistocene glaciation in northern Labrador ... 343
White Tank quartz monzonite, California, Textural and spectrochemical studies of the. By J. J. W. Rogers ... 449
WHITTINGTON, H. B. (WITH C. H. KINDLE): Stratigraphy of the Cow Head region, western Newfoundland ... 315
WILSON, M. E.: Precambrian classification and correlation in the Canadian Shield ... 757
Wombeyan marble, Experimental deformation and faulting in. By M. S. Paterson ... 465

X-ray spectrometer studies
Alteration of clay minerals in Illinoian till by weathering. By J. B. Droste and J. C. Tharin ... 61

Yellowstone River
Drainage evolution in northeastern Montana and northwestern North Dakota. By A. D. Howard ... 575

Zambales, Luzon, Philippine Islands, Geology and petrology of the Masinloc chromite deposit. By W. C. Stoll ... 419
Zinc deposits
Geochemistry of the Sterling Hill zinc deposit, Sussex County, New Jersey. By R. W. Metsger, C. B. Tennant, and J. R. Rodda ... 775

40. Hadrosaurian Dinosaurs of North America. R. S. Lull and N. E. Wright. 1942. 242 p., 31 pls., 90 figs. $2.70.
48. North American Pleospongia. V. J. Okulitch. 1943. 112 p., 19 figs. $1.50.
49. Ozarkian and Canadian Cephalopods. Part II: Brevicones. E. O. Ulrich, A. F. Foerste, and A. K. Miller. 1943. 240 p., 70 pls., 15 figs. $3.00.
50. Bibliography of Economic Geology of South America. J. T. Singewald, Jr. 1943. 159 p. $1.00.
58. Ozarkian and Canadian Cephalopods. Part III. Longicones. E. O. Ulrich, A. F. Foerste, A. K. Miller, A. G. Unklesbay. 1944. 226 p., 68 pls., 9 figs. $3.00.
60. Glacial Map of North America. By Committee on Glacial Map. R. F. Flint, *Chairman*. 1945. $2.00.
62. Crust of the Earth. Arie Poldervaart, *Editor*. 1955. 762 p. $6.50.
63. De Natura Fossilium, by Georgius Agricola. Translated by M. C. Bandy and J. A. Bandy. 1955. 240 p. $3.00.
64. Marysvale, Utah, Uranium Area. Paul F. Kerr *et al.* 1957. 212 p., 21 pls., 106 figs. $6.00.

## MEMOIRS

1. Stratigraphy of Western Newfoundland. Charles Schuchert and C. O. Dunbar. 1934. 123 p., 11 pls., 8 figs. $2.40.
2. Paleozoic Plankton of North America. Rudolf Ruedemann. 1934. 141 pp., 26 pls., 6 figs. $2.40.
3. Evolution of the Congo Basin. A. C. Veatch. 1935. 183 p., 10 pls., 8 figs. $2.10.
4. Geology in the Coastal Atlas of Western Algeria. R. van V. Anderson. 1936. 450 p., 19 pls., 2 figs. $4.20.
11. Mollusca of the Tertiary Formations of Northeastern Mexico. Julia Gardner. 1945. 332 p., 28 pls., 1 fig. $3.90.
12. Revision of the Upper Cambrian Fauna of New Jersey. B. F. Howell. 1945. 46 p., 8 pls. $1.00.
13. Pennsylvanian Geology of a Part of the Southern Appalachian Coal Field. H. R. Wanless. 1945. 162 p., 40 pls. 1 fig. $3.90.
14. Brachiopoda of the Independence Shale. M. A. Stainbrook. 1945. 76 p., 6 pls., 2 figs. $1.20.
15. Tungsten Mineralization in the United States. P. F. Kerr. 1946. 241. p., 23 pls., 34 figs. $3.50.
16. Eocene Faunas from the Department of Bolivar, Colombia. B. L. Clark and J. W. Durham. 1946. 126 p., 28 pls. 1 fig. $2.10.
18. Lineation: A Critical Review and Annotated Bibliography. Ernst Cloos. 1946. 122 p., 10 pls., 15 figs. Supplement Literature for 1942-1952), 16 pages. 1953. Reprinted 1957 as one volume. $2.00.
21. Origin and Development of Craters. T. A. Jaggar. 1947. 508 p., 87 pls., 14 figs. $6.00.
25. Evolution of the Horse Brain. Tilly Edinger. 1948. 177 pl., 24 figs. $2.00.
26. Bibliographic Index of Permian Invertebrates. C. C. Branson. 1948. 1049 p. $9.50.
27. Propagation of Sound in the Ocean. J. L. Worzel, Maurice Ewing, C. L. Pekeris. 1948. 205 p., 23 pls., 89 figs. $2.75.
28. Origin of Granite (Conference). James Gilluly, *Chairman*. 1948. 139 p., 13 pls., 5 figs. $1.80.
34. Permian Crinoid Calceolispongia. Curt Teichert. 1949. 132 p., 26 pls., 24 figs. $2.50.
35. Geology of the Coast Ranges Immediately North of the San Francisco Bay Region, California. C. E. Weaver, 1949. 242 p., 14 pls., 2 figs. $6.50.
36. Geology of the Lake Titicaca Region, Peru and Bolivia. N. D. Newell. 1949. 111 p., 21 pls., 14 figs. $5.00.
37. Bibliography of Fossil Vertebrates, 1939-1943. C. L. Camp, S. P. Welles, and Morton Green. 1949. 371 p. $4.50.
38. Lower Cretaceous Stratigraphy in Southeastern Arizona. Alexander Stoyanow. 1949. 169 p., 27 pls., 2 figs. $2.50.
39. Sedimentary Facies in Geologic History. C. R. Longwell, *Chairman*. 1949. 171 p. $1.75.
40. Revision of the Families and Genera of the Devonian Tetracorals. E. C. Stumm. 1949. 92 p., 25 pls. $2 00.
41. American Permian Nautiloids. A. K. Miller and Walter Youngquist. 1949. 218 p., 50 pls., 39 figs. $3.00.
42. Maquoketa Brachiopoda of Iowa. Y. Wang. 1950. 55 p., 12 pls. $1.40.
43. 1940 E. W. Scripps Cruise to Gulf of California. C. A. Anderson *et al.* 1950. 362 p., 65 pls., 28 figs. $6.50.
45. Interpretation of Ore Textures. E. S. Bastin. 1950. 101 p., 28 figs. $1.75.
47. Interpretation of Aeromagnetic Maps. V. Vacquier *et al.* 1951. 151 p., 14 pls., 83 figs. $2.25.
48. North American Geosynclines. Marshall Kay. 1951. 143 p., 16 pls., 20 figs. $2.00.
50. Deformation, Metamorphism and Mineralization in Gypsum-Anhydrite Cap Rock. Marcus Goldman. 1952. 16 p., 5 figs., 64 pls. $3.00.
51. Catalogue of the Cenozoic Plants of North America through 1950. Robert S. LaMotte. 1952. 381 p., 5 figs. $5.50.
52. Selected Petrogenic Relationships of Plagioclase. R. C. Emmons, *Editor*, 1953. 142 p., 38 figs., 16 pls. $2.00.
53. Paleozoic and Mesozoic Arachnida of Europe. Alexander Petrunkevitch. 1953. 128 p., 58 pls. $3.00.
54. Biostratigraphy of the Maqfi Section, Egypt. L. W. LeRoy. 1953. 73 p., 4 figs., 14 pls. $1.75.
55. Trilobites from the Lower Champlainian Formations of the Appalachian Valley. Byron N. Cooper. 1953. 68 p., 1 fig., 19 pls. $1.75.
56. North American and European Strophedontids: Morphology and Systematics. Alwyn Williams. 1953. 67 p., 5 figs., 13 pls. $1.50.
57. Bibliography of Fossil Vertebrates, 1944-1948. C. L. Camp *et al.* 1953. 455 p. $5.50.
59. Silicified Middle Ordovician Trilobites. H. B. Whittington and W. R. Evitt II. 1954. 137 p., 27 figs., 33 pls. $3.00.
60. Crystal Data. J. D. H. Donnay and Werner Nowacki. 1954. 719 p. $5.00.
61. Stratigraphy and History of the Moenkopi Formation of Triassic Age. E. D. McKee. 1954. 133 p., 19 figs., 12 pls. $3.00.
64. Sunken Islands of the Mid-Pacific Mountains. E. L. Hamilton. 1956. 97 p., 12 figs., 13 pls. $2.50.
65. Handbook of South American Geology. W. F. Jenks, *Editor*. 1956. 378 p., 13 figs., 11 pls. $5.50.
66. Cenozoic Foraminifera from Micronesia. Shoshiro Hanzawa. 1957. 163 p., 12 figs., 41 pls. $4.50.
67. Treatise on Marine Ecology and Paleoecology. Volume 1, Ecology. Joel W. Hedgpeth, *Editor*. 1957. 1296 p. $12.50. Volume 2, Paleoecology. H. S. Ladd, *Editor*. 1957. 1078 p. $10.00.
68. Beekmantown Group (Lower Ordovician) of Maryland. W. J. Sando. 1957. 161 p., 20 figs., 15 pls. $5.00.
69. Genus *Pentremites* and Its Species. J. J. Galloway and H. V. Kraska. 1957. 104 p., 5 figs., 13 pls. $2.50.
70. *Fenestella* from the Permian of West Texas. M. K. Elias and G. E. Condra. 1957. 158 p., 17 figs., 23 pls. $3.50.

# *Publications of the Geological Society of America*

Publications currently in stock may be purchased at prices indicated below, on order accompanied by remittance addressed to The Geological Society of America, 419 West 117 Street, New York 27, N. Y. Consult lists on current Bulletins to be assured that items of interest are in stock.

## BULLETIN

Monthly. Advance subscription, $15 per year; separate number $1.50; back yearly volumes, as available: prior to 1925, $12.00 per volume; 1925–, $15.00 per volume. Ten-year indexes covering vols. 31–40, 41–50, $1.50 per copy; covering vols. 51–60, $1.00 per copy.

## GUIDEBOOKS FOR ANNUAL MEETING FIELD TRIPS

GUIDES TO SOUTHEASTERN GEOLOGY. (New Orleans). Richard J. Russell, *Editor*. November 1955. $3.00.

GUIDEBOOK FOR FIELD TRIPS. (Minneapolis). G. M. Schwartz, *Editor*. November 1956. $4.00.

## BERKEY VOLUME

APPLICATION OF GEOLOGY TO ENGINEERING PRACTICE, SIDNEY PAIGE, *Chairman*. By 18 Authors (13 papers), 327 p. $2.75.

## PENROSE VOLUME

LIFE AND LETTERS OF R. A. F. PENROSE, JR., H. R. Fairbanks and C. P. Berkey. 1932. 765 p. $4.00.

## BIBLIOGRAPHY OF GEOLOGY EXCLUSIVE OF NORTH AMERICA

Annually, 1933–1940; biennially, 1941–1946; annually, 1947–. By Marie Siegrist, Marcia Lakeman, and Mary Grier, Vols. 1–7 inclusive, $2.50 per volume; Volumes 8–12, out of stock; Volume 13, $3.25; Volume 14, $3.00; Volume 15, $3.00; Volume 16, $4.50; Volume 17, $5.75; Volume 18, $5.50; Volume 19, $7.50; Volume 20, $8.00; Volume 21, $10.00.

## SPECIAL COLORED MAPS

GLACIAL MAP OF NORTH AMERICA (Special Paper 60). By Committee on Glacial Map. R. F. Flint, *Chairman*. 1945. $2.00.

GEOLOGIC MAP OF SOUTH AMERICA. By South American Map Committee, A. I. Levorsen, *Chairman*. 1950. $4.00.

GEOLOGIC-TECTONIC MAP OF VENEZUELA. By W. H. Bucher. 1950. $2.50.

TECTONIC MAP OF CANADA. By Geological Association of Canada. 1950. $1.50.

PLEISTOCENE EOLIAN DEPOSITS OF THE UNITED STATES, ALASKA, AND PARTS OF CANADA. James Thorp and H. T. U. Smith, *Cochairmen*. 1952. $3.00.

## ROCK COLOR CHARTS

Prepared by Committee of National Research Council. $7.00 per set.

## GEOLOGICAL ABSTRACTS

Volume 4 (1956) $2.50; Volume 5 (1957) $3.00; Subscriptions for Volume 6 (1958) $3.00.

## TREATISE ON INVERTEBRATE PALEONTOLOGY

Raymond C. Moore, *Editor*

Part D. PROTISTA 3 (Chiefly Radiolarians and Tintinnines). By A. S. Campbell and R. C. Moore. 1955. 195 p., 92 figs. $2.50.

Part E. ARCHAEOCYATHA AND PORIFERA. By V. J. Okulitch and M. W. de Laubenfels. 1955. 122 p., 88 figs. $3.00.

Part F. COELENTERATA. By F. M. Bayer *et al.* 1956. 498 p., 358 figs. $7.00.

Part G. BRYOZOA. By Ray S. Bassler. 1954. 253 p., 175 figs. $3.00.

Part L. MOLLUSCA 4—CEPHALOPODA; AMMONOIDEA. By W. J. Arkell *et al.* 1957. 490 p., 558 figs. $8.50.

Part P. ARTHROPODA 2 (Chelicerata, Pycnogonida, Palaeoisopus). By L. Störmer, A. Petrunkevitch, J. W. Hedgpeth, 1955. 181 p., 123 figs. $3.50.

Part V. GRAPTOLITHINA. By O. M. B. Bulman. 1955. 101 p., 72 figs. $3.00.

## SPECIAL PAPERS

1. BIBLIOGRAPHY AND INDEX OF PALEOZOIC OSTRACODA. R. S. Bassler and Betty Kellett. 1934. 500 p., 24 figs. $3.00.
2. FOSSIL CRUSTACEA OF THE ATLANTIC AND GULF COASTAL PLAIN. M. J. Rathbun. 1935. 160 p., 26 pls., 2 figs. $1.50.
3. FOSSIL NON-MARINE MOLLUSCA OF NORTH AMERICA. Junius Henderson. 1935. 313 p. $2.10.
5. GEOLOGY OF SAINT JOHN, NEW BRUNSWICK. A. O. Hayes and B. F. Howell. 1937. 146 p., 9 pls., 4 figs. $1.50.
7. ATLANTIC SUBMARINE VALLEYS OF THE UNITED STATES AND THE CONGO SUBMARINE VALLEY. A. C. Veatch and Paul A. Smith. 1939. 101 p., 5 charts, 10 pls., 28 figs. $3.50.
9. FOSSIL SNAKES OF NORTH AMERICA. C. W. Gilmore. 1938. 96 p., 4 pls., 38 figs. $0.90.
11. GEOLOGY AND PALEONTOLOGY OF THE MINGAN ISLANDS, QUEBEC. W. H. Twenhofel. 1938. 122 p., 24 pls., 1 fig. $1.50.
12. TERTIARY FLORA FROM THE RIO PICHILEUFU, ARGENTINA. E. W. Berry. 1938. 149 p., 56 pls., 11 figs. $2.10.
21. PALEONTOLOGY AND STRATIGRAPHY OF THE SILURIAN ROCKS OF THE PORT DANIEL-BLACK CAPE REGION, GASPE. S. A. Northrop. 1939. 302 p., 28 pls., 1 fig. $3.00.
23. BIBLIOGRAPHIC INDEX OF NORTH AMERICAN DEVONIAN CEPHALOPODA. E. M. Kindle and A. K. Miller. 1939. 179 p. $1.25.
28. REVIEW OF THE PELYCOSAURIA. A. S. Romer and L. I. Price. 1940. 538 p., 46 pls., 71 figs. $4.20.
29. PHACOPID TRILOBITES OF NORTH AMERICA. D. M. Delo. 1940. 135 p., 13 pls. $1.20.
33. NUMERICAL STRUCTURE FACTOR TABLES. M. J. Buerger. Reprinted 1953. 119 p., 4 figs. (Cloth bound) $1.50.
37. OZARKIAN AND CANADIAN CEPHALOPODS, Part I, Nautilicones. E. O. Ulrich, Aug. F. Foerste, A. K. Miller and W. H. Furnish. 1942. 157 p., 57 pls., 23 figs. $2.40.
38. TEREBRATULOID BRACHIOPODA OF THE SILURIAN AND DEVONIAN. P. E. Cloud, Jr. 1942. 182 p., 20 pls., 17 figs. $1.50.

*(Continued on inside back cover)*